



THE UNIVERSITY OF QUEENSLAND
AUSTRALIA

**Measuring motor-training induced neuroplasticity using diffusion and
functional MRI: A Sensitive, Pathology-Robust Approach**

Lee Bremner Reid

MSc (1st class hon), PGDipSci, BSc

A thesis submitted for the degree of Doctor of Philosophy at

The University of Queensland in 2017

Faculty of Medicine

Abstract

Brain injury constitutes a significant health burden worldwide, and outcomes are generally poor. To improve treatment, we must better understand how injury affects brain function, how the brain responds to learning pressures (neuroplasticity), and the interaction between the two. This is difficult, however, because of current technological shortcomings.

This thesis focusses on the measurement of neuroplasticity in response to motor training in situations such as rehabilitation following brain injury. Although the principles and methods discussed generalise to many forms of brain pathology, discussion is generally focussed on unilateral cerebral palsy (UCP) because altered brain-development in UCP makes analyses particularly difficult. This begins with a literature review (Chapter 2) that outlines UCP, rehabilitative approaches, and the relationship between atypical brain organisation and early-life brain injury. Also discussed is how novel rehabilitation strategies may stem from studying brain changes induced by rehabilitation, and why the most informative findings are likely to come from studies utilising multiple imaging modalities.

Blood Oxygen-Level Dependent Functional Magnetic Resonance Imaging (fMRI) measures brain activity indirectly and has been used to study neuroplasticity in both healthy participants and those with brain pathology. Although fMRI confounds are well understood, no published work has explored their cumulative effect when brain injury is present. Resultantly, confounds have largely been ignored, leading to heterogeneous findings that have provided little toward understanding brain changes, biologically speaking. Chapter 3 examines the cumulative effect of fMRI confounds, assumptions, and other issues, when attempting to measure neuroplasticity in participants with brain injury. This work concludes that, although fMRI can be expected to locate approximate regions of brain activation in an individual scan, numerous confounding factors make its interpretation, in terms of neuroplasticity, difficult without additional information acquired through alternative means.

Diffusion MRI (dMRI) is an imaging modality that is typically used to identify the brain's white-matter pathways and calculate metrics that are influenced by factors such as myelination or axonal density. Standard dMRI analyses are ill suited to studying brain injury due to their reliance on brain 'atlases' which indicate relationships between brain regions and brain functions. Brain pathology can prevent reliable atlas registration, and alter relationships between structure and function. Chapter 4 details a novel dMRI analysis designed to measure neuroplasticity, addressing the need for a sensitive and reliable alternative to standalone-fMRI. This method utilises surface-based fMRI analyses, rather than brain atlases, to locate regions involved in motor execution. Corticospinal (CST) and thalamocortical tracts emanating from these regions are delineated using dMRI tractography and

machine learning. This method was applied to children with UCP - the majority of whom presented with significant brain pathology. Relationships between dMRI measures of CST microstructure and clinical measures of motor function were identified. In these and other measures, the present method outperformed a cutting-edge voxelwise fMRI+dMRI technique applied to the same data.

Studying plasticity in participants with brain injury requires first understanding the neuroplastic processes of healthy people. Imaging literature in this area is largely fragmented: studies are typically mono-modal and have incomparable methodologies. Chapter 5 and Chapter 6 address this through a multimodal investigation into motor-learning driven neuroplasticity. Twenty-four healthy adults practised a finger-thumb opposition sequence with their non-dominant hand daily. After four weeks, task performance improved and fMRI activation associated with trained-sequence execution decreased. In 'trained' motor areas, transcranial magnetic stimulation mean evoked potentials (MEPs; at the pollicis brevis) increased; MEP map volume did not. These responses overlapped spatially with fMRI and potential cortical thickness increases. These results imply that a long-term-potential-like process occurred predominantly in regions *already responsible* for conducting the task, improving task-processing efficiency. Potential cortical thickness increases were also found in the dorsolateral prefrontal cortex (dlPFC). Diffusion changes were seen in striatal regions connected to the dlPFC and connections between these regions. The aforementioned fMRI-driven dMRI method revealed changes to the CST consistent with myelination.

Chapter 7 describes an attempt to take this analysis further: to measure brain changes in 14 children with UCP who participated in 20 weeks of virtual reality therapy. Clinical improvements were limited and no changes in associated white matter microstructure were detected. The fMRI-driven dMRI method demonstrated a high degree of test-retest reliability in the 13 enrolled controls, and so it is likely that statistical power was limited by degrees of clinical improvement. The number of enrollees required to achieve meaningful power for such measurements, however, was unexplored in the literature.

These results make clear that a barrier to investigating neurorehabilitation-induced neuroplasticity is uncertainty surrounding statistical power. Chapter 8 describes power analyses for paediatric UCP neurorehabilitation trials measuring cortical thickness and dMRI changes. Calculations were based on results presented in the preceding chapters. The results can be utilised to formally plan study numbers, preventing underpowered trials. This analysis also allowed a number of recommendations to be made that may further reduce barriers to successful neurorehabilitative trials.

Declaration By Author

This thesis is composed of my original work, and contains no material previously published or written by another person except where due reference has been made in the text. I have clearly stated the contribution by others to jointly-authored works that I have included in my thesis.

I have clearly stated the contribution of others to my thesis as a whole, including statistical assistance, survey design, data analysis, significant technical procedures, professional editorial advice, and any other original research work used or reported in my thesis. The content of my thesis is the result of work I have carried out since the commencement of my research higher degree candidature and does not include a substantial part of work that has been submitted to qualify for the award of any other degree or diploma in any university or other tertiary institution. I have clearly stated which parts of my thesis, if any, have been submitted to qualify for another award.

I acknowledge that an electronic copy of my thesis must be lodged with the University Library and, subject to the policy and procedures of The University of Queensland, the thesis be made available for research and study in accordance with the Copyright Act 1968 unless a period of embargo has been approved by the Dean of the Graduate School.

I acknowledge that copyright of all material contained in my thesis resides with the copyright holder(s) of that material. Where appropriate I have obtained copyright permission from the copyright holder to reproduce material in this thesis.

Publications during candidature

Peer-reviewed Journal Papers

Sahama I, Sinclair K, Fiori S, Doecke J, Pannek K, **Reid L**, et al. Motor pathway degeneration in young ataxia telangiectasia patients: A diffusion tractography study. *NeuroImage Clin.* 2015;9:206–15.

Reid LB, Rose SE, Boyd RN. Rehabilitation and neuroplasticity in children with unilateral cerebral palsy. *Nat Rev Neurol.* 2015;11(7):390–400.

Reid LB, Cunnington R, Boyd RN, Rose SE. Surface-Based fMRI-Driven Diffusion Tractography in the Presence of Significant Brain Pathology: A Study Linking Structure and Function in Cerebral Palsy. Yap P-T, editor. *PLoS One.* 2016 Aug 3;11(8):e0159540.

Scheck SM, Fripp J, **Reid L**, Pannek K, Fiori S, Boyd RN, et al. Extent of altered white matter in unilateral and bilateral periventricular white matter lesions in children with unilateral cerebral palsy. *Res Dev Disabil.* 2016 Aug;55:368–76.

Reid LB, Boyd RN, Cunnington R, Rose SE. Interpreting Intervention Induced Neuroplasticity with fMRI: The Case for Multimodal Imaging Strategies. *Neural Plast.* 2016;2016:1–13.

Reid LB, Sale M V, Cunnington R, Mattingley JB, Rose SE. Brain changes following four weeks of unimanual motor training: evidence from fMRI-guided diffusion MRI tractography. *Hum Brain Mapp.* (In Press)

Reid LB, Pagnozzi AM, Fiori S, Boyd RN, Dowson N, Rose SE. Measuring Neuroplasticity Associated with Cerebral Palsy Rehabilitation: A Power Analysis. *International Journal of Developmental Neuroscience.* (In Press)

Conference Proceedings

Reid LB, Cunnington R, Boyd RN, Rose SE. Mesh-based fMRI-driven-tractography for automated analyses of non-parcellateable brains with pathology. In: 23rd Annual Meeting and Exhibition of the International Society for Magnetic Resonance in Medicine. Toronto; 2015.

Reid LB, Sale M V., Cunnington R, Rose SE. Motor Learning Induced Neuroplasticity, Revealed By fMRI-Guided Diffusion Imaging. In: 24th Annual Meeting and Exhibition of the International Society for Magnetic Resonance in Medicine. Singapore; 2016.

Houston E, **Reid LB**, Fiori S, Rose S, Ware R, Boyd R. Relationship between clinical assessment of mirror movements and microstructural integrity of corticospinal and thalamocortical tracts in children with congenital hemiparesis. In: 8th Biennial Scientific Conference of the Australian Academy of Cerebral Palsy and Developmental Medicine. Adelaide; 2016

Houston E, **Reid LB**, Fiori S, Rose S, Ware R, Boyd R. Relationship between clinical assessment of mirror movements and microstructural integrity of corticospinal and thalamocortical tracts in children with unilateral cerebral palsy. In: 28th Meeting of the European Academy of Childhood Development. Stockholm; 2016

Reid LB, Pagnozzi A, Fiori S, Boyd RN, Rose SE. Measuring Neuroplasticity Associated with Cerebral Palsy Rehabilitation: An MRI based Power Analysis In: International Symposium on Biomedical Imaging. Melbourne; 2017.

Publications included in this thesis

Chapter 2

Reid LB, Rose SE, Boyd RN. Rehabilitation and neuroplasticity in children with unilateral cerebral palsy. *Nat Rev Neurol*. 2015;11(7):390–400.

Contributor	LR	SR	RB
Literature Search	80%		20%
Writing	65%		35%
Editing/Reviewing	15%	50%	35%

Chapter 3

Reid LB, Boyd RN, Cunnington R, Rose SE. Interpreting Intervention Induced Neuroplasticity with fMRI: The Case for Multimodal Imaging Strategies. *Neural Plast*. 2016;2016:1–13.

Contributor	LR	RC	RB	SR
Conception	50%			50%
Literature Search	100%			
Writing	100%			
Editing/Reviewing		20%	40%	40%

Chapter 4

Reid LB, Cunnington R, Boyd RN, Rose SE. Surface-Based fMRI-Driven Diffusion Tractography in the Presence of Significant Brain Pathology: A Study Linking Structure and Function in Cerebral Palsy. Yap P-T, editor. *PLoS One*. 2016 Aug 3;11(8):e0159540.

Contributor	LR	RC	RB	SR
Method Conception	50%			50%
Method Implementation	100%			
Data Acquisition	50%		50%	
Data Analysis	100%			
Interpretation	80%			20%
Writing	100%			
Clinical Trial Planning		10%	70%	20%
Editing/Reviewing		33%	33%	33%

'Clinical Trial Planning' and 'Data Acquisition' refer solely to components of the clinical trial that were utilised in this specific publication.

Chapter 6

Reid LB, Sale M V, Cunnington R, Mattingley JB, Rose SE. Brain changes following four weeks of unimanual motor training: evidence from fMRI-guided diffusion MRI tractography. *Hum Brain Mapp. (In Press)*

Lee Reid and Martin Sale were joint-first authors on this publication

Contributor	LR	MS	RC	JM	SR
Whole-Study Planning		60%		35%	5%
Sub-study Conception	34%	33%			33%
Data Acquisition		100%			
Data Analysis	100%				
Interpretation	60%	25%			15%
Writing	90%	10%			
Editing/Reviewing	20%	30%	10%	10%	30%

Chapter 8

Reid LB, Pagnozzi AM, Fiori S, Boyd RN, Dowson N, Rose SE. Measuring Neuroplasticity Associated with Cerebral Palsy Rehabilitation: A Power Analysis. *International Journal of Developmental Neuroscience. (In Press)*

Lee Reid and Alex Pagnozzi were joint-first authors on this publication

Contributor	LR	AP	RB	ND	SR
Conception and Planning	25%	25%		25%	25%
Data Acquisition	50%		50%		
Data Analysis	50%	50%			
Interpretation	50%	50%			15%
Writing	75%	25%			
Editing/Reviewing	20%	20%	20%	20%	20%

Some data used in this paper were utilised from Chapters 5 and 6. Acquisition of this data is detailed in the appropriate tables above. Dr James Doeke also dedicated approximately half an hour to providing statistical advice.

Contributions by others to the thesis

Collection of raw cerebral palsy data was conducted as part of the Mitii randomised controlled trial. The Mitii team included Roslyn Boyd, Paul Colditz, Stephen Rose, Jenny Ziviani, Anthony Smith, Paul Scuffham, Lynne McKinlay, Stephanie Ross, Sarah James, Louise Mitchell, Emmah Baque, Carly Mayberry, Melinda Lewis, Kerstin Pannek, Naomi Westwood, Julien Savina, Amy Cutrer, and myself. Naomi Westwood contributed particularly-substantially toward collection of the MRI data from this trial.

Chapter 5 and Chapter 6 are verbatim copies of two papers submitted to *Human Brain Mapping*, for which I am joint-first author. Chapter 5 is presently undergoing peer review, and Chapter 6 has been accepted. Planning of these analyses was primarily conducted by Jason Mattingly and Martin Sale, with contributions also from Stephen Rose and myself. Collection of this data was conducted by Jason Mattingly's Cognitive Neuroscience laboratory group at the Queensland Brain Institute, including Martin Sale, Luca Cocchi, Daniel Stjepanovic, and Amanda Robinson. The manuscript appearing in Chapter 5 was reviewed by Jason Mattingly, Stephen Rose, Martin Sale, Amanda Robinson, Alex Pagnozzi, and Luca Cocchi prior to submission. The manuscript appearing in Chapter 6 was reviewed by Jason Mattingly, Stephen Rose, Martin Sale, and Ross Cunnington prior to submission.

Chapter 8 is verbatim copy of a paper accepted by the *International Journal of Developmental Neuroscience*. I am joint-first author on this publication with Alex Pagnozzi. I wrote the vast majority of this manuscript, and shared responsibility for analysis and interpretation with Alex Pagnozzi. Data collection was conducted by the Mitii team (see above), which includes myself. Study planning and manuscript reviewing was shared between Alex Pagnozzi, Roslyn Boyd, Nicholas Dowson, Stephen Rose and myself. Dr James Doeke also dedicated approximately 30 minutes to providing statistical advice.

All remaining academic contributions by others are stated in Publications during candidature.

Statement of parts of the thesis submitted to qualify for the award of another degree

None

Acknowledgements

On the academic side, naturally, I would like to thank my supervisors Professors Stephen Rose, Roslyn Boyd, and Ross Cunnington. Stephen, in particular, deserves thanks for spending considerable time and energy on guiding my project – and manuscript wording – through the various hurdles it faced. Stephen always has had time to hear and discuss ideas with me, more or less immediately, and has well balanced challenging me and 'leaving me to it'. Although we both know (and have exercised) our relative positions, my steps have been predominantly guided, rather than ordered, for which I am extremely grateful. Stephen also successfully clinched, at short notice, the majority of my living allowance through CSIRO, the importance of which cannot be understated. Professor Boyd has been particularly enabling in terms of opportunities: the Cerebral Palsy data used in much of my work has come from her group at The University of Queensland, and the opportunity to publish in Nature Reviews Neurology was borne through her academic reputation. She has also agreed to provide a top-up to my CSIRO funding which has helped relieve the financial burden that three (more) years of study can bring. Although my contact with Professor Cunnington has been relatively limited, his several hour teaching session on functional MRI analysis (including a degree of honesty about what is and is not 'fluff') gave me a large leg-up at the outset. I am also very grateful for having someone to challenge my ideas in terms of biology; this has proven valuable, if not critical, multiple times.

Special mention must also go to Dr Kerstin Pannek, whose final three months of PhD were spent patiently answering endless questions from a new student nicknamed 'Kerstin's replacement', rather than writing her thesis. Her own elaborate diffusion tractography pipelines provided a foundation upon which mine could be built. After Kerstin's return from the UK two years later, our decidedly different skill-sets made it clear that I never was 'true' a replacement, and have really highlighted for me the benefits in both collaboration and drinking tea.

On the personal side, I'm blessed to have such supporting parents who have been more than happy to listen to my frustrations and difficulties, offered extensive useful advice, reminded me to relax, and made concerned "ohh dear"-like statements, even when they probably had no idea what I was blathering on about. My siblings are kind of alright too, I guess.

I never feared the scale, or academic challenge, of my PhD; my biggest challenge has been letting it go at the end of the day. Sincere thanks must go out to Elyse, who I met near the beginning of my PhD and has since done little but take me out, tell me to go home, feed me dinner, help me unwind (well, sometimes), and at least *attempt* to get me to live more amongst the physical world than amongst the ideas in my head. Similarly, the various forms of support I have received from Juju,

Beck, Wes and 'Nick have been invaluable, and the absurdist sense of humour readily offered by Alex Pagnozzi, and Josh Drummond throughout my candidacy have been a real highlight.

Finally, a big thanks to Andrew Timms. I had the pleasure of knowing Andrew for 25 years. A fellow Kiwi, Andrew showed me how life worked in Australia. We explored much of Queensland together, including dozens of mountains, waterfalls, and beaches; built furniture; fixed cars; taught one-another our trades; swim-trained weekly; had innumerable BBQs; riled up the locals at rugby matches; and complained to one-another incessantly about the beer. Andrew's untimely death was an unwelcome reminder on the importance of focusing on tangible progress in medical science. Chur. Double thumbs-up. Rest in Peace.

Keywords

diffusion-weighted magnetic resonance imaging, blood-oxygen level dependent functional magnetic resonance imaging, neuroplasticity, neurorehabilitation, cerebral palsy, cortical thickness, magnetic resonance imaging, multimodal imaging

Australian and New Zealand Standard Research Classifications (ANZSRC)

ANZSRC code: 110903, Central Nervous System, 40%

ANZSRC code: 080106, Image Processing, 40%

ANZSRC code: 111403, Paediatrics, 20%

Fields of Research (FoR) Classification

FoR code: 1109 Neurosciences, 40%

FoR code: 0801 Artificial Intelligence and Image Processing, 40%

FoR code: 1114 Paediatrics and Reproductive Medicine, 20%

Dedicated To Mum & Dad,
Who never discouraged me from asking questions

Table of Contents

Chapter 1 Thesis Aims and Structure	1
Chapter 2 Rehabilitation and neuroplasticity in children with unilateral cerebral palsy	3
Publication Information	4
Abstract	5
Key points	6
Review criteria	6
Introduction	7
Existing rehabilitative strategies	8
Neuroplasticity-informed rehabilitation.....	11
Measuring neuroplasticity	12
Conclusions	24
Chapter 3 Interpreting Intervention Induced Neuroplasticity with fMRI: The Case for Multimodal Imaging Strategies	25
Publication Information	26
Abstract	27
Introduction	29
Common Findings.....	30
The Challenge	34
Disease Confounds.....	39
Summary and Recommendations.....	40
Conclusion	46
Addendum.....	47
Chapter 4 Surface-Based fMRI-Driven Diffusion Tractography in the Presence of Significant Brain Pathology: A Study Linking Structure & Function in Cerebral Palsy	48
Publication information.....	50
Abstract	51
Introduction.....	52
Methods.....	57

Surface Method	61
Results	69
Discussion	77
Conclusions	81
Supporting Information	83
Chapter 5 Brain changes following four weeks of unimanual motor training: evidence from behaviour, neural stimulation, cortical thickness and functional MRI.....	85
Publication information.....	87
Abstract	89
Introduction	90
Materials and Methods.....	92
Results.....	100
Discussion	107
Conclusion	111
Supplementary Material	113
Chapter 6 Brain changes following four weeks of unimanual motor training: evidence from fMRI- guided diffusion MRI tractography	119
Publication information.....	120
Abstract	121
Introduction.....	122
Methods.....	125
Results.....	130
Discussion	135
Conclusion	139
Supplementary Materials	140
Chapter 7 Measuring Neuroplasticity in the Mitii Cerebral Palsy Rehabilitation Trial	142
Introduction.....	143
Methods.....	144
Results.....	146

Discussion	148
Chapter 8 Measuring Neuroplasticity Associated with Cerebral Palsy Rehabilitation: An MRI based Power Analysis	151
Publication Information	152
Abstract	153
Highlights.....	154
Introduction.....	155
Methods.....	156
Results.....	165
Discussion	168
Conclusions.....	171
Supplementary Materials	172
Chapter 9 Grand Discussion	177
Novel Contributions.....	178
Implications, Limitations and Future Work.....	181
References.....	183

Table of Figures

Figure 1	The influence of periventricular lesions on corticospinal laterality.....	19
Figure 2	An example of functional-MRI-guided diffusion MRI tractography	20
Figure 3	Commonly seen fMRI activation changes	31
Figure 4	Voxel-wise fMRI analyses of a block-design hand-tapping task.....	32
Figure 5	Task-based fMRI activation changes, in the presence of bilateral activation, require additional information for useful interpretation.....	37
Figure 6	Utilising fMRI in conjunction with a number of other modalities	45
Figure 7	Functional MRI activation for a hand tapping task, and corresponding T1 images for two children with unilateral cerebral palsy	55
Figure 8	Examples of participants with unilateral cerebral palsy, for whom neurological abnormalities include distortion of the midbrain, and/or loss of contrast between the thalamus and posterior limb of the internal capsule	56
Figure 9	Examples of pathology seen in the enrolled cohort	58
Figure 10	Summary of the pipeline for the surface-based fMRI-guided dMRI tractography	60
Figure 11	Example tractography from the surface-based and voxel-based methods, in a single participant with left-hemispheric pathology	64
Figure 12	Examples of pathology and impacts on analyses	70
Figure 13	Typical significant fMRI activation detected through surface and voxelwise methods for tapping of the ‘impaired’ hand in a single participant	71
Figure 14	Trained finger-to-thumb opposition sequences	93
Figure 15	Cortical thickness pipeline	98
Figure 16	Increase in performance of motor training tasks following training	100
Figure 17	Mean of participants’ normalised TMS responses, positive BOLD activation during the learned task, and positive t-value map contrasting BOLD for control sequence > trained sequence	102
Figure 18	Training-related differences in BOLD activation	103
Figure 19	Training-related changes in motor cortical excitability	104
Figure 20	Areas of increase in cortical thickness overlaid on the FSL MNI 152 template	106

Figure 21	Example of volbrain ROI placement on a single participant template and to a diffusion FA image.....	131
Figure 22	fMRI-tractography for a representative participant	133
Figure 23	Change in unadjusted FA in the right corticomotor tract, by bin	134
Figure 24	The Mitii system in action	144
Figure 25	Change in clinical scores and diffusion statistics of the corticospinal tracts in children with CP after 20 weeks	147
Figure 26	An illustration of the cortical thickness pipeline used to estimate the effect size for the power analysis	159
Figure 27	Example of cortical thickness, projected onto the pial surface; ROI-seeded diffusion tractography; and surface-fMRI seeded tractography in a participant with CP.....	163
Figure 28	Power analysis curves	166
Figure 29	Number of participants needed to scan in order to successfully analyse 25 participants	167
Supplementary Figure 1	Illustration of functional MRI motion artefact and/or supplementary activation rejection	83
Supplementary Figure 2	Region of interest for cortical thickness analysis.....	113
Supplementary Figure 3	Coronal and Axial views of final hard segmentations achieved for a single-subject template, as calculated by ANTs.....	115
Supplementary Figure 4	Longitudinal changes in functional MRI for control sequence execution.....	117
Supplementary Figure 5	Training-related changes in white matter.....	141
Supplementary Figure 6	Representative axial slices illustrating the brain pathology the five children with UCP, whose scans were used estimate of measurement variance.....	173
Supplementary Figure 7	Power analysis curves.....	174
Supplementary Figure 8	Power analysis curves: posterior parietal lobe and supplementary motor cortex	175

Abbreviations

AHA	Assisting Hand Assessment
AI	Asymmetry Index
ANOVA	Analysis of Variance
AMPS	Assessment of Motor and Process Skills
BOLD	Blood-Oxygen Level Dependent
COPM	Canadian Occupational Performance Measure
CP	Cerebral Palsy
dIPFC	Dorsolateral Prefrontal Cortex
dMRI	Diffusion Magnetic Resonance Imaging
FA	Fractional Anisotropy
fMRI	BOLD Functional Magnetic Resonance Imaging
FSL	FMRIB (Oxford Research Centre) Software Library
GM	Grey Matter
GMFCS	Gross Motor Function Classification System
HARDI	High Angular-Resolution Diffusion Weighted Imaging
JHFT	Jebsen-Taylor Hand Function Test
LTP	Long-Term Potentiation
M1	Primary Motor Cortex
mCIMT	Modified Constraint-Induced Movement Therapy
MD	Mean Diffusivity
MEG	Magnetoencephalography
MRI	Magnetic Resonance Imaging
MUUL	Melbourne Unilateral Upper Limb Assessment
PET	Positron Emission Tomography
PLIC	Posterior Limb of the Internal Capsule
RD	Radial Diffusivity
ROI	Region Of Interest
RMS	Root Mean Squared
S1	Primary Sensory Cortex
S1M1	Primary Sensorimotor Cortex
sMRI	Structural Magnetic Resonance Imaging
TBI	Traumatic Brain Injury
t-fMRI	Task-Based Functional Magnetic Resonance Imaging

TMS	Transcranial Magnetic Stimulation
UCP	Unilateral Cerebral Palsy
VBA/VBM	Voxel Based Analysis/Morphology
WM	White Matter

Chapter 1

Thesis Aims and Structure

Neurorehabilitative strategies are presently hampered by a lack of understanding of the relationship between motor learning and neuroplasticity. This lack of understanding is, in large part, due to a lack of longitudinal studies investigating these processes in humans. In turn, this lack of studies is predominantly a reflection of the difficulties in measuring such change. There are several sources of such difficulty. *Firstly*, most standard tools fail outright when trying to process MRI data from brains with substantial pathology. *Secondly*, the relationship between any detected signal changes (for example, change in BOLD fMRI patterns) and biological changes is not well documented, and the interpretability of standard approaches has not been discussed in depth for longitudinal scenarios. Similarly, what sort of approach is ‘ideal’ to achieve an interpretable result is not clear, and discussions of this type are absent from the present literature. This can mean that even studies reporting significant changes have limited impact on our ability to harness neuroplasticity. *Finally*, it is reasonable to expect that degrees of brain change are small when a person has practised a new task for a period of only a few weeks or months. By contrast, most structural measures that could be applied to measure brain change are relatively insensitive in their standard forms. Functional measures are often considered substantially more sensitive to brain differences or changes but, as mentioned previously, their reliability and interpretability have not been formally assessed. In either case, one can reasonably ascertain that very large study enrolments would be required to reliably measure brain changes in response to learning or rehabilitation. With these points in mind, the current thesis has the following aims and structure:

First, to critically review the potential for functional MRI, when used alone, to measure brain changes in a rehabilitative context. Functional MRI is focused upon because it is perhaps the most commonly used technique for investigating brain changes. This aim is addressed in Chapter 3, which was published in the peer-reviewed journal *Neuroplasticity*. From this exploration, it was concluded that a multimodal imaging approach was the best means of reliably measuring brain change in humans.

Second, to address the need for algorithms that can reliably detect subtle structural brain changes and that perform well in the presence of pathology. This aim is addressed in Chapter 4, through description of a diffusion-MRI analysis pipeline which utilises information from functional MRI in order to measure characteristics of white matter microstructure in specific sensorimotor

pathways. This method is robust to pathology. This work was published in the peer-reviewed journal *Plos One*. It was also published in abstract form and presented in Toronto at the 23rd annual meeting of the International Society of Magnetic Resonance in Medicine.

Third, to combine the aforementioned principles and methods in order to measure a variety of brain changes in healthy adults learning a novel motor task, then to interpret such information together in a way that may improve our understanding of neuroplasticity at a biological level. This aim is addressed in Chapter 5 and Chapter 6. These chapters have been submitted as two papers to the journal *Human Brain Mapping*, and are currently undergoing peer review. The majority of results from the second of these papers have been published in abstract form and presented in Singapore at the 24th annual meeting of the International Society of Magnetic Resonance in Medicine.

Last, to utilise the information above to perform a power analysis that can be used to plan neuro-rehabilitative studies in children with cerebral palsy. A goal of this power analysis is to make a number of recommendations for future study designs to (A) minimise resource wastage and (B) ensure adequate enrolment numbers, such that studies can reasonably expect to be able to ascertain the efficacy of their chosen treatment strategy with regards to inducing measurable brain changes. This analysis appears in Chapter 8, which has been submitted to the *Journal of Developmental Neuroscience* and is currently undergoing peer review. An abstract form of these results is currently undergoing peer review for presentation in Hawaii at the 25th annual meeting of the International Society of Magnetic Resonance in Medicine.

This thesis is presented as a series of papers that have been published, or are currently undergoing peer review, in international peer-reviewed journals. Chapter 7 presents unpublished work. I am the first, or joint-first, author of all presented manuscripts. My contributions, as well as the contributions of my co-authors are listed in the preliminary pages of this thesis. All works are included in this thesis with permission from the publishing journals or other copyright holders.

Chapter 2

Rehabilitation and neuroplasticity in children with unilateral cerebral palsy

This chapter consists of the paper *Rehabilitation and neuroplasticity in children with unilateral cerebral palsy*, published in *Nature Reviews Neurology*. This paper introduces the neurobiology of unilateral cerebral palsy, current rehabilitative therapies, and current knowledge regarding intervention-induced neuroplasticity. It also discusses how better knowledge of rehabilitation-induced neuroplasticity may shape future therapies and the imaging modalities that are available to perform such measurements.

This work acts as an introduction to this thesis that provides a relatively broad overview of the current state of knowledge regarding CP, the future work needed, the basics of the imaging modalities available, and how imaging can advance our knowledge regarding neuroplasticity.

As first author of this paper, I planned the structure of this paper, performed the majority of writing, and conducted the literature searches required for its construction. Professor Roslyn Boyd contributed writing for the initial draft for the section *Existing rehabilitative strategies*. All three authors reviewed and edited the paper.

Publication Information

Reid LB, Rose SE, Boyd RN. Rehabilitation and neuroplasticity in children with unilateral cerebral palsy. *Nat Rev Neurol*. 2015;11(7):390–400.

DOI: 10.1038/nrneurol.2015.97

Published online 16 June 2015

Minor changes have been made in response to examiner feedback.

Abstract

Cerebral palsy is a lifelong neurological disorder that primarily impairs motor function. Onset occurs during childhood. Unilateral cerebral palsy (UCP), which impairs use of one hand and impairs bimanual co-ordination, is the most common form of the condition. The main contemporary upper limb rehabilitation strategies for UCP are constraint-induced movement therapy and bimanual intensive therapy. In this Review, we outline the factors key to the success of motor rehabilitation in children with UCP, including the dose of training, the relevance of training to daily life, the suitability of training to the age and goals of the child, and the ability of the child to maintain close attention to the tasks. Emerging evidence suggests that the first 2 years of life are a critical period during which interventions for UCP could be more effective than in later life. Abnormal brain organization in UCP and the way in which development affects rehabilitation must be understood to develop new effective interventions. Therefore, we also consider neuroimaging methods that can provide insight into the neurobiology of UCP and how it responds to existing therapies. We discuss how these methods could shape future rehabilitative strategies that are based on the neurobiology of UCP and the therapy-induced changes seen in the brain.

Key points

- Activity-based therapy is the major clinical rehabilitation strategy for children with unilateral cerebral palsy
- Therapies can be considered effective if they bring about improvements that transfer to daily activities and help children to meet their individual needs and goals
- Current research suggests that motor impairments in children with unilateral cerebral palsy result from damage to the corticospinal tract as well as impairments of sensorimotor pathways and motor planning
- A variety of tools and imaging modalities are available that will enable the measurement of neuroplasticity in future clinical trials
- Future therapies for unilateral cerebral palsy are likely to be multimodal and derived from research into the neurobiology of the condition

Review criteria

Searches of the authors' personal collections of literature, the PubMed database, Google, and Google Scholar were reviewed for influential and original publications that were relevant to the discussion. Search terms used were "cerebral palsy", "hemiplegia", "stroke", "rehabilitation", "CIMT", "BIM", "robot therapy", "robot assisted", "MRI", "fMRI", "EEG", "TMS", "PET", "MEG", "neuroplasticity", "reorganization", or "tDCS". References from these articles were inspected for additional material.

Introduction

Cerebral palsy encompasses a heterogeneous group of neurodevelopmental conditions that primarily present as disorders of movement and posture, often accompanied by epilepsy, secondary musculoskeletal problems, and impaired sensation and cognition.¹ Symptom onset occurs during early childhood, typically before 18 months of age;¹ on average, diagnosis is confirmed at 13–19 months of age.^{2–4} The most common form of the condition is unilateral cerebral palsy (UCP), which impairs the use of one hand, as well as bimanual co-ordination. Cerebral palsy, by definition, results from abnormal brain development and/or brain damage that is non-progressive and occurs during very early development. In most cases, the cause is periventricular white matter damage that is presumed to occur during the third trimester of pregnancy, but other abnormalities, such as diffuse grey matter injury, focal infarcts, lesions of the basal ganglia, and/or cerebral malformations, can underlie the condition.^{5–7} Early brain injury in cerebral palsy can lead to atypical brain development and reorganization, particularly during the first 2 years of life,⁸ which can complicate the understanding of the condition and the selection of appropriate rehabilitation.

The current definition of cerebral palsy includes the word permanent, but notes that the physical symptoms of the condition are “not unchanging”: the initial disruption to normal brain structure and function “may be associated with changing or additional manifestations over time”.¹ In children with UCP, the type and extent of impairment is primarily determined by the location and size of the brain lesion.⁹ The ability of patients to gain functionality with therapy might be influenced by comorbidities such as impaired vision, impaired concentration, learning difficulties, and epilepsy.¹⁰

We commence this Review by summarizing current evidence for the efficacy of existing rehabilitation therapies for children with UCP and discussing factors that can increase effectiveness, such as the mode, dose, context, motivation, relevance, and timing of intervention. We then discuss how future therapies for children with UCP could be informed by research into the neuroplasticity of the condition. We present imaging technologies that should be used in future studies to examine neuroplasticity, and the current knowledge that could direct future research that will ultimately shape the future of rehabilitation for children with this lifelong condition.

The appropriate rehabilitation for children with cerebral palsy depends greatly on the motor subtype of cerebral palsy, the type and extent of brain damage or abnormalities, and other factors, such as age and cognitive ability. Current knowledge is primarily limited to children with UCP, so in this paper, we concentrate on rehabilitation that targets the principal symptoms of this condition: sensorimotor deficits. In particular, the focus is on upper-limb rehabilitation.

Existing rehabilitative strategies

Rehabilitation for children with UCP should be evidence-based, activity-based (that is, the child performs the activity themselves), relevant to the environment and the child's motivation, and goal-directed. The therapy should be delivered by the parents as a series of challenging but achievable activities, conducted in the appropriate environment and context, and designed according to what the child will learn. The two most heavily investigated contemporary approaches to upper-limb therapy in children with UCP are modified constraint-induced movement therapy (mCIMT) and bimanual intensive therapy (BIM; Box 1). Hybrid CIMT, in which the child trains with mCIMT prior to BIM, is another approach.¹¹

mCIMT and BIM are increasingly being delivered to individuals and groups in real-life situations to provide context to motor skill learning.¹² However, such therapy requires expertise, can be costly, and is not always accessible. For these reasons, the usual upper-limb therapy for children with UCP includes occupational therapy in conjunction with adjunctive treatments, such as medications to reduce spasticity, that target secondary symptoms. Although occupational therapy can include mCIMT or BIM, the time allotted for these therapies is typically only a small fraction of what is carried out in clinical trials. In response to this multifactorial challenge, alternative modes of delivery, such as web-based training and virtual reality platforms, have been developed. Early studies of web-based multimodal training have shown that these approaches can improve motor and motor planning skills in children with UCP.¹³⁻¹⁵ Pilot trials¹⁶⁻¹⁸ and larger studies^{19,20} of robot-assisted virtual reality therapy (Box 1) have also provided preliminary evidence that highlights the potential of such therapy for rehabilitation in children with UCP.

The efficacy of currently used activity-based therapies, as determined by large systematic reviews and meta-analyses, can be used to gauge the appropriate dose, environmental context and intensity of optimal upper-limb intervention for children with UCP.^{12,21} A meta-analysis of 42 randomized controlled trials that assessed the efficacy of 14 approaches to upper-limb therapy concluded that moderate to strong evidence supports the use of intensive activity-based, goal-directed interventions (such as mCIMT and BIM) rather than usual care to improve the quality and efficiency of upper-limb movement and to achieve individual goals.¹² The conclusions drawn in this systematic review, in combination with knowledge of the factors that are barriers to or enablers of implementation of therapy, have led to the current consensus on the essential elements of effective upper-limb therapy. These elements are intensive structured task repetition, progressive incremental increases in difficulty, and goal-directed approaches that enhance the motivation and engagement of individuals receiving therapy.²²

Box 1 | Contemporary rehabilitative therapies for unilateral cerebral palsy

Constraint-induced movement therapy (CIMT) and bimanual intensive therapy (BIM) are the two contemporary primary upper-limb motor rehabilitative schemes increasingly used for children with unilateral cerebral palsy (UCP).

CIMT was originally designed to address ‘learned disuse’ of the impaired hand after stroke in adults, but has since been adapted to aid the development of motor skill in the impaired hand of children with UCP.²⁵ A child-friendly protocol, called modified CIMT, involves constraint of the more-functional upper limb for several hours per day over several days. During this period, the impaired arm is trained in an intensive and repetitive manner in activity-based practice.²⁶

Patients undergoing BIM intensively practice bimanual tasks that become progressively more difficult. This therapy is based on the premise that co-ordination of both hands is important to the improvement of performance in everyday tasks, as these tasks are predominantly bimanual in nature. BIM focuses on tasks that require use of both hands; as the unimpaired hand acts as a template for learning motor control of the impaired hand.^{290,291}

Robot-assisted therapy is an emerging modality for rehabilitation that uses robotics to aid and/or objectively record movement of limbs during repetitive exercises. Robot-assisted therapies can allow participants with moderate impairment to experience a wider range of motion (and thus sensory feedback) than other therapies, and can be linked to virtual reality environments that provide haptic feedback. The technique is in the very early experimental phase and is primarily used in adults after stroke; its potential for therapy in UCP is currently unclear.²⁹²

Current activity-based therapies are thought to provide both specific (unimanual or bimanual) and global (occupational performance) improvements in motor function. For example, when mCIMT and BIM were delivered in a block of 60 h over 10 days in the INCITE randomized comparison trial ($n = 64$), mCIMT was more effective than BIM at increasing the use of the impaired limb, but intensive BIM was more effective than mCIMT at improving bimanual co-ordination.²¹

This observation confirms that these training techniques have specific effects. Motor-evoked potential recruitment curves, which were measured with transcranial magnetic stimulation (TMS), were also changed more substantially by intensive group-based mCIMT than by BIM (Boyd *et al.* unpublished data). Several barriers to implementation of intensive group-based therapy have been identified, including the cost and perceived barriers to implementation.²²

Another randomized trial has made a direct comparison between intensive group-based hybrid CIMT over 2 weeks and a comparable amount of individual therapy distributed over 12 weeks.¹¹ Improvements in bimanual co-ordination (evaluated with the Assisting Hand Assessment) and occupational performance (assessed with the Canadian Occupational Performance Measure) in the two groups were similar. These results show that, with a constant total dose of activity-based therapy, similar results can be achieved despite variations in child:therapist ratios (1:2 or 1:1) and the delivery of therapy (groups or individuals).²³ The similar outcomes attained with the use of intensive group-based therapy and individual therapy means that therapists can choose to deliver upper-limb therapy in the way that is best-suited to family circumstances and characteristics of the child. In this trial, the willingness of children to independently persevere, solve problems, master challenging tasks, and use their impaired hand for bilateral activities contributed to occupational performance outcomes.²⁴ Family ecology and the therapeutic context were also identified as critical factors that influenced children's mastery motivation and engagement in therapy.²⁴

Although long-term retention of the functionality gained from upper-limb therapies is not frequently assessed, some evidence suggests that gains in functionality can last for at least 6–12 months after therapy in children with UCP.^{25–27}

The majority of research into the effectiveness of rehabilitation and the mechanisms that underlie responses to therapy has been conducted with school-aged children with UCP, but major brain growth and development occurs in the first 2 years of life. This period could represent a critical window during which rehabilitation might be most effective, but which is missed by modern rehabilitative approaches.²⁸ Empirical evidence for the effectiveness of currently used therapies in infants with UCP is limited, but evidence from animal studies indicates that a critical period might exist.^{29–31} For example, in kittens, inactivation of the primary motor cortex in one hemisphere during post-natal weeks 5–7 results in seemingly permanent impairment of contralateral motor skill, and a variety of abnormalities in neural organization.³¹ Motor training and limb restriction that is similar to CIMT can reverse these motor deficits when carried out during early development at 8–13 weeks of age, but is much less effective when carried out at 20–24 weeks of age.³¹ Such critical periods of development might primarily reflect time windows during which abnormal neural organization can be prevented, rather than periods during which the brain is simply more able to repair existing damage.³² One pilot study ($n = 5$) of lower-limb rehabilitation has indicated that intense rehabilitation is feasible and effective in children with UCP aged <2 years, and a follow-up clinical trial is in progress.²⁸ Whether this approach is equally feasible and efficacious in upper-limb rehabilitation is currently under investigation.^{33,34}

Neuroplasticity-informed rehabilitation

Behavioural and outcomes data have improved intervention strategies for children with UCP by providing insight into how learning and skill development are influenced by factors such as the dose and intensity of therapy, as well as its relevance to daily life. Although intervention strategies such as mCIMT and bimanual training have been derived from and improved by these data, strategies and improvements based on a mechanistic understanding of the brain remain largely unexplored in children with UCP. Exploitation of this opportunity for the development of rehabilitation strategies requires an improved understanding of the neurobiology of UCP and the neuroplastic potential possessed by children with this condition.

Two complementary arms of research are likely to inform and shape future rehabilitation strategies for people with UCP. One is the investigation into patterns of atypical brain development. The abnormal brain structures seen in children with cerebral palsy reflect more than focal damage to a single system: early focal brain damage probably influences the development of related systems *in utero*, influences and modifies critical developmental periods, and has further effects in later life owing to adaptive and impaired behaviours.^{31,32,35,36} The other research arm is the characterization of therapy-induced neuroplasticity that aims to determine how and when brain networks respond to therapy. In combination, these research arms might not only identify networks that are commonly impaired or maladapted in UCP, but also determine how different initial insults lead to differences in the ability of the brain to respond to rehabilitation. For example, future research might reveal that the limited effectiveness of movement-based rehabilitation in some children with UCP is explained by indirect factors, such as attentional deficits or disrupted network dynamics that prevent neuroplastic changes.^{37–39}

With these points in mind, one could reasonably surmise that translational neuroscience might suggest not only treatments that improve existing skills, but also pretraining regimens that aim to improve the learning capacity of children and/or to ‘reset’ maladaptive brain states, in the same way that mCIMT aims to ‘reset’ the learned disuse of the impaired hand. One example of such a pretraining regimen is the use of TMS to enhance the effects of CIMT, an approach that has been used in one small-scale randomized controlled trial.⁴⁰ In this trial, 19 children aged 8–17 years with UCP received mCIMT alongside either repetitive TMS or sham TMS. Improvements in bimanual coordination (evaluated with the Assisting Hand Assessment) were significantly greater in children who received therapy than in children who received sham therapy, although the researchers noted that the results could have been complicated by differing baseline scores between the treatment groups.

In other fields, brain mapping/neurostimulation studies have informed rehabilitation. For example, the use of TMS has revealed that maladaptive neuroplasticity, seen as increased contralesional sensorimotor activity, can undermine recovery from stroke in adults.⁴¹ Trials in which transcranial direct current stimulation (tDCS) has been used to restore the interhemispheric balance of activation in the sensorimotor system and thereby improve clinical upper-limb motor scores^{42–45} and acquisition of motor skills⁴⁶ have had some success. These findings have led to an investigation in which children with spastic diplegia underwent treadmill training and concurrent anodal tDCS over the primary motor cortex contralateral to the dominant side of the body.⁴⁷ Some improvements in gait variables and functional mobility were reported and maintained for at least one month.⁴⁷

Another similar approach is paired associative stimulation, in which peripheral sensory stimulation is paired with TMS of the motor cortex; this approach is thought to induce long-term potentiation in sensorimotor networks.⁴⁸ This method has been shown to induce changes in motor-evoked potentials in healthy adults at 60 minutes after stimulation⁴⁸ and in healthy children 75 minutes after stimulation.⁴⁹ After a single session of stimulation, these potentials returned to baseline after 24 h in adults.⁴⁸ The fact that this method was well tolerated in healthy children suggests that it could be suitable for children with UCP.

Measuring neuroplasticity

Although the atypical patterns of brain organization and the potential neuroplasticity in people with UCP are not yet well understood, several findings hint at specific targets for future therapies.

Measurement of brain organization and therapy-driven neuroplasticity can be beneficial in clinical trials beyond contributing to an understanding of how and for whom rehabilitation is effective. The measurement of baseline brain organization might enable selection of a more homogeneous cohort of participants, or better matching of participant pairs prior to randomization. This approach can minimize between-group differences at baseline, thereby boosting statistical power, improving interpretability and increasing clinical significance. Furthermore, the demonstration of neuroplastic changes in response to therapy provides confidence that clinically important changes in functional outcomes are an index of neurological improvement rather than a reflection of changes in task strategy between tests.

Methods for the measurement of neuroplasticity and brain organization that currently show promise are discussed below, together with some of the key insights these methods have provided into neuroplasticity in children with UCP. Table 1 and Table 2 summarize these methods and findings.

Modality	Common measures	Spatial and/or temporal resolution*	Advantages	Disadvantages
TMS	Nerve conductivity, functional organization	~1 cm, ~1 ms	Direct objective measure, sensitive to neuroplastic change ⁵⁰	Can induce headaches in some children
dMRI	Tissue microstructure, structural connectivity	2–3mm	Simple biological interpretation, correlates well with clinical scores ⁵¹	Large lesions can preclude automated analyses
EEG	Neuronal signalling	≥1 cm, <1 ms	Can distinguish between different stages of sensorimotor processing	Complex to interpret; Sensitive to motion artefacts
MEG	Neuronal signalling	<1 cm, <1 ms	As EEG, but often provides higher spatial resolution	Similar to EEG; Scanning facilities are rare due to high costs
sMRI	Cortical thickness, grey matter volume	1 mm	Simple biological interpretation, moderately sensitive to neuroplastic change ^{52,53}	Large lesions can preclude automated analyses
BOLD fMRI	Functional organization of the brain	3–12 mm, 2–4 s	Simple to analyse data and visualize results with respect to brain structure	Sensitive to motion artefacts and haemodynamic abnormalities; lesions can prevent group analyses

*Table 1. Characteristics of noninvasive neuroimaging modalities used to measure neuroplasticity. *Stated resolutions are typical and do not reflect the theoretical limits. The spatial resolutions of TMS, EEG, MEG, and fMRI are strongly dependent on the methods of data acquisition and analysis. Abbreviations: dMRI, diffusion MRI; BOLD fMRI, blood oxygen-level dependent functional MRI; MEG, magnetoencephalography; sMRI, structural MRI; TMS, transcranial magnetic stimulation.*

Study	Age range (years)*	Condition (n)*	Design	Comparison group	Imaging	Primary finding
Holmefur <i>et al.</i> ⁹	1.5 – 5	UCP (32), GMFCS I–III [§]	Longitudinal	None	sMRI or CT	Hand function at age 8 years was crudely predicted by lesion characteristics
Staudt <i>et al.</i> ⁵⁴	16 – 25	Periventricular UCP (12, 4 with excellent motor outcomes)	Case-control	10 healthy adults	fMRI, TMS	fMRI activity was seen in ipsilateral or bilateral S1–M1 in individuals with UCP (n = 8), but not in controls. Corticospinal tracts ipsilateral to the impaired hand were seen only in those with larger lesions
Staudt <i>et al.</i> ⁵⁵	5 – 27	UCP (14)	Observational	None	dMRI, fMRI, TMS	Ipsilateral M1 corticospinal connections to the impaired hand were observed and associated with poorer diffusion metrics
Farmer <i>et al.</i> ⁵⁶	2-5	UCP with mirror movements (4)	Case-control	10 CTD	TMS	Ipsilateral M1 corticospinal connections to the impaired hand were seen in children with UCP, but not in controls
Guzzetta <i>et al.</i> ⁵⁷	10 - 28	UCP (12)	Observational	None	fMRI	Contralesional somatosensory representations were uncommon in UCP and poor at improving function
Rose <i>et al.</i> ^{51¶}	10.6 ± 3	Periventricular UCP (16)	Observational	None	dMRI, sMRI	Upper-limb function correlated inversely with corticothalamic tract connectivity asymmetry
Pannek <i>et al.</i> ^{58¶}	5 - 17	Periventricular UCP (50), GMFCS I–II [§]	Case-control	17 CTD	dMRI	Motor function was associated with the integrity and connectivity of many white matter tracts
Tsao <i>et al.</i> ^{59 ¶}	11.5 ± 3.1	Periventricular UCP (40), GMFCS I–II [§]	Case-control	15 CTD	dMRI	Upper-limb function correlated with asymmetries of the sensorimotor white matter tract microstructure
Hoon <i>et al.</i> ⁶⁰	1.3 - 13	Cerebral palsy (16, various subtypes)	Case-control	35 CTD	dMRI	Microstructural integrity of posterior thalamic radiations correlated with sensory and motor function
Staudt <i>et al.</i> ⁶¹	20 - 28	UCP (4)	Observational	None	dMRI, MEG, fMRI, TMS	Unilateral somatosensory organization, but bilateral motor activity was observed. Evidence for thalamocortical tract bypassing of lesion sites was observed.
Kurz <i>et al.</i> ⁶²	10–18	Spastic diplegia (9), UCP (4). GMFCS I–III [§]	Case-control	13 CTD	MEG	Event-related desynchronization of beta-waves suggested that the participants with cerebral palsy had difficulty planning knee joint movements
Scheck <i>et al.</i> ^{63¶}	5–17	UCP (70), GMFCS I–II [§]	Case-control	19 CTD	sMRI	Lower grey matter volumes in patients with UCP were observed, particularly in subcortical regions compared to CTD
Sterling <i>et al.</i> ⁶⁴	2–7	UCP (10)	Intervention	mCIMT	sMRI	Therapy increased grey matter volumes in the sensorimotor cortex that was associated with the greatest impairment
Golomb <i>et al.</i> ⁶⁵	13–15	Severe UCP (3)	Intervention	Virtual reality therapy	fMRI	Activation cluster volumes were larger after virtual reality therapy than at baseline
Sutcliffe <i>et al.</i> ⁶⁶	7–15	Cerebral palsy (4), GMFCS I [§]	Intervention	mCIMT	fMRI	Laterality of cortical activation in response to a motor task changed in two children, even though one child did not improve clinically
Cope <i>et al.</i> ⁶⁷	7–14	UCP (7)	Intervention	mCIMT	fMRI	Mixed changes were detected by fMRI, despite improvements in upper-limb function in most children

Juenger <i>et al.</i> ⁶⁸	10–30	UCP (8)	Intervention	mCIMT	fMRI	S1–M1 activation was increased by intervention for sensory and motor tasks in ~50% of all participants, but motor performance differed
Juenger <i>et al.</i> ⁶⁹	10–30	UCP (16)	Intervention	mCIMT	fMRI, MEG, TMS	Brain changes in response to therapy differed in patients with ipsilateral corticospinal tracts innervating the impaired hand, compared with those in patients without such tracts

*Table 2. Key findings in neuroimaging studies of children with unilateral cerebral palsy. *Age range reflects age at enrolment of individuals with CP; errors given are standard deviations. ‡n reflects the number of participants with UCP included in the specified measures. § The GMFCS enables individuals to be classified according to the motor severity of their condition. ||Participants of the indicated studies overlapped. ¶Participants of the indicated studies overlapped. Abbreviations: CTD, children with typical development; dMRI, diffusion MRI; GMFCS, Gross Motor Function Classification System; mCIMT, modified constraint-induced movement therapy; MEG, magnetoencephalography; S1, primary sensory cortex; M1, primary motor cortex; sMRI, structural MRI; UCP, unilateral cerebral palsy.*

TMS and atypical brain organization

TMS is a noninvasive method that depolarizes neurons with strong, brief magnetic pulses. When applied over the primary motor cortex, TMS can induce measurable electromyographic responses via the corticospinal tract.⁷⁰ This method is widely considered to be the gold standard noninvasive technique for mapping the corticospinal pathways, as it provides a direct measure of functional connectivity between the primary sensorimotor cortex (S1–M1) and muscle activation.⁷¹ For the measurement of neuroplasticity in the context of rehabilitation, several additional metrics can be obtained before and after rehabilitation, including motor thresholds, motor-evoked potential (MEP) recruitment curves, and trans-callosal inhibition.^{70,72–74} The motor threshold is the lowest level of stimulus intensity that produces a reliable MEP in ~50% of 10-20 consecutive stimuli.⁷⁰ MEP recruitment curves characterize the amplitude of MEPs across a range of stimulus intensities, relative to the maximum amplitude of compound muscle action potentials obtained with supramaximal stimulation of the median nerve at the wrist.⁷⁵

TMS provides data with high temporal resolution, but poor spatial resolution.⁷³ The procedure can induce headaches in children, and its use is restricted by some researchers owing to concerns that it might induce seizures in people with epilepsy (a condition commonly seen in children with CP⁷⁶), though reports of seizures are rare.⁷⁴ Furthermore, cortical mapping by TMS can be challenging and the procedure can be uncomfortable for some recipients. The acceptability of using repetitive TMS in children needs to be considered alongside the benefits when planning such treatment.⁷⁷

One striking finding with respect to brain organization in UCP was made by using TMS: in approximately one third of children with the condition, the impaired hand is directly controlled by the ipsilateral hemisphere.^{54–57} This brain organization is particularly common among patients who exhibit mirror movements.^{55,56} During the first ~18 months of typical post-natal development, interhemispheric competition reduces the number of ipsilateral corticomotor connections.⁸ In children with early brain lesions, such as those with UCP, damage to the contralateral corticomotor connections is proposed to prevent this interhemispheric competition, or alter its balance, leaving ipsilateral connections intact (Figure 1).³² Such atypical development is not necessarily mirrored in the somatosensory system though: TMS has been used to show that the somatosensory system is often still contralaterally organized in such children (Figure 1).⁵⁷ Children with ipsilateral motor control of their impaired hand typically have poorer motor control than do children with contralateral motor control. A major cause of motor dysfunction in UCP could, therefore, be impaired transmission of sensory feedback from the impaired hand to the motor cortex that controls that hand.⁵⁷ In addition to

visual hemianopias, such impaired sensorimotor function and mirror movements probably account for much of the poor bimanual co-ordination exhibited by children with UCP.

Diffusion MRI and thalamocortical pathways

Diffusion MRI measures the directional diffusion of water molecules, which enables inferences to be made about the structural characteristics of brain tissue.⁷⁸ Diffusion MRI images can be used for tractography, which elucidates white matter pathways and structural connectivity between brain regions (Figure 2). Diffusion MRI can also provide measures that reveal information about the microstructural integrity and density within these white matter pathways. These measures include the tensor metrics of mean diffusivity, fractional anisotropy and radial diffusivity, as well as measures, such as apparent fibre density, that rely on more-modern higher-order mathematical models of tissue structure.⁷⁹

Few studies to date have used diffusion measures to longitudinally assess neuroplasticity in children with UCP. Diffusion MRI has, however, demonstrated that the microstructural integrity of white matter in the corticospinal tract is lower in children with UCP than in children with typical development,^{58,59} and correlates with performance on a variety of clinical assessments.^{51,58,59} Tensor measures of white matter microstructural integrity also seem to change in response to motor training in healthy adults.⁸⁰

In line with evidence from studies that used TMS and suggested that disrupted sensorimotor integration is important in UCP, studies that used diffusion MRI have suggested that damage to the thalamocortical radiations and consequent impairment of sensory feedback might be a key factor that underlies impaired motor function in children with cerebral palsy.^{51,60,81} Diffusion MRI data also suggest that thalamocortical fibres can bypass periventricular injuries as they project to the cortex, explaining how somatosensory networks can develop connections to the contralateral (impaired) hand, even when white matter damage has already disrupted the equivalent corticomotor tract (Figure 1).⁶¹

EEG, MEG, and motor planning

EEG and magnetoencephalography (MEG) are noninvasive methods that measure electrical activity in the brain—primarily in the cortex—via electrodes on the scalp (EEG) or magnetometers above the scalp (MEG). Both methods can be used to elucidate the timing, amplitude and direction of signals from groups of neurons that respond to stimuli. Both methods provide a millisecond or sub-millisecond temporal resolution.^{82,83}

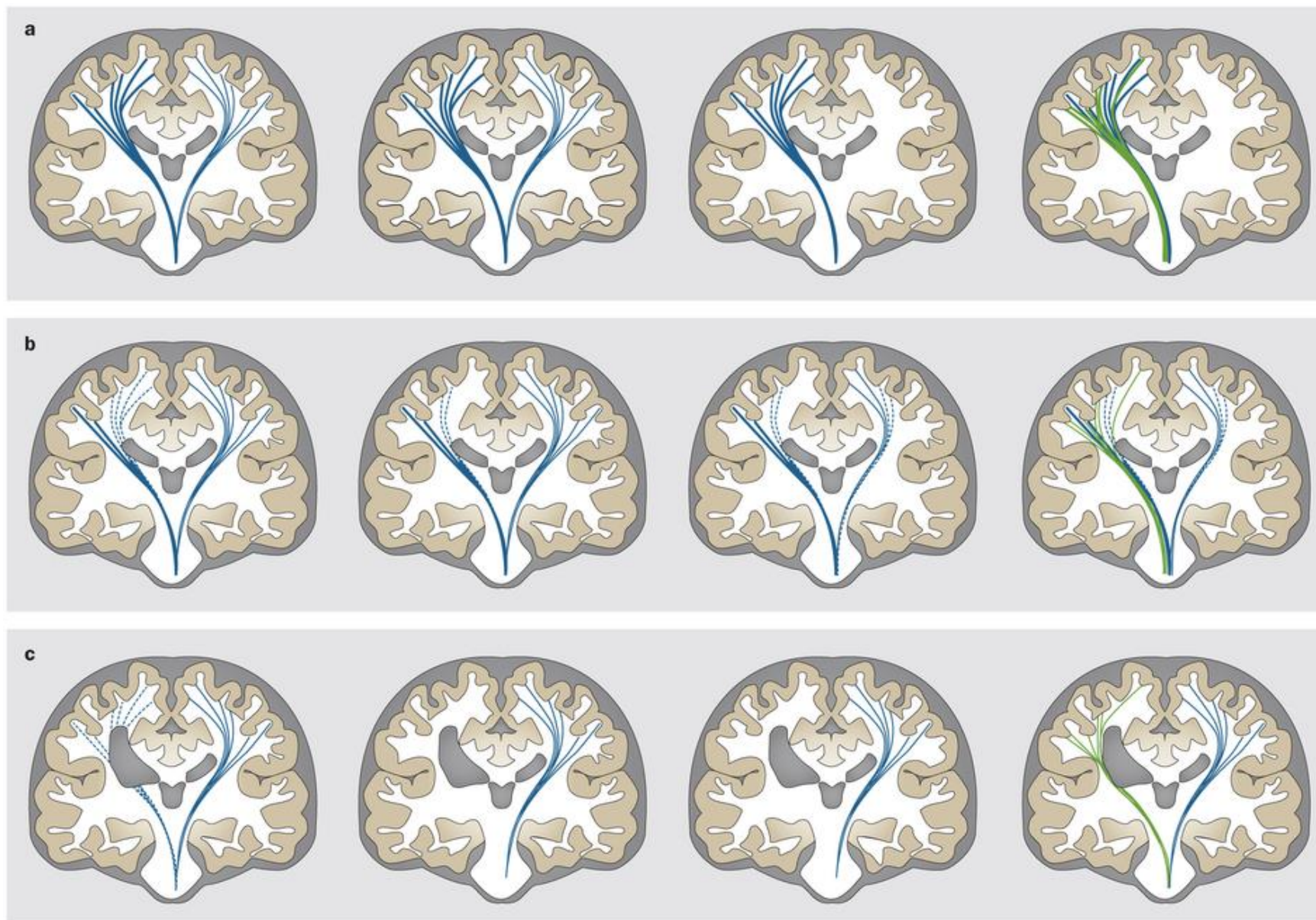


Figure 1. The influence of periventricular lesions on corticospinal laterality. The images show corticospinal (blue) and thalamocortical (green) connection pathways. a | In typical development, bilateral corticospinal connections develop and are unperturbed during early development. After birth, interhemispheric competition that is mediated by cross-callosal connections (not shown) results in the removal of connections that project to the ipsilateral side of the body. b | During early development in cerebral palsy with small periventricular lesions, the lesions can weaken or eliminate the corticospinal connections, which are consequently unable to compete effectively with the opposite side of the brain during later development. The result is bilateral motor cortex control of the impaired side of the body. c | During early development in cerebral palsy with focal or large lesions, the lesions might completely eliminate corticospinal connections in one hemisphere. The result is ipsilateral motor cortex control of the impaired side of the body. If the insult occurs prior to development of somatosensory connections, the primary somatosensory system can still develop on the ipsilesional side of the brain, causing a discrepancy between the laterality of sensory feedback and motor signalling

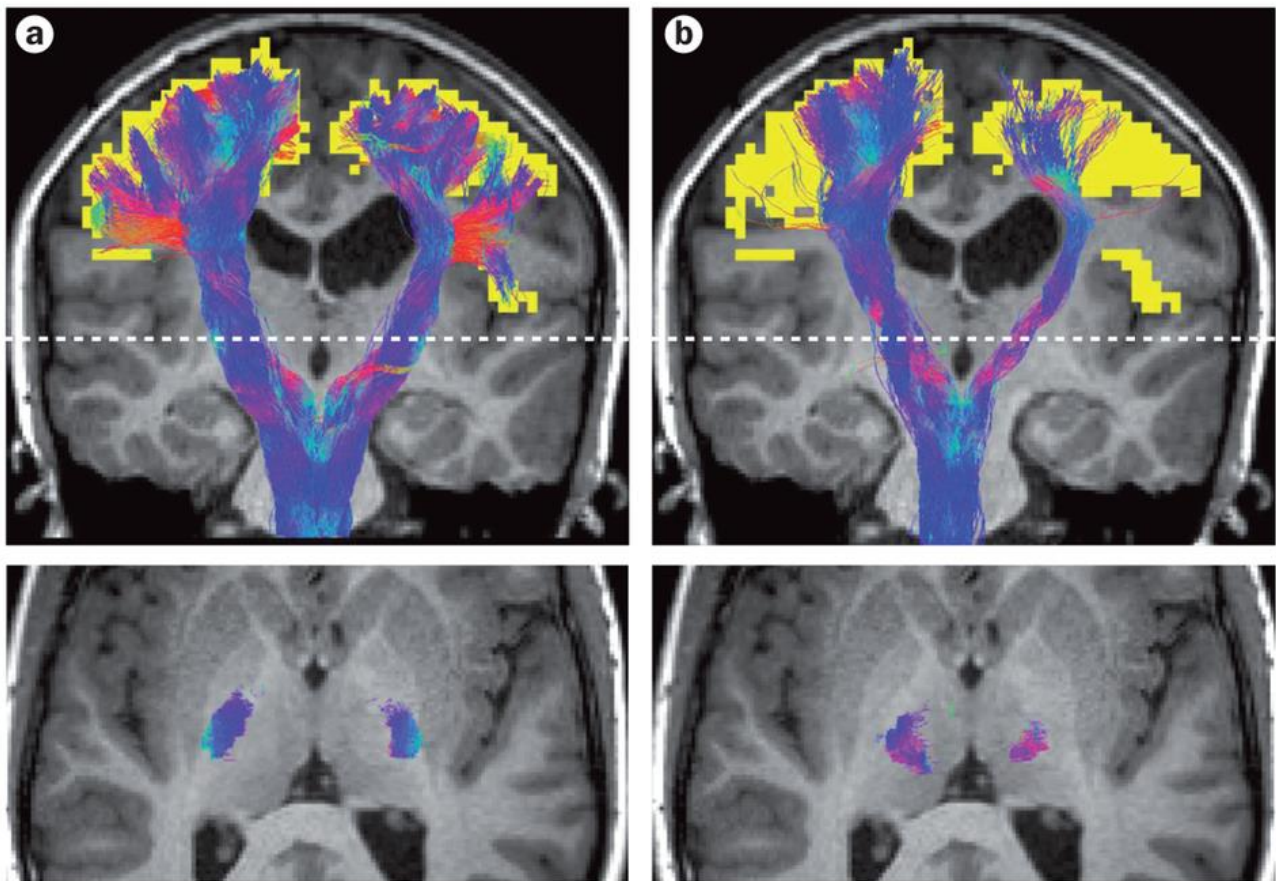


Figure 2. An example of functional-MRI-guided diffusion MRI tractography. This method provides information about the structural connectivity of functionally relevant brain regions, and eliminates the need to register brains to templates, which is often impossible when malformations or pathology are present. Here, a child with unilateral cerebral palsy performed hand-tapping tasks during a functional MRI session. Voxels that were significantly activated (yellow) were used as the seed (starting) region for diffusion tractography. Activated voxels from several slices are overlaid here for illustrative purposes. The bottom images are axial sections at the level of the dashed line in the top images. a | Corticospinal tracts. These were identified as tracts that passed from the seeding region through the posterior limb of the internal capsule, then to the brainstem inferior to the pons. b | Corticothalamic tracts. These were identified as tracts that passed from the seeding region through the thalamus, then to the brainstem inferior to the pons

Although the spatial resolution of MEG (often in the order of single millimetres) is often higher than that of EEG, MEG is only sensitive to signals that travel tangentially to the cortical surface.^{83,84}

One small-scale study that used MEG revealed locations in the brain at which tactile stimulation of the first, third and fifth digits initially evoked a response; these sites seemed to be further apart in children with spastic motor type cerebral palsy than in children with typical development.⁸⁵

Another study that used MEG reported abnormal beta-wave activity in children with spastic hemiparesis during the planning stage of a knee extension task.⁶² This finding suggested that motor planning, rather than muscular recruitment, might have been the limiting factor in the controlled execution of the motor task. If similar impairments are found to occur commonly in UCP, an increased therapeutic focus on motor planning and sensorimotor integration, rather than motor output, might accelerate or improve the effectiveness of rehabilitation in the population with this condition.

Studies that used EEG have also reported that infants with typical development exhibit different neural responses when observing goal-directed and non-goal-directed actions from as young as 6–8 months.^{86–89} Such responses of the mirror neuron system suggest that novel rehabilitation approaches that involve action observation might be possible in very young children.^{90,91}

Imaging of grey matter and cortical thickness

Intervention-induced grey matter changes can be investigated with whole-brain, region-of-interest or voxel-based morphometry approaches, the results of which complement diffusion MRI measures of white matter tissue integrity. These approaches require a high-resolution structural MRI scan that enables reliable delineation of the boundaries between white matter and grey matter, and identification of the pial surfaces. Increases in grey matter volume or thickness are particularly interesting in relation to neurorehabilitation, as they reflect improvements that are mediated by tissue ‘growth’, rather than by novel use of pre-existing neural substrates.

Studies have shown that motor training in healthy adults⁵² and CIMT in adults after stroke⁵³ increases the volume of cortical grey matter in brain regions that are functionally relevant to the training. Decreases in cortical thickness have also been shown in the first 3 months after traumatic brain injury in children, after which some areas ‘recover’ and others continue to thin.⁹² Another study showed that the cortical thickness of the right precentral gyrus inversely correlates with upper-limb motor function in children with congenital left-sided hemiplegia.⁹³ Encouragingly for the therapy of UCP, a pilot study of young children ($n = 10$, mean age 3 years and 3 months) found that the volume of grey matter in the sensorimotor cortex increased after 3 weeks of CIMT.⁶⁴

It is not known as to which cellular processes underlie these grey matter changes, but a combination of glial, vascular, dendritic, synaptic and axonal changes is probable.⁹⁴ Neurogenesis might also contribute, but its role is thought to be minor.^{94,95}

fMRI and potential neural recruitment

Functional MRI (fMRI) is used in neurorehabilitation either to identify cortical areas that are active under certain conditions (an approach known as task-based fMRI that is used for cortical mapping)

or to identify cortical areas that are likely to be functionally connected (an approach known as resting state fMRI). The most frequently used type of fMRI is blood oxygen-level dependent imaging, which relies on a detectable oversupply of oxygenated blood to localized areas during periods in which their neural activity is increased. Unlike TMS, fMRI offers whole-brain coverage in less than 10 minutes for each task. The final resolution of fMRI after processing is ~3–12 mm.⁹⁶ fMRI cannot, however, provide information on whether activity is excitatory or inhibitory, and its temporal resolution is inferior to that of TMS, EEG and MEG: each frame typically averages ~2–4 seconds of brain activity.

Measurement of neuroplasticity with fMRI ideally involves obtaining scans during a motor or cognitive task before and after intervention for at least 20 people per experimental group.⁹⁷ Groupwise analyses can then be used to identify voxels with significantly different activity between time points, and thereby determine whether the location or area of activation has changed substantially. Conventional voxel-based group comparisons can be ill-suited to the study of children with cerebral palsy, however, owing to the heterogeneous size and location of brain lesions seen within most cohorts. The effects of this issue can be reduced by performing region-of-interest analyses that measure the interhemispheric balance of activation between the sensorimotor cortices before and after therapy in the same child with UCP.⁹⁸ In any case, as fMRI is an indirect measure of neuroplasticity, all such analyses should ideally be supported with other evidence of changes, such as TMS measurements, and correlated with functional improvements in a motor task that is not performed in the scanner.

In practice, conducting an fMRI study with good statistical power is a challenge because it requires a homogeneous cohort of children with UCP who are able to perform tasks consistently in the noisy and constrained environment of the MRI scanner. In our experience, preparation with mock scanners and the presence of people who are familiar to the child during experimental scanning improves success. The use of cluster-based fMRI analyses to improve the sensitivity of comparisons between pre-therapy and post-therapy conditions should be avoided, as these analyses do not provide voxel counts that are genuinely quantitative of the ‘true’ activation volume.^{99,100}

Several small-scale studies have reported changes in children with UCP in response to therapy that were detected with fMRI. For example, in a pilot study of virtual reality therapy, cluster-based S1–M1 voxel counts were increased after therapy in three adolescents aged 13–15 years with UCP, whose Jebsen–Taylor hand function test scores also indicated meaningful improvements in speed and dexterity.⁶⁵ Another study found a change in the balance of activation between hemispheres in two of four children with UCP after they received CIMT.⁶⁶ One of these two children, however, showed no clinical improvement, rendering the practical significance of such fMRI changes unclear. A similar study that included seven children with UCP highlighted the difficulties involved in scanning this

population: the results were mixed, and the researchers noted that standard analyses were not feasible owing to movement artefacts in the fMRI scans.⁶⁷

Multimodal studies and CIMT

Multimodal neuroimaging offers unique opportunities to improve our understanding of neuroplasticity by combining complementary information. For example, such an approach could help to determine the dynamics of structure–function relationships (Figure 2). Three related studies of children with UCP have used a multimodal approach to investigate brain changes that occur in response to mCIMT.^{68,69,101} These reports, which used data from two studies with overlapping participants, used fMRI to assess how brain activation changed when a ball-squeezing task was performed with the impaired hand. After exclusion of scans that were influenced by confounding factors, the first of these studies found no activation changes in two participants, and increased bilateral activation of the hand knob of the sensorimotor cortices in one individual aged 16 years with UCP.⁶⁸ The second study combined data from five patients aged 10–20 years with UCP: group analysis of contralateral corticospinal connections showed an increase in cluster-based S1–M1 voxel counts after mCIMT.¹⁰¹ In the third study, an associated analysis showed bilateral activation of S1–M1 in adolescents with corticospinal projections ipsilateral to the impaired hand; the balance of this activation shifted towards the impaired hemisphere after training.⁶⁹ In the same study, CIMT increased TMS-evoked MEPs in the primary descending corticospinal connection to the impaired hand, but not to the unimpaired (constrained) hand, in children with UCP, regardless of whether the impaired hand was controlled by the contralateral or ipsilateral motor cortex. MEG data that was acquired at the same time also found that somatosensory-evoked magnetic fields increased marginally in both groups after mCIMT.⁶⁹ In combination, data from these three studies suggest that mCIMT reorganizes the sensorimotor system and/or promotes recruitment of additional grey matter and thereby enables more-effective processing of sensory inputs and conversion of these inputs into corticospinal signals.

Conclusions

Current rehabilitation for children with UCP focuses on single-mode activity-based therapies that are selected on the basis of behavioural observations. The effectiveness of these therapies relies on the intensity and timing of treatment, the way in which improvements transfer into the patients' daily lives, and on the child's ability to maintain close attention to the training task.

Ongoing research that has the aim of improving treatment outcomes is investigating therapy-induced neuroplasticity and the way in which brain injuries sustained during early life can result in large-scale atypical brain organization. The extent of these factors is currently unclear, and their clinical manifestations not well understood, although several findings suggest that the impairments observed in many children with UCP result from disrupted integration of sensorimotor information and motor planning. A wide variety of tools can be used in future clinical trials for the measurement of brain structure and function, including TMS, EEG, MEG and diffusion, structural and/or functional MRI. Approaches that combine complementary information from more than one of these tools are also likely to be beneficial. Studies that use these tools are likely to improve our understanding of the neurobiology of UCP and the neuroplastic processes that are promoted by effective rehabilitation. This greater understanding could ultimately transform rehabilitation for this condition.

Chapter 3

Interpreting Intervention Induced Neuroplasticity with fMRI: The Case for Multimodal Imaging Strategies

The previous chapter detailed a number of non-invasive methods by which neuroplasticity can be measured. Functional MRI is one of the most common tools researchers use to index brain changes in response to therapy or learning. Unfortunately, despite the collection of reasonable amounts of data, fMRI studies have been unable to reasonably improve our understanding of biological changes in response to intervention. Common interpretations for changes in functional MRI are also sometimes contradictory and its validity in the context of brain injury has not been rigorously assessed.

The present chapter consists of the paper *Interpreting Intervention Induced Neuroplasticity with fMRI: The Case for Multimodal Imaging Strategies*, which was published in *Neural Plasticity*. This paper critically analyses the validity of BOLD task-based functional MRI for the measurement of neuroplasticity in brain injured cohorts. This paper summarises many findings in this area, explores the issues which have inhibited interpretation of functional MRI data, and suggests a way forward.

This chapter addresses Aim 1 of this thesis: *to critically review the potential for functional MRI, when used alone, to measure brain changes in a rehabilitative context*. The overarching goal of the thesis was to provide means by which neuroplasticity can be measured, and to attempt to do so in a way that is biologically informative. Toward this ultimate goal, this chapter rules out the use of standalone fMRI for this purpose, concluding that the more promising strategy involves multimodal imaging.

As the first author of this paper, I performed all literature searches, planned the paper structure, evaluated issues discussed, formed the arguments, and wrote the paper. Professors Boyd, Cunnington, and Rose edited and critically reviewed the manuscript. Professor Rose and I conceptualised the paper in the broad sense.

Publication Information

Reid LB, Boyd RN, Cunnington R, Rose SE. Interpreting Intervention Induced Neuroplasticity with fMRI: The Case for Multimodal Imaging Strategies. *Neural Plast.* 2016;2016:1–13.

DOI: 10.1155/2016/2643491

Accepted for Publication on 27 September 2015

Minor changes have been made in response to examiner feedback.

Abstract

Direct measurement of recovery from brain injury is an important goal in neurorehabilitation, and requires reliable, objective, and interpretable measures of changes in brain function, referred to generally as “neuroplasticity.” One popular imaging modality for measuring neuroplasticity is task-based functional magnetic resonance imaging (t-fMRI). In the field of neurorehabilitation, however, assessing neuroplasticity using t-fMRI presents a significant challenge. This commentary reviews t-fMRI changes commonly reported in patients with cerebral palsy or acquired brain injuries, with a focus on studies of motor rehabilitation, and discusses complexities surrounding their interpretations. Specifically, we discuss the difficulties in interpreting t-fMRI changes in terms of their underlying causes, that is, differentiating whether they reflect genuine reorganisation, neurological restoration, compensation, use of preexisting redundancies, changes in strategy, or maladaptive processes. Furthermore, we discuss the impact of heterogeneous disease states and essential t-fMRI processing steps on the interpretability of activation patterns. To better understand therapy-induced neuroplastic changes, we suggest that researchers utilising t-fMRI consider concurrently acquiring information from an additional modality, to quantify, for example, haemodynamic differences or microstructural changes. We outline a variety of such supplementary measures for investigating brain reorganization and discuss situations in which they may prove beneficial to the interpretation of t-fMRI data.

Introduction

Broadly speaking, “neuroplasticity” refers to the phenomenon of neurons and neural networks modifying their connections and/or behaviour in response to new information, sensory stimulation, development, damage, or dysfunction. The ultimate goal of neurorehabilitation is to induce neural plasticity in a manner that restores the full original function and potential of the injured brain (“neurological restoration”), but a variety of other patterns of neural plasticity may also occur during recovery, including compensatory activity, use of redundant networks, or changes in behavioural or cognitive strategy. Direct measures of such changes are critical to understanding how and when recovery from brain injury takes place and ultimately may lead to improved or novel rehabilitative treatments. One very popular modality used to measure neuroplasticity is task-based functional MRI (t-fMRI). This technique infers from local changes in cerebral blood flow (CBF) and oxygenation to identify brain regions that are more “active” while subjects execute a task than during a comparison or resting state. For a more in-depth explanation of fMRI, readers are referred to Logothetis.¹⁰²

The accessibility and noninvasive nature of fMRI are important strengths. When used to measure neuroplasticity, however, t-fMRI suffers from a unique set of challenges that are not always fully acknowledged. With the accelerating development of neurorehabilitation strategies researchers need to be cognisant of the limitations of commonly used neuroimaging technologies, including t-fMRI, in order to collect information capable of advancing our understanding of the neurorehabilitative process. In particular, it is critical that researchers can correctly interpret what a change in t-fMRI signal reflects, if they are to understand the mechanisms of functional recovery.

To aid researchers in this regard, this review explores two important questions: “What are the challenges in interpreting changes in t-fMRI signal as intervention-induced neuroplasticity?” and “How can complementary information from other modalities aid such interpretations?” To contextualise our discussion, we define four basic criteria that we believe are essential for informative interpretation of any neuroimaging signal change in terms of brain changes. We propose that detected changes should (1) be moderately stable or evolve reliably, (2) be meaningfully distinguishable from day-to-day variation in brain activity, (3) offer biological insight into the recovery process, and (4) reliably relate to (or influence) clinical changes. These criteria are somewhat straightforward: to advance neurorehabilitative science, reported changes must be unambiguous, reliable, related to recovery, and clearly a direct or indirect effect of the intervention at hand.

With this in mind, we begin this review by outlining t-fMRI findings associated with intervention-induced neuroplasticity and discuss uncertainties surrounding their interpretations. We highlight that change in t-fMRI activation patterns can be difficult to extrapolate to brain

reorganisation and, in some cases, may be confounded by processing inherent to the technique. We follow this overview by offering supporting strategies, focussing on the supplementation of t-fMRI findings with information from other modalities, such as structural MRI or transcranial magnetic stimulation (TMS). Examples are provided as to how incorporating such information can improve interpretation of t-fMRI data, strengthening specific claims about intervention driven neuroplasticity.

Though some points made here may be generalised to other contexts, this commentary restricts discussion to studies targeting motor impairment and movement rehabilitation in patients with cerebral palsy (CP) or acquired brain injuries, such as traumatic brain injury (TBI). As relevant literature describing therapy-driven brain reorganisation is limited in patients with acquired brain injuries, we also make reference to neuroimaging studies based on adult stroke populations and some nonlongitudinal studies. It must be kept in mind that while subject groups may all undergo neuroplasticity in response to rehabilitation, they may do so from a vastly different baseline, particularly due to the impacts of brain injury on early development.¹⁰³ Further, for the sake of brevity, discussion here is restricted to standard GLM-analyses of t-fMRI, as this is the dominant technique in published literature; resting state fMRI and other forms of fMRI are not considered.

Common Findings

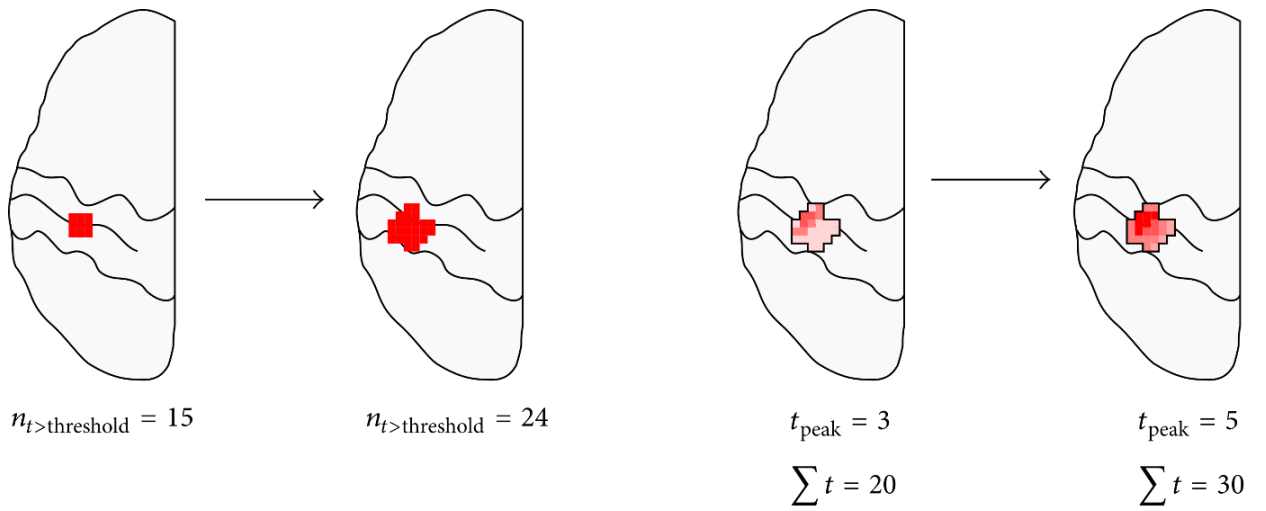
There are three primary findings that are commonly reported in t-fMRI studies of neurorehabilitation, summarised in Figure 3.

Intensity and Size Changes

Altered ipsilesional activated-voxel counts, or heightened peak intensities, are commonly reported for patients with brain injuries who have received treatment, improved function, or when compared with controls (Figure 3 (a), Figure 3 (b), and Figure 4 (a)).

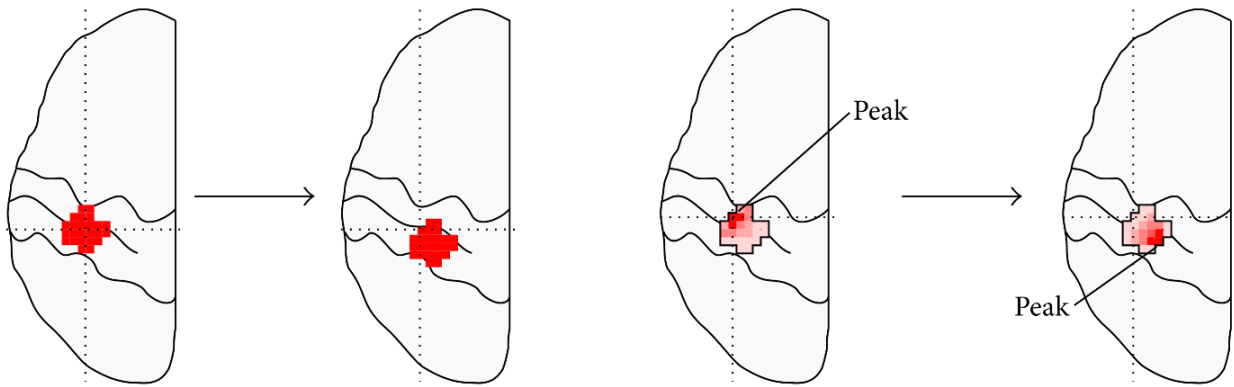
Heightened activation of motor regions has been reported for children with TBI¹⁰⁴ and adolescents with CP¹⁰⁵ when compared with controls. A recent systematic review reported seven longitudinal t-fMRI studies of treatment interventions for unilateral CP, drawn from four unique subject cohorts.¹⁰⁶ After therapy, area of activation of the (most) impaired hemisphere reportedly increased in a subset of subjects within each study.¹⁰⁶

In TBI, one study of seven adult subjects with primarily-nonchronic injury showed changes in the activation volumes of several sensorimotor-related regions in response to motor rehabilitation.¹⁰⁷ The location and relative changes in activation volumes varied greatly between subjects. Increased ipsilesional premotor activation has been shown in response to constraint-induced movement therapy,



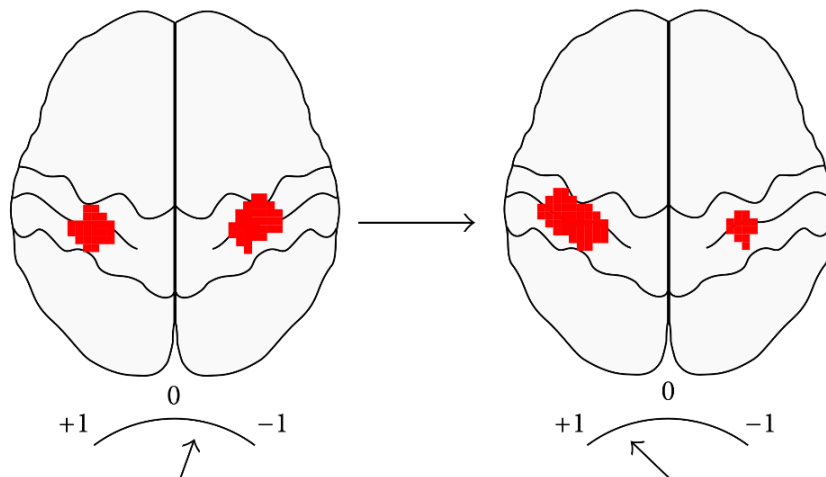
(a) Suprathreshold voxel count

(b) Peak t -value or sum of suprathreshold t -values



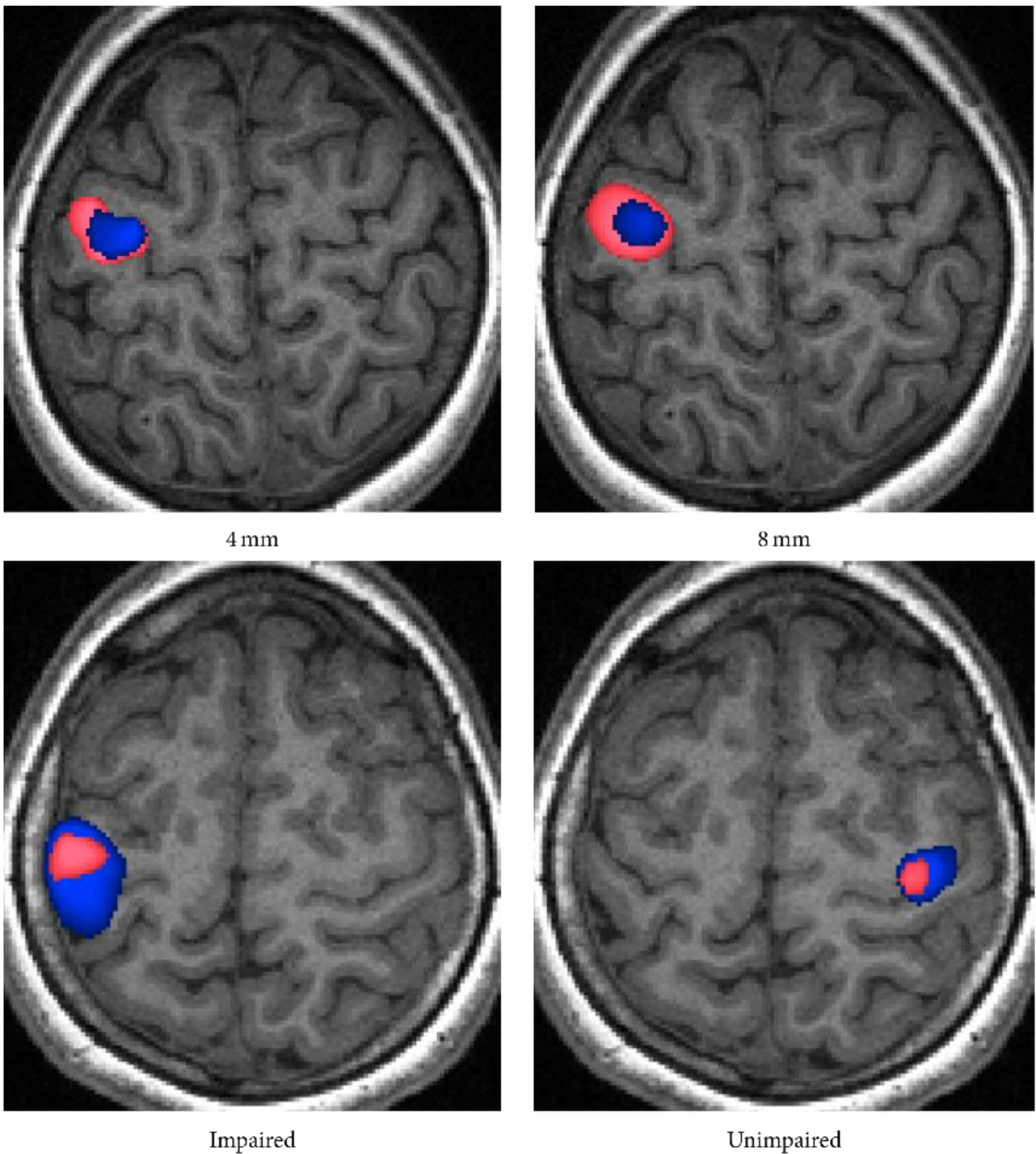
(c) Activation location

(d) Peak intensity location



(e) Laterality index

Figure 3. Commonly seen fMRI activation changes. Common fMRI activation pattern changes reported in the literature include suprathreshold voxel counts (a), peak t -values or sum of suprathreshold t -values (b), activation location (c), peak t -value location (d), and changes in laterality index (e). Some studies report changes over time, while others report differences between groups. The degrees of changes shown here are for illustrative reasons only.



■ Baseline
■ +25 weeks

Figure 4. Voxel-wise fMRI analyses of a block-design hand-tapping task recorded at baseline (blue) and after ~25 weeks (pink). (a) A subject with chronic traumatic brain injury who underwent virtual reality therapy during the 25-week period. In the affected hemisphere, the 25-week scan showed a 2.2 times or 3.3 times larger activation volume than the baseline scan, depending on whether a 4 mm (left) or 8 mm (right) smoothing kernel was used. The 4 mm and 8 mm processing options were associated with peak voxel shifts of 8.6 mm and 5 mm, respectively. (b) A subject with cerebral palsy demonstrating large changes in activation between scans, for tapping of the impaired (left image) and unimpaired (right image) hands. The subject underwent no treatment during the 25-week period but was less anxious and followed the auditory cue marginally more accurately during the follow-up scans.

alongside improvements in Fugl Meyer assessment scores, in a single adult with chronic traumatic damage to the primary sensorimotor cortex (S1M1).¹⁰⁸ Similarly, increased S1M1 activation has been found in two adult TBI subjects after robotic therapy.¹⁰⁹ Likewise, following adult stroke, regions of sensorimotor activation are reportedly larger in recovered patients than in partially recovered patients¹¹⁰ and can further enlarge with motor training.¹¹¹

Laterality Shifts

The second common t-fMRI finding in patients with brain injuries is a shift in the hemispheric-balance of activation (Figure 3 (e)). In normal subjects, basic motor tasks overwhelmingly activate the contralateral S1M1.¹¹² Both stroke and unilateral CP patients, however, regularly demonstrate robustly bilateral activation.^{105,113,114} These balances of activation are typically calculated as laterality index (LI):

$$LI = (\sum C - \sum I) / (\sum C + \sum I)$$

where $\sum C$ and $\sum I$ are supra-threshold voxel counts, or t-value sums (weighted LI, also referred to here as LI for simplicity), for the contralateral and ipsilateral hemispheres, respectively. LIs fall between -1 (only ipsilateral activation) and $+1$ (only contralateral activation).

In stroke, S1M1 LI values for the paretic hand are lowest in acute stroke, due to both decreased ipsilesional activity and increased contralesional activity.¹¹⁴ Over time, these values become more positive^{111,114} but do not typically return completely to “normal” values,¹¹⁵ even in well-recovered patients.^{110,116} In chronic stroke patients, LI values are often,^{117,118} but not always,¹¹⁹ reported to shift toward the lesioned hemisphere in response to rehabilitative therapy.

In children with unilateral CP, activation of ipsilateral sensorimotor regions can be evoked with active movements, passive movements, and tactile stimulation of the impaired limb,¹⁰⁵ the patterns of which depend on their type of reorganisation.^{55,69} Small-scale studies of children with unilateral CP suggest that virtual reality and constraint-induced movement therapies can alter the balance of activation toward the contralateral hemisphere.^{106,120} This may prove functionally beneficial: contralateral somatosensory activation during motor tasks appears to be associated with improved unimanual capacity.¹¹²

Numerous studies have proposed that laterality shifts demonstrate an adaptive bihemispheric reorganisation of motor networks.^{115,116,118,120,121} This is a key point that we will return to later.

Intrahemispheric Relocation of Activation

Differences in intrahemispheric location of S1M1 activation, between either time points or subject groups, are also frequently reported as evidence of neurological reorganisation (Figure 3 (c) and Figure 3 (d)). This metric is principally reported in adult stroke literature, where longitudinal dorsal “shifts” in peak activation have been described 4, 12,¹¹¹ and 24 months after stroke.¹²² Different loci of activation have been reported between stroke and control subjects numerous times.^{110,123} One study¹²⁴ has reported a correlation between peak S1M1 activity location and motor impairment.

The Challenge

It is clear that changes in t-fMRI measures have been reported in a variety of studies and pathologies. This section identifies several challenges that make the interpretation of such results in terms of neuroplasticity particularly difficult. These issues include subject variability, biological ambiguity, methodological considerations, and confounds introduced by disease states. As we shall discuss, these factors impede informative interpretation of the t-fMRI signal by obscuring two key facts: (1) whether neurological change has genuinely taken place and (2) if so, what type of change has been observed. Possible solutions to reduce the impact of these variables are summarised within the final section of this review. These incorporate the use of information from other modalities within the study design, providing complementary support for t-fMRI measured brain changes, to provide more robust evidence of neuroplasticity.

t-fMRI Results Are Variable

One of the greatest challenges for t-fMRI in studies of neurorehabilitation is the heterogeneity in findings, both within and between studies of patients with brain injury. Intrahemispheric “relocations” of activation, for example, are not always reported and have been variable even within studies, differing, for example, by patient subgroup¹¹⁰ or task performed.¹²² In addition, changes in activation patterns do not consistently correlate with behavioural improvements (Figure 4 (b)). Distinct changes in activation patterns have been reported in rehabilitative studies of adult stroke (postrehabilitation versus retention),¹¹¹ hemispherectomy (pre- versus postrehabilitation),¹²⁵ and paediatric CP (pre- versus postrehabilitation),⁶⁶ despite subjects demonstrating stable motor scores. In unilateral CP, the degree of S1M1 activation for active and passive movements may not correlate with motor scores,^{105,113} and results for sensory impairment are mixed.^{57,105,126} Similarly, for stroke, activation of the ipsilateral primary motor cortex has been associated with both good and poor behavioural outcomes.¹¹⁴ Such variability can render the physiological significance of t-fMRI differences unclear.

One probable source of this heterogeneity is patient variability. Factors such as anatomical location, extent, type, and timing of insult can have profound influences on neurological impairments, response to treatment, and the type of neuroplasticity required for recovery.¹²⁷ Controlling for such factors can be very difficult. Restricting a study to patients in the chronic stage of injury, for example, may not remove effects due to progressive Wallerian degeneration and/or volumetric changes, which take place during the first few years following stroke¹²⁸ and, potentially, TBI.¹²⁹ Response to treatment also appears to be subject to intact contralateral corticothalamic connections in stroke subjects¹³⁰ and ipsilateral corticospinal connections in children with CP.⁶⁹ Such factors can dramatically alter the interpretation and biological significance of measures such as LI, but their identification requires utilisation of additional modalities, such as TMS or diffusion imaging.

Attempts to limit such variability is probably one reason why most t-fMRI studies investigating neuroplasticity include only ~4–10 subjects with brain injury.^{106,114} Reproducibility studies have demonstrated that even well-controlled longitudinal t-fMRI studies of normal subjects likely have a high degree of intrasubject measurement error¹³¹ and require at least 20 subjects per group to perform reliable and sensitive group analyses.⁹⁷ The higher degree of variability seen within brain injury cohorts means that required numbers are likely to be substantially higher.

Biological Ambiguity

It is common in the t-fMRI literature to refer to activation differences as direct evidence of adaptive neuroplasticity. What is rarely addressed is the fact that activation differences, in isolation, do not allow researchers to differentiate between a variety of substantially different biological processes, many of which do not indicate regained, novel, or improved neurological capabilities and may not be positive or adaptive at all.

Compensatory Activation

One of the most obvious alternative explanations to adaptive neuroplasticity is that activation changes reflect normal system dynamics compensating for poor performance. One possible compensatory method is more intensive processing in already-activated tissue. This ties in with the topic of task equivalency and is discussed later. Another mechanism is the compensatory activation of redundant motor areas.¹³²

It is already established that the brain can switch between apparently functionally equivalent sensorimotor representations in response to disrupted activity, for example, during a tumour removal operation,¹³³ or reversibly within minutes of direct inactivation of motor areas.¹³⁴ Equivalent dynamics are probably, then, likely to occur in brain injury. Importantly, t-fMRI alone is unable to

determine whether such dynamics reflect a switch (1) to an equipotent area (reflecting ongoing impairment), (2) back to the original area (restored function), or (3) to an area previously incapable of such responsibility (novel gain in function). Given the three distinctively different take-home messages for the intervention investigated, there is a strong argument for researchers to seek secondary evidence (e.g., microstructural, conduction, or connectivity changes) before assuming that an activation change necessarily indicates novel or regained function.

Strategic Shifts

Rather than relying on neurological recovery, subjects can improve task performance by altering the role of muscle groups, improved motor planning, or better attending to feedback. Some adult stroke patients rely more heavily on proprioceptive feedback than healthy subjects,¹³⁵ for example. Adult stroke patients have also been shown to adopt compensatory movement patterns, including atypical-muscle use for pointing and reaching tasks, during rehabilitation.^{136,137} Importantly, such compensation can result in “improved” motor scores, despite unimproved motor capabilities,¹³⁶ and is associated with poorer recovery.¹³⁷ In addition, studies combining TMS and t-fMRI have revealed that attention, anticipation, and/or the forward-planning of motor movements dramatically alters cortical excitability in button pressing tasks.^{138,139}

Given these points, it is not unreasonable to surmise that subtly different behavioural strategies may underlie subtle changes in t-fMRI activation patterns. While it could be argued that learning is a form, or the result, of neuroplasticity, again the usability of information becomes limited if one cannot differentiate between “working around” ongoing disability and neurological restoration.

Task Difficulty

Task equivalency is another, related, source of uncertainty in t-fMRI. Typically, studies have all subjects perform identical tasks at all time points. One argument is that controlling for differential performance is essential to avoid different workloads or feedback confounding results (Figure 4 (b)).¹⁴⁰ In order to perform similarly to controls, however, impaired patients have to apply more effort or execute different strategies, such as a more heavy reliance on feedback, which can increase recruitment of S1M1, attentional networks, and/or supplementary areas.¹⁰⁴ These sustained attentional demands are also more difficult for brain injured subjects to meet^{141–143} and may influence activation of some sensorimotor areas, independently of motor output.¹³⁸ Increased cognitive fatigue may also result in more frequent head movement, which can impact analyses.¹⁴⁴ To avoid this issue, the equivalency of perceived effort can, instead, be controlled for (e.g., by modulating the range of motion or force exerted). Subjects performing different tasks, however, may use different task strategies, musculature, and/or receive different somatosensory feedback, all of which may alter

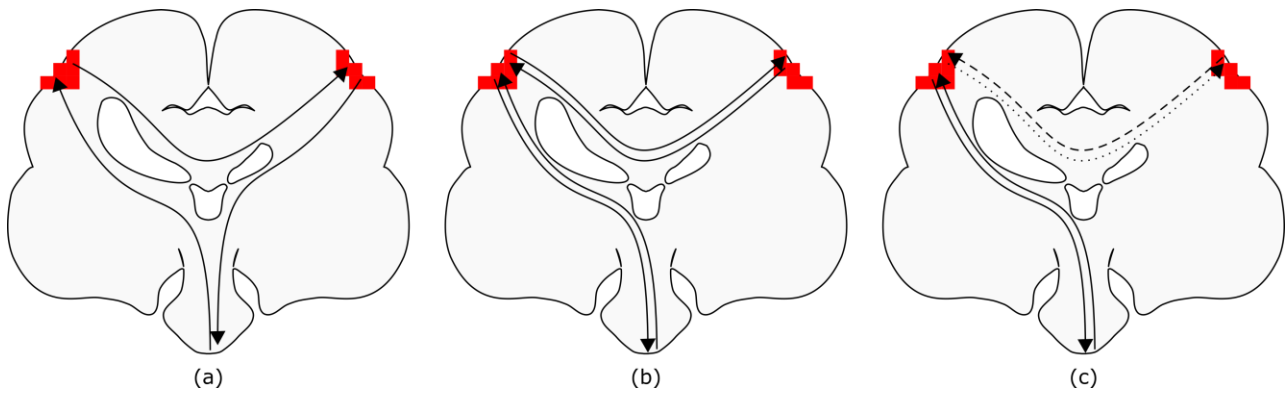


Figure 5. Task-based fMRI activation changes, in the presence of bilateral activation, require additional information for useful interpretation. Activation changes are often interpreted with the assumption that sensorimotor processing occurs primarily contralaterally, with interhemispheric relaying of information for supplementary processing (b). In cerebral palsy, however, sensory processing is often contralaterally organised, while motor signals emanate from the ipsilateral hemisphere (a). In addition, in cerebral palsy, stroke, and acquired brain injuries, imbalances in interhemispheric inhibition ((c); dashed lines) may be the primary factor influencing t-fMRI activation. Such organisations, and thus meaning of t-fMRI activation changes, can be elucidated via supplementary methods such as TMS and MEG recordings.

activation patterns. In some instances, it may be possible to conduct two tasks, one controlling for perceived effort and another where performance is controlled between participants. These two sets of functional results can then be interpreted in the context of one another and the behavioural observations noted during scanning. Researchers should carefully consider their participants before selecting this course of action as the attention required to perform multiple tasks without head movement may be beyond the means of young children, people with moderate-to-severe disability, and participants with acute brain injury (such as concussion).

Another option is the use of trivial tasks with limited cognitive load, for which perceived task difficulty and performance are likely to be identical across sessions. Scans using these tasks, however, may be insensitive to subtle reorganisation and would require exclusion of most moderately impaired patients, for whom no task is “trivial.” Passive movements of the impaired limb are a final option¹¹² but may miss genuine activity and reorganisation associated with motor planning and execution.¹⁰⁵ As such, most rehabilitation studies that incorporate fMRI of motor tasks are best positioned by accepting the task equivalency problem, choosing a simple/stable task, and making claims in the context of secondary, independent evidence of neurological change.

Disinhibition

Shifts in LI toward the contralesional hemisphere have been previously interpreted as neuroplastic compensation for a damaged sensorimotor cortex. At least in stroke, however, contralesional activation does not appear to be a good predictor of functional recovery.¹⁴⁵

Given that the motor cortices inhibit one another in normal subjects,¹⁴⁶ an alternative explanation is interhemispheric disinhibition (Figure 5): damage to the lesioned hemisphere reduces its inhibitory ability, leading to contralesional hyperactivation. TMS and fMRI + TMS studies have provided direct evidence for this hypothesis in subjects with CP,¹⁴⁷ TBI,¹⁴⁸ and stroke.^{41,110} Contralesional activity may even have a net-negative influence: direct inhibition of such activity with transcranial direct current stimulation can improve motor scores⁴² and motor-skill acquisition⁴⁶ in adults with chronic stroke.

Unknown anatomy and functional dynamics can further undermine interpretation of changes in LI. In CP, preserved ipsilateral corticospinal connections may exist,⁵⁵ which t-fMRI-only studies are unable to discern. In stroke, one fMRI + TMS study revealed that contralesional dorsal-premotor-cortex activity was correlated with poorer clinical scores, facilitating the ipsilesional motor cortex in impaired patients but inhibiting it in patients exhibiting good recovery.¹²⁴ These results highlight how difficult correctly interpreting t-fMRI activation differences can be in subjects with impairment. Activations may be adaptive, maladaptive, pathological, excitatory, inhibitory, and/or net-neutral. Which interpretation is correct is something that cannot be determined by t-fMRI alone.

Methodological Considerations

Smoothing

There are methodological considerations to consider when evaluating changes, or differences, in the spatial extent and location of t-fMRI activation peaks. Smoothing of voxel intensities is a common step in t-fMRI analyses and varies greatly between studies, often without supplied justification.⁹⁶ Smoothing can have dramatic nonlinear effects on voxel variances which can alter the volume and shape of activation, as well as the location of peaks (Figure 4 (a)).¹⁴⁹ Even kernels as small as 4 mm can shift peak-intensity localisation of motor centres by several millimetres.¹⁵⁰ Such effects should be kept in mind when inferring from activation characteristics, especially with larger smoothing kernels, which are more optimal for the small cohort sizes seen in this field.

Spatial Normalisation

When conducting group analyses, it is typical to nonlinearly register scans to a standardised “normal brain” template. This normalisation step can, however, inappropriately distort the location of tissues surrounding brain lesions.¹⁵¹ This may lead to shifts in activation location and activation-size differences between groups in damaged hemispheres. Performing affine-only registration, cost-function marking, or unified segmentation may reduce such effects but does not guarantee their elimination.¹⁵² These effects should be given consideration when interpreting group-wise analyses,

especially given that reported location differences are typically in the millimetre range and derived from small sample sizes.

Cluster Analyses

Care must also be taken with interpretation of cluster analyses, which comprise the majority of recent t-fMRI analyses.^{96,100} A cluster of voxels discovered through a cluster analysis does not infer that all voxels within that cluster were significantly active during the task. A cluster indicates a region that meets a minimum size requirement, somewhere inside of which there is evidence against the null hypothesis.^{99,153,154} A consequence of this is that the spatial specificity of these analyses is typically low, especially with larger clusters,¹⁵⁴ and one cannot make specific inferences about particular voxels within the cluster. When studying neuroplasticity, an enlarged cluster does not, thus, necessarily mean that neurons on the periphery of that region are newly utilised for a task. Similarly, a cluster that has changed shape or shifted slightly may still only have the “true” activation in the same location. This is of particular concern when liberal primary voxel-level thresholds (e.g., $p < 0.01$) are used, as these further dilute the ability to make claims about spatial location of activation.¹⁵⁴ Use of liberal thresholds is not uncommon: a recent review of 814 cluster-based fMRI studies published in high-impact journals described use of liberal thresholds as “both endemic and detrimental to the neuroimaging field”.¹⁰⁰

Disease Confounds

Beyond their most obvious motor impairment, subjects with brain injuries may also present with a number of complicating factors that cannot easily be controlled for between groups or time points and may impact t-fMRI analyses in unexpected ways.

Acute Effects

In acute and subacute stages of brain injury, fMRI signal may be heavily influenced by temporary vascular changes.¹⁵⁵ Evolution of activity patterns during this time may also simply demonstrate the temporary effects of a regressing oedema, mass effect, and/or inflammation, all of which are expected to acutely impact function.¹⁵⁶ As such, special care should be taken not to misconstrue t-fMRI changes during early disease states as neuroplasticity, without secondary evidence ruling out such causes.

The Haemodynamic Response Function

Standard BOLD analyses rely on a number of assumptions, including that neurovascular coupling (1) is consistently overcompensatory, (2) is adequately regionally invariant, and (3) has a sufficiently standard time-course between regions and subjects. These assumptions may be invalidated by the

substantial cerebrovascular damage that is associated with many forms of stroke, TBI, and congenital hemiplegia. Altered CBF has been reported for all clinical stages of both stroke^{157–159} and TBI.^{155,160} Stroke patients' haemodynamics may be additionally impacted nonglobally by concurrent vascular disease caused by risk factors such as advanced age, smoking, hypertension, and diabetes mellitus.

As normal haemodynamic responses overcompensate for metabolic needs, reduced cerebrovascular reactivity can present as a diminished BOLD signal, despite unaltered levels of neural activity. As such, in longitudinal designs involving nonchronic patients, it may be impossible to differentiate between changes in neural activation and cerebrovascular reactivity using t-fMRI alone.¹⁵⁷ Of particular concern, several studies have found that the haemodynamic response near a lesioned site is more strongly impacted by injury than nonlesioned regions, even in chronic disease states.^{155,158,159} Finally, there is evidence that aspects of cerebrovascular reactivity may be correlated with motor performance in certain stroke patients,¹⁶¹ even in the absence of marked vascular disease.¹⁶² It is noteworthy that dynamic causal modelling, a more advanced fMRI analysis method, may be more robust to haemodynamic inhomogeneities by modelling haemodynamics in a region-wise fashion.^{163,164}

Head Movement

Head movement can have profound impacts on the fMRI signal. Although movement between frames can be reversed through reslicing, there are other sources of signal changes associated with movement (e.g., spin history effects) that will remain. Even after statistical adjustment, submillimetre RMS movement can lead to measurably reduced statistical power.¹⁶⁵ Such movement is more likely in subjects with movement disorders (i.e., dystonia) or reduced cognitive abilities or who find the task difficult.¹⁴⁴ Movement artefacts can be reduced by excluding subjects or censoring frames with movements,¹⁶⁵ but this may systematically reduce the statistical power for one subject group and can lead to sampling biases.¹⁴⁴

Summary and Recommendations

There is little doubt that t-fMRI is an important neuroimaging modality. The aim of this review is not to critique t-fMRI per se nor to blanket-prescribe a specific method by which to quantify functional images when measuring neuroplasticity. Rather, we wish to make researchers and clinicians aware of the systematic and methodological challenges affecting common t-fMRI study designs, which are often not addressed or acknowledged, and elucidate how these issues can be mitigated through a multimodal approach. To summarise our case so far, even if confounds such as movement, acute effects, and haemodynamic differences are eliminated, it is still possible that some findings may be

explainable by unavoidable data processing steps, such as smoothing and spatial normalisation. These issues are particularly concerning given the vast patient variability and low subject numbers seen in this field. Even when overcoming such issues, assumptions of brain plasticity based on t-fMRI evidence alone are problematic due to difficulties in differentiating between recovery, compensation, use of preexisting redundancies, changes in strategy, and maladaptive processes. In studies of neurorehabilitation, it is critical that researchers can correctly interpret what a change in t-fMRI signal actually means in order to understand the mechanisms of functional recovery.

In this review our basic criteria for informative interpretation required that signal changes were moderately stable, meaningfully distinguishable from day-to-day variation, reliably related to clinical changes, and offered biological insight into the recovery process. The first, imperative, step to meeting these criteria with t-fMRI is to relate changes to valid and reliable measures of motor function. Planning longitudinal studies can also provide certainty that any activation changes seen are not due to patient heterogeneity. To overcome the remaining challenges, multimodal imaging can help in four ways. Firstly, multimodal information can allow more homogenous cohorts to be selected or subgroups identified for analysis. Secondly, by providing contextual information, other modalities can narrow down which biological process t-fMRI may have indexed. Relatedly, additional modalities can quantify potentially influential covariates, such as haemodynamic differences, to assess their impact on t-fMRI. Finally, when uncertainties and/or ambiguities are still prevalent, change measured through an independent method can provide confidence that t-fMRI is genuinely indexing a stable functional change. Many multimodal configurations are available that have already proven valuable in helping studies meet these criteria; examples are listed in Table 3.

Structural MRI

Structural MRI allows measurement of cortical thickness: essentially an index of locally or globally available grey-matter. While cortical thickness can be challenging to measure precisely, especially in patient cohorts presenting with cortical lesions or malformations, such analyses are typically automated, simple to visually assess, and can be easily overlaid with t-fMRI statistical parametric maps. Adequate structural images are routinely acquired within fMRI-scan sessions and usually simple to acquire motion-free. While structural imaging is probably less sensitive to change than t-fMRI, these methods share few sources of uncertainty and provide one another with useful contexts for plausible interpretation. In particular, as locally increased grey-matter thickness likely reflects newly ongoing utilisation of that tissue,¹⁶⁶ increases in this measure may indicate that any accompanying t-fMRI activation increases are moderately stable and reflect some form of gain-in-

Reference	Disorder	Additional measures(s)	Significance
Werring et al. ¹⁵⁶	TBI	dMRI	Earliest known combined fMRI + dMRI study for a recovering patient. Combined imaging revealed which corticospinal tracts were partially damaged and whether they were still in use.
Palmer et al. ¹⁷⁶	Healthy subjects	dMRI tractography	fMRI-guided tractography elucidated minute longitudinal structural changes; changes were not detected by fMRI alone.
Cherubini et al. ¹⁷⁴	TBI	dMRI tractography	In patients, fMRI-guided tractography identified additional corticospinal connections and more normal connectivity patterns than atlas-based seeding.
Staudt et al. ⁵⁵	CP	dMRI, TMS	TMS, dMRI, and fMRI of motor areas showed good agreement, except in the only successfully scanned subject with bilateral fMRI activation. For this subject, TMS and dMRI ruled out an ipsilateral CST connection.
Rijntjes et al. ¹⁶⁷	Stroke	TMS	Integrity of the pyramidal tract was required for patients to show lasting responses to CIMT. Long term outcomes, fMRI patterns, and correlations between these factors were dependent on such integrity.
Wilke et al. ¹²⁶	CP	TMS, MEG	Multimodal imaging demonstrated that sensory organisation was preserved despite motor reorganisation.
Schaechter et al. ²⁹³	Stroke	Cortical thickness	fMRI activations correlated with cortical thickness specifically in putative area 3b of the lesioned hemisphere.
Xiong et al. ¹⁶⁹	Healthy subjects	PET	The fact that fMRI “returns to baseline” in long term motor training may be due to an increased baseline rCBF, rather than the assumed decrease in activation during task performance.

Table 3. Example of multimodal studies of brain injury and neuroplasticity. TBI: traumatic brain injury; dMRI: diffusion MRI; CIMT: constraint-induced movement therapy; CP: cerebral palsy; TMS: transcranial magnetic stimulation; MEG: magnetoencephalography; PET: positron emission tomography.

function rather than, for example, a switch to an unchanged “backup” network. Changes seen in cortical thickness are particularly beneficial to studies with limited subject numbers, where well-powered group analyses, which can rule out day-to-day variability in neural or vascular dynamics, are difficult or impossible to perform.

Analyses of structural images and diffusion MRI (below) can also quantify potential covariates (such as degeneration, regressing oedema, or developmental maturation) that may affect t-fMRI metrics longitudinally and are likely to vary by subject-cohort and time-point.

TMS

TMS is unique in its ability to directly characterise structural-functional connectivity, including intercortical inhibition, corticospinal tract conductivity, and motor thresholds. TMS may prove particularly useful for studies that need to characterise the functional meaning of t-fMRI determined LI changes. TMS has been used in multiple studies to differentiate between subject subgroups, allowing researchers to understand the biological significance of bilateral fMRI activation patterns in CP^{55,126} and reveal correlations between fMRI changes and long term outcomes in stroke.¹⁶⁷

EEG and MEG

Magnetoencephalography (MEG) and electroencephalography (EEG) can improve certainty in t-fMRI changes by providing direct measures of net neuronal activity that are not likely to be impacted by factors such as haemodynamics, or the aforementioned methodological considerations. The very high temporal resolution of these methods can also allow researchers to distinguish between stages of processing, such as motor planning and execution.¹²⁰ Concurrent EEG + fMRI is now possible, although caution may be advised in cohorts for whom head movement is an issue, as concurrent artefacts may result in plausible type-I errors.¹⁶⁸

EEG and MEG information can profoundly change the interpretation of changes in t-fMRI metrics, such LI or activation volume, and elucidate whether comparisons between subject groups are valid. For example, MEG has been used in conjunction with fMRI and TMS to demonstrate that, in some subjects with CP, bilateral t-fMRI S1M1 activation reflects contralateral somatosensory processing alongside ipsilateral (reorganised) motor processing.¹²⁶ This illustrates clearly how categorisation of such subjects into homogeneous subgroups can be critical for t-fMRI metrics to be appropriately interpreted (Figure 5). The researchers highlighted that, particularly for motor-based t-fMRI, “[d]efinitively disentangling such bilateral activation is... only possible when complementary methods are used, like TMS and MEG”.¹²⁶

PET and ASL

Positron emission tomography and arterial spin labelling are neuroimaging methods that can provide measurements of regional CBF, and so reveal whether haemodynamic differences are affecting fMRI measurements. Arterial spin labelling is a contrast-agent-free MRI technique that can be carried out in ~10 minutes, during the same session as an fMRI. PET is advantageous in that it can additionally provide direct measures of glucose metabolism in brain tissue but requires access to PET imaging equipment and associated radiopharmaceutical facilities. Because both of these methods provide quantitative measures of local haemodynamics, they can quantify precisely how fMRI measurements in each region are affected by factors such as angiogenesis or vascular impairments. This may provide certainty in situations involving lesions, suggest adjustment of haemodynamic parameters, provide guidance on study design (i.e., indicate whether a block-design should be chosen over an event-related design), or shed light on otherwise-unclear findings. In one illustrative study of healthy adults, increases in t-fMRI activation volumes were shown in the supplementary motor area and M1 after two weeks of motor training.¹⁶⁹ These volumes subsequently declined to near-baseline values during the following two weeks of training, despite ongoing improvements in motor performance. PET scans showed that regional CBF increased between all time points, revealing that fMRI decreases were probably due to increased blood flow at rest, rather than actual decreases in brain activity during task execution.

Diffusion MRI

Diffusion MRI (dMRI) measures the directional diffusivity of water in tissue and can provide a variety of useful metrics. In subacute head injury or stroke, dMRI can be used to ensure that t-fMRI differences reflect more than inflammation or oedema. “Microstructural integrity” indices, such as fractional anisotropy and mean diffusivity, can provide evidence that t-fMRI changes represent ongoing changes in brain activity outside of the scanner: these metrics correlate with, and are sensitive to, myelination, which increases in response to ongoing electrical activity.¹⁷⁰ Advanced analyses can identify white matter pathways, calculate their intra-axonal volumes, and index the physical “connection strength” between cortical and subcortical regions. These measures correlate with functional measures in CP⁵¹ and may help provide a more complete picture when interpreting changes between balances of activation between brain regions. Another form of dMRI, neurite orientation dispersion and density imaging,¹⁷¹ provides the opportunity to reveal whether shifts or enlargements of t-fMRI activation reflect local network changes in, for example, the cortex or thalamus.¹⁷²

Diffusion MRI data are easily acquired in the same session as an fMRI scan, usually in 8–12 minutes. As dMRI is acquired at rest, overt movement is easier to avoid than with t-fMRI and is

unlikely to be correlated with factors such as ability. Standard preprocessing methods can also correct or “scrub” moderately ($\leq 10\%$) motion-corrupted dMRI data without compromising the final result.¹⁷³

t-fMRI Fusion

Finally, a promising alternative approach is to not infer directly from t-fMRI activation patterns, but rather to use t-fMRI to identify functionally important regions-of-interest in which other modalities

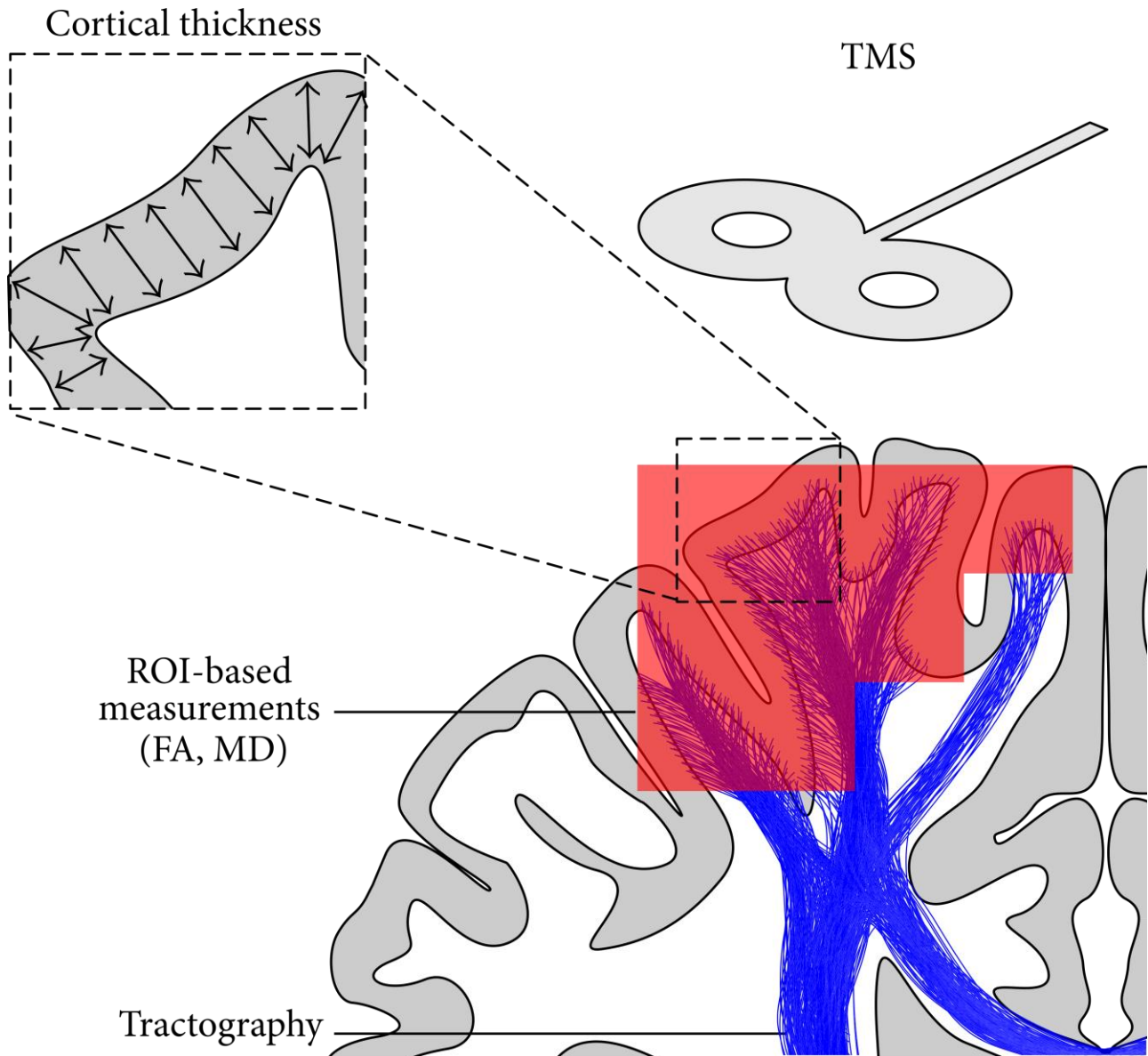


Figure 6. Utilising fMRI in conjunction with a number of other modalities. The red region indicates an area of significant activation, determined with fMRI. When combined with structural MRI, these activated regions can be used as ROIs in which targeted measures of cortical thickness can be made. When combined with diffusion MRI, the fMRI ROIs can be used as sample regions for FA and MD values within subcortical white matter, both of which provide information about tissue microstructure. These ROIs can also act as seed regions to drive tractography, from which white matter connectivity and integrity can be measured. Combining fMRI with TMS measures can also provide context to and certainty about the functional-relevance of fMRI-based findings. ROI: region of interest; FA: fractional anisotropy; MD: mean diffusivity; TMS: transcranial magnetic stimulation.

should make measurements (Figure 6). This fusion of information can avoid some pitfalls of overanalysing changes in activation patterns, while considerably improving the sensitivity and interpretability of other modalities.^{174,175} One fusion method which is being progressively adopted is the use of t-fMRI activation patterns to guide diffusion tractography, allowing this method to focus microstructural and structural-connectivity measurements on functionally relevant areas.^{174–176}

Optimising Multimodal Study Designs

Asking a specific research question is fundamental to optimising a study design. Focussed questions (e.g., “How does rehabilitation alter S1M1 connectivity?”) are not only inherently more testable than very broad questions (e.g., “What does rehabilitation change in the brain?”), but can also provide guidance on which study design is appropriately powerful, which modalities and behavioural measures can contribute to the overall picture, and how t-fMRI metrics may require supplementation or disambiguation with additional information. For example, investigations into somatosensory processing may require teasing apart t-fMRI activation using temporally precise signals (MEG) and/or information about integrity of the corticothalamic tracts (TMS or dMRI).

With a specific question in place, one should then consider which factors may primarily impair t-fMRI interpretability. Modalities that can minimise such issues are those which can either quantify their extent or provide supplementary evidence that is unaffected by such issues. For example, if a difference in t-fMRI activation volume is expected between two groups, but one group may have impaired haemodynamics, quantifying regional-CBF with arterial spin labelling, or directly measuring brain activity with MEG, may be of great benefit. As a contrasting example, a t-fMRI study of subjects displaying dyskinesia is unlikely to benefit greatly from dMRI, as both may be confounded by movement artefacts.

Finally, in some situations, the benefits of multimodal imaging may be limited. Studies with very low subject numbers, particularly cross-sectional studies, may see limited benefit from modalities that are less sensitive to change or have high intersubject variance. In such cases, resources may be better spent on boosting subject numbers or collecting additional behavioural information than on additional neuroimaging. In addition, studies that are unable to collect relevant and reliable clinical measures have limited abilities to discern the relevance of neuroplastic changes, regardless of how many imaging measures are taken.

Conclusion

For measures of neuroplasticity in subjects with brain injuries, the reliability and interpretability of t-fMRI is hampered by a unique set of systematic and methodological challenges. Multimodal imaging

provides the opportunity for t-fMRI results to be interpreted with more confidence and biological specificity, ultimately providing greater understanding of the rehabilitative process. Which complementary imaging modality offers the most benefit depends on the study question and subjects selected. Many of these modalities have a minimal time and financial cost for acquisition while still offering exciting, novel opportunities to explore the relationship between structure, function, and clinical outcome which simply cannot be investigated in any other way.

Addendum

Since the publication of this Chapter as a peer-reviewed paper, it has been suggested that a topic missing from its discussion was the use of alternative statistical models, particularly resting state fMRI and multivoxel pattern analyses. The scope of the above Chapter was purposefully limited to GLM analyses not only because these are overwhelmingly popular, but also because their relative simplicity means that associated issues are generally applicable to more complex models. For example, while multivoxel pattern analysis may allow one to test more sensitively the activation differences of two tasks, task equivalency, abnormal haemodynamic responses, head movement, spatial normalization, and so on still present as compounding issues in brain injured cohorts. To the author's knowledge there is no evidence that such an approach is more robust to these issues than GLM analyses. In fact, it seems logical that such an approach is potentially *more* susceptible to such issues, given that it relies on machine learning that is 'trained' on a subset of the data, and then applied to the rest: these issues may present more strongly at some time point or in some patients than others. Regardless of the statistical methodology, the benefits of using multimodal imaging, rather than standalone fMRI, seem clear.

Chapter 4

Surface-Based fMRI-Driven Diffusion Tractography in the Presence of Significant Brain Pathology: A Study Linking Structure & Function in Cerebral Palsy

The previous chapters identified a number of means by which neuroplasticity could potentially be measured noninvasively in humans. One large issue with many standard structural methods is that they rely on assumptions about brain organisation which are invalidated by pathology. For example, such methods typically utilise standard brain parcellation maps (atlases) to identify specific functional regions, but brain shape and functional organisation may be altered substantially by brain injury. Another issue is that the presence of pathology results in standard processing steps, such as aligning volumes with atlases, behaving unreliably or failing outright. Although much more conservative regions could be utilised to improve reliability, the inclusion of unrelated areas may also reduce the sensitivity of methods to detect longitudinal change.

This chapter consists of the paper *Surface-Based fMRI-Driven Diffusion Tractography in the Presence of Significant Brain Pathology: A Study Linking Structure and Function in Cerebral Palsy*, published in *Plos One*. This paper outlines a novel, specialised, method for delineating the corticospinal and thalamocortical tracts specifically associated with hand use. The properties of these tracts can then be assessed with diffusion MRI. The technique is particularly novel in that it is robust to severe pathology, and utilises machine learning to differentiate corticospinal tracts from thalamocortical tracts. This reduces the need for atlases and/or manual delineation, and providing more coherent tract estimations.

This work addresses Aim 2 of this thesis: *address the need for algorithms that can reliably detect subtle structural brain changes and that perform well in the presence of pathology*. Although this chapter does not formally calculate the reliability of this method, it demonstrates that the produced measures correlate with several clinical scores and, in this regard, performs substantially better than state-of-the-art fMRI-guided tractography. In detecting such correlations, the present chapter identifies that such measures are a sensible region in which to search for neuroplastic change in a motor rehabilitative trial. The sensitivity of this method is demonstrated in Chapter 6, its ability

to perform in a longitudinal study is demonstrated in Chapter 7, and a formal analysis of its reliability is conducted in Chapter 8.

As first author of this paper, I designed and programmed the described imaging pipeline, analysed and interpreted the data, and wrote the manuscript. All authors reviewed and edited the paper. Stephen Rose also aided in initial conception of the pipeline.

Publication information

Reid LB, Cunnington R, Boyd RN, Rose SE. Surface-Based fMRI-Driven Diffusion Tractography in the Presence of Significant Brain Pathology: A Study Linking Structure and Function in Cerebral Palsy. Yap P-T, editor. *PLoS One*. 2016 Aug 3;11(8):e0159540.

DOI: 10.1371/journal.pone.0159540

Accepted July 4th 2016

Published August 3rd 2016

Minor changes have been made in response to examiner feedback.

This work also appeared in abstract form and was presented at an international conference as follows:

Reid LB, Cunnington R, Boyd RN, Rose SE. Mesh-based fMRI-driven-tractography for automated analyses of non-parcellateable brains with pathology. In: 23rd Annual Meeting and Exhibition of the International Society for Magnetic Resonance in Medicine. Toronto; 2015.

Abstract

Diffusion MRI (dMRI) tractography analyses are difficult to perform in the presence of brain pathology. Automated methods that rely on cortical parcellation for structural connectivity studies often fail, while manually defining regions is extremely time consuming and can introduce human error. Both methods also make assumptions about structure-function relationships that may not hold after cortical reorganisation. Seeding tractography with functional-MRI (fMRI) activation is an emerging method that reduces these confounds, but inherent smoothing of fMRI signal may result in the inclusion of irrelevant pathways. This paper describes a novel fMRI-seeded dMRI-analysis pipeline based on surface-meshes that reduces these issues and utilises machine-learning to generate task specific white matter pathways, minimising the requirement for manually-drawn ROIs. We directly compared this new strategy to a standard voxelwise fMRI-dMRI approach, by investigating correlations between clinical scores and dMRI metrics of thalamocortical and corticomotor tracts in 31 children with unilateral cerebral palsy. The surface-based approach successfully processed more participants (87%) than the voxel-based approach (65%), and provided significantly more-coherent tractography. Significant correlations between dMRI metrics and five clinical scores of function were found for the more superior regions of these tracts. These significant correlations were stronger and more frequently found with the surface-based method (15/20 investigated were significant; $R^2 = 0.43-0.73$) than the voxelwise analysis (2 sig. correlations; 0.38 & 0.49). More restricted fMRI signal, better-constrained tractography, and the novel track-classification method all appeared to contribute toward these differences.

Introduction

Cerebral palsy is a term describing a group of permanent disorders of movement and posture owing neurological insult, or non-progressive disturbances of neurological development, that are presumed to have occurred by the time of birth.¹ The majority of cases are due to periventricular white-matter damage that is assumed to occur during the third trimester.⁵⁻⁷ Children with cerebral palsy often have learning impairments, and are restricted in both their mobility and ability to participate in everyday activities.¹⁷⁷ As with disorders caused by acquired brain injuries, current rehabilitative efforts are hampered by a limited understanding about the relationship between brain structure, function, and brain pathology.¹⁰³ In cerebral palsy, this picture is complicated further by ongoing neural development that occurs during childhood. Structural MRI is one modality that has been utilised to investigate cerebral palsy, but relationships between gross structure and functional outcomes are not straightforward, and have proven difficult to ascertain.¹⁷⁸

Diffusion MRI (dMRI) is an increasingly popular modality that is used to investigate links between white matter (WM) injury and clinical outcomes. A number of dMRI studies investigating WM injury in cerebral palsy have reported relationships between microstructural characteristics of the cerebrospinal tract and functional outcomes.^{103,179} In unilateral cerebral palsy, questions still remain as to whether the primary contributor to upper-limb motor impairment is damage to corticomotor tracts or associated damage to the thalamocortical sensory pathways.^{51,59} Although standard analyses might have the potential to provide answers to these questions, such approaches are often difficult or impossible to perform on moderately impaired children with cerebral palsy due to the presence of pathology and potentially-atypical brain organisations.

Most diffusion analyses provide metrics that can be used to make inferences about the brain's underlying microstructure. When studying motor function, such approaches require robust delineation of cortical motor regions and/or subregions (such as the hand knob). Cortical parcellation performs this role reliably in healthy individuals, but problems often emerge when applying analyses to individuals with brain pathology. These problems are twofold. Firstly, tools such as Freesurfer (<http://surfer.nmr.mgh.harvard.edu>) often fail to delineate the cortical surface when pathology or abnormal morphology is present. For example, in our experience, Freesurfer fails to delineate this surface acceptably in around 30% of children and adolescents with mild-to-moderate cerebral palsy, even after repeated manual adjustment. Consequently, the majority of studies measuring dMRI metrics in cerebral palsy (and similar conditions) so far have relied on manual-parcellation.¹⁷⁹ Unfortunately, manual parcellation is prone to bias or human error and is extremely time consuming, especially when pathology is present. The second issue is that cortical parcellation, both automated

and manual, may be invalidated by functional reorganization that occurs in response to pathology (Figure 7). Using coarser regions of interest (ROIs; such as the entire sensorimotor cortex) might improve confidence that tissue that is functionally-relevant to the hypothesis is included, but will likely also include tissue that is functionally irrelevant to the hypothesis at hand. Tracking towards the surface using multiple hand-drawn ‘include’ ROIs is an alternative approach. This can often identify the corticomotor tracts reasonably, but is unable to reliably locate specific subregions of interest (such as those innervating the hand knob) and in a clinical situation often results in tracks that fail to reach the cerebral surface.

In situations where specific regions of interest are known a-priori, the need for cortical parcellation can be circumvented through the use of task-based functional MRI (fMRI).^{103,175} In such a method, areas of significant fMRI activation are used as seeding regions for diffusion tractography. This method has been used in several studies of healthy subjects,¹⁷⁵ by utilising standard voxel-based software packages such as SPM (<http://www.fil.ion.ucl.ac.uk/spm/software>) and MRTrix.¹⁸⁰ Standard fMRI analyses include an appreciable amount of implicit and explicit smoothing, which can artificially increase the size of the detected activation beyond its true boundaries.^{103,181} Additional smoothing also takes place when fMRI images are converted into dMRI seed images (i.e. reslicing and/or expanding activation ROI into WM). This is not usually a meaningful issue in standard fMRI interpretation, but when expanded ROIs are used for tractography seeding or filtering, this issue might result in the inclusion of irrelevant WM tracts. Applying binary inclusion/exclusion ROIs to tractography may filter out some of these tracks, but this method relies totally on assumptions of brain connectivity patterns that may not hold true in participants with pathology. The challenge of creating fair ROIs for such filtering that do not filter or miscategorise legitimate plasticity can be as difficult as manual parcellation, and is prone to the same challenges we have already discussed.

One method that can improve the specificity of fMRI-determined activation is surface-based smoothing.¹⁸² That is, explicitly smoothing the data along the brain’s topology, rather than in image space. Theoretically, this method could constrain fMRI activation legitimately, providing a tighter seed for tractography that circumvents having to rely on highly-accurate individually-tailored ROIs for track filtering. Standard pipelines that use this method (e.g. FS-FAST), however, will also still include some implicit cross-sulci smoothing during motion correction, projection between surface and voxel-based representations, and subsequent conversion into dMRI-seed ROIs. More importantly, these methods rely on Freesurfer-based meshes that are often impossible to generate when moderate pathology or abnormal morphology is apparent.

This paper describes a surface-based fMRI protocol that performs reliably in people with moderate or significant pathology, and minimizes the aforementioned difficulties related to

smoothing by eliminating reslicing. The resulting surface is used to both seed and anatomically constrain diffusion tractography. Rather than requiring high quality 3D ROIs of the midbrain, which can be difficult to obtain in the presence of pathology (Figure 8), the method optionally provides track categorisation through simple clustering algorithms that accept roughly-drawn 2D ROIs as hints. This method was demonstrated in a cohort of children with mild-moderate unilateral cerebral palsy, and the resultant diffusion measures were correlated with participants' clinical characteristics. These results were compared with results obtained using a more standard voxel-based-fMRI + dMRI pipeline on the same dataset. The surface-based method was also run without track clustering to determine the contribution of this element to the quality of tractography.

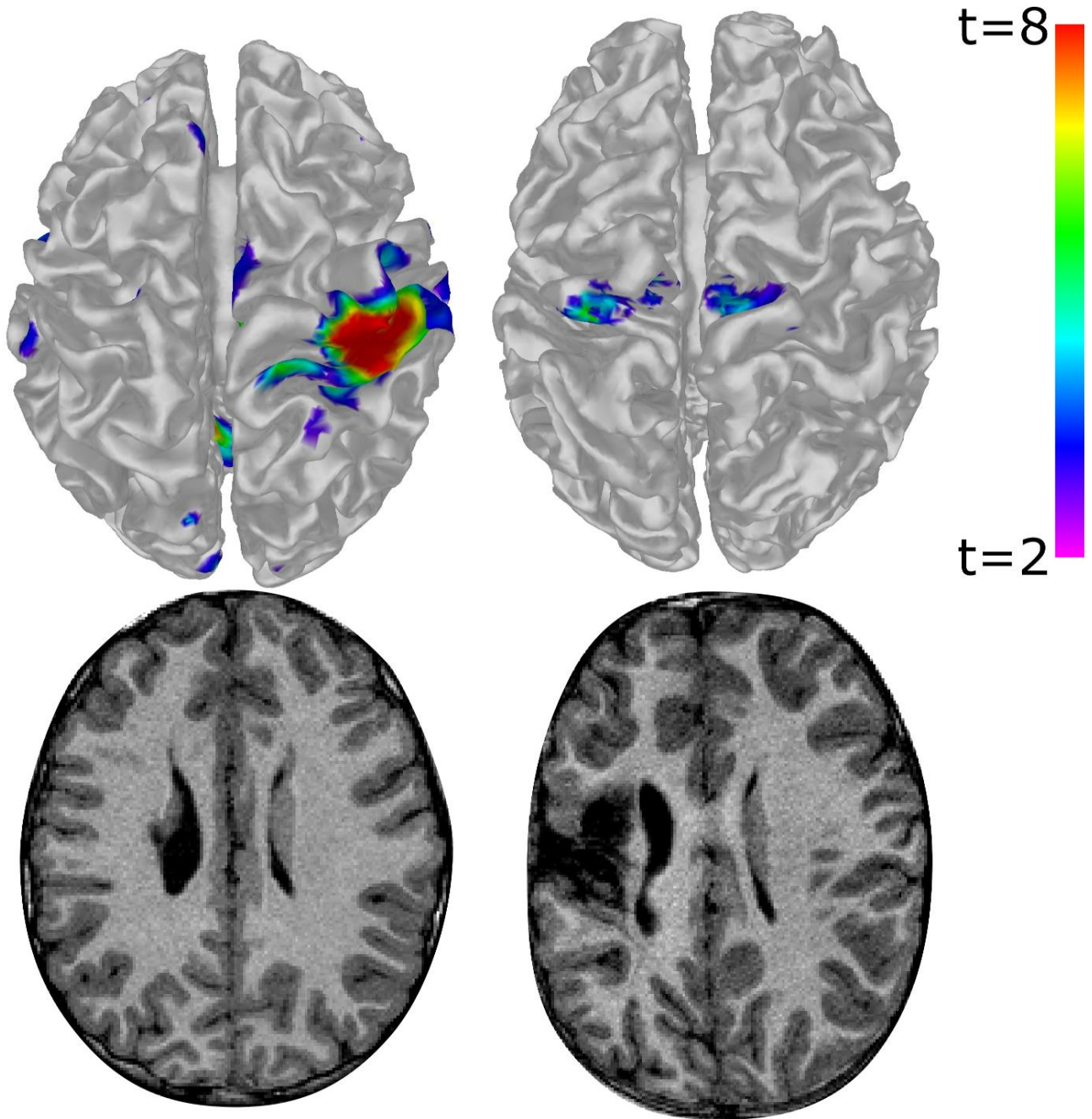


Figure 7. Functional MRI activation for a hand tapping task (top), and corresponding T1 images (bottom) for two children with unilateral cerebral palsy. The top-left of each image represents the anterior-left of each brain. Left Column: a higher-functioning child tapping their less-impaired (right) hand. Robust unilateral activation can be seen in the ‘typical’ hand knob location of the sensorimotor cortex, as may be expected from a typically developing child. Right Column: a child with higher degrees of brain damage tapping their more-impaired (left) hand. Activation appears more medially, bilaterally, and anteriorly; predominantly in the assumed supplementary motor areas rather than in the typical hand-knob locus. These differences may illustrate potentially abnormal brain organisation occurring in response to the early-life brain injury sustained. Images are not to scale.

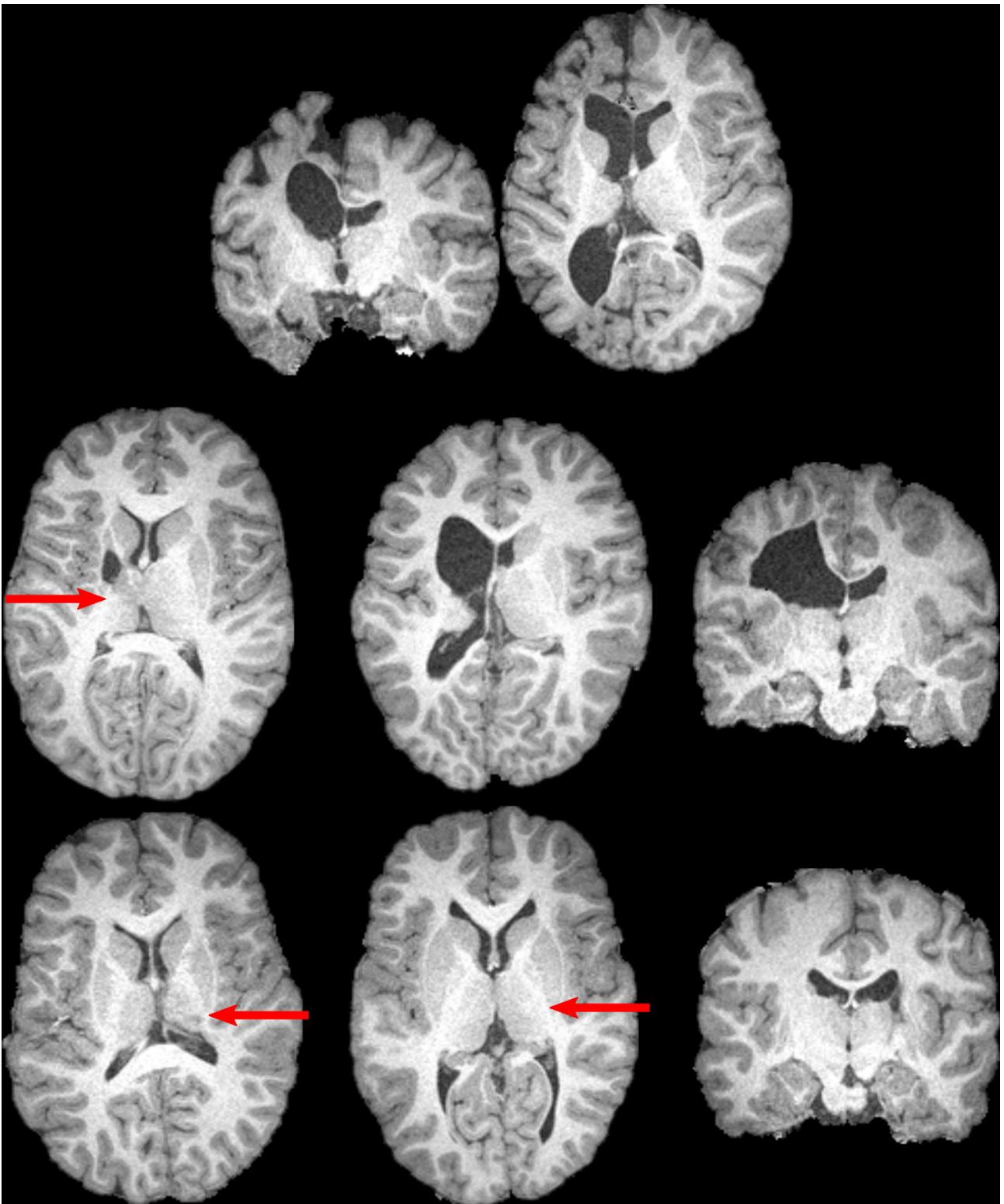


Figure 8. Examples of participants with unilateral cerebral palsy, for whom neurological abnormalities include distortion of the midbrain, and/or loss of contrast between the thalamus and posterior limb of the internal capsule. Subtler losses in contrast are indicated by arrows. Such abnormalities can make reliable delineation of these structures difficult to perform. The top row displays two slices from a single participant. The remaining images are from six different participants. All displayed participants contributed data that was utilized for one or more analyses.

Methods

Overview

Two pipelines were used to obtain corticomotor and thalamocortical tracks, from which measurements of fractional anisotropy (FA) and mean diffusivity (MD) were obtained. The Surface method utilized a simple tissue segmentation approach to generating a mesh. This mesh was then used in a surface-fMRI analysis that identified the sensorimotor area for each participant. Diffusion tractography was then seeded from this sensorimotor surface, and constrained by this mesh. Corticomotor and thalamocortical tracts were then delineated using a clustering algorithm. The Voxel-Based analysis used a standard SPM fMRI analysis in voxel space to identify the sensorimotor area. This area was then used to seed tractography, which was constrained by a brain mask. Corticomotor and thalamocortical tracks were then delineated using hand-drawn midbrain ROIs.

Participants

Imaging and clinical data were acquired as part of the Mitii clinical trial.¹³ This analysis included data from 37 children (Mean age 11.7y; SD 2.7y), who had acceptable dMRI scans and did not exhibit behavioural issues that impaired data quality (e.g. repeated purposeful head movement) during fMRI or structural scans. All had a diagnosis of mild to moderate spastic-type unilateral cerebral palsy, with injury to the periventricular white matter (65%) or cortical deep grey matter (35%), a Gross Motor Function Classification System Level I (43%) or II, and Manual Abilities Classification scale (MACS) I (32%) or II. Diagnoses of CP subtype were made by a paediatric neurologist based on T1, T2 HASTE, and T2 TIRM volumes; the neurologist was blinded to clinical information. Detailed clinical characteristics are provided in Table 4. Representative examples of pathology are shown in Figure 8 and Figure 9. Written informed consent was obtained from the parent or legal guardian of each child. Ethical approval was obtained by the Medical Ethics Committee of The University of Queensland (2011000608), The Royal Children's Hospital Brisbane (HREC/11/QRCH/35), and the Cerebral Palsy Alliance Ethics Committee (2013-04-01). The Mitii study was registered with the Australian clinical trials register (www.anzctr.org.au): ACTRN12611001174976.

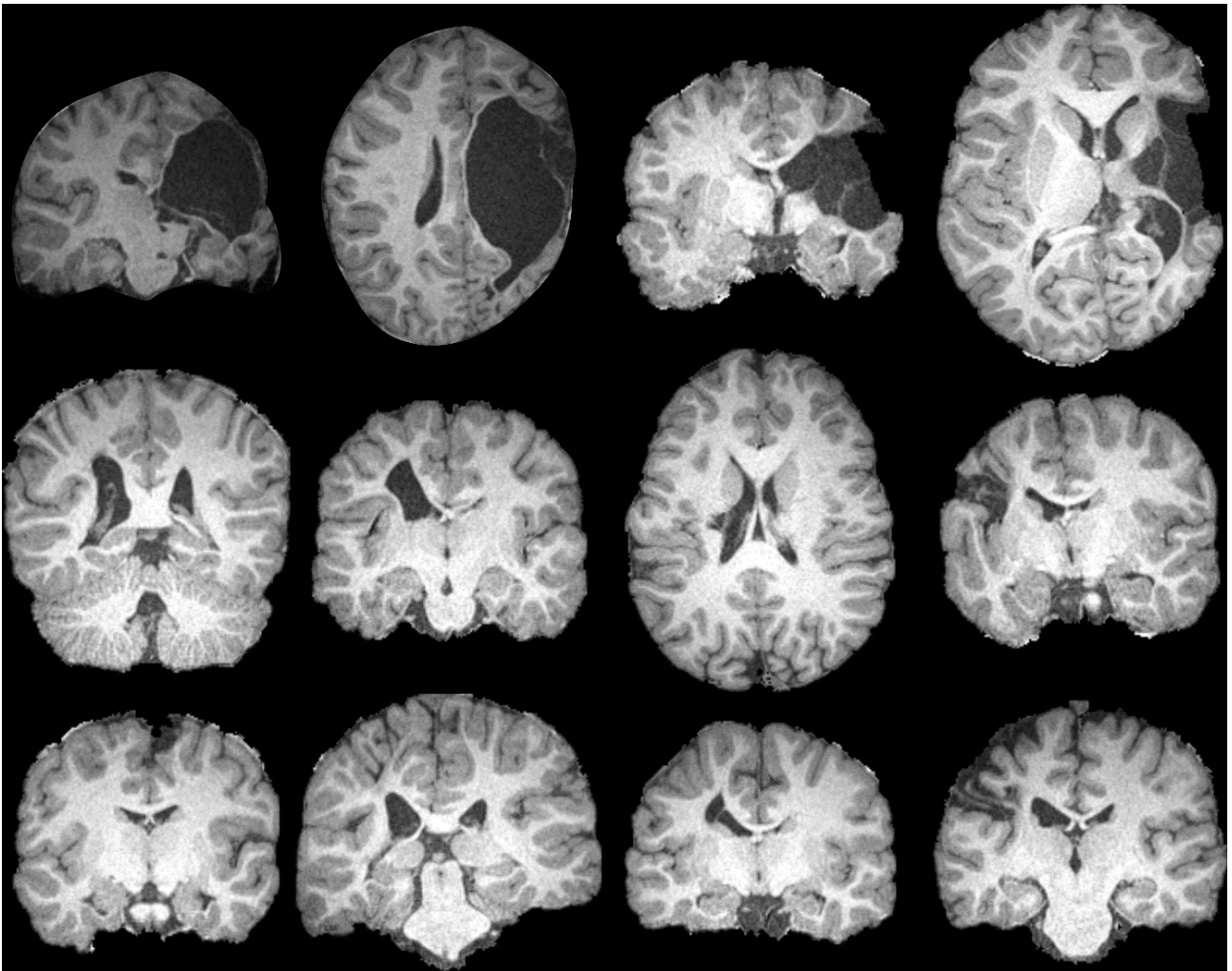


Figure 9. Examples of pathology seen in the enrolled cohort. The top row displays one coronal and one axial image from two participants with severe brain pathology. The remaining two rows display images of eight unique participants. No participants are duplicated from Fig 2. All displayed participants contributed data that was utilized for one or more analyses. These images, combined with those in Figure 8, are representative of the range of pathology severity seen across enrolled participants.

Analysis Stage	N	Age	Left-sided Hemiplegia	Male	GMFCS I	MACS I	PWM	AMPS-M	JHFT-AI	COPM-P	AHA	MUUL
Enrolment	37	11.7±2.7	41%	51%	43%	32%	65%	1.29±0.37	0.46±0.28	4.50±1.27	70.1±14.8	85.9±16.9
Attempted	31	11.8±2.9	45%	45%	48%	32%	71%	1.32±0.36	0.44±0.27	4.58±1.26	70.8±13.2	88.5±12.3
Surface Succeeded	27	12.0±2.7	41%	44%	48%	37%	74%	1.37±0.33	0.39±0.25	4.65±1.18	73.8±10.7	90.8±9.9
Surface Correlations	24	11.6±2.4	44%	48%	50%	38%	79%	1.39±0.33	0.40±0.25	4.68±1.25	74±11.4	91.1±9.9
Voxelwise Succeeded	20	12.0±2.7	45%	50%	40%	30%	75%	1.26±0.31	0.45±0.28	4.54±1.19	71±12.6	89.9±10.8
Voxelwise Correlations	18	12.0±2.8	50%	50%	39%	28%	83%	1.26±0.30	0.48±0.28	4.53±1.26	70.7±13.3	89.5±11.0
Reanalysis	16	12.0±3.0	44%	56%	38%	31%	88%	1.28±0.30	0.43±0.27	4.41±1.28	72.8±12.4	90.1±11.0

Table 4. Left-sided hemiplegia refers to percentage of participants whose left arm was more impaired than their right. GMFCS I and MACS I refers to the percentage of patients scored as classification I for these scores; all others are level II. PWM refers to the percentage of participants with periventricular white-matter damage; all others had cortical deep grey matter injury. ‘Attempted’ rows include participant-datasets for whom fMRI analysis was attempted. ‘Succeeded’ include all datasets that were successfully processed through to diffusion metrics, inclusive. ‘Correlations’ rows include all participants included in correlation analyses (i.e. excludes participants with distinctively non-unilateral lesions). ‘Reanalysis’ row refers to the subset of data used during reanalysis of overlapping voxelwise and surface-based data. Ages and clinical scores are provided as mean ± standard deviation. All percentages are to 2 sf. Acronyms: GMFCS, Gross Motor Function Classification System; MACS, Manual Ability Classification System; PWM, periventricular white-matter damage; AMPS-M, motor component of the Assessment of Motor and Process Skills; MUUL, the Melbourne Unilateral Upper Limb Assessment; AHA, the Assisting Hand Assessment logit; JHFT-AI, the Jebsen-Taylor Hand Function Test asymmetry index; COPM-P, The Canadian Occupational Performance Measure performance score.

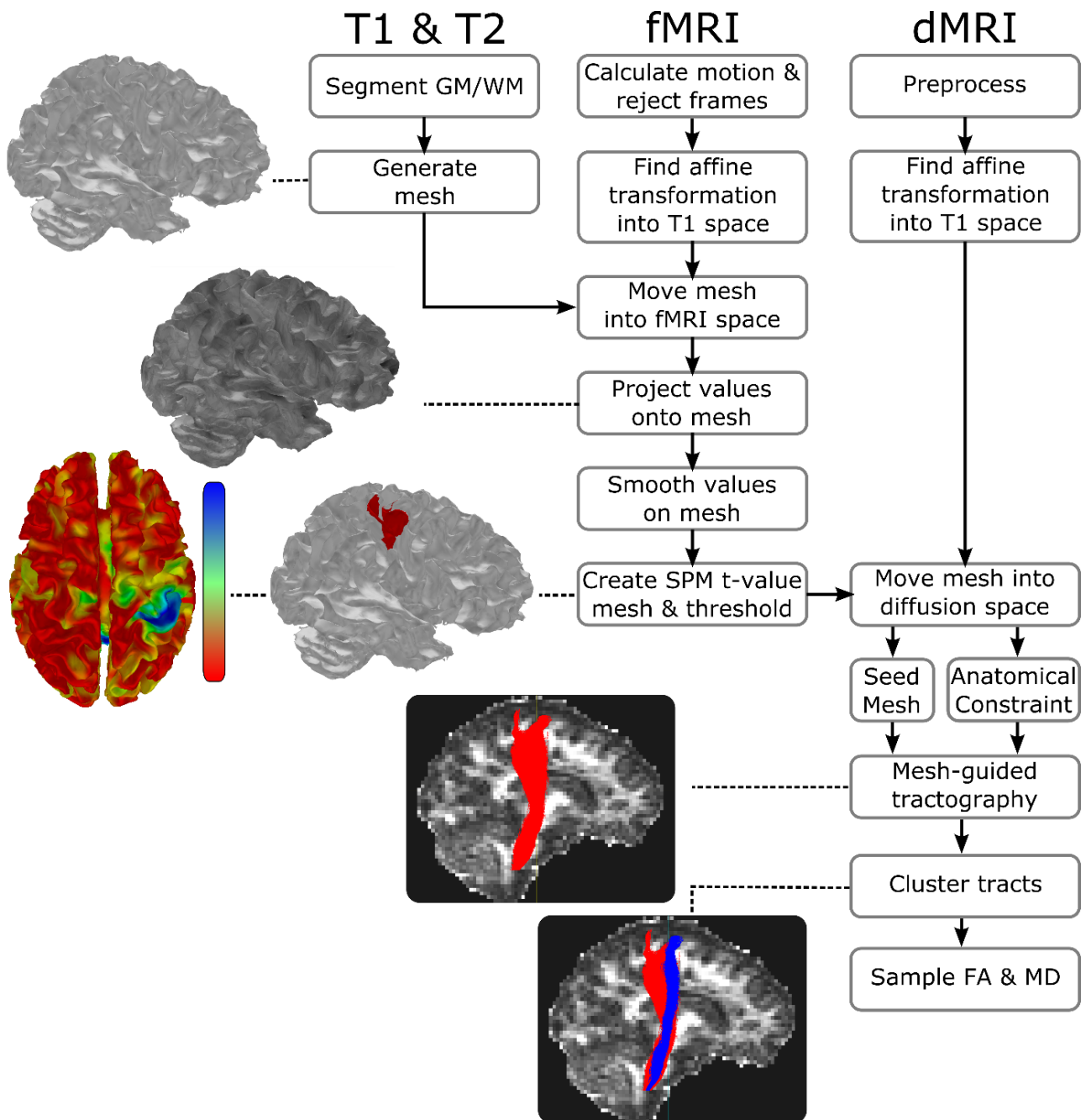


Figure 10. Summary of the pipeline for the Surface-based fMRI-guided dMRI tractography. Images and meshes associated with each major step depict real results from a single participant enrolled in this study. Major steps of the pipeline include tissue segmentation, mesh generation, projection of fMRI echo-planar image values onto the mesh, statistical fMRI calculation on the mesh, fMRI-seeded tractography, and tract clustering. See text for additional details.

Surface Method

The surface method pipeline is summarised in Figure 10.

Mesh Generation

A mesh of the grey matter-white matter interface was generated using a tissue segmentation driven by an expectation-maximization algorithm that has been described previously.^{183,184} In this study, high resolution T1 MPR (TR/TE: 1900/2.32ms; 0.9mm isotropic) and T2 HASTE images (TR/TE 1500/81ms; 0.69 x 0.69 x 4mm) were used for tissue segmentation, and six age-appropriate atlases (from typically developing children) were utilized for each participant. Two Gaussians were fit to describe to gray-matter tissue intensities, and one Gaussian was fit to each of the other tissue classes. To improve this segmentation, a white-matter exclusion mask was generated by dilating the inverted brain mask three times. Clusters of voxels classed as WM were reclassified as gray matter if they both (i) overlapped this mask at any position and (ii) were smaller than 40 voxels in volume. The marching squares algorithm then produced a mesh of the gray-matter/white-matter interface with a mean vertex-to-neighbour-vertex distance of ~0.9mm. Meshes were in participant T1 space and checked visually before further analysis.

Surface-based fMRI

Two block-design task-based fMRI scans, each consisting of 90 echo planar images (TR/TE 3000/30ms; 3mm isotropic; full brain coverage), were collected for each participant in a single scan session on a Siemens Tim Trio 3T (Siemens, Erlangen, Germany) scanner. Distortion correction was applied online by the scanner. Each scan consisted of nine 30-second blocks, alternating between 'stop' and 'move' conditions. A visual cue consisting of the words 'stop' or 'move' was visible at all times, in addition to an auditory click that was delivered at 1Hz. Participants were instructed to tap their hand, by full extension at the wrist, in time with this cue in the 'move' condition, and to remain still during the 'stop' condition. Participants who were unable to perform a full-wrist extension due to physical impairment were asked to perform the largest tap that they could comfortably maintain (e.g. with fingers) without moving their forearm. Participants tapped using their more able hand in the first scan and more impaired hand during the second scan. We shall refer to these as the 'able' and 'impaired' hand tasks for brevity, but it should be noted that many participants displayed some degree of impairment in their more-able upper limb. These tasks were practiced out of the scanner immediately before the session began.¹³ During the scan, an observer noted the quality of movements, the number of successful taps per block, as well as timing and degree of any body movements.

The long block lengths used in this scan eliminated the need for slice-timing corrections and reduced the potential impact of abnormal haemodynamic responses, which have been documented multiple times in participants with brain injuries.^{155,159,160}

Motion and Projection: The required coregistration between EPI images was estimated using `mcflirt`,¹⁸⁵ and applied to each frame's header (i.e. without reslicing). The registration between the T1 and mean EPI image used by `mcflirt` were calculated using the `epi_reg` script from FSL 5.0, which utilises boundary-based registration to generate rigid registration parameters.¹⁸⁶ The mesh was then moved into EPI space using these parameters, and visually inspected. To ensure analysis of grey-matter activation, the registered mesh was expanded outwards by 1mm before values were projected onto each vertex mesh using nearest-neighbour interpolation. The result for each dataset was a motion corrected cine-mesh of grey-matter EPI intensities.

Head motion larger than 2mm is common in children with cerebral palsy during fMRI scans, which can preclude standard fMRI analyses. Framewise displacement¹⁶⁵ was, therefore, calculated and frames with a framewise displacement above 0.9mm were rejected. Datasets with 20 or more rejected frames across the two fMRI scans were excluded from further analysis.

On the surface, our original node-to-node distance was around three times the EPI image resolution. Decimation was employed to halve the number of triangles in the mesh. This reduced computational complexity, whilst maintaining a sufficiently high-resolution surface to represent the underlying image data accurately. Surface-based smoothing of vertex values was then carried out using a Laplacian-Beltrami filter.¹⁸⁷ An 8mm FWHM smoothing kernel was selected based on the large cortical representation for hand and forearm movements described in anatomical studies of healthy participants¹⁸⁸ and fMRI studies of children with cerebral palsy.^{68,105}

Analysis: Required SPM 8 code was ported into the .NET framework and modified to accept meshes, rather than images, as input for all fMRI processing steps. Meshes were treated as two dimensional surfaces with anisotropic spacing between vertices. Due to frame rejection in the previous step, aspects of this code were changed to avoid implicit assumptions that frames were evenly spaced temporally. In line with a previous report,¹⁶⁵ preliminary analyses demonstrated that the addition of translation (head-motion) parameters as GLM regressors in the presence of motion censoring made little difference to the degree of motion artefacts in participants with movement (visually assessed). Furthermore, in some instances these parameters sufficiently reduced the statistical power to the point where plausible significant activation shrank visibly in participants demonstrating weaker activation. Because of this, we included only rotation parameters as covariates-of-no-interest for our analysis. A high-pass filter of 120s and the standard SPM8 hemodynamic

response function were used. Temporal autocorrelation was modelled using the standard white noise and autoregressive AR(1) model. Contrasts between ‘move’ and ‘stop’ conditions were calculated for the able- and impaired-hand scans separately, and the resulting standard parametric maps for each scan were thresholded at $p < 0.05$ (FWE corrected) and binarised. Group analyses were not performed for the surface or voxel-based fMRI, as the purpose of the fMRI analysis was to locate the functionally relevant primary sensorimotor area for each individual, rather than interpret activation metrics.

Filtering: Significant activation was often seen in regions such as the supplementary motor area and cerebellum that were not of interest for this particular analysis. The largest plausible activation clusters near the presumed hand knob on the precentral gyri were retained and other activation clusters (including minor motion artefacts) were manually discarded (Supplementary Figure 1). Participants noted to have moderate degrees of motion artefacts in this step were rejected. The two resulting binarised SPM meshes for each participant were then combined with logical ‘OR’ for a final seeding mesh.

Tractography

We acquired a 64-direction high-angular resolution diffusion image sequence with $b = 3000\text{s/mm}^2$,¹⁸⁹ , one $b = 0$ image, whole brain coverage, and $2.34\text{mm} \times 2.34\text{mm} \times 2.5\text{mm}$ spatial resolution (NEX = 1). An extensive preprocessing procedure that has been described previously^{58,190} was utilised to correct for image artefacts caused by cardiac pulsation, head motion, and image distortions. FA and MD maps were calculated using a copy of MRTrix 2.9 that was modified to utilise surfaces as masks during tractography. Constrained spherical deconvolution was used to estimate the fibre orientation distributions utilised for tractography.

The registration between the T1 and FA map was calculated using the `epi_reg` script from FSL. The seeding mesh was returned to the grey-matter/WM interface in T1 space, then registered to diffusion space using these parameters. At this stage, the seeding mesh was duplicated to provide an anatomically-constraining mesh (mesh ‘brain mask’). The seeding mesh was then shrunk inward 1mm at all points to ensure tracks started in the WM.

As we were interested in both the thalamocortical and corticomotor tracks, two-dimensional inclusion ROIs of (1) the thalamus and (2) the posterior limb of the internal capsule were drawn with ITK SNAP¹⁹¹ on a 1mm-isotropic track density image¹⁹² at the most superior axial slice inferior to the corpus callosum (Figure 11). An inclusion ROI of the brainstem was drawn on the first axial slice inferior to the pons. ROIs were drawn by a researcher blinded to participants’ clinical scores. For each participant, a target of 20,000 tracks were generated that passed from the seeding region, through either of the midbrain ROIs, then terminated in the brainstem ROI. A similarly-drawn two-

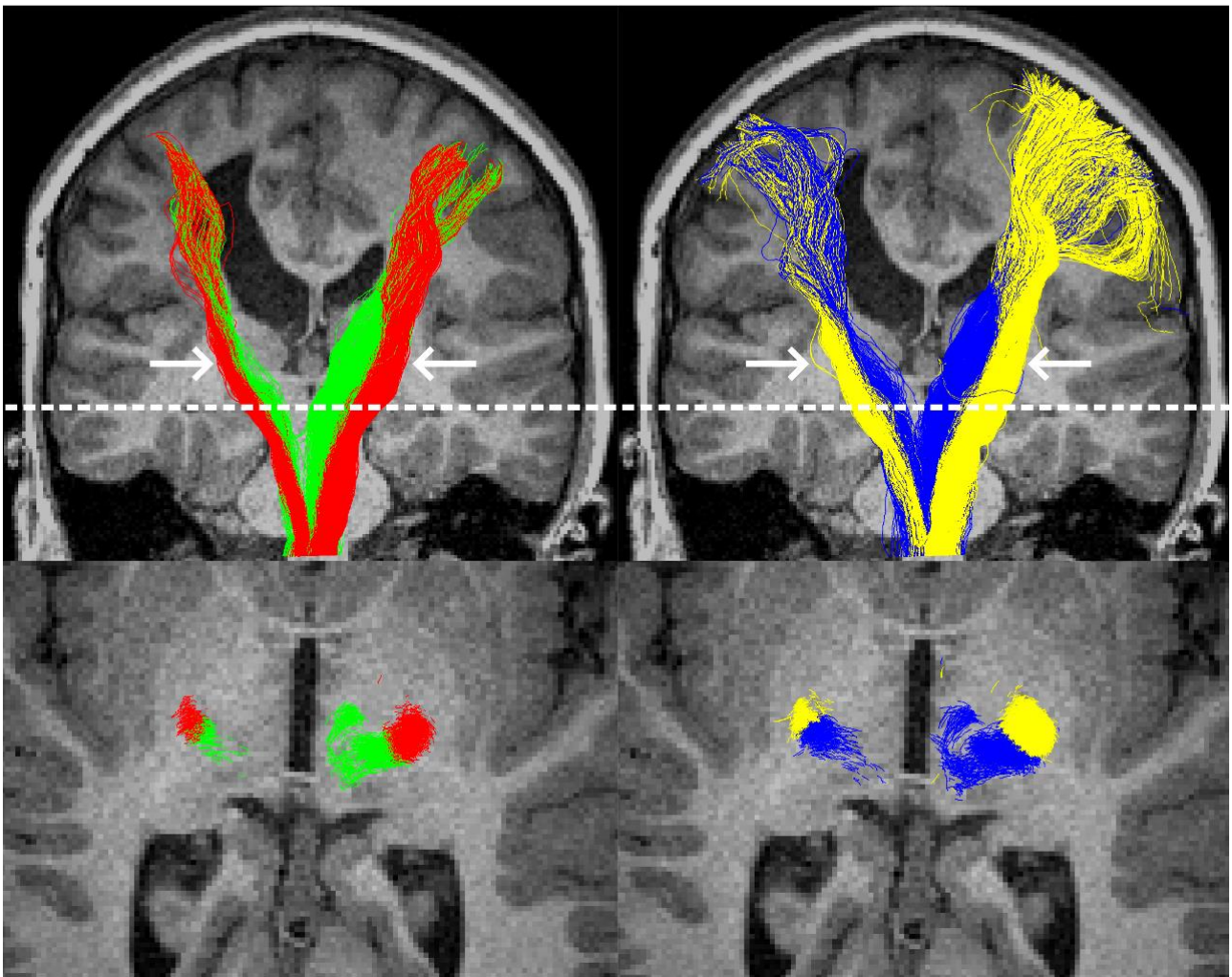


Figure 11. Example tractography from the surface-based (left column) and voxel-based (right column) methods, in a single participant with left-hemispheric pathology. The top row shows all tracks from all slices, with thalamocortical tracts in green or blue and corticomotor tracts in red or yellow. In this participant, the superior sections of the tracts were considerably more coherent when delineated with the surface-based method. The bottom row shows an axial slice at the level of the dotted white line. For this participant, at this level, track clustering (left) provided visually similar results to the region-of-interest based approach to track classification. Arrows indicate the approximate location of the midbrain regions of interest that were used to filter tracks.

dimensional ROI of the corpus callosum was used as an exclusion mask to exclude inter-hemispheric connections.

Seeding for probabilistic tractography took place from all triangles consisting of three neighbouring vertices that survived the statistical thresholding described earlier. Seeding was probabilistic and approximately uniform across the seeding area: the likelihood of each triangle being chosen to be seeded from on any given iteration was linearly-proportional to its surface area. The seed positions within each triangle were random and resultantly uniform. The initial direction for each track was inward, and perpendicular to the triangle from which it was seeded from. Tracks were terminated upon entering any voxel with an $FA \leq 0.1$ or crossing any triangle in the anatomically-constraining mesh. A step size of 0.2mm and minimum curvature radius of 1mm were used.

Semi-Automated Track Identification: In preliminary analyses, manually drawn 2D posterior-limb-of-the-internal capsule and thalamic ROIs often proved ineffective for filtering thalamocortical from corticomotor tracks, primarily due to the partial overlap of such tracks in the midbrain. Manually drawing 3D ROIs, however, is extremely time consuming, especially in the presence of pathology or with large numbers of participants, and may be subject to human biases. To circumvent this problem, tracks were classed as either thalamocortical or corticomotor using the following two stage k-means clustering algorithm.

Track identification used a standard k-means clustering algorithm. Input was a single MRTrax track file containing all tracks passing from the assumed sensorimotor cortices, through the posterior limb of the internal capsule or thalamus, and to the brainstem inferior to the pons. Care was taken to draw the 2D midbrain ROIs as accurately as possible in this study due to the voxelwise analysis' reliance on these ROIs. Experimentation suggested that clustering algorithm was very robust to roughly drawn ROIs, however, including when ROIs overlapped by several voxels in areas of uncertainty.

The first stage of the process split input tracks into those in the left and the right hemispheres. The mean features of each cluster were initially set to the features from a random track. The algorithm was allowed a maximum of two clusters. Each track was converted into four features: the X and Y coordinates of a track's first node (i.e. at the cortex), and the X and Y coordinates of the first node inside either of the midbrain ROIs, in standard space. Upon each iteration, the clustering algorithm assigned each track to the cluster that minimised the following cost function:

$$Cost = \sum_{i,f} (t_{i,f} - \mu_f)^2$$

Where t_i indicates track i , feature f , and μ_f indicates the mean value for feature f of the cluster in question. Convergence was defined as when no tracks were swapped between clusters on an iteration, or when 1000 iterations was reached. Clustering was attempted three times; results from the attempt with the lowest global cost were kept. The resulting clusters were automatically defined as either left- or right-hemispheric, based on their mean midbrain coordinates.

The second stage of the process separated motor from thalamic tracks, and was run on each hemisphere's tracks separately. Twelve features were selected: the X and Y coordinates of the first node inside either of the midbrain ROIs; the X, Y, and Z coordinates of the 50th node after (inferior to) the midbrain ROI; the X, Y, and Z coordinates of the node 50 nodes before the end of the track; the X and Y coordinates of the final node (i.e. brainstem); whether the track passed through the

posterior limb of the internal capsule ROI (0 or 1); and whether the track passed through the thalamic ROI (0 or 1). The cost function used for this stage was:

$$Cost = \sum_{i,f} (t_{i,f} - \mu_f)^2 \times w_f$$

Where w_f indicates weight for feature f for the current cluster, and other parameters have identical meaning to those in the previous equation. Weights were based predominantly on expected anatomy, but fine-tuned during preliminary analyses on four-participant datasets. For the thalamocortical cluster, all weights had a value of 1. For the corticomotor cluster, the weight for the midbrain Y coordinate was 0.49, reflecting the elongated shape of this tract at the midbrain; and weights were 1.69 for the X, Y, and Z coordinates at the 50th node inferior to the midbrain, reflecting high spatial coherence at this position. Other weights for this cluster were 1. The thalamocortical cluster was initialised with the track closest to a point 5cm posterior to the centre of the brain. The corticomotor cluster was initialised with the track that was furthest from this posterior-central point at the midbrain ROI, with only those that passed through the medullary pyramids as eligible. The medullary pyramids in this context were defined as the anterior third of the brainstem ROI, or as the anterior third of all brainstem nodes if no tracks were found with the ROI criteria. Iteration and convergence criteria were identical to the previous stage. Clustering was attempted 20 times; results from the attempt with the lowest global cost were kept.

With exception of the manually drawn 2D ROIs, the entire track identification process was entirely automated and ran in under 30 seconds per 20,000 track dataset on a standard desktop PC.

Voxel-Based Method

The voxel-based approach was carried out on the same dataset as the surface approach.

Voxel-Based fMRI

Analysis. The voxel based fMRI was carried out with a standard pipeline using SPM 8. As motion scrubbing is not available in this package, frames that were excluded from the Surface-based analysis due to movement were replaced with interpolated frames for this analysis. As with the surface analysis, an 8mm smoothing kernel was used. Other parameters and contrast were identical to the surface fMRI analysis. The resulting t-value maps were resliced into dMRI space using the same transform used for the surface analysis, before being thresholded at $p < 0.05$ (FWE corrected) and binarised.

Filtering. Filtering of significant clusters followed the same protocol as for the surface-based approach. For the voxel-based approach, activation maps were overlaid with structural (T1) images during this procedure to ensure correct filtering.

Tractography

Tractography was carried out on the same diffusion images used for the surface-based analysis. The same inclusion ROIs were used as the surface based method to identify a target of 20,000 tracks passing from the cortex to the brainstem via the midbrain. Filtered fMRI activation from the previous step was used to seed tractography bi-directionally, with the brainmask used as a stop mask. Other parameters were identical to the surface-based method.

Tracks passing through the posterior limb of the internal capsule at any point were classed as corticomotor tracks; tracks passing through the thalamus and not the posterior limb of the internal capsule were classed as thalamocortical tracks.

Tract Dispersion

One argument made for our surface-based approach was to reduce the number of non-relevant tracts included in tractography. If only tracks from a single white-matter bundle are identified, these tracks should be directionally coherent. To quantify this, we calculated tract dispersion for each motor and sensory tract as the mean square error in stepping direction at 20 node-positions that are evenly spaced across each track (i.e nodes at 0%, 5.3% ... 94.7%, 100% of track length). Error here was defined as the geodesic difference from the mean direction (at that point of the track) across all tracks in the collection. Conceptually, if tracks are pointed in similar directions at equivalent nodes

throughout their length, dispersion will be low. If tracks are commonly pointed in different directions at these equivalent positions, dispersion will be high. Mathematically:

$$\text{dispersion} = \frac{\sum_{n=1}^{20} \sum_i^t \left(\text{Geo}(\theta_{n,i} - \bar{\theta}_n, \phi_{n,i} - \bar{\phi}_n) \right)^2}{20t}$$

where n is the node-position; t is the number of tracks in the collection; $\theta_{n,i}$ indicates inclination of direction at node-position n , track i ; $\bar{\theta}_n$ indicates the mean inclination across all tracks at node-position n ; $\phi_{n,i}$ indicates azimuth of direction at node-position n , track i ; $\bar{\phi}_n$ indicates the mean inclination across all tracks at node-position n ; and Geo is the function for calculating geodesic distance. Each spherical coordinate was calculated from the Euclidean coordinates, in standard space, of the node at node-position n , and the immediately following track node.

Tract dispersion was calculated to compare not only the voxelwise and surface-based methods but also to determine whether the track clustering algorithm positively influenced the coherency of the surface-based tractography method.

Diffusion Metrics and Clinical Assessments

Diffusion metrics were calculated identically for the Surface and Voxel-Based approaches. FA and MD values were calculated with MRTrix 2.9 using CSD images. Each tract was split into superior (superior to the midbrain ROI) and inferior segments (inferior to the midbrain ROI), to provide measures for these locations separately. Asymmetry indices of sampled FA and MD measures were calculated the formula $AI = (A-I)/(A+I)$, where A and I refer to the mean sampled values for the hemispheres opposite to the ‘able’ and ‘impaired’ hands, respectively. Asymmetry indices were adjusted for age and correlated with five clinical assessments. Correlations were conducted for all successfully processed datasets from the voxelwise method, all successfully processed datasets from the surface-based method, and all datasets successfully processed by both methods. Clinical assessments were carried out on the same day as scanning. These assessments were the Assessment of Motor and Process Skills motor component (AMPS-M),¹⁹³ a observational assessment of the quality of performance of activities of daily living; the Melbourne Unilateral Upper Limb Assessment (MUUL)¹⁹⁴, an objective measure of upper-extremity function; The Assisting Hand Assessment logit (AHA), an index of the impaired hand as an assisting hand in bimanual tasks; the Jebsen-Taylor Hand Function Test asymmetry indices (JHFT-AI), a test of uni-manual hand speed and dexterity, converted here into an asymmetry index; and The Canadian Occupational Performance Measure performance score (COPM-P), the participants self-reported satisfaction with their ability to carry out everyday tasks.

Results

Participants, fMRI, and Movement

Of the 37 children included in this investigation, four demonstrated clear head movement in time with hand tapping—a consequence of participants exerting substantial effort in order to achieve muscular contraction and/or an inability to dissociate hand from total body movement. Two additional children who were not noted as exhibiting excessive motion during scanning still demonstrated framewise displacement greater than 0.9mm in more than 20 frames. After exclusion of these participants, 31 children remained. Across the remaining datasets, the mean and median numbers of rejected frames were 4.6 and 1, respectively. The rejected frame counts did not correlate significantly with any clinical score (all $p > 0.05$ and $R^2 < 0.1$). Scans revealed large bilateral pathology in three of the remaining participants (despite being clinically assessed as unilateral CP). These participants were still processed to determine the success of the investigated methods in the presence of such pathology, but were excluded from final correlation analyses as asymmetry indices would be a poor reflection of tissue integrity in these instances.

Surface Method

Automated tissue segmentation succeeded in 30 of 31 participants, including several with moderate or severe pathology and both participants with distinct bilateral injury (Figure 12D). Of these, minor manual editing to delineate dura from brain tissue was required in two instances. Tissue segmentation failed in one case where severe pathology was present (Figure 12A); cost-function marking or manual delineation of pathology may have allowed segmentation to succeed in this case but was not attempted. Generation of the surface mesh from segmentation succeeded in all instances. Segmentation and mesh generation time took ~75mins per participant on a desktop PC.

Functional MRI analyses were completed successfully for the 30 remaining participants. Figure 13 shows an example of activation in the presumed sensorimotor cortex (S1M1) and anterior lobe of the cerebellum for a single participant during the ‘impaired’ hand task. Significant activation was seen in the region physically resembling the S1M1 for all of the 60 tasks across the 30 participants (Table 5). This was bilateral in seven instances (six during the able task). Significant activation was also seen in the supplementary motor area (16 participants), anterior lobe of the cerebellum (21 participants), and superior parietal lobule (7 participants). Such activation was discarded prior to tractography. Small areas of significant activation that were considered to be motion artefacts or statistical anomalies also appeared in thresholded results for eight participants, and were similarly discarded. In no instance were motion artefacts severe enough to justify rejection of the participant.

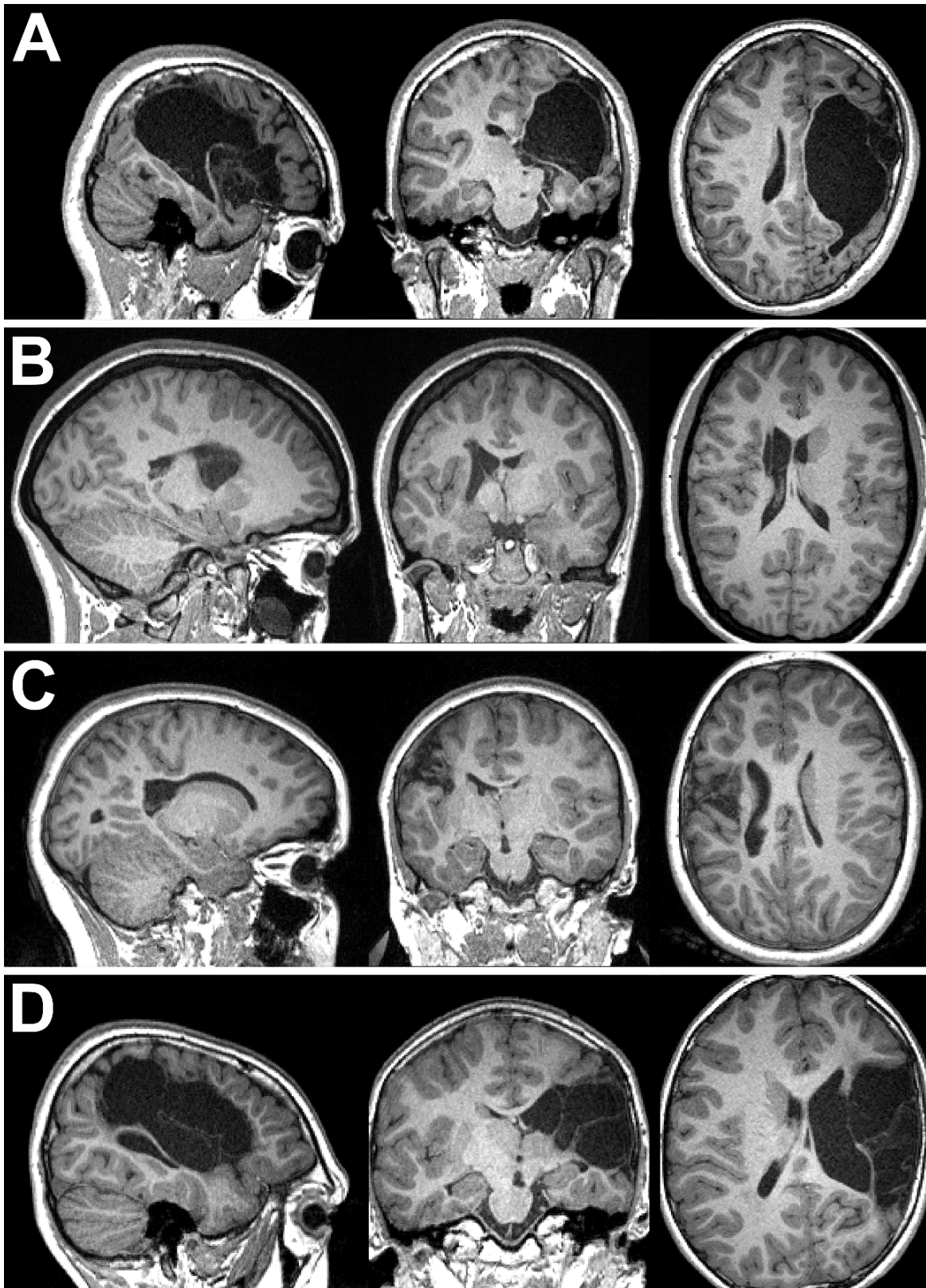


Figure 12. Examples of pathology and impacts on analyses. Row A: The child for whom a surface could not be generated. Tissue segmentation failed as the allowed magnitude of warping was insufficient to match any atlas, leading to cerebrospinal fluid being classed as grey and white matter. Voxelwise analyses were successful. Rows B and C: Two participants for whom surface analyses were successful, but voxelwise analyses failed to detect significant fMRI activation. Row D: A child with severe pathology for whom both voxelwise and surface analyses detected fMRI activation. Both methods found no corticomotor or thalamocortical tracks in the hemisphere with pathology; no genuine connections of this type were probably present.

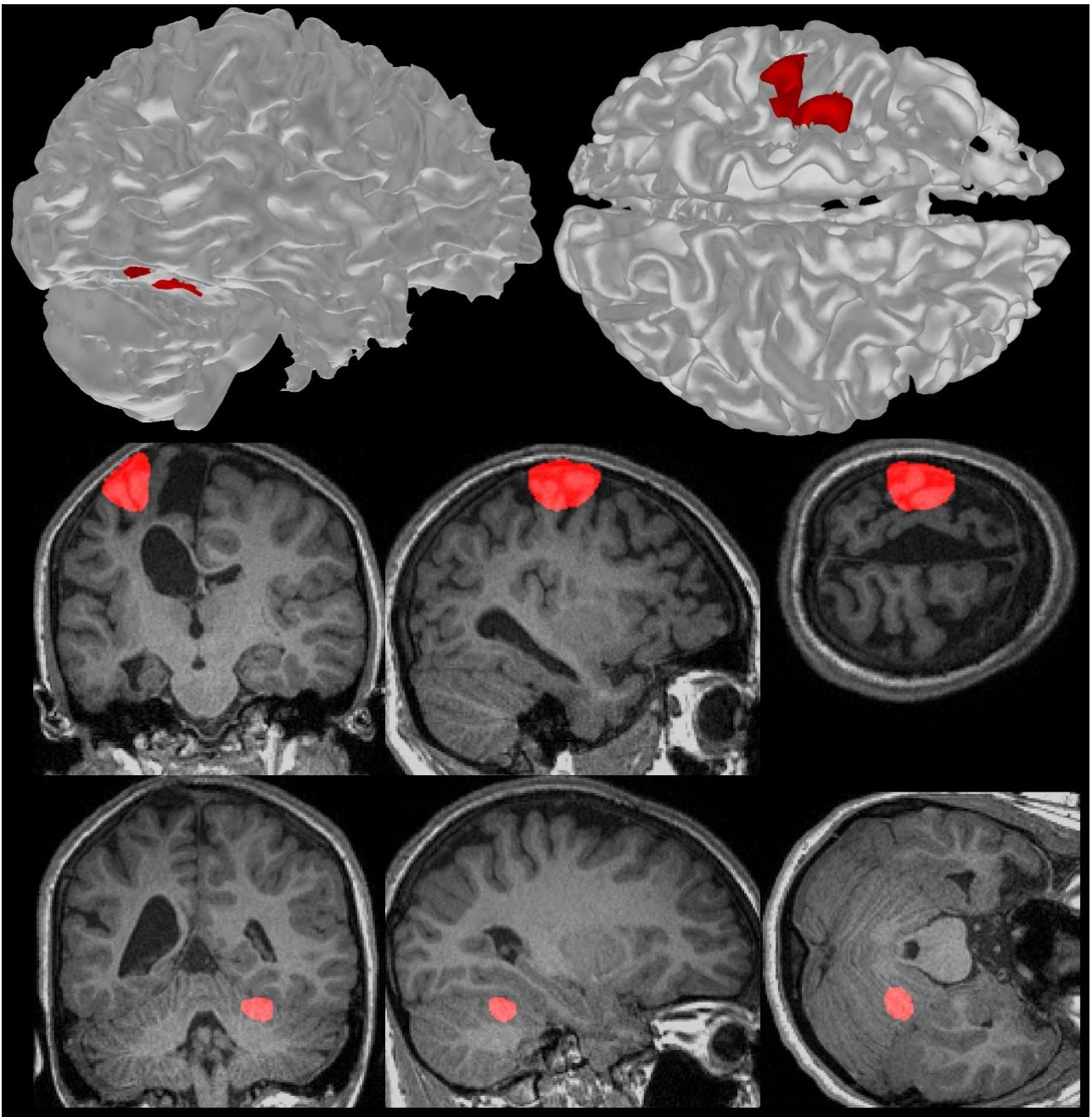


Figure 13. Typical significant fMRI activation detected through surface (top row) and voxelwise (middle and bottom rows) methods for tapping of the 'impaired' hand in a single participant. The middle and bottom rows show coronal, sagittal, and right-facing axial sections in the left, middle, and right columns respectively. Both methods show activation (red) in the approximate pre- and post-central gyri of the left hemisphere, and the right anterior lobe of the cerebellum. The voxelwise analysis resulted in approximately oval shaped activations that include grey-matter, white-matter, and cerebrospinal fluid. The surface-based method resulted in less-uniformly shaped activation patterns and two activation sites on the cerebellum.

Surface Method (n=30)

	S1M1		SMA	Ant. Cerebellum	SPL	None
	Unilateral	Bilateral				
Able Hand Task	24	6	14	19	4	0
Impaired Hand Task	29	1	10	10	3	0
Either	30	7	16	21	7	0

Voxel Based Method (n=30)

	S1M1		SMA	Ant. Cerebellum	SPL	None
	Unilateral	Bilateral				
Able Hand Task	24	2	10	14	3	0
Impaired Hand Task	23	2	8	6	2	6
Either	29	3	14	16	4	6

Table 5. Counts of Participants Displaying Significant Activation. Significant activation was defined as values of $p < 0.05$ FWE in three or more connected vertices (Surface method), or one or more voxels after reslicing to diffusion space (Voxel-Based method), for five motor regions. 'Either' refers to the number of participants in which the specified activation pattern was seen for either task performed. None indicates that no significant activation was seen in any of these regions in either task. Abbreviations: Ant. Cerebellum, anterior lobe of the cerebellum; S1M1, sensorimotor cortex, comprising of the precentral and post central gyri; SMA, supplementary motor area; SPL, superior parietal lobule.

To alleviate concerns that tractography correlations could be the product of different degrees of fMRI activation, we calculated correlations between thresholded-fMRI activation area in the presumed S1M1 and clinical scores. Data from all 30 remaining participants were used. No informative correlations between clinical scores and impaired-hemisphere activation area, or activation-area asymmetry, were found (all $R^2 \leq 0.15$).

Voxel-Based Approach

Voxel-wise fMRI was completed acceptably in 30 of 31 participants: one participant-dataset was rejected due to the presence of severe motion artefacts. Significant activation was seen in the region physically resembling the S1M1 for 51 of the 60 tasks across the remaining participants (Table 2). This was bilateral in four instances (two during the able task). Compared with the surface method, clusters of significant activation were seen less frequently in the supplementary motor area, cerebellum, and superior parietal lobule (Table 5), but, visually, appeared to more frequently span

multiple functional areas (e.g. both S1M1 and the supplementary motor cortex; data not shown). Thalamic activation was seen in two participants. Six participants displayed no significant activation during the impaired hand task (Figure 12). As our metrics were based on a ratio between hemispheres, nine participants who displayed significant S1M1 activation in only one hemisphere (across their two tasks) were excluded from further analysis.

No informative correlation was found between clinical scores and impaired-hemisphere S1M1 activation-volume, or activation-volume asymmetry (all $R^2 \leq 0.10$; $n = 30$). Results were similar when this analysis excluded the nine participants displaying unilateral-activation, with exception of activation volume asymmetry, which correlated weakly with JHFT-AI ($R^2 = 0.24$).

Tractography

For the surface method, no or very-few tracks were found on the side of the brain with pathology in three participants (Figure 12D). Based on inspection of structural MRIs, it was highly plausible that these participants were ipsilaterally-organised for one or both of these tracts. These participants were excluded from further analysis. Tractography and clustering in the remaining 27 participants was successful (visually assessed; Figure 11). It is noteworthy that clustering provided sensible results for one participant with pathology to the midbrain, and in one excluded participant who lacked thalamocortical tracks in the hemiplegic hemisphere (data not shown).

For the voxel-based approach, one participant was excluded from analysis as tractography was unable to find sufficient tracks on the side of the brain with pathology. This participant was likely to be ipsilaterally organised (Figure 12D). Tractography was successful in the remaining 20 participants.

Tract dispersion was calculated for each tract in the 18 participants for whom tractography was successful using both methods. Tracts generated by the voxel-based approach had significantly poorer (i.e. wider) dispersion than those generated by the surface-based method for the ipsilesional thalamocortical, contralesional thalamocortical, ipsilesional corticomotor, and contralesional corticomotor tracts (all $p < 0.01$; Wilcoxon signed-rank test with Holm-Bonferroni Correction for multiple comparisons).

To calculate the influence of track clustering on tractography results, the surface method was re-run using midbrain ROIs to classify tracks. In this sub-analysis, no ipsilesional thalamocortical tracks were able to be identified for 5 of the 27 datasets. This ROI approach provided significantly poorer dispersion for the ipsilesional thalamocortical ($p < 0.01$), contralesional thalamocortical ($p < 0.01$), and contralesional corticomotor ($p < 0.05$) tracts (Wilcoxon signed-rank test with Holm-

	Superior Thalamocortical		Superior Corticomotor	
	FA	MD	FA	MD
Surface Method (n=24)				
AMPS-M	ns	0.33	0.43	0.26
JHFT-AI	ns	0.48	0.37	0.55
COPM-P	0.23†	0.33	0.28	0.26
AHA	ns	0.41	0.34	0.42
MUUL	ns	0.47	0.34	0.46
Voxelwise Method (n=18)				
AMPS-M	ns	ns	ns	ns
JHFT-AI	ns	ns	0.44	ns
COPM-P	ns	ns	ns	ns
AHA	ns	ns	0.27†	ns
MUUL	ns	ns	ns	ns

Table 6. Correlations (R^2) between clinical scores and age-adjusted diffusion metrics recorded via tractography for two tracts superior to the midbrain ROIs. Correlation analyses included all participant-datasets possible. ‘ns’ indicates that correlations were not statistically significant ($p \geq 0.05$). † indicates values that were not significant but for which $p < 0.1$. Abbreviations: AHA, The Assisting Hand Assessment logit; AMPS-M, Assessment of Motor and Process Skills motor component; COPM-P, The Canadian Occupational Performance Measure performance score; FA, fractional anisotropy; MD, mean diffusivity; MUUL, the Melbourne Unilateral Upper Limb Assessment; JHFT-AI the Jebsen-Taylor Hand Function Test asymmetry index.

Bonferroni Correction for multiple comparisons). Despite this poorer performance, all four types of tract generated by the surface + ROI method were still significantly more coherent than those generated by the voxelwise method in identical participants (all $p < 0.01$; Wilcoxon signed-rank test with Holm-Bonferroni Correction for multiple comparisons).

Diffusion Metrics

Surface Method

After exclusion of the three participants with large bilateral injuries, 24 participant-datasets were available for correlations between age-adjusted diffusion metrics and clinical scores. For the upper corticomotor tract, both MD asymmetry and FA asymmetry correlated significantly ($p < 0.05$) with all five clinical scores investigated (Table 6). For the upper thalamocortical tract, MD asymmetry correlated significantly ($p < 0.05$) with all five clinical scores investigated, but FA asymmetry was not predictive of clinical scores. FA asymmetry of the lower corticomotor tract correlated significantly with AMPS-M ($R^2 = 0.44$) and JHFT-AI (0.33), and approached significance correlating weakly with AHA logit ($R^2 = 0.24$, $p = 0.06$), but not with other clinical scores. Clinical scores did not correlate

with FA asymmetry of the upper or lower thalamocortical tract, nor MD asymmetry of either lower tract.

Voxelwise Method

After exclusion of the participants with large bilateral injuries, 18 participant-datasets were available for correlation between age-adjusted diffusion metrics and clinical scores (Table 6). Significant correlations were only found between JHFT-AI and FA asymmetry, in the upper ($R^2 = 0.44$; $p = 0.01$) and lower (0.35; 0.04) corticomotor tracts. All other correlations were not significant, although correlations between upper corticomotor FA asymmetry and AHA ($R^2 = 0.27$; $p = 0.07$), and lower thalamocortical FA and JHFT-AI (0.28; 0.09) approached significance.

Analysis with Identical Participants

To determine whether differences between the surface and voxelwise methods were simply due to a difference in participants or participant numbers, correlation analyses were repeated with only the 16 participants with unilateral lesions who were able to be analysed by both methods. Fourteen of these participants had periventricular white matter injury. In this sub-analysis, for the surface method, all correlations between clinical scores diffusion metrics in the upper tracts strengthened considerably (Table 7), as did the correlation between lower corticomotor FA and JHFT-AI ($R^2 = 0.39$), but the correlation between lower corticomotor FA and AMPS-M weakened ($R^2 = 0.31$; $p = 0.08$). Other lower-tract correlations remained non-significant. For the voxelwise analysis, correlations remained for upper corticomotor FA asymmetry with JHFT-AI ($R^2 = 0.49$; $p = 0.01$) and AHA remained (0.38; 0.05), and JHFT-AI and FA of the inferior corticomotor tract reached significance (0.46; 0.02), but all other correlations remained non-significant (Table 7). In this 16-participant group, the number of fMRI frames rejected due to motion was not significantly correlated with any clinical score.

	Superior Thalamocortical		Superior Corticomotor	
	FA	MD	FA	MD
Surface Method				
AMPS-M	0.31†	0.50	0.73	0.50
JHFT-AI	ns	0.58	0.49	0.71
COPM-P	0.30†	0.52	0.37	0.54
AHA	ns	0.54	0.48	0.62
MUUL	ns	0.61	0.43	0.64
Voxelwise Method				
AMPS-M	ns	ns	ns	ns
JHFT-AI	ns	ns	0.49	ns
COPM-P	ns	ns	ns	ns
AHA	ns	ns	0.38	ns
MUUL	ns	ns	ns	ns

Table 7. Correlations (R2) between clinical scores and age-adjusted diffusion metrics recorded via tractography for two tracts superior to the midbrain ROIs. Correlation analyses used the 16 participant-datasets available to both methods. ‘ns’ indicates that correlations were not statistically significant ($p \geq 0.05$). † indicates values that were not significant but for which $p < 0.1$. Abbreviations: AHA, The Assisting Hand Assessment logit; AMPS-M, Assessment of Motor and Process Skills motor component; COPM-P, The Canadian Occupational Performance Measure performance score; FA, fractional anisotropy; MD, mean diffusivity; MUUL, the Melbourne Unilateral Upper Limb Assessment; JHFT-AI the Jebsen-Taylor Hand Function Test asymmetry index.

Discussion

In this study, a novel data-processing pipeline was demonstrated that allows diffusion metrics to be obtained from participants with moderate to severe brain pathology in functionally-relevant regions of the thalamocortical and corticomotor tracts. This pipeline utilised a surface-based fMRI analysis to replace often-problematic parcellation, and minimized cross-sulcal smoothing present in standard fMRI analyses. This mesh was then used to both seed and anatomically constrain tractography that was subsequently dissected into tracts using a clustering algorithm. When applied to children with unilateral cerebral palsy, plausible correlations between diffusion metrics and functional ability were demonstrated, particularly for the superior aspect of the tracts.

Method Comparison

The surface method was able to successfully process substantially more datasets (27) than the voxelwise method (20). This was primarily due to an apparently heightened sensitivity to fMRI activation (Table 5), reflected here by more-frequent detection of activation in supplementary areas, and in S1M1. Similar findings of heightened sensitivity have been reported in other comparisons of surface- and voxel-based analyses.^{149,195}

The surface method was also able to consistently find correlations between symptom severity and diffusion metrics in the superior aspect of the both corticomotor and thalamocortical tracts, but equivalent correlations using the voxelwise method were mostly absent. This was not due to participant numbers or different groups of participants as no obvious bias in dataset rejection in terms of age or ability was identified (Table 4), and reanalysis of these data using matched datasets strengthened correlations for the surface-based approach substantially more than those of the voxelwise approach (Table 7). One potential source of this difference may have been spatial sensitivity: areas of significant activation appeared qualitatively to be better restricted to within the S1M1 in the surface-based approach than rather than the voxel-based approach. This factor was not able to be quantified here, as this would require atlas-based parcellation, but better spatial specificity for surface or surface-like methods have been reported in several other studies.^{149,182,196,197} Tracts elucidated using the surface method were also significantly more coherent, indicating that they each better represent a single population of fibres, than those generated via the voxelwise method. This was likely not only due to the tractography seeding, but also due to the clustering method, which resulted in superior track dispersion compared to ROI-based filtering. The surface-based tractography may have also played a role by preventing tracks from crossing sulcal boundaries in locations where the FA cut-off was undermined by partial volumes of grey and white matter (Figure 11).

It may be argued that the primary issue with the voxelwise analysis is the use of 2D, rather than 3D, midbrain ROIs. It is certainly possible that these results may have improved with 3D ROIs, but in any dataset where pathology prevents parcellation, these 3D ROIs must be manually delineated, which is very time consuming and difficult to perform accurately, even with super-resolution track density images. Even with 3D ROIs, the best method to classify tracks is not obvious, as the majority of thalamocortical tracks will also pass through voxels containing the posterior limb of the internal capsule at some point. Better voxelwise tractography may have resulted from a smaller fMRI blurring kernel, but the sensitivity of the fMRI analysis will likely have also suffered, resulting in rejection of even more participants than was seen here. Higher statistical thresholds are an alternative approach to constraining fMRI but, again, reduce the sensitivity of the fMRI analysis and may result in additional participant rejection. Tailoring statistical thresholds to each individual are a related approach but raises issues of data equivalency when data is pooled. For example, if one participant must have a threshold set at $p < 0.05$ FWE, but another must have it as low as $p < 0.005$ FWE, is the resultant tractography functionally equivalent? Surface based methods, however, provide equal-or-better statistical power than voxel-based smoothing,¹⁴⁹ without such issues. For this reason we believe that surface smoothing is more appropriate for group-wise studies.

Clinical Findings

In this study, significant correlations were found between five clinical scores of motor ability (AMPS-M, JHFT-AI, COPM-P, AHA and MUUL) and MD of the superior (i.e. cortical) section of both the thalamocortical and corticomotor tracts (Table 7). These scores also correlated with FA of the upper corticomotor tract, but not of the upper thalamocortical tract. Previous studies of unilateral cerebral palsy in non-overlapping subject cohorts have reported moderate correlations between FA of these tract sections and AHA,⁵⁸ as well as between corticothalamic tract streamline-count asymmetry and JHFT, MUUL, and AHA.⁵¹ Our findings here contrast with the latter of these studies, which concluded that damage to the sensory tracts may hold more importance to clinical outcomes than damage to the motor tracts. Rather than contradicting the hypothesis that thalamocortical tracts are ‘more influential’ for function than motor tracts, this discrepancy more likely highlights that this condition is highly heterogeneous, and complex. I.e. the relative influences of lesions depend on additional factors such as the lesion’s type, specific location, and timing. The results presented from the two methods used here also highlight how different quantification methods can have distinctly different patterns of sensitivity. It is worthy of note that our analysed data came overwhelmingly from participants with unilateral periventricular white-matter injury (Table 4), and so results may not be generalizable to other forms of CP.

There were very limited correlations found between functional clinical scores and diffusion metrics of the inferior section of the tracts investigated. This is an interesting result, considering the strong correlations found for the superior aspects of the tracts. In one respect, this is not unexpected as all participants in this study had either diffuse axonal injury, or injuries predominantly at or superior to the level of the midbrain. If taken at face value, this would indicate that upper-tract damage, long term, is not strongly reflected further along those tracts, as may be expected from Wallerian degeneration or constrained neurological development. An alternative explanation is that the tensor diffusion metrics used here are not sufficiently sensitive to measure such differences, especially when measuring voxels that include ‘unimpaired’ fibre populations. Some evidence for this hypothesis was identified using apparent fibre density⁷⁹ as a metric, but due to uncertainties regarding the effects of intensity normalisation, we did not formally include this metric in this analysis. More advanced measures, such as ‘SIFT’ed track counts¹⁹⁸ are one way that this could be resolved, but these currently rely on full-brain tractography and require midbrain parcellation, which is not currently possible to automate in participants with the levels of pathology seen here. A final possibility is that these structures are impaired more bilaterally than more superior aspects of the tracts, limiting the sensitivity of asymmetry measures. One earlier study of unilateral cerebral palsy has provided some evidence for this hypothesis, finding that periventricular WM lesions are often associated with bilateral cortical or deep grey-matter lesions.⁶³

Strengths and Limitations

One potential criticism of fMRI-dMRI methods, including these, is that acceptable quality functional scans are required for each participant, which can be difficult to achieve, and so such methods offer little-to-no advantage over the traditional parcellation-based approach. In our experience, acquiring most types of MRI in children with simultaneous learning and physical impairments can be a challenge as such disabilities can impair their ability to remember and follow instructions. In this study, four of the six excluded participants were excluded due to unconsciously nodding while tapping, a consequence of participants exerting excessive effort to achieve meaningful isolated muscular contraction. The issue of movement was thus primarily an instructional one that may be preventable in future studies by allowing extra practice time before scan sessions, or more dedicated preparation procedures.¹⁹⁹ These rates of data rejection are still lower than our earlier attempts to parcellate brains using Freesurfer, where we were unable to successfully process ~30% of participants with only mild to moderate pathology. Another option is manual parcellation, but this is costly in terms of time, may introduce biases or errors. These issues aside, the primary advantages to fMRI-based seeding are that they enable investigation into participants with obvious pathology, who would otherwise be continually excluded from analyses. Functional MRI based seeding also theoretically

provides higher specificity in tract identification than parcellation-based approaches. This is not only because fMRI tasks can be designed to provide specific subregions (e.g. the hand knob), but also because there is little certainty that regions defined by parcellation accurately identify only the desired functional areas when used in brains that have undergone atypical development or reorganisation. A final option is to use hand-drawn ROIs of the brainstem and midbrain, and track toward the cortex without use of any cortical ROIs. For identification of the entire corticomotor tract this is the obvious solution, though a degree of stray-track pruning may be required if tract metrics wish to be measured. There are numerous situations in which this is not sufficient however, such as studies looking at the relationship between upper limb abilities and diffusion metrics, or attempts to measure rehabilitation-evoked plasticity. In such studies, it is critical to identify the location specific to the upper-limb (or other body part) in question. Failure to do so can undermine sensitivity and biological interpretability of any resultant metrics.

A related criticism is that task fMRI results can be variable,¹⁸¹ and so could lead to differences in tractography that do not exist anatomically. We concede that single-participant activation maps based on a single time point are prone to such variability. Head motion can often correlate with participant ability,²⁰⁰ but was controlled for to the best of our ability in the present study. Task performance may also affect fMRI activation maps,¹⁸¹ but we aimed to minimise any such effects by utilising a very simple task and ensuring adequate task performance for each participant. Activation volume and area did not correlate meaningfully with clinical scores, so are unlikely to have biased diffusion results. Even with such controls, all fMRI-based seeding methods, particularly when applied to participant data that cannot be pooled, are at risk of fMRI variability leading to spurious correlations. This must be weighed up against the opportunity fMRI provides to perform tractography in datasets that otherwise would be discarded from atlas-based analyses. Regarding our method comparison, however, we consider it unlikely that the surface-based method outperforming the other in almost all aspects was simply a product of biased seeding. This is because these methods utilised identical raw data, and so we should expect task-difficulty differences or other sources of variation to equally influence both methods investigated. I.e., it is unclear how sources of fMRI variability could artificially generate correlations between diffusion and clinical-test metrics for only one of these methods.

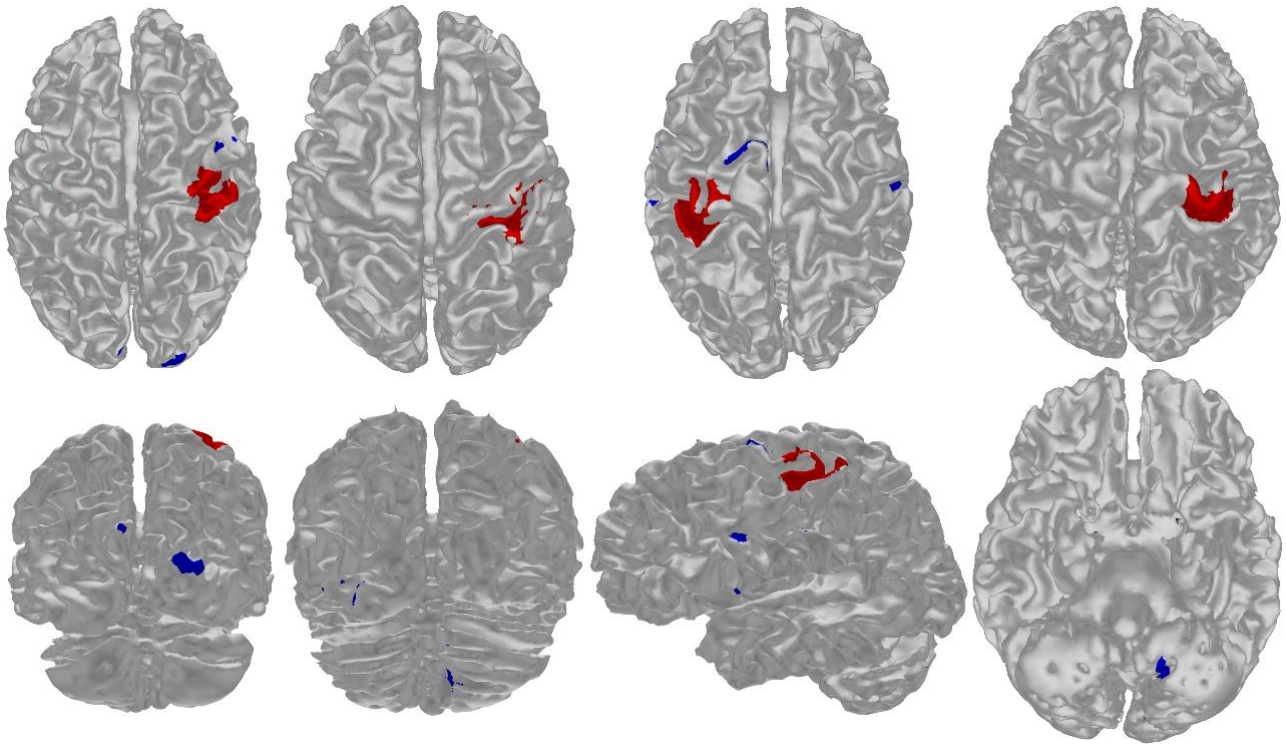
Finally, brain pathology can be accompanied by haemodynamic abnormalities. Quantifying these is potentially critical for a study with a difficult task, when differences in fMRI patterns intend on being directly interpreted. It is also important for event-related designs where changes between action/rest blocks are frequent. The present study, however, involved a very simple task with very long blocks. This design minimises the influence of abnormal haemodynamic response curves, and

was only used to identify the ‘hand’ region of the S1M1. Again, as the activation area and volume did not correlate with any clinical test recorded, this design likely fulfilled its purpose, without introducing confounds that could lead to type-I errors.

Conclusions

Investigating diffusion characteristics of people with moderate brain pathology is difficult or impossible to perform with standard parcellation-based approaches, and has led to fMRI-seeding of dMRI data. In this work, a novel highly-automated fMRI-dMRI fusion pipeline that identified distinct correlations between functional clinical scores and dMRI metrics of sensorimotor tracts in children with unilateral cerebral palsy was presented. These relationships were substantially stronger when delineated with this approach than when delineated with a standard voxelwise fMRI-seeding approach, and were minimally apparent in the inferior aspect of these tracts, where pathology was absent. The approach demonstrated here may prove valuable to studies of brain pathology, especially where sensitive analyses are required, such as the measurement of neuroplastic changes induced by intervention. The presented method may also ultimately prove useful for presurgical planning—for example, planning of neurosurgery aiming to treat intractable epilepsy in children with pre-existing brain injuries.

Supporting Information



Supplementary Figure 1. Illustration of functional MRI motion artefact and/or supplementary-activation rejection. Four participants (one per column) with motion artefacts are shown. The third column additionally displays activation of the supplementary motor area. Selected activation is shown in red, according to the criteria set out in Methods. Rejected activation is shown in blue. Note how only unambiguous activation within the major cluster of activation is selected in each instance. For surfaces in the top row, the front left of each image represents the anterior left of that participant. For surfaces in the second row within the first and second columns, a view from behind the participants are used: left of the image is left of the participant; top of the image is superior. The 'sagittal' view in the second row, third column, shows the left side of the brain; the left of the image is anterior. The bottom right image shows a view of the underside of the brain; the top of the image is anterior; the left of the image is the patient's right.

Chapter 5

Brain changes following four weeks of unimanual motor training: evidence from behaviour, neural stimulation, cortical thickness and functional MRI

This chapter consists of the paper *Brain changes following four weeks of unimanual motor training: evidence from behaviour, neural stimulation, cortical thickness and functional MRI*. This and the following chapter form a pair of papers which are both available on the preprint server *bioRxiv* and have been submitted to the journal *Human Brain Mapping* (Chapter 5, under review; Chapter 6, accepted). Together, these papers describe a wide-scale multimodal analysis of motor learning in healthy adults. The measures focussed on in the present chapter are transcranial magnetic stimulation (TMS), fMRI, cortical thickness, and behavioural changes. The following chapter reports changes in behaviour and diffusion metrics, including diffusion changes in the corticospinal tract elucidated using the methodology described in Chapter 4.

These two chapters, together, address the third aim of this thesis: *to combine the aforementioned principles and methods in order to measure a variety of brain changes in healthy adults learning a novel motor task, then to interpret such information together in a way that may improve our understanding of neuroplasticity at a biological level*. These works are a critical step toward analysis of similar measures in a rehabilitative context for three reasons.

First, Chapter 4 revealed correlations between diffusion measures of corticomotor tract and motor function in children with UCP. This indicates that this is a sensible location to search for neuroplastic change in response to motor rehabilitation. However, no direct evidence exists that the microstructure of this white matter tract responds to motor training. Arguably the most sensible next step is to demonstrate that motor training can induce neuroplasticity in this region. By initially using healthy adults, rather than children with CP, for this purpose, we can expect an improved signal-to-noise ratio and interpretability, as such a cohort are more likely to achieve meaningful behavioural improvements and are free of potential confounders such as ongoing brain development (maturity). An inability to induce changes here in a healthy cohort would likely scuttle the idea of measuring such a change in brain-injured populations.

Second, although the analysis method described in Chapter 4 demonstrated superior results to the present state-of-the-art fMRI driven method, whether this method is sufficiently sensitive for the measurement of neuroplasticity has yet to be demonstrated. As with the previous point, there are several advantages associated with first assessing this in healthy adults, rather than children with CP.

Thirdly, as discussed in both Chapter 2 and Chapter 3, adequate interpretation of imaging data requires that a range of modalities are collected, or at least that the relationships between structural and functional change are well known. Presently, there is a paucity of longitudinal studies that have collected multimodal information, and so neuroplasticity associated with motor learning is poorly understood. Although one may consider jumping straight into collecting such information in a neurorehabilitative context, collecting this in healthy cohorts undergoing motor training allows inclusion of valid functional data which may greatly improve biological insight. As previously discussed, in people with brain injury, fMRI changes are difficult to interpret, and there are ethical considerations toward the use of TMS. The work here, then, is important in not only demonstrating how a multimodal neuroplasticity study can be conducted, but also in providing a foundation of understanding into the patterns of brain change that are associated with motor learning.

Dr Martin Sale and I were joint-first authors on this publication. Dr Sale predominantly planned the study and collected the raw data. I analysed fMRI, cortical thickness, and behavioural data, and played a minor role in the statistical analysis of TMS data. The interpretation of results, writing of the manuscript, and data visualisation were predominantly done by myself. Dr. Luca Cocchi, Alex Pagnozzi, and Prof. Stephen Rose all contributed academic input regarding final data analysis. All authors reviewed the manuscript.

Publication information

Sale M V., **Reid LB**, Cocchi L, Pagnozzi AM, Rose SE, Mattingley JB. Structural brain changes following four weeks of unimanual motor training: evidence from behaviour, neural stimulation, cortical thickness and functional MRI. *Hum Brain Mapp.* (Under Review)

and

Sale M V, **Reid LB**, Cocchi L, Pagnozzi AM, Rose SE, Mattingley JB. Structural and functional brain changes following four weeks of unimanual motor training: evidence from behaviour, neural stimulation, cortical thickness and functional MRI. *bioRxiv.* 2016 Nov 17.

DOI: 10.1101/088302

Martin Sale and Lee Reid were joint-first authors on this publication.

Minor changes have been made in response to examiner feedback.

Abstract

Although different aspects of neuroplasticity can be quantified with behavioural probes, brain stimulation, and brain imaging assessments, no study to date has combined all these approaches into one comprehensive assessment of brain plasticity. Here, 24 healthy right-handed participants practised a sequence of finger-thumb opposition movements for 10 minutes each day with their left hand. After four weeks, performance for the practised sequence improved significantly ($p < 0.05$ FWE) relative to a matched control sequence, with both the left (mean increase: 53.0% practised, 6.5% control) and right (21.0%; 15.8%) hands. Training also induced significant (cluster p -FWE < 0.001) reductions in functional MRI activation for execution of the learned sequence, relative to the control sequence. These changes were observed as clusters in the premotor and supplementary motor cortices (right hemisphere, 301 voxel cluster; left hemisphere 700 voxel cluster), as well as sensorimotor cortices and superior parietal lobules (right hemisphere 864 voxel cluster; left hemisphere, 1947 voxel cluster). Transcranial magnetic stimulation over the right ('trained') primary motor cortex yielded a 58.6% mean increase in a measure of motor evoked potential amplitude, as recorded at the left abductor pollicis brevis muscle. Cortical thickness analyses based on structural MRI suggested changes in the right precentral gyrus, right post central gyrus, right dorsolateral prefrontal cortex and potentially the right supplementary motor area. Such findings are consistent with LTP-like neuroplastic changes in areas that were already responsible for finger sequence execution, rather than improved recruitment of previously non-utilised tissue.

Introduction

The brain is capable of remarkable structural and functional change to allow it to optimise performance. Such changes, collectively referred to as plasticity, are key to understanding a variety of real-life phenomena, such as the learning of new skills,²⁰¹ the storing of memories,²⁰² and recovering neurological function after brain injury.²⁰³

By definition, plasticity results in functional and/or structural change.¹³² At the microscopic level, plasticity in the central nervous system can manifest in several different ways. Sprouting of new connections, unmasking of hidden or inhibited synaptic connections, and withdrawal of inhibition are some examples of these changes.^{204–206} Another form of plasticity is referred to as long-term potentiation (LTP), which reflects an increase in synaptic efficacy.^{207,208} Behaviourally, neuroplastic changes typically manifest as altered task performance, such as improved speed of movement. Measuring performance of learned tasks before and after training provides a means of assessing the functional impact of training. Although such an approach can allow for an investigation of the effects of various factors on plasticity (e.g. aging, attention, hormones), a purely behavioural approach is unable to shed light on the location and type of brain changes that occur after training. In order to probe the biological changes subserving plasticity, brain stimulation and brain imaging techniques are required, each with their own relative advantages and disadvantages.¹⁸¹

In the area of motor-skill learning, almost all studies investigating neuroplasticity have, so far, relied on animal models, cross-sectional data, or functional measures of brain change.²⁰⁹ In rodents, motor learning appears to upregulate synaptic plasticity in the primary of motor cortex,²¹⁰ and may also be associated with altered neural recruitment in this area.²¹¹ In humans, early work using structural magnetic resonance imaging (MRI) suggested that differences in morphology of the primary motor cortex may exist between expert musicians and the general population.²¹² Since then, functional MRI (fMRI) studies have reported altered activity in motor planning in professional sports people,²¹³ and transcranial magnetic stimulation (TMS) studies have similarly reported that skilled racquet players have a larger cortical representation of the hand than the general population.²¹⁴ Functional MRI work has also suggested that the supplementary motor area, dorsolateral prefrontal cortex (dlPFC), and caudate nuclei may play integrated roles in error correction and learning of motor sequences.^{215,216}

Longitudinal studies are particularly useful for studying neuroplasticity as they eliminate the possibility that neural differences are the cause, rather than result, of participants deciding to learn a skill. Several reports exist of changes in brain function in response to motor training,^{E.g. ,209,217}

including in the pre- and post-central gyri, dlPFC and basal ganglia.²¹⁸ Many extensive reviews of such work are available, including Chang et al,²⁰⁹ Dayan and Cohen,²¹⁹ Doyon,²²⁰ and others. In brief, trained tasks in such studies have been somewhat heterogeneous, and both increases²²¹ and relative decreases in fMRI activation have been reported, often within the same study.^{169,218,222} The direction of change appears to depend on the duration of training,^{169,218,219} potentially due to increases in baseline cerebral blood flow,¹⁶⁹ though what constitutes ‘short-term’ or ‘long-term’ training appears to be task dependent.²¹⁹ A small number of reports have also detailed minute structural changes in grey matter in response to visuo-motor tasks, particularly in the sensorimotor cortex,²²³ visual cortex, and superior parietal lobule,^{52,80} all areas associated with visuo-motor skills.

So far, research in this area has predominantly relied on single data collection modalities, such as TMS, or fMRI. Unfortunately, the differences in study design, contrasts, time-period, and imaging modalities of these studies can make it difficult to achieve a deeper understanding of the critical experimental parameters that yield reliable brain changes, whether such changes are typically concurrent or independent, and so on. In addition, each modality has its own limitations regarding reliability or interpretability, which can hamper insight into biological processes when only a single modality is acquired. For example, due to its indirect method of measuring brain activity, it is difficult to unambiguously interpret changes in fMRI in terms of biology without independent concurrent information, particularly given that controlling for task equivalency across scans can be difficult to achieve.¹⁸¹ Collecting multiple modalities can also alleviate concerns that results in one modality simply reflect statistical anomalies, rather than subtle brain changes. For these reasons, the longitudinal study of motor learning presented here concurrently acquired data on four different measures of neuroplasticity – behaviour, TMS, fMRI, and cortical thickness. Findings from a fifth measure, diffusion MRI, appear in a second study.²²⁴ Each of these modalities helps to build a global picture of the changes that occur with motor training, by reporting on a slightly different aspect of the neuroplastic response.

TMS can evoke a clearly discernible and quantifiable motor response when motor cortical neurons are stimulated at sufficient intensity.²²⁵ This TMS-evoked response, referred to as a motor evoked potential (MEP), reflects the excitability of underlying cortical neurons. Measuring the amplitude of the MEP before and after a training paradigm provides objective measurement of changes attributed to cortical motor plasticity.⁴⁸ This is different from other, non-motor regions, where brain stimulation-evoked responses are more difficult to quantify (e.g., prefrontal brain regions), yet which also undergo changes via the same, ubiquitous, mechanisms. Although TMS is ideally suited to quantify training-related change arising in the motor cortex, there are several

limitations to the technique. In particular, TMS can only penetrate superficial grey matter structures,²²⁶ and can only probe the activity of one area of cortex at a time. Therefore, TMS is unable to provide information on whole-brain changes arising from training.

Whole-brain assessment of plastic change arising with training can be investigated with both functional and structural MRI. Functional MRI of local blood oxygenation level-dependent (BOLD) signals provides information about changes in brain activity during tasks with high sensitivity and excellent spatial resolution. However, fMRI cannot readily distinguish whether any measured changes following training reflect excitatory or inhibitory activity,¹⁰² something that TMS can do. Changes in BOLD signals are also more straightforward to interpret, in terms of biological change, when in the context of information from other modalities, such as TMS.¹⁸¹ By contrast, if conducted carefully, structural MRI can measure changes in cortical thickness that are more directly interpretable in terms of biology but, without accompanying functional measures, are difficult to link to any changes in brain activity.

With these points in mind, the aim of the present study was to use a multi-modal approach to investigate plasticity in the human cortex. We measured behaviour, TMS evoked MEPs, BOLD changes using fMRI, and cortical thickness, before and after four-weeks of motor training. To make interpretation of the results more straightforward, we opted for training that did not have any visual component. Our TMS analyses were conducted on the trained hemisphere and tested for increased MEP amplitude which could reflect altered connectivity induced by an LTP-like process underlying motor learning. For our fMRI analysis, we tested for both task-induced increases and decreases in activation within sensorimotor cortices, supplementary motor areas, and superior parietal lobes. These phenomena may reflect altered processing in the ‘trained’ hemisphere, and potentially an altered balance of interhemispheric inhibition. Although fMRI changes in higher areas, such as the dorsolateral prefrontal cortex, were possible, we did not test for these explicitly. Finally, we tested for increased cortical thickness in motor areas of the trained hemisphere, given reports of subtle changes in visuomotor areas associated with visuomotor learning.^{52,80,223} In combination with our parallel analysis of white matter and network changes,²²⁴ this work provides a comprehensive assessment of the functional and structural brain changes associated with motor learning in humans.

Materials and Methods

Overview

Twenty-four participants were recruited (14 female; aged 28.8 ± 1.5 years; range 18 – 40 years). Participants were all right-handed (laterality quotient 0.92 ± 0.03 ; range 0.58 – 1.0) as assessed by

the Edinburgh Handedness questionnaire. Participants trained daily on a finger-thumb opposition task²²¹ for four weeks. Behavioural, MRI, and TMS measures were obtained before and immediately after the training period to quantify training-related changes. Participants were instructed to refrain from the consumption of known neuroactive substances (including caffeine and alcohol) before and during the training and quantification sessions. No participants reported any adverse effects. The study was approved by the University of Queensland Human Research Ethics Committee and all participants gave written informed consent.

Motor training task

The training task has been used in a previous independent study, in which it was reported to induce robust behavioural and functional changes.²²¹ The task involved participants performing a sequence of finger-thumb opposition movements with their non-dominant (left) hand (Figure 14). Participants were pseudo-randomly assigned one of two sequences that were mirror-reverse copies of each other. Participants were instructed to perform their assigned sequence as quickly and as accurately as

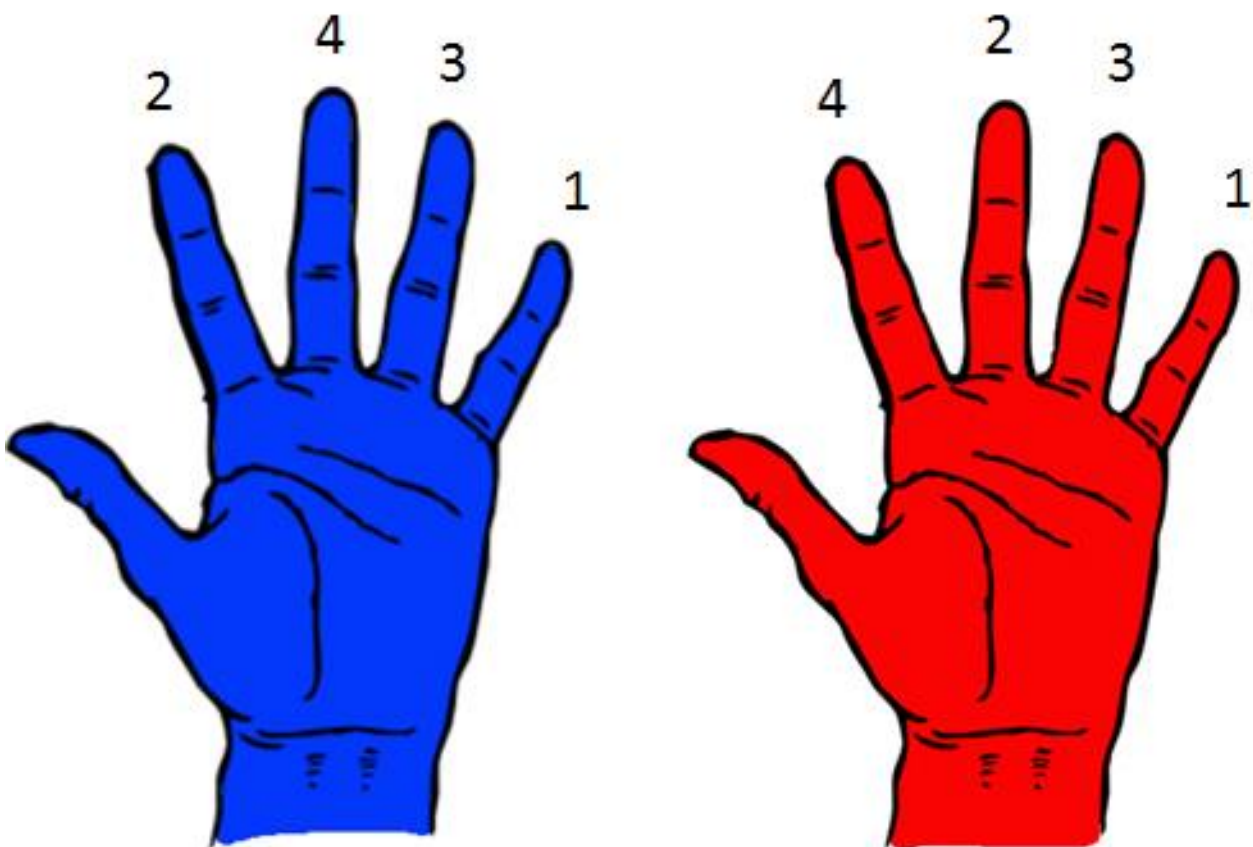


Figure 14. Participants were randomised to practising one of two finger-to-thumb opposition sequences. For the 'Blue' sequence (left), the order of fingers required to make contact with the thumb were little, index, ring, middle. For the 'Red' sequence (right) the order was little, middle, ring, index. These sequences were mirror images of one another.

possible for 10 minutes each day for 4 weeks, and not to look at their hand during training. To help remember the correct sequence, participants were given a printed copy of their allotted sequence (red or blue; see Figure 14). In order to minimize any circadian effects on motor learning,²²⁷ each participant was randomised to practising either during the morning or evening, and conducted training at the same time each day. Participants kept a log-book to record their training, and were instructed to be honest when training sessions were missed, or were performed outside of the specified training time.

Behavioural measure

Participants' performance on the finger-thumb opposition tasks was assessed as the number of correct sequences completed in 30 sec. Performance was documented online with a hand-held video camera, and quantified off-line. Participants performed both red and blue (Figure 14) sequences with both their left and their right hands. This was to investigate whether training induced any spill-over of effects to a non-trained sequence and/or the contralateral hemisphere. The order of the sequences performed was randomised for each participant. To minimize errors, and to assist in performance, a print-out of the sequence to be performed was placed in front of the participant for the duration of that task. Further, prior to the quantification of baseline performance of the sequences (before training), participants were given a brief period of time (~ 5-10 sequences) to practice the two sequences.

Performance on the finger-thumb opposition sequences was analysed using a three-way repeated measures ANOVA with within-participant factors of *training* (Baseline, Post), *hand* (Left, Right), and *sequence* (Trained, Control). Where appropriate, post hoc analyses were performed using Holm-Bonferroni corrected paired t-tests.

Functional MRI

Functional MRI images were acquired in the same session as structural MRI images. We acquired 41 axial slices (slice thickness, 3.3 mm) using a gradient EPI sequence (TR 2.67 sec; TE, 28 ms; flip angle, 90°; field of view, 210 x 210 mm; voxel size, 3.3 x 3.3 x 3.3 mm). A liquid crystal display projector back-projected the stimuli onto a screen positioned at the head-end of the scanner bore. Participants lay supine within the bore of the magnet and viewed the stimuli via a mirror that reflected the images displayed on the screen. Participant head movement was minimized by packing foam padding around the head.

Prior to entering the scanner, participants familiarised themselves with the two movement sequences – ‘trained’ and ‘control’ – they were going to perform within the scanner. The sequences are shown in Figure 14. Within the scanner, participants performed these finger-thumb opposition movements with their left hand in blocks of 16 seconds, each followed by 16 seconds of rest. During rest blocks, a visual display showed a “Rest” command. At the start of each movement block a visual cue - displaying either the red or blue hand and corresponding movement sequence - notified participants whether they would be performing the trained or the control sequence. This was displayed for 2 seconds, then removed. Participants then performed the required sequence at a rate of two movements (of the sequence) per second. As a cue to aid in this timing, a fixation cross flashed at 2 Hz on the screen. A tone also sounded at 2 Hz intervals throughout the acquisition. The last two tones in each movement block were at progressively lower pitches to notify participants that a rest block was imminent. Immediately following completion of each movement block (i.e., following the last fixation cross), a “Stop” command was presented for 1 second, which was then replaced with the “Rest” command. Four consecutive ‘runs’ were performed. Each run consisted of four trained-sequence blocks, four control-sequence blocks, and seven rest blocks. The order of the trained/control sequence blocks was randomised but kept consistent between participants. Correct performance of the sequence was verified by recording the movements with a video camera, which were later reviewed for accuracy.

Image processing and statistical analyses were performed using SPM12 (Wellcome Department of Imaging Neuroscience, UCL, London, UK). Functional data volumes were slice-time corrected and realigned to the first volume. The mean image of the resultant time series was co-registered with the participant’s temporally-unbiased T1 template (see Methods: Cortical Thickness). The time series was then normalised into MNI space, an MNI brain mask was applied, and the result smoothed with an 8-mm FWHM isotropic Gaussian kernel. For first level statistical analyses, contrasts were conducted for (a) movement > rest (b) trained > rest, and (c) control > trained sequence blocks. All six motion parameters for each run were included as nuisance regressors. The second level analysis looked at the interaction between sequence and time point (i.e., baseline [control > trained] versus post [control > trained]). This was designed to test whether motor training altered the brain’s response to performance of the learned sequence, taking into account any changes that were unrelated to learning, or pre-existing differences between responses to the control and learned sequences (although no baseline differences were expected). It was possible that the trained or control sequence would show greater BOLD responses after training, and so we treated this as a two-tailed test. To account for this, we set a more conservative cluster significance level of $p < 0.025$ FWE with minimum cluster size of 200 voxels, after voxel-wise thresholding at $p < 0.0005$ uncorrected.

TMS mapping

Mapping of motor cortical excitability with TMS was performed in a separate laboratory, after MRI acquisition. Surface electromyographic recordings were obtained from the left abductor pollicis brevis (APB) muscle. Recordings were made using silver/silver-chloride surface electrodes with the active electrode placed over the muscle belly, and the reference electrode placed over the adjacent metacarpophalangeal joint. Signals were amplified (x1000) and band-pass filtered (20-1000 Hz) using a NeuroLog system (Digitimer), then digitized (2000 Hz) with a data acquisition interface (BNC-2110; National Instruments) and custom MATLAB software (MathWorks). Signals were monitored online for movement-related activity using high-gain electromyography and a digital oscilloscope.

Mapping of motor cortical excitability before and after training involved applying TMS to the right hemisphere in a grid like pattern (described below). The TMS was delivered using a Magstim 200² stimulator (Magstim, UK) and a figure-of-eight coil (70 mm diameter). The coil was positioned with the handle pointing backwards at a 45° angle to the sagittal plane to preferentially induce current in a posterior-to-anterior direction in the cortex. The optimal scalp position for evoking electromyographic responses in the APB was established as the position that consistently evoked the largest MEP amplitude in this muscle with a slightly suprathreshold intensity. Resting motor threshold (RMT) was determined and defined as the minimum stimulus intensity which evoked an MEP of at least 50 μ V in at least 5 out of 10 successive stimuli. The TMS intensity used for the mapping procedure was set at 120% of RMT. This stimulus intensity was established for both pre- and post-training sessions.

Prior to participants' first TMS mapping session, their individual T1 MRI scan was processed with the neuro-navigation software ASA-Lab (ANT, The Netherlands). Markers were placed on the scalp surface of the structural scan in a grid-like pattern spanning the entire right hemisphere. The grid commenced at the vertex, and markers were placed every 1 cm anteriorly and posteriorly from the vertex, and then extended out laterally (to the right) in 1 cm increments. Marker sites were targeted with TMS using a Polaris-based infrared frameless stereotaxic system and Visor software (ANT, The Netherlands). Five TMS pulses were applied to these markers every 5 sec. The markers were stimulated systematically, moving in a medial-to-lateral direction. Stimulation of the marker sites continued until the average MEP amplitude from a marker site fell below 50 μ V. Those sites where average MEPs met or exceeded this amplitude were referred to as *active*. Once a row of markers had been assessed, stimulation was moved either 1cm anteriorly or posteriorly (chosen randomly), until all active marker sites had been stimulated and identified. The MEP *volume*²²⁸ was also calculated

before and after training. This was calculated by summing the mean MEP amplitude of all the active sites.

Training-related increases in the number of active sites and MEP volume were investigated using separate one-tailed, paired t-tests to compare pre-training measurements with those acquired after training. Significance was set as $p < 0.05$ after Holm-Bonferroni multiple comparisons correction.

Cortical Thickness

We examined cortical thickness changes arising in response to motor training. We acquired MPRAGE T1 images (0.9mm isotropic) immediately before (“baseline”) and after (“post”) the four-week training period using a 3T MR system (Magnetom Trio, Siemens) and a standard 32 -channel head coil. Images were processed with Advanced Normalization Tools (ANTs; v2.1.0, source pulled 9th Feb 2016). An overview of the processing pipeline is shown in Figure 15.

Single Participant Analyses

In longitudinal analyses, it is important to utilise templates that are invariant to either time-point, in order to boost statistical power and avoid false-positives induced by registration bias.²²⁹ Although ANTs provides a longitudinal cortical thickness script, we found that the templates produced by this script on our system were commonly biased toward one time-point. Therefore, we constructed templates for each participant by rigid-registering the baseline and post structural images together using ANTs SyN (symmetric) transform²³⁰ after skull-stripping, N4 bias-field correction and intensity normalisation. Time points were transformed by half of the resulting matrices then averaged, producing an approximate template that was unbiased with respect to time point. This initial template was converted into a sharper, segmented, template using the *antsMultivariateTemplateConstruction* script, followed by the *antsCorticalThickness* script using the ANTs NKI template. Each axial, coronal, and sagittal slice was then carefully visually inspected. In instances where dura or skull were classified as grey matter, or the brain under-segmented, edits were made to the brain mask using ITK Snap v3.4.0,¹⁹¹ and the script was re-run with the updated brain mask. For this study, particular emphasis was placed on achieving highly precise segmentations of the parietal and frontal lobes (Supplementary Figure 2) due to their known association with, or proximity to, areas involved in motor training and/or learning. The process was repeated until we were satisfied with the final segmentations. Examples of acceptable and unacceptable segmentations are provided in Supplementary Figure 3. Posterior tissue probabilities were then converted into priors in a manner consistent with ANTs *antsCookTemplatePriorsCommand* script.

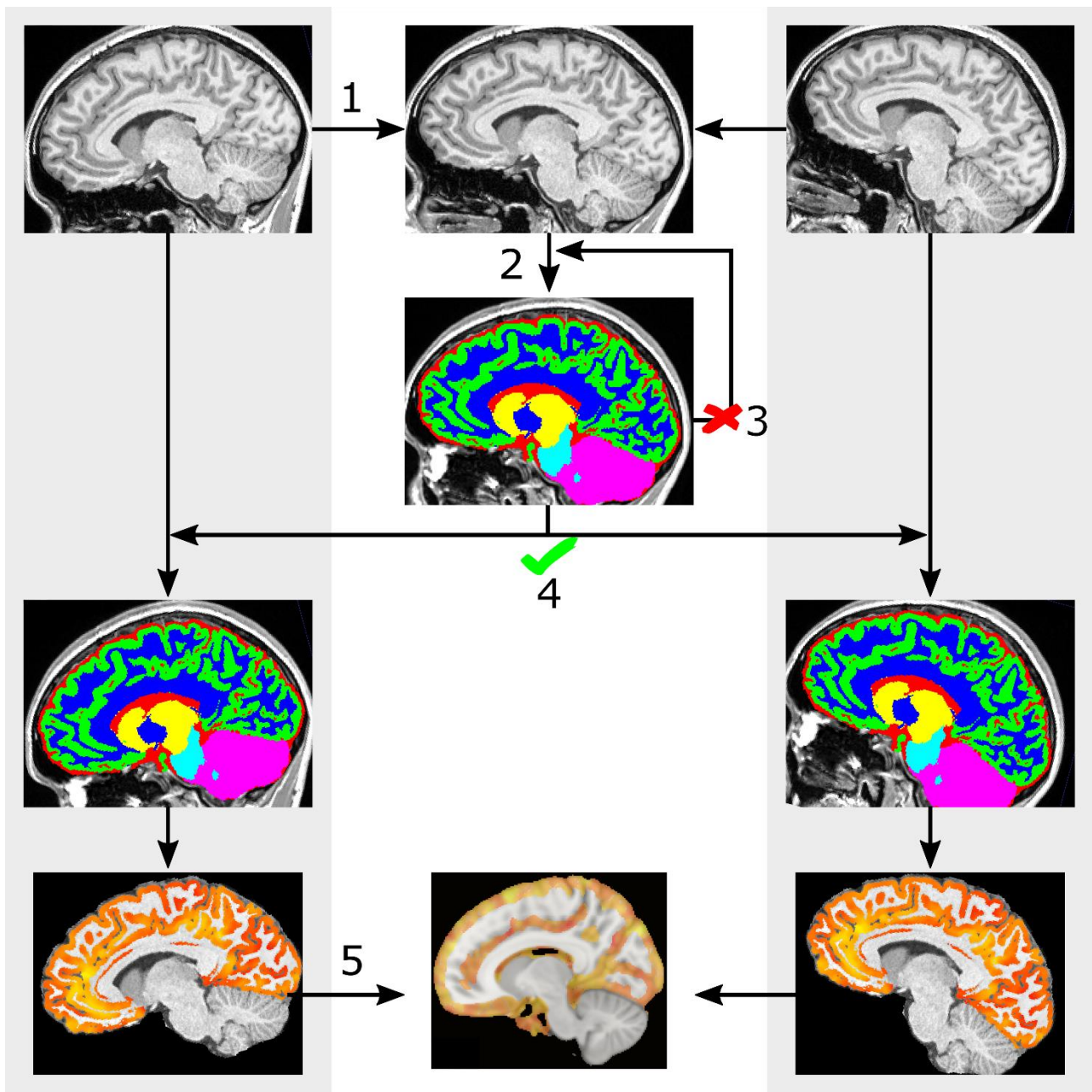


Figure 15. Cortical thickness pipeline. Steps are indicated with numbers. 1) Structural volumes from the baseline (left column) and post (right column) were pre-processed, skull-stripped, and registered using a symmetrical registration. The resulting half transforms were applied to non-skull-stripped images to achieve an intermediate image (top, middle column), which was processed into a sharp single subject template. 2) The single-subject template was then skull-stripped and segmented. The result was carefully visually inspected. 3) If the segmentation was considered inaccurate, the brain mask was manually edited and Step 2 was re-run. 4) If the segmentation was successful, each time point was then re-skull-stripped and segmented using the single subject template (middle row of left and right columns), and cortical thickness calculated (bottom row of left and right columns). 5) Cortical thickness at each time point was moved into single-subject template space, subtracted, and this difference transformed into MNI space for statistical analysis using the known transform between the single-subject template and MNI space. Statistical analyses were then performed across all subjects, resulting in statistical maps (bottom row, middle column). Images here are purely illustrative; orientation differences have been exaggerated in order to convey concepts clearly.

The *antsCorticalThickness* script was applied to structural images from both time points, utilising the single subject template, producing a cortical thickness map in single-subject-template space. Subtraction of the pre-training from post-training cortical thickness images produced a cortical thickness difference image.

Statistical Analysis

We hypothesised that any region of change would likely be substantially smaller than atlas ROIs, and so opted for voxel-based morphometry. Single subject template T1s were registered to FSL's 1mm isotropic MNI152 atlas (Figure 15) using ANTs SyN, and the resultant transforms applied to cortical thickness difference images. Voxels where the white matter was the most probable tissue, as defined by the mean of all single-subject tissue priors, were excluded. Images were then smoothed with a 5mm FWHM kernel and placed into a factorial model in SPM 12 (<http://www.fil.ion.ucl.ac.uk/spm/software/spm12/>). This model regressed change in cortical thickness against time point. This model included sex as a factor to account for its previously-reported effects on cortical thickness,²³¹ and included ANCOVA normalisation for nuisance effects to account for any remaining global differences. In the interests of accuracy and statistical power, we restricted our analysis to the parietal and frontal lobes – the areas which received particular focus during segmentation correction (Figure 15). We set our significance criteria as $p < 0.05$ FWE corrected, or a cluster comprising more than 20 voxels expressing values $p < 0.001$ uncorrected.

TMS and MRI overlay

In order to interpret TMS, fMRI, and cortical thickness results together, it was important to show reasonable anatomical correspondence between the methods. To achieve this, TMS MEP responses were projected into MNI 152 space. This was achieved by converting each active site from Talairach to MNI coordinates, using the Lancaster transform,²³² then connecting neighbouring measurement nodes to form a mesh. An edge of zero-value nodes was added to the outside of this mesh, based on the position of neighbouring nodes. A duplicate of this mesh was projected 20mm toward the midline of the base of the brain ($x=0, y=0$), reflecting the approximate penetration of the TMS pulse. Values on the grid were normalised between 0-1 on a per-participant basis. For each participant, a volume was generated by linearly interpolating all voxels in MNI space between the inner and outer surfaces of the grid by the nearest surrounding 8 nodes. All participants' volumes were averaged to produce a mean image. This overlay was used for visual comparison of the modalities only; it was not used for quantification of TMS MEPs.

Results

Behavioural performance

There was no difference in behavioural performance for the morning and evening training groups, and therefore the data for the two groups were pooled for subsequent analyses. Prior to training, participants were equally proficient at performing the trained and control sequences with their left and right hands. Following training, there was a significant improvement in the number of sequences participants could complete in the 30 sec period (Figure 16; effect of time $p < 0.001$, partial $\eta^2 = 0.16$; side \times sequence \times time interaction $p < 0.01$, partial $\eta^2 = 0.026$). Using the left (trained) hand, the number of correct sequences completed on the trained sequence increased by 53%, from 24.0 ± 1.2 (Mean \pm SEM) to 36.7 ± 2.1 (Holm-Bonferroni adjusted $p = 2.73 \times 10^{-9}$). There were also smaller, but significant improvements in performance of the control sequence with the left hand (24.48 ± 0.94 to 25.65 ± 0.79 [Mean \pm SEM]; 6.5% increase; $p = 0.025$ [Holm-Bonferroni adjusted]), the trained

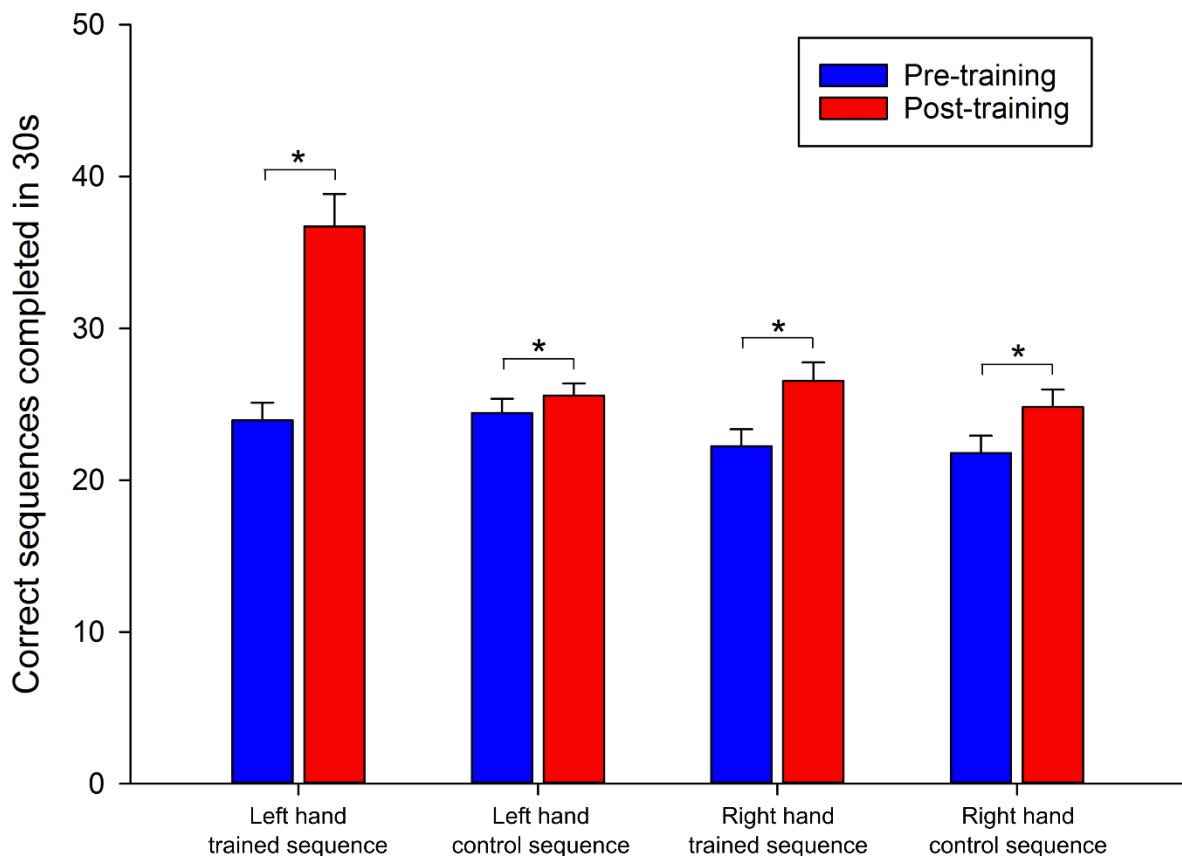


Figure 16. Increase in performance of motor training tasks following four-weeks of training. Group data ($n = 24$) showing number of correct sequences performed prior to (blue bars) and following (red bars) four weeks of training of a finger-thumb opposition movement sequence (trained sequence). Participants performed the trained and control sequence with their left hand (trained) and right hand (not trained). Training improved execution speed for all four hand-sequence combinations assessed (Each $p < 0.05$ FWE). Data represent mean \pm SEM.

sequence with the right hand (22.22 ± 1.11 to 26.48 ± 1.22 ; 21.0% increase; $p = 7.53 \times 10^{-6}$), and the control sequence with the right hand (21.82 ± 1.4 to 24.74 ± 1.15 ; 15.8% increase; $p = 9.85 \times 10^{-6}$). Although participants improved to a greater degree on the trained sequence than the control sequence (both hands $p < 0.05$ FWE), this difference between sequences was substantially greater for the left than the right hand ($p < 0.05$ FWE).

fMRI analysis

Of the 23 participants included in the fMRI analysis, none exhibited excessive ($>2\text{mm}$ or 2°) head movement during any session. Prior to training (Figure 17), the learned sequence versus rest contrast revealed four significant ($p < 0.05$ FWE) clusters that were located across a variety of motor areas, predominantly in a bilateral manner, including the precentral gyri, postcentral gyri, supplementary motor areas and superior parietal lobule. At this time, the activation of the trained and control sequences were, as expected, equivalent (i.e., there were no significant clusters when contrasted). Following training, however, the *control* sequence evoked *greater* activation than the trained sequence in a number of sensorimotor areas (Figure 17), despite slight reductions in control-sequence activation in these areas after training (Supplementary Figure 4). To formally compare these differences we calculated the interaction between training type and time point (baseline [control $>$ trained] versus post [control $>$ trained]). For this contrast, positive t-values indicated locations in which the trained sequence showed reduced signal after training, relative to the control sequence. In the left hemisphere, a significant cluster overlapped the post-central gyrus and superior parietal lobule (1947 voxels, cluster p-FWE < 0.001 ; Table 8). In the right hemisphere, a similar cluster overlapped the pre-central gyrus, post-central gyrus, and superior parietal lobule (864 voxels, cluster p-FWE < 0.001 ; Figure 18). Both hemispheres also each demonstrated a significant cluster crossing the premotor cortex and supplementary motor area (left hemisphere, 700 voxels; right hemisphere, 301 voxels; each cluster p-FWE < 0.001). Reversal of this contrast, highlighting areas of increased relative activation of the learned sequence, revealed no significant clusters.

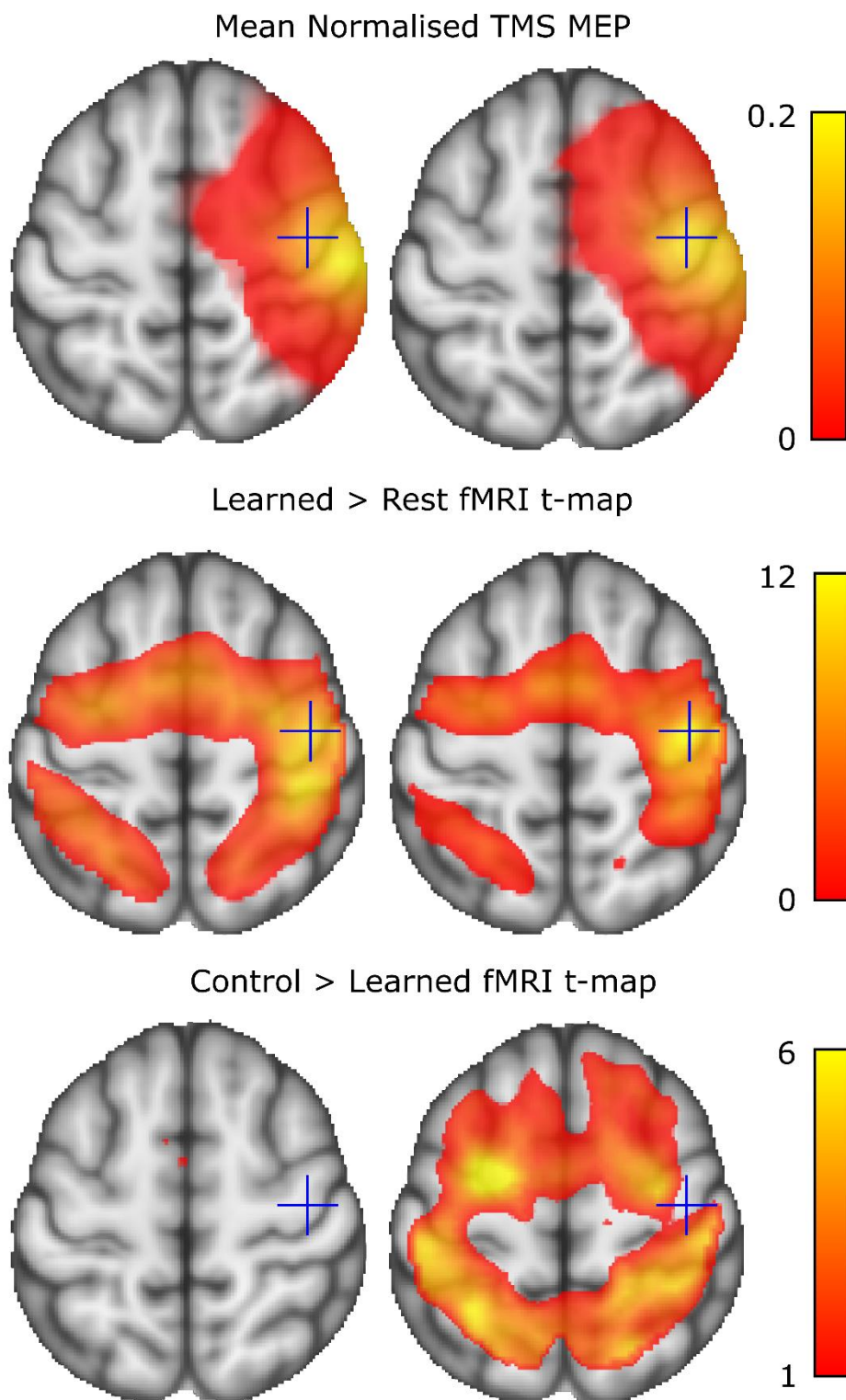


Figure 17. Mean of participants' normalised TMS responses (Top; normalised mV), positive BOLD activation during the learned task (Middle; t-values for task vs rest), and positive t-value map contrasting BOLD for control sequence > trained sequence (Bottom), overlaid on an MNI 152 T1 image. The left and right columns show measures before and after the training period, respectively. Crosshairs show equivalent anatomical positions (MNI 152 coordinate: 37, -16, 57) to aid viewing. TMS and BOLD signals show a large degree of overlap in the primary motor cortex. The TMS responses were centred more anteriorly (motor+premotor), particularly after training, than the BOLD responses (predominantly motor+ sensorimotor). Details of TMS projection into MNI space is contained in the text.

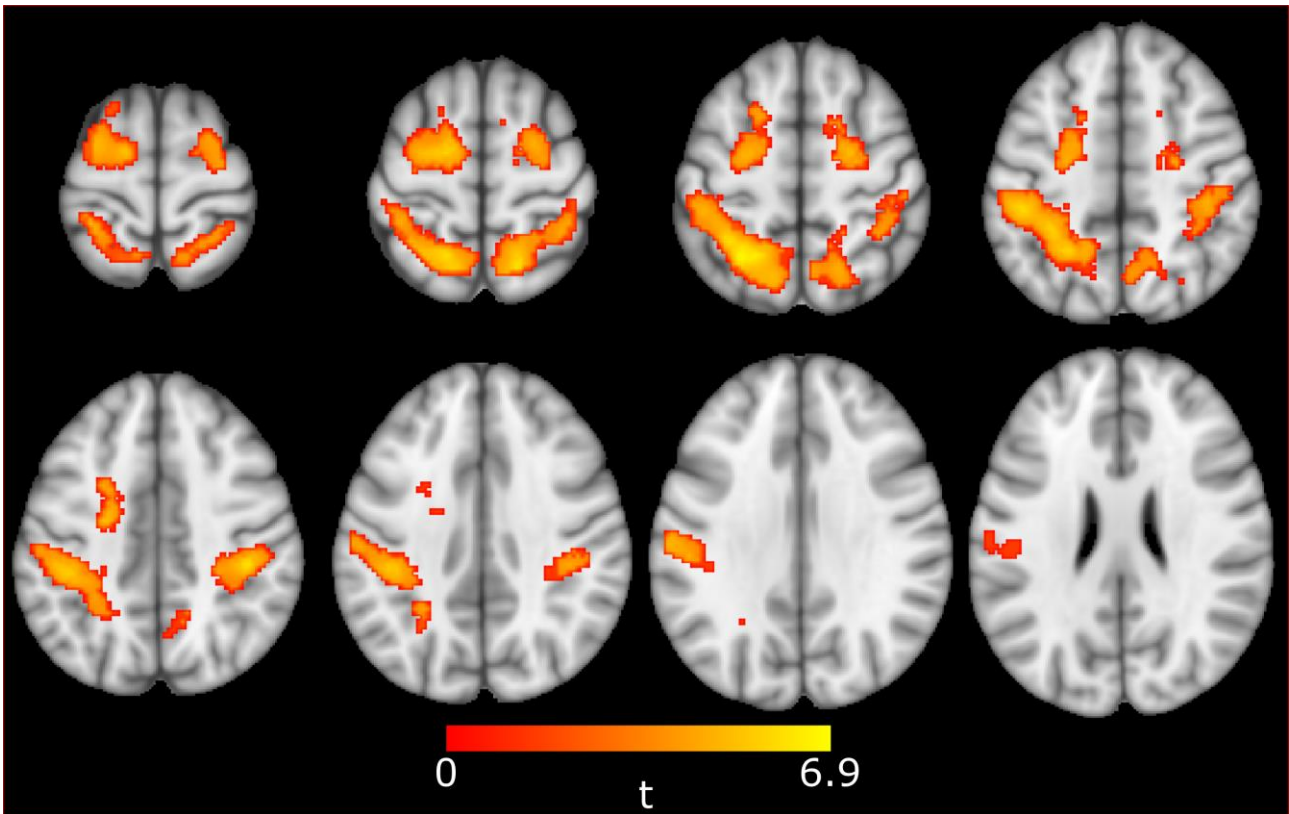


Figure 18. Training-related differences in BOLD activation. Groupwise functional MRI t-map, showing voxels which, after training, demonstrated higher signal during the control sequence than the trained sequence. A series of axial slices is shown. Significant clusters were apparent in the superior parietal lobule and primary sensorimotor cortices in the right (864 voxels; $p < 0.001$ FWE) and left (1947 voxels; $p < 0.001$ FWE) hemispheres. Significant clusters were also seen in the supplementary motor area / superior premotor area of the right (301 voxels; $p < 0.001$ FWE) and left (700 voxels; $p < 0.001$ FWE) hemispheres. Only voxels belonging to significant clusters are shown; a structural template is displayed for anatomical reference only. Left of image is left of brain. Axial slices shown are evenly spread between MNI-152 z-slices 67 and 26 inclusive.

Cluster Size	Peak Coordinates	Anatomical Locations
1947	-26, -54, 54	L SPL
	-44, -34, 36	L PoG
	-32, -44, 52	L SPL
864	18, -56, 60	R SPL
	40, -30, 42	R PrG/PoG
	20, -48, 62	R SPL/PoG
700	-12, -6, 64	L SMA
	-24, 6, 40	L Premotor/SMA
	-24, 10, 42	L Premotor
301	24, -8, 54	R Premotor/SMA
	24, -2, 64	R Premotor/SMA
	28, -10, 62	R Premotor

Table 8. Locations of significant cluster fMRI peaks for the timepoint-sequence interaction (Baseline [Control > Trained] > Post [Control > Trained]). Cluster size is in voxels. Peaks are in MNI 152 standard space. Abbreviations: L, Left; PrG, Precentral Gyrus; R, Right; SMA, Supplementary Motor Area; SPL, Superior Parietal Lobule

TMS mapping

There was no significant change in RMT following training (40.8% vs 41.6% maximum stimulator output; $p > 0.05$). By contrast, training induced an increase in the *volume* of MEP amplitudes evoked at the targeted sites by an average of 58.6% ($p = 0.015$; Figure 19). That is, with the same relative TMS intensity (120% of RMT), MEPs evoked by TMS at the active sites were significantly larger following training. There was no significant increase in the number of active sites evoked with TMS ($p=0.09$). A cortical heat-map from a representative participant is shown in Figure 19, together with group-wise changes. A normalised group-wise heat map (see Methods) is also shown in Figure 17.

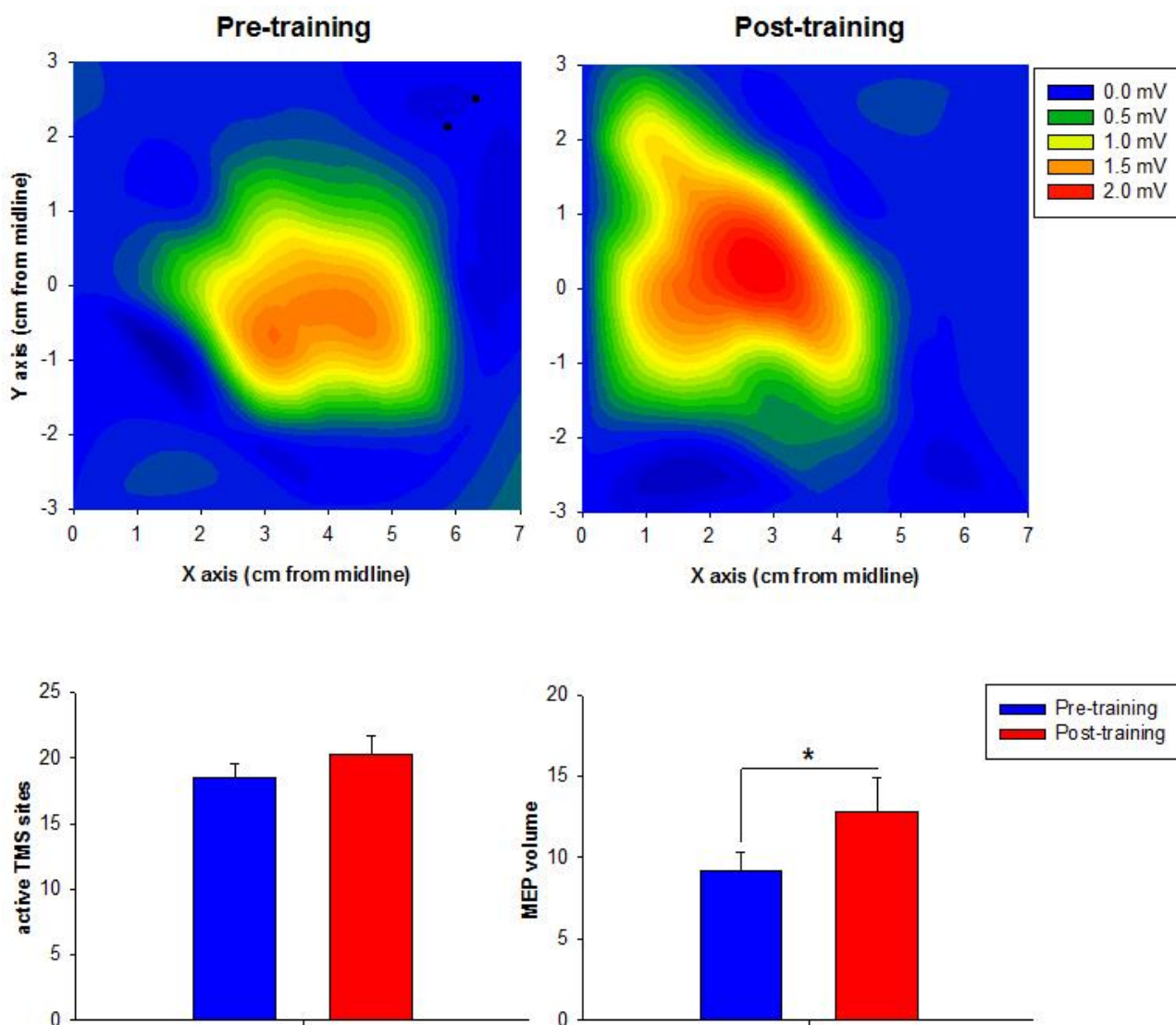


Figure 19. Training-related changes in motor cortical excitability. Top: A heat-map representation of the cortical representation of the abductor pollicis brevis before (left) and after (right) training in one representative participant. Coordinates are referenced to the vertex (0, 0). The average MEP amplitude evoked at each site is indicated by the colour scale (mV). Bottom: Mean number of active sites (left) and MEP map volume (right) before (blue) and after (red) training across all participants. There was no increase in active sites following training, but MEP volume increased significantly.

Cortical Thickness

One participant's dataset was lost during transfer to the server, and so was excluded from both cortical thickness and fMRI analyses. A second participant displayed slight MRI artefacts on the T1 images in the right sensorimotor cortex, and so was excluded from cortical thickness analyses. For a third dataset we were unable to achieve a high-quality tissue segmentation and so we excluded this dataset from cortical thickness analyses, leaving 21 participants in total for these analyses. At an uncorrected threshold of $p < 0.001$, training resulted in an increase in cortical thickness in the right precentral gyrus (81 voxel cluster), right post central gyrus (34 voxel cluster) and right dlPFC at approximately Brodmann's area 9 (22 voxels; Figure 20). The right supplementary motor area (SMA) also contained two nearby clusters, 11 and 13 voxels in size, whose individual volumes did not cross our prespecified threshold, but whose sum did. Although these five clusters did not survive multiple comparisons correction ($p < 0.05$ FWE) all changes were observed in regions that are likely to be involved with motor tasks, and all were in the right ('trained') hemisphere. Notably, clusters at the pre- and post-central gyri were consistent with the expected location of sensory and motor finger representations,^{233,234} and close to peaks in the (post time-point) TMS and fMRI maps. All clusters were within the group-wise region of successful TMS excitation, and all but the prefrontal cluster were consistent with regions of group-wise fMRI activation. To test the robustness of these findings, we removed data from the two participants who displayed the strongest performance improvements. In this reanalysis, the previously found clusters in the pre-central gyrus, post-central gyrus, and prefrontal cortex were still apparent (data not shown).

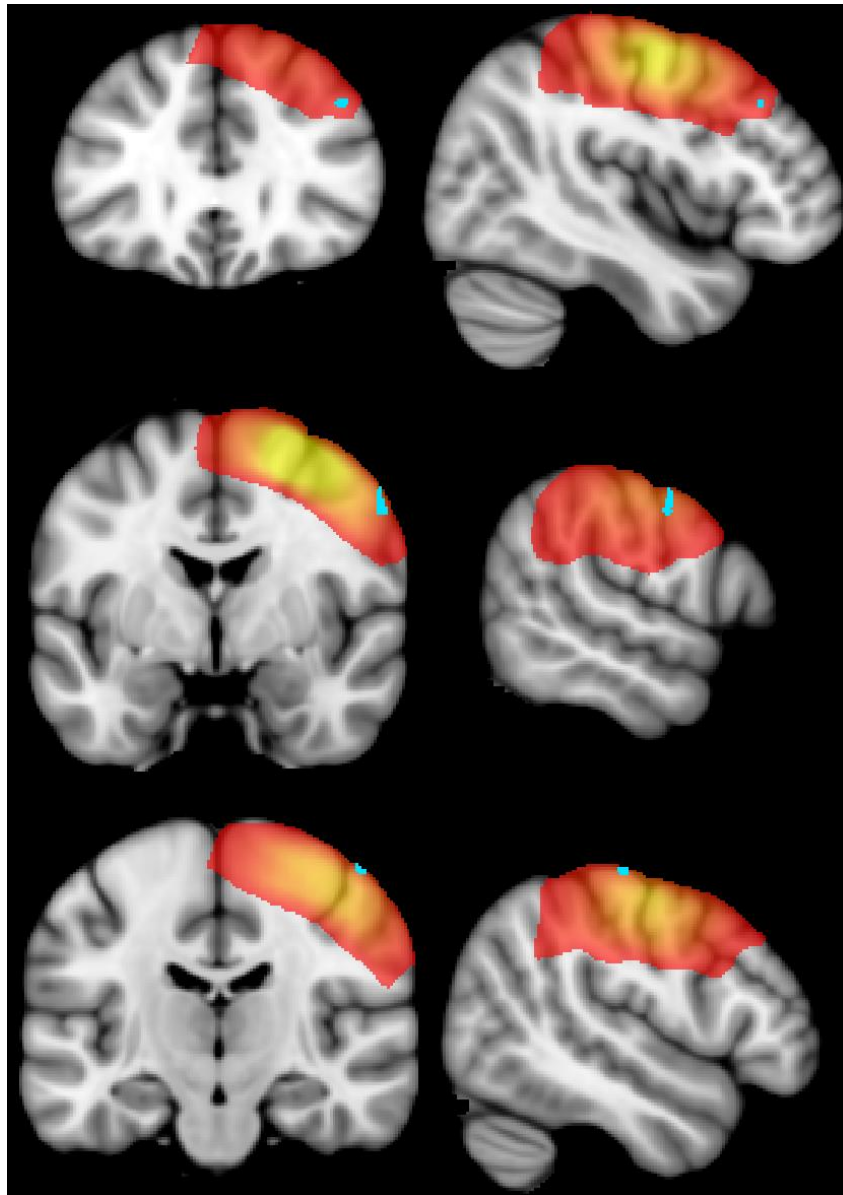


Figure 20. Areas of increase in cortical thickness overlaid on the FSL MNI 152 template. Light blue indicates voxels with significant (cluster size > 20 voxels at $p < 0.001$ unc) increases in cortical thickness estimation. Increases were seen in the right prefrontal cortex (top row), and approximate hand areas of the right precentral (middle row) and postcentral (bottom row) gyri. Red-Yellow indicates mean normalised TMS response, where yellow indicates a strong response (mean $\geq 30\%$ normalised peak motor evoked potential) and red indicates a weaker response (mean $\geq 1\%$ of normalised peak motor evoked potential); see text for details. Left of coronal and axial images indicates left of brain. Axial slices (top-to-bottom) show MNI y-coordinates 30, -3 and -18. Sagittal slices show MNI x-coordinates 44, 58 and 61.

Discussion

The neural changes that accompany a period of motor training contribute to the increase in performance. Understanding how these neural changes manifest themselves is important in both guiding rehabilitation strategies,¹⁰³ and understanding normal brain function. Such neural changes can be quantified in several ways, each with their respective advantages and limitations. Here, we show how utilising several different methods to concurrently quantify plasticity – behavioural, brain stimulation, functional brain imaging, and structural brain imaging – can offer broad insight into the plastic changes that arise following training. To our knowledge, these multimodal data from healthy adults provide the most comprehensive assessment of the functional and structural changes that occur following training to date.

Four weeks of training of a sequence of finger-thumb opposition movements resulted in a substantial improvement in performance. This was particularly true of the trained sequence performed with the trained hand, for which correct sequence completions improved by 53% (Figure 16). This was similar (albeit slightly lower) than reported in two similar, yet smaller, studies.^{169,221} To further investigate the brain changes arising from training, we incorporated several other probes of cortical structure and function. Although transfer of skill did occur, both between sequences and between hands, our fMRI and TMS analyses were not explicitly designed to investigate such effects. Diffusion MRI analyses detailed in a companion paper²²⁴ explored transfer effects in the same participant group in more detail.

fMRI

Our fMRI analyses revealed that, only after training, the trained sequence evoked *lower* cortical activation bilaterally than the control sequence (Figure 18), predominantly in the sensorimotor cortices and superior parietal lobe (Table 8). The apparent relative reduction in functional activation reported here is at odds with an earlier smaller (n=6) study that used a very similar training and scanning approach.²²¹ A subsequent replication of this work showed that fMRI activation decreased during the 3rd and 4th weeks of training, and PET data suggested that this was, at least in part, due to an increase in baseline blood flow rather than a decrease in actual brain activity.¹⁶⁹ Changes in baseline blood flow may certainly have taken place in the present study, but are unlikely to explain our results because our contrast focused on the interaction between time point and task. Specifically, since both the control and learned tasks evoked the same patterns of activation at baseline (Figure 17), changes in resting cerebral blood flow would be expected to affect both equally, and so cannot explain the statistical interaction reported here. An alternative, non-mutually exclusive, explanation

is that local changes, such as LTP, allowed local grey matter to perform the learned sequence more efficiently, reducing the need for recruitment of surrounding areas. Although motor training paradigms, similar to the one employed in the present study, have been shown to induce LTP-like changes in cortical activity,²³⁵ it would be fair to consider this hypothesis speculative if based on fMRI alone. In the present work, however, it is supported by two additional lines of evidence: changes in TMS-evoked responses, and changes in cortical thickness.

TMS

TMS provides an indirect way to assess LTP-like changes in cortical excitability. Since TMS activates motor cortical output neurons trans-synaptically, if synaptic efficacy is increased, this should lead to an increase in the amplitude of the MEP at a given stimulus intensity.²³⁶ Here, we showed that MEP amplitudes were larger following training (Figure 19). Notably, there was no significant change in the area that could evoke an MEP in the APB. This suggests that the changes indexed by TMS were predominantly driven by changes in neural networks that already played a role in contraction of the APB.

In order to consider TMS and MRI evidence together, it is important that these are viewed with respect to one another, to ascertain that regions of measurement (or signal change) for these modalities have reasonable anatomical overlap. In the present study, the areas of cortex that were activated by the trained sequence (in the trained hemisphere) during fMRI scans were very similar, though not identical, to areas eliciting MEPs during TMS mapping (Figure 17). TMS and fMRI map markedly different aspects of motor control, and so perfect overlap between them should not be expected: fMRI here contrasted BOLD responses to sequential movement of the fingers and thumb versus rest, while TMS targeted neurons functionally relevant to activating the APB muscle.

Keeping in mind that there was no increase in the RMT, the TMS findings suggest that at least one of three processes have taken place: enhanced trans-synaptic transmission (e.g., through LTP), increased neurite density, and/or improved conduction of the corticospinal tract. Both the first and second of these possibilities support our earlier hypothesis introduced in the context of the fMRI results. The third possibility, regarding changes in white matter, is investigated in detail in our follow-up publication.²²⁴

Cortical Thickness

Increased cortical thickness was observed after motor training within the right SMA, right middle-frontal gyrus, as well as right pre-central gyrus and right post-central gyrus. Although cortical

thickness changes did not reach our stricter FWE-corrected threshold, the clusters of significant voxels seen were sizeable (22 - 81 voxels @ $p < 0.001$) and striking in their location. The location of clusters in the pre- and post-central gyri were consistent with our fMRI maps, our TMS maps (Figure 20), and with areas responsible for sensorimotor representation of the fingers elucidated through electrocorticographic and brain stimulation techniques.^{233,234} The neighbouring clusters seen in the right SMA were also within the TMS and fMRI maps from our study, and consistent with previous findings that this area plays a role in motor learning.²³⁷ That these changes appeared near the peaks of fMRI and TMS maps adds further credibility to the suggestion that changes in fMRI and TMS patterns were a reflection of altered neurite organisation, density, and/or connection strength in regions that, at baseline, were already predominantly responsible for execution of the (to-be) learned sequence, rather than altered responsibility of surrounding areas.

The final location in which we saw changes in cortical thickness was the dlPFC, which is known to play an important role in error-correction of motor output (along with the caudate nucleus).^{215,216} Structural changes in the dlPFC were toward the edge of the TMS response map, and not in an area of fMRI change. The role of the dlPFC is to *modulate* motor responses, not generate them directly, and so it should not be surprising that only small TMS responses were recorded. Furthermore, we do not consider cortical thickness change here to be at odds with fMRI findings because the fMRI analysis was optimised for detection of motor output and conducted at around half the speed participants were capable of at baseline; it did not contrast very-challenging-versus-relaxed motor performance, as would be optimal to highlight an area that plays a role in error detection. In fact, we believe this apparent discrepancy highlights the usefulness of multimodality imaging in measuring neuroplasticity to provide a more accurate overview of changes that take place during learning.¹⁸¹ The dlPFC and related areas were further investigated with diffusion imaging; these analyses are described in a separate publication.²²⁴

Generalisation to the Untrained Hand

We report improvements in task performance for both sequences in both hands, despite only one sequence with the non-dominant hand being trained. Such cross-hemisphere generalisation is at odds with one smaller study ($n=6$) that employed a similar learning task,²²¹ but is consistent with findings from several other motor studies that utilised other tasks.^{238,239} Our fMRI analyses revealed that, after training, execution of the trained sequence with the left hand elicited reduced activation relative to the control sequence, *bilaterally*. However, the present results and those of our companion paper²²⁴ revealed no changes in the left hemisphere as measured with structural or diffusion MRI. This discrepancy suggests that altered fMRI and behavioural measures of the ‘untrained’ side may reflect

changes in grey matter, such as LTP or altered neurite density, that were too subtle to be detected by structural MRI. Techniques such as neurite orientation dispersion and density imaging,¹⁷¹ or bilateral TMS, EEG, or fMRI tasks targeting the opposite hand, might allow future studies to shed further light on this issue.

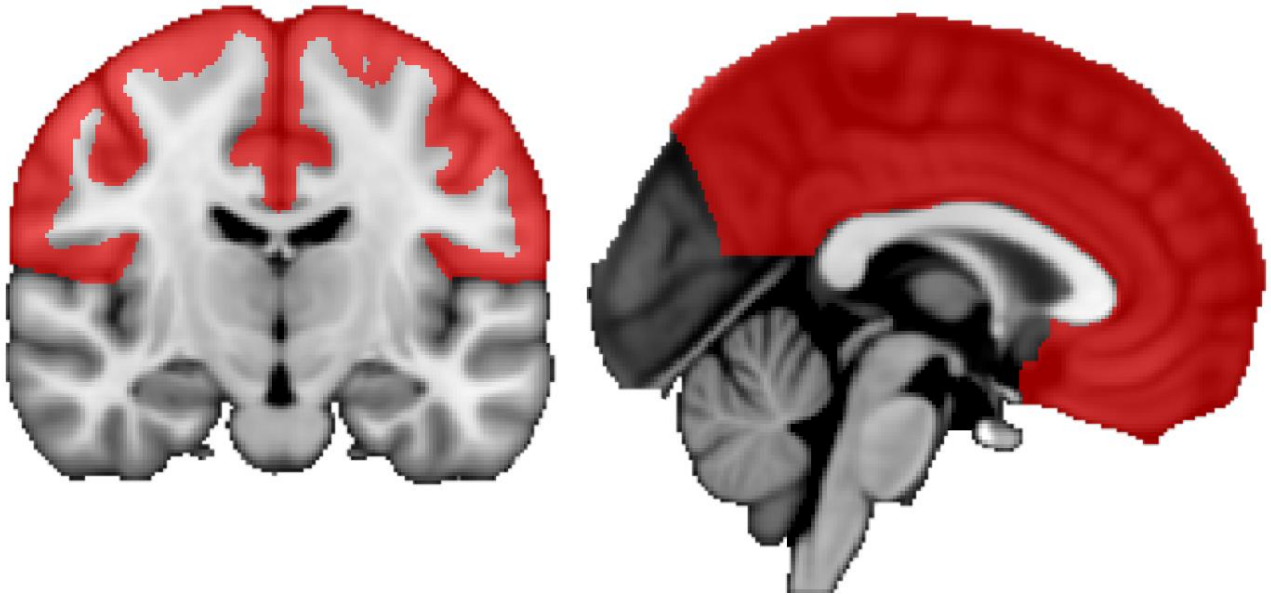
Limitations

The present study was designed to maximise the amount of concurrently acquired information. Practical considerations, however, meant that the depth of investigations with each modality had to be limited, leaving some open questions for future studies. For example, more challenging rates of task execution were not assessed using fMRI. Including such a manipulation might have helped us interpret the changes in dlPFC and related structures, as reported both here and in our diffusion MRI work.²²⁴ Similarly, TMS was not acquired for the ‘untrained’ hemisphere. Including such a condition might help to understand processes responsible for skill transfer between hemispheres. Future work could also further illuminate these processes by including an additional time point, several days or weeks following the cessation of training. Another possibility would be to include daily behavioural assessments, to assess whether training-related brain changes reflect continuous skill acquisition, or instead track ongoing learning processes themselves and subside once skill level reaches a plateau. In a multiple-time point study of this nature, collecting behavioural error rates, in addition to successful-sequence completion rates, would also be advantageous.

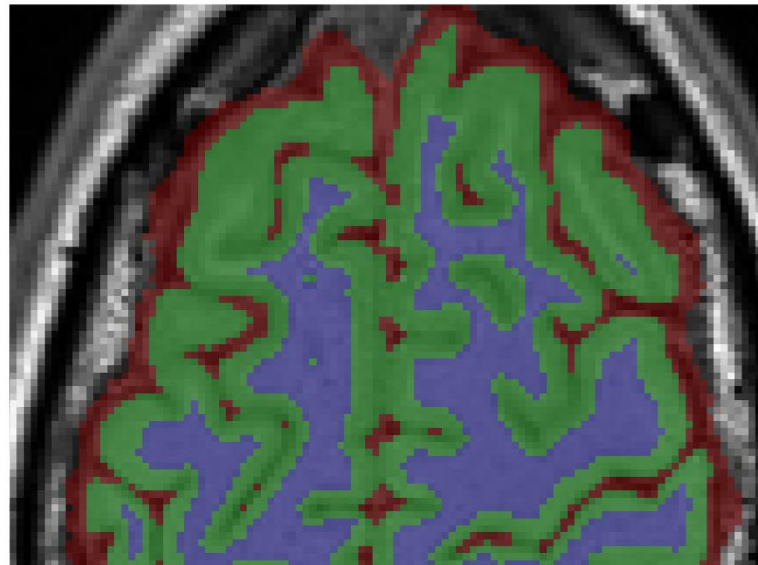
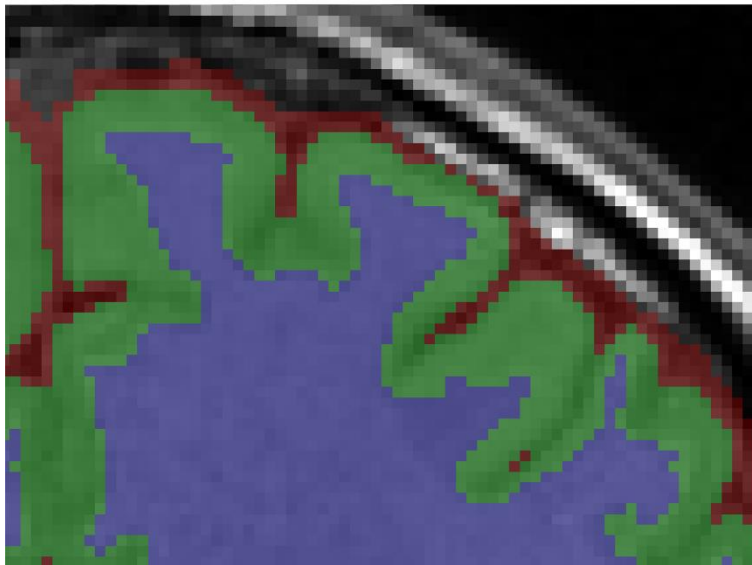
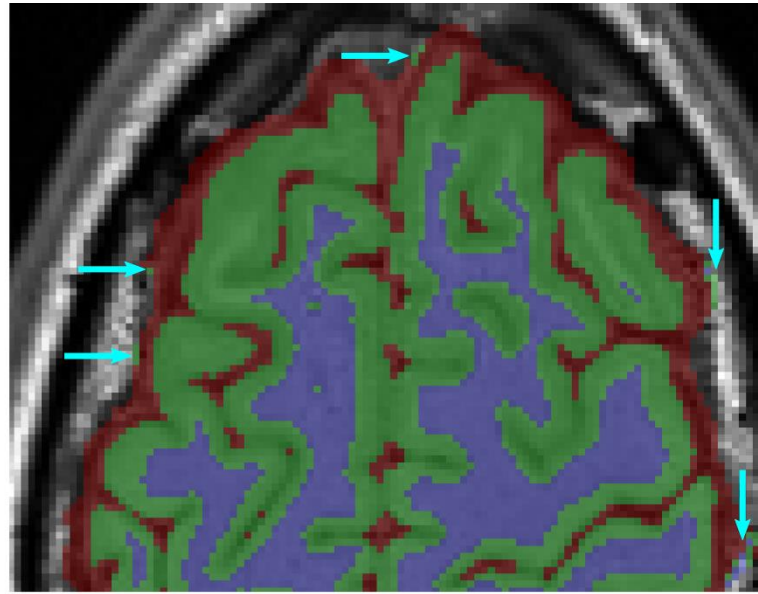
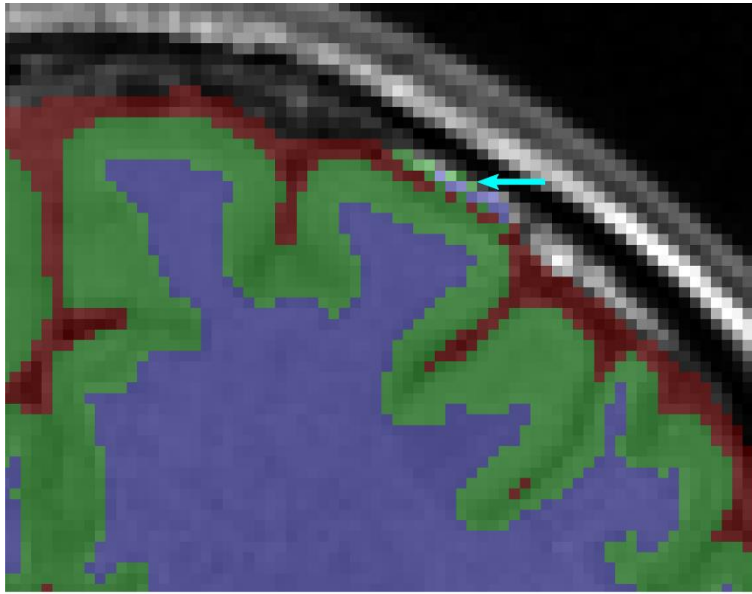
Conclusion

We have shown that four weeks of motor training can invoke robust changes in behaviour, cortical thickness, fMRI activation, and TMS-evoked motor maps in motor regions of the brain. Taken together with our diffusion MRI findings,²²⁴ the work presented here provides the most cohesive and comprehensive longitudinal study of motor plasticity in healthy adult humans to date. All three brain measures suggested that motor learning was driven by LTP-like plasticity that was relatively widespread across the sensorimotor system – even when a participant is trained on a simple task solely on the basis of proprioceptive feedback.

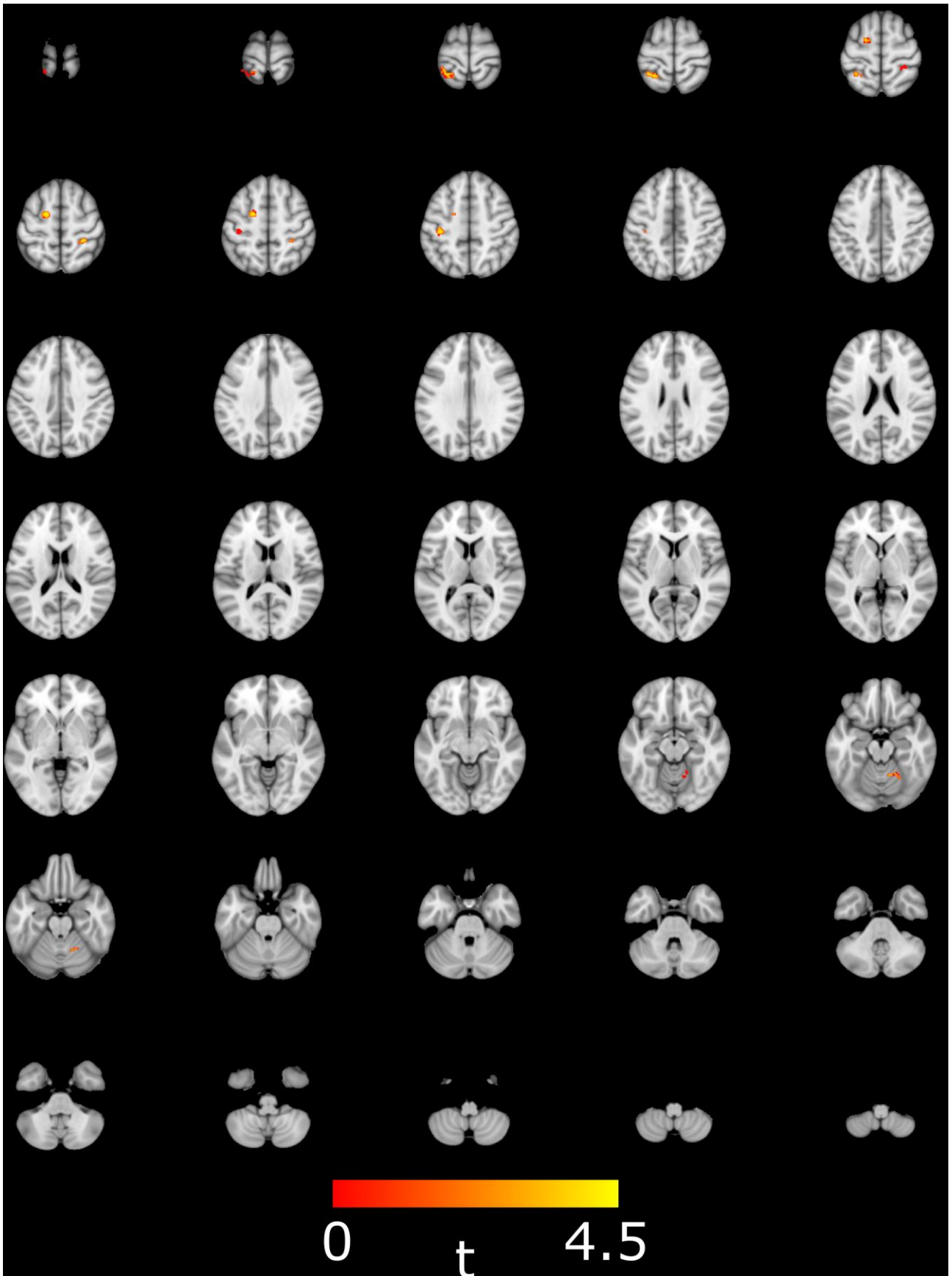
Supplementary Material



Supplementary Figure 2. Region of interest for cortical thickness analysis (red) overlaid on the FSL MNI template used to coregister participants. To correct segmentation errors, brain masks for single-subject templates were manually edited in every sagittal, axial, and coronal slice prior to warping to MNI space. Final segmentation acceptability was based predominantly on the frontal and parietal lobes (red). Voxel-based morphology statistics were solely calculated for these regions.



*Supplementary Figure 3. Coronal (left column) and Axial (right column) views of final hard segmentations achieved for a single-subject template, as calculated by ANTs. Blue, green, and red indicate white matter, grey matter, CSF, respectively. **Top Row:** segmentation performed without any form of manual correction. Arrows indicate locations where dura has been categorised as grey and/or white matter. The existence of any of these errors would deem the segmentation unacceptable in the present study. Small (<5 voxel) clusters of grey matter labelling of the dura in the temporal and occipital lobes were generally corrected but did not automatically deem an entire segmentation as unacceptable if the only error present. **Bottom Row:** segmentation of the same template using repeated brain mask correction to correct segmentation errors. The displayed images are representative of the typical error-correction performed, and final segmentation quality obtained, in the present study. Left of images is subject's left. Top of axial images is anterior. Top of coronal images is superior.*



Supplementary Figure 4. Functional MRI for baseline [control_sequence > rest] > post [control_sequence > rest]. Result is thresholded at $p < 0.001$ uncorrected with minimum cluster size of 20 voxels; no voxels survived at a voxelwise threshold of $p < 0.05$ FWE. Left of image is left of brain. This map indicates areas where brain activation was lower after training than before training, as participants undertook a novel tapping sequence. Activation can be seen in several motor regions, including regions ipsilateral to the trained hand. Note that this scan was not intended to be directly interpreted; instead, it was intended as a control for execution of the learned sequence, allowing statistics to account for daily fluctuations and other changes unrelated to motor learning. The opposite contrast was also conducted (baseline [control_sequence > rest] < post [control_sequence > rest]). This revealed increased activation in the right superior parietal lobe at $p < 0.001$ (uncorrected) with minimum cluster size of 20 voxels (not shown).

Chapter 6

Brain changes following four weeks of unimanual motor training: evidence from fMRI-guided diffusion MRI tractography

This chapter consists of the paper *Structural and functional brain changes following four weeks of unimanual motor training: evidence from fMRI-guided diffusion MRI tractography*. This and the preceding chapter form a pair of papers which are both available on the preprint server *bioRxiv*. The present chapter has been accepted to the journal *Human Brain Mapping*; the previous chapter was still under peer review for the same journal at the time of writing. Together, these papers describe a wide-scale multimodal analysis of motor learning in healthy adults. The present chapter focusses on behavioural data and diffusion MRI of the corticospinal tract, basal ganglia, and dorsolateral prefrontal cortex.

The opening to the previous chapter describes how this pair of chapters contribute toward Aim 3 of this thesis. In addition, the present chapter contributes toward Aim 2: *address the need for algorithms that can reliably detect subtle structural brain changes and that perform well in the presence of pathology*. Specifically, this chapter demonstrates that the fMRI-driven diffusion method previously described is sufficiently sensitive to detect minute changes in white matter microstructure associated with motor learning. A similar analysis in children with UCP is demonstrated in Chapter 7. A formal analysis of the reliability of this method in children with UCP appears in Chapter 8.

As joint-first author on this publication, I analysed all data, and was the primary contributor in terms of data and manuscript construction. I also made substantial contributions toward planning of analyses. Contributions by others were predominantly study planning, data acquisition, manuscript editing, and critiquing the biological interpretation of final results.

Publication information

Reid LB, Sale M V, Cunnington R, Mattingley JB, Rose SE. Brain changes following four weeks of unimanual motor training: evidence from fMRI-guided diffusion MRI tractography. *Hum Brain Mapp. (In Press)*

and

Reid LB, Sale M V., Cunnington R, Mattingley JB, Rose SE. Structural and functional brain changes following four weeks of unimanual motor training: evidence from fMRI-guided diffusion MRI tractography. *bioRxiv*. 2016 Nov 17;

DOI: 10.1101/088328

Martin Sale and Lee Reid were joint-first authors on this publication.

This work also appeared in abstract form and was presented at an international conference as follows:

Reid LB, Sale M V., Cunnington R, Rose SE. Motor Learning Induced Neuroplasticity, Revealed By fMRI-Guided Diffusion Imaging. In: 24th Annual Meeting and Exhibition of the International Society for Magnetic Resonance in Medicine. Singapore; 2016.

Abstract

We have reported reliable changes in behaviour, brain structure and function in 24 healthy right-handed adults who practiced a finger-thumb opposition sequence task with their left hand for 10 mins daily, over four weeks. Here we extend these findings by employing diffusion MRI to investigate white-matter changes in the corticospinal tract, basal-ganglia, and connections of the dorsolateral prefrontal cortex. Twenty-three participant datasets were available with pre-training and post-training scans. Task performance improved in all participants (mean: 52.8%, SD: 20.0%; group $p < 0.01$ FWE) and widespread microstructural changes were detected across the motor system of the ‘trained’ hemisphere. Specifically, region-of-interest based analyses of diffusion MRI ($n=22$) revealed significantly increased fractional anisotropy in the right caudate nucleus (4.9%; $p < 0.05$ FWE), and decreased mean diffusivity in the left nucleus accumbens (-1.3%; $p < 0.05$ FWE). Diffusion MRI tractography ($n=22$), seeded by sensorimotor cortex fMRI activation, also revealed increased fractional anisotropy in the right corticospinal tract (mean 3.28%; $p < 0.05$ FWE) predominantly reflecting decreased radial diffusivity. These changes were consistent throughout the entire length of the tract. The left corticospinal tract did not show any changes. FA also increased in white matter connections between the right middle frontal gyrus and both right caudate nucleus (17/22 participants; $p < 0.05$ FWE) and right supplementary motor area (18/22 participants; $p < 0.05$ FWE). Equivalent changes in FA were not seen in the left (‘non-trained’) hemisphere. In combination with our functional and structural findings, this study provides detailed, multifocal evidence for widespread neuroplastic changes in the human brain resulting from motor training.

Introduction

The science of motor rehabilitation for patients with brain injury is hampered by a lack of understanding of how experience changes brain structure and function at microscopic and macroscopic scales. A small number of publications have reported such changes in animal models, cross-sectional comparisons, and/or functional measures of brain change.²⁰⁹ The majority of such studies have reported results from single imaging modalities (e.g. fMRI) with different study protocols and learning tasks, which can make it difficult to interpret the available research to construct a cohesive picture. In addition, despite decades-old reports of electrical activity inducing myelination *in vitro*,^{170,240} evidence that myelin is continuously turned over *in vivo*,^{241,242} and evidence that electrical potentials evoked by stimuli can change in response to some other forms of learning,²⁴³ there have been very few longitudinal studies of white matter (WM) change associated with motor learning in humans. In the few works published, changes in diffusion MRI (dMRI) have predominantly indicated possible changes near the GM/WM interface in visuo-motor areas in participants undergoing visuo-motor skill learning⁸⁰ and in the frontal lobe of participants learning a balancing task.²³⁷ Curiously, this latter study reported a reduction, rather than increase, in fractional anisotropy (FA), and a variety of decreases in cortical thickness amongst its results. All of these studies have relied on voxel based morphometry (VBM). Unfortunately, when applied to dMRI, VBM can be greatly influenced by the parameters used, and false positive results can arise through registration biases.^{229,244,245} Although VBM is still considered a valuable family of methods, the voxelwise statistics produced can have low statistical power and, in most instances, leave researchers unable to confidently interpret their results in terms of specific tracts,²⁴⁶ which precludes insight into precisely which networks are undergoing change.

Diffusion tractography allows measurement of microstructural properties of specific WM tracts, but is a largely unexplored method in this area, potentially because of several limitations that accompany its most common implementation. First, the method traditionally relies on parcellation-based tract classification, which is likely to include aspects of WM tracts that are functionally irrelevant to the learned task.¹⁸¹ For example, effects of practicing a hand-based motor task would be ideally investigated in only the part of the corticospinal tract responsible for hand movement, but parcellation-based seeding would typically also include fibres responsible for movement of the face, trunk, and legs. Failure to restrict measures to fibres involved with hand use theoretically weakens the method's sensitivity and, in longer-term studies, increases the likelihood that any changes found might reflect other processes, such as developmental maturation.^{e.g. ,247} Diffusion metrics from tractography are also typically calculated on a whole-tract-mean basis, opening the possibility of missing changes in a subset of voxels or – if artefactual or due to changes in a crossing fibre – falsely

concluding that the entire tract has changed. Finally, neither voxel-based morphometry nor traditional tractography integrate functional information, which limits the ability to infer functional relationships between changes seen, brain function, and skill acquisition.

Previously, we reported a multimodal study of motor learning which used fMRI, TMS, cortical thickness and behaviour (task performance) to assess structural and functional brain changes in 24 healthy adults who practiced a non-visual motor task for ten minutes a day for four weeks.²⁴⁸ These findings suggested that improvements in task performance were driven, at least in part, by changes within the grey-matter, such as long-term potentiation of synapses. These changes appeared to take place in cortical regions that were already responsible for task performance at baseline, rather than representing gained function in neighbouring areas. The amplitude of TMS-evoked motor evoked potentials reported in this previous work increased significantly following training, which could reflect both grey matter changes (either locally within the stimulated brain region, or in remote but functionally related brain regions), improved white-matter conductivity, or both. Changes in cortical thickness of the dorsolateral prefrontal cortex (dlPFC) were also reported, but neither TMS nor fMRI were optimised for investigating this area.

Here, we report the effects of four-weeks of motor learning on the microstructure of the basal ganglia, corticospinal tract, and related intracortical white matter networks. We hypothesised that, solely in the ‘trained’ hemisphere, fractional anisotropy would increase in the corticospinal tract, dlPFC connection to the caudate nucleus, and dlPFC connection to the supplementary motor cortex, due to the importance of these networks in voluntary movement and motor learning. We also hypothesised that the basal ganglia may exhibit microstructural changes, reflecting sub-cellular reorganisation evoked by an LTP-like process associated with motor practice. Unlike previous studies, this experiment was carried out with a pure motor-coordination task, and on a dataset for which a variety of brain changes and performance improvements are known to have occurred.²⁴⁸ To overcome the aforementioned limitations of traditional dMRI methods, where possible, we utilised a recently-validated fMRI-guided diffusion tractography method²⁴⁹ that allows for sensitive measurement of diffusion metrics in specific functionally-relevant tracts. The novelty of the present findings lies in the unique (and broad) loci over which changes were detected, in the specific hypotheses addressed, and in the high-degree of anatomical specificity provided by the utilised methods. Furthermore, the present results yielded relatively clear-cut biological interpretations, and we believe generate a number of testable predictions for future work. This is due in part to concurrent changes that were detected in a number of independent measures, including TMS-induced motor-evoked potentials.²⁴⁸ We also performed a series of subanalyses to confirm results were not a reflection of participant selection, tensor fitting algorithms, voxel exclusion criteria, tractography

seeding biases, or variable region-of-interest placement. In combination with our functional and structural findings, this study provides compelling evidence that neuroplasticity can be induced throughout the motor system by a relatively focussed form of motor training, and interpreted more robustly when measured with a comprehensive multimodal imaging approach.

Methods

Participants and Task

Details of the task and participants have been published elsewhere.²⁴⁸ In brief, 24 participants were recruited (14 female; aged 28.8 ± 1.5 years; range 18 – 40 years) who were all right-handed (laterality quotient 0.92 ± 0.03 ; range 0.58 – 1.0) as assessed by the Edinburgh handedness questionnaire. Participants practiced a finger-thumb opposition sequence with their left hand for ten minutes each day, for four weeks. Participants were randomised to practice one of two sequences, and instructed to practice as quickly and accurately as possible but not to watch their hand while doing so. We collected MRI (3T Siemen's Magnetom Trio) and behavioural data for 23 participants immediately before (*baseline*) and after (*post-training*) this period. Task performance was assessed as the number of correct sequences that could be performed in a 30-second period. This was recorded for each hand by video, outside of the scanner, and quantified offline. Participants gave informed consent and the study was approved by The University of Queensland Human Research Ethics Committee.

Single Participant T1 Templates

In longitudinal analyses, it is possible for variable regions of interest to induce biases that result in false positive or false negative results. To avoid this, diffusion measures which required atlas-based regions of interest utilised *single participant templates* – T1 images for each participant that were unbiased with respect to time point. The steps used to generate these are described in detail elsewhere.²⁴⁸ In brief, a participant's T1 images (MPRAGE, 0.9mm isotropic) at pre- and post-training were N4 corrected, intensity normalised, and registered to one another using half of a symmetrical transform, calculated with ANTS Syn,²³⁰ after skull stripping. This initial template was converted into a sharper template using the *antsMultivariateTemplateConstruction* script. Segmentation was achieved by using ANTs tools with the ANTs NKI template. If the segmentation was not satisfactory, the brainmask was carefully manually edited and this process repeated. Examples of satisfactory and unsatisfactory segmentations can be found with detailed descriptions of this process elsewhere.²⁴⁸ Cortical labels were calculated for each participant's templates using *antsJointLabelFusion* with the ANTS IXI and NKI templates. To identify structures of the basal ganglia, single-participant template T1s were processed with volBrain,²⁵⁰ which has been demonstrated to provide accurate delineation of deep GM structures.²⁵¹

Diffusion MRI of the Basal Ganglia

Several structures of the basal ganglia are thought to play key roles in motor learning and goal directed behaviour.^{215,216,219,252} It is therefore possible that extensive practice of a motor task could drive an

LTP-like process that subtly modifies sub-cellular organisation within these regions. We aimed to determine whether changes in microstructure were apparent in the basal ganglia. At both time points, we acquired a 64-direction high-angular resolution diffusion image sequence with $b=3000\text{s/mm}^2$, one $b = 0$ image, whole brain coverage, and $2.34 \times 2.34 \times 2.5\text{mm}$ spatial resolution. Our HARDI dMRI pipeline has been published in detail elsewhere.^{58,190} In brief, dMRI data underwent extensive preprocessing, and constrained spherical deconvolution was used to estimate fibre orientation distributions. We used MRTrix 3 (<https://github.com/MRtrix3/mrtrix3>)¹⁸⁰ to calculate tensor metrics across the whole brain.

Registration between T1 and diffusion b_0 diffusion images was calculated with FSL's *epi_reg*, using the previously generated single-participant template white-matter segmentation. By applying the inverse of this transform, labels for the basal ganglia were moved into diffusion space. Mean FA and MD values were then sampled within the labels for the globus pallidus, putamen, caudate nucleus, and nucleus accumbens (NAcc). Although volBrain also provides a label for the amygdala, we considered this area unsuitable for analysis as it is often heavily distorted in dMRI images.

We hypothesised that changes would likely be in the right hemisphere, and in specific ROIs, rather than across the entire basal ganglia. We performed a factorial ANOVA to determine whether changes had occurred differentially in any of these regions. This model was as follows:

$$\text{diffusionMetric} \sim (\text{subject} + \text{timepoint}) * \text{structure} * \text{hemisphere}$$

where structure refers to the basal ganglia structure type (putamen, caudate nucleus, etc). This model was used to better account for the non-independence of diffusion metrics between structures in each hemisphere (e.g. left and right putamen) than is possible by treating left and right structures as independent categorical variables. A significant interaction between structure, hemisphere, and time-point was used as the criterion for performing post-hoc paired t-tests to determine which individual ROIs had changed with respect to timepoint. Post-hoc tests were corrected for eight multiple comparisons using the Holm-Bonferroni method ($\alpha < 0.05$ FWE). We tested for decreases in MD (one-tailed), but bi-directional changes in FA (i.e. two-tailed), as interpreting FA change is not straightforward in deep grey-matter.

Diffusion MRI of the Frontal Cortex

Previously, we reported cortical thickness changes in the right ('trained') dlPFC in the region of Brodmann's area 9.²⁴⁸ Top-down control of motor output, for error-correction, is predominantly associated with activation of the dlPFC, as well as the caudate nucleus.^{215,216} The dlPFC is thought to connect strongly with premotor areas, including the supplementary motor area (SMA)²⁵³ – a region

which displayed changes in fMRI, cortical thickness, and TMS measures after training in the present cohort.²⁴⁸ For these reasons, we measured FA in connections between the middle frontal lobe and SMA, and the middle frontal lobe and caudate nucleus, with diffusion tractography.

Probabilistic whole-brain tractography was performed on constrained spherical deconvolution images using MRTrix 3.0. For each dataset, 20 million streamlines were generated using anatomically constrained tractography (iFOD2), with *dynamic seeding* and *backtrack* flags, but otherwise default settings. For each hemisphere, we sampled FA for tracts connecting (A) the middle frontal gyrus and caudate nucleus and (B) the middle frontal gyrus and SMA. Functional MRI-driven tractography was not possible for this subanalysis due to practical limitations regarding scan time, and so a standard parcellation-based approach was used. Labels used were from the single participant T1 templates (see above) to avoid temporal bias. The SMA label included both pre-SMA and SMA-proper. Sampling was weighted according to the output of MRTrix SIFT2.²⁵⁴ Difference in FA (post-training – pre-training) values violated assumptions of normality and were non-symmetrical. As such, a binomial test was conducted to calculate for an over-representation of FA increases ($H_0: \pi \leq 0.5$) with Holm-Bonferroni correction for four multiple comparisons ($\alpha < 0.05$ FWE).

Diffusion MRI of the Corticospinal Tract

We aimed to determine whether diffusion MRI metrics of the right corticospinal tract changed in response to the motor learning task. To focus on functionally-relevant white-matter, we analysed these images with an fMRI-seeded dMRI-tractography protocol that has been published in detail elsewhere.²⁴⁹ In brief, T1 images were used to generate surface meshes, upon which fMRI activations were calculated (see below). Statistically significant activation within the right S1M1 was used to seed probabilistic tractography from the white matter near the grey-matter/white-matter interface. The same mesh and seed were used for each time point. Tractography was performed on constrained spherical deconvolution images using MRTrix software that had been modified to utilise surface meshes as masks. For each dataset, 40,000 streamlines were generated that passed from the seeding region, through either the posterior limb of the internal capsule or the thalamus (as defined by manually-drawn regions of interest) and terminated in the brainstem. Meshes constrained tractography to the WM. Streamlines were classified as corticospinal or thalamocortical using k-means clustering and streamlines belonging to thalamocortical tracts were discarded. Although complex, this method has recently been shown to reveal more significant and robust relationships between motor performance and diffusion metrics than naïve voxel-based fMRI+dMRI methods, and also provides more coherent tracts than ROI-based classification.²⁴⁹ Our method here deviated from the previously published version by fMRI task and filtering method (see below). In order to rule out that any changes in the right corticospinal tract were due to biases in registration or tensor-fitting, the

procedure was repeated for the left corticospinal tract in all participants who displayed bilateral activation during the functional MRI.

Functional MRI

Functional MRI was used to identify functionally-relevant cortical areas for each participant, from which tractography was seeded. We acquired a 2D gradient-echo EPI (TE 28 ms, TR 2670 ms), with online distortion correction and 41 axial slices providing full-brain coverage at a voxel size of 3.28 x 3.28 x 3.3mm (matrix size 64 x 64; FOV 210 x 210 mm; slice gap 0.3mm). Prior to entering the scanner, participants familiarised themselves with the two movement sequences – ‘trained’ and ‘control’ – that they were going to perform within the scanner. Within the scanner, participants performed these finger-thumb opposition movements with their left hand in blocks of 16 seconds, each followed by 16 seconds of rest. During rest blocks, a visual display showed a “Rest” command. At the start of each movement block a visual cue - displaying either the red or blue hand and corresponding movement sequence - notified participants whether they would be performing the trained or the control sequence. This was displayed for 2 seconds, then removed. Participants then performed the required sequence at a rate of two movements per second. As a cue to aid in this timing, a fixation cross flashed at 2 Hz on the screen. A tone also sounded at 2 Hz intervals throughout the acquisition. The last two tones in each movement block were at progressively lower pitches to notify participants that a rest block was imminent. Immediately following completion of each movement block (i.e., following the last fixation cross), a “Stop” command was presented for 1 second, which was then replaced with the “Rest” command. Four consecutive ‘runs’ were performed. Each run consisted of four trained-sequence blocks, four control-sequence blocks, and seven rest blocks. The order of the trained/control sequence blocks was randomised but kept consistent between participants. Correct performance of the sequence was verified by recording the movements with a video camera, which were later reviewed for accuracy.

Each fMRI-session was analysed individually in surface space, using methods and parameters described previously.²⁴⁹ This included 5mm of surface-smoothing, and motion scrubbing where framewise displacement¹⁶⁵ exceeded 0.9mm. Contrast was set as learned-sequence > rest, for which statistical significance was set at $p < 0.05$ FWE. As this study enrolled healthy adults, we were able to utilise non-linear registration (NiftyReg)²⁵⁵ to propagate labels from the Harvard-Oxford atlas to the mesh in order to crop significant activation to the right S1M1. Manual filtering of significant activation was then carried out, as described previously.²⁴⁹ to retain only the largest ROI near the hand-knob on the right S1M1. For each participant, regions of significant activation from each time-point were combined with logical ‘OR’ to provide an identical seeding region for each time-point’s tractography. This seeding region was expanded such that total seeding area was at least 200mm² in

participants who displayed significant fMRI activation, but whose total seeding area was below this size.

Statistical Analysis of Tractography

We sought to determine whether FA had changed over time for the corticospinal tracts. Diffusion metrics were sampled for each tract, and the mean taken. Paired t-tests were applied to pre- and post-training tensor values to determine whether change in FA or MD occurred with training. It has become commonplace in VBM analyses to exclude voxels with FA values < 0.2 , in order to exclude GM voxels.²⁴⁶ Tractography naturally avoids such voxels, but to maintain comparability with previous works in this area, which have relied on VBM analyses, we repeated our analysis excluding all samples from voxels with an FA < 0.2 .

Changes in diffusion metrics were expected to be subtle. Although probabilistic tractography is robust to minor deviations in seeding position (especially with multiple inclusion ROIs), the possibility remains that deviations in tractography and/or errors in tensor fitting could cause a small number of voxels to artificially raise the mean FA of a tract, particularly near the seed point. The nature of axonal ‘all-or-nothing’ signalling and relationships between activity and subsequent myelination^{170,240} imply that genuine changes in white matter should occur throughout the entire length of a tract. To confirm that any detected changes reflected genuine change throughout the length of the corticospinal tract, each streamline was binned into seven equal-length sections, using a method previously described,²⁵⁶ and intensities were sampled for each section. An example of this binning is shown in Figure 22. Means for each bin were entered into a factorial ANOVA, with *time-point*, *participant*, and *bin* as factors, as well as *participant * time-point* and *time-point * bin* interactions, using R.²⁵⁷ *Bin* was treated as a categorical, rather than continuous, variable due to the non-linear nature of FA values across the tract length. The significance of the *time-point * bin* interaction in this model was inspected to determine whether any mean change was due to differences in a small cluster of voxels, or local variations in tractography, rather than biologically plausible changes. Criteria for further investigation into any such issues was set as (A) a loss of significance ($p \geq 0.05$) for the ‘time-point’ factor, and/or (B) trends towards significance ($p < 0.1$) for this interaction term.

TBSS

To facilitate comparison with previous works, we also ran tract based spatial statistics on our data. As voxelwise approaches are largely outside of the intended goals of this work, they are detailed and discussed in Supplementary Materials.

Results

Results are summarised in Table 9. Results for each participant are provided in Supplementary Materials. One participant displayed MRI artefacts on the T1 images in the right sensorimotor cortex, and so was excluded from all results reported here, leaving 22 participants. For these 22 participants, increased execution speeds were observed in the post-training assessment for both the trained (Left hand: $53 \pm 4.0\%$ [Mean \pm SEM]; Right hand: $23 \pm 4.2\%$) and control sequences (Left hand: $7.6 \pm 3.0\%$; Right hand: $17 \pm 3.9\%$). These mean increases were all statistically significant (One-tailed paired T-Test; Holm-Bonferroni corrected $p < 0.01$). The degree of performance improvement was

Sequence Execution Speed (n=22)

Sequence	Hand	Mean Change	Significance
Trained	Left	$\uparrow 53\%$	$P < 0.01$ FWE
Control	Left	$\uparrow 7.6\%$	$P < 0.01$ FWE
Trained	Right	$\uparrow 23\%$	$P < 0.01$ FWE
Control	Right	$\uparrow 17\%$	$P < 0.01$ FWE

fMRI Driven Tractography (n=22)

Measure	Tract	Mean Change	Significance
FA	Right Corticomotor	$\uparrow 3.28\%$	$p < 0.05$ FWE
FA	Left Corticomotor	$\uparrow 0.67\%$	ns ($p > 0.3$)

Diffusion MRI of Basal Ganglia (n=21)

Measure	Structure	Mean Change	Significance
FA	Right Caudate	$\uparrow 4.9\%$	$p < 0.05$ FWE
MD	Right Caudate	$\downarrow 0.9\%$	$p = 0.087$
FA	Right NAcc	$\downarrow 3.2\%$	$p = 0.071$
MD	Left NAcc	$\downarrow 1.3\%$	$p < 0.05$ FWE

Middle Frontal Gyrus FA Increases (n=22)

Hemisphere	Connection To	Increase Frequency	Significance
Right	Right Caudate	17/22	$p < 0.05$ FWE
Right	Right SMA	18/22	$p < 0.05$ FWE
Left	Left Caudate	ns	ns ($p > 0.5$)
Left	Left SMA	ns	ns ($p > 0.2$)

Table 9. Summary of major findings. Values are rounded to 2 significant figures. Significance is uncorrected for multiple comparisons, except where 'FWE' is signified. Abbreviations: FA, fractional anisotropy; FWE, Family-wise error (multiple comparisons) corrected; n, number of participants; ns, not significant; MD, mean diffusivity; NAcc, Nucleus Accumbens; RD, radial diffusivity; SMA, supplementary motor area

greater for trained than untrained sequence in the left hand ($p=1.2E-9$) but not in the right hand ($p=0.07$).

Diffusion MRI of the Basal Ganglia

No additional datasets were excluded from the diffusion MRI analysis of the basal ganglia ($n=22$). An example of ROI placement is shown in Figure 21. A significant interaction between structure, hemisphere, and time-point was found ($p=0.025$) and so post-hoc tests were performed. In the right caudate nucleus, FA increased significantly ($4.9\pm 1.4\%$ [Mean \pm SEM]; $p=0.002$; p -corrected <0.05), and there was a trend towards an MD decrease ($-0.8\pm 0.7\%$; $p=0.087$; p -corrected=ns). In the NAcc, a trend toward a decrease in FA was apparent in the right hemispheric nucleus ($-3.2\pm 1.8\%$; $p=0.07$; p -corrected=ns), and a decrease was seen in MD of the left hemispheric nucleus ($-1.3\pm 0.6\%$; $p=0.005$; p -corrected <0.05). We did not see changes in the globus pallidus or putamen. To test the robustness of these findings, we reran analyses using ANTs-generated basal ganglia labels, instead of those from

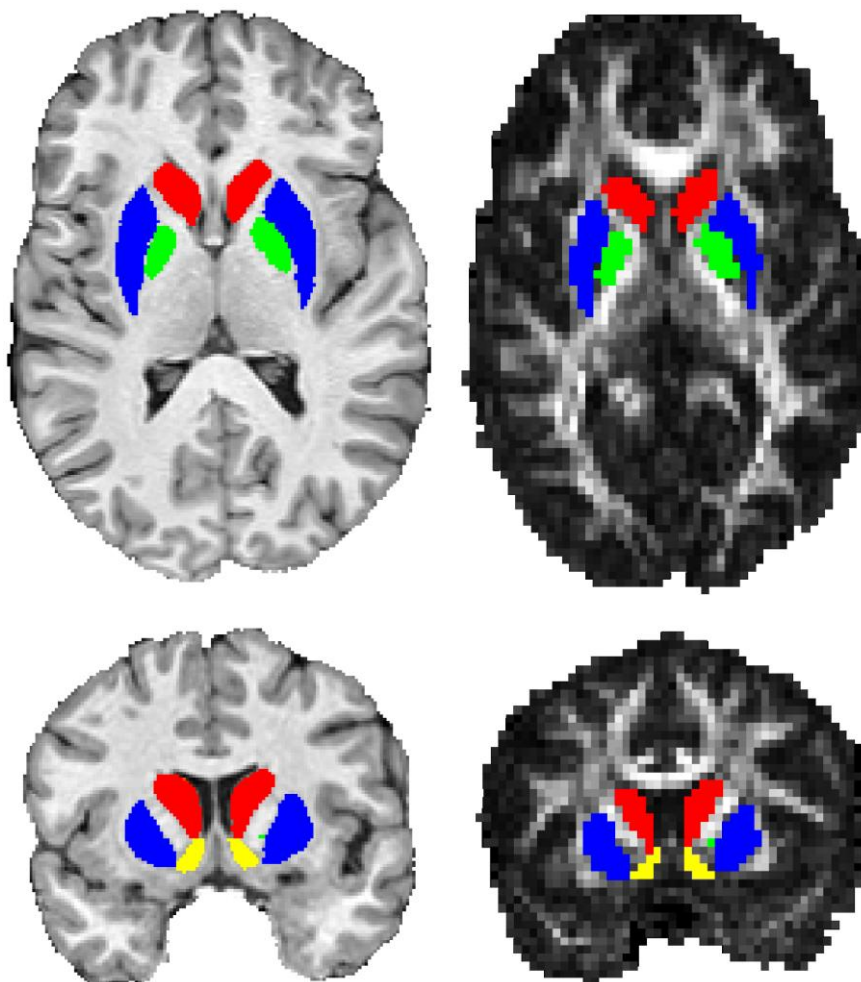


Figure 21. Example of volbrain ROI placement on a single participant template (left) and to a diffusion FA image (right). Colours: Red, Caudate Nucleus; Blue, Putamen; Green, Globus Pallidus; Yellow, Nucleus Accumbens.

volBrain, and utilised tensor maps calculated with an older version of MRTrix (2.9), which uses a different tensor fitting method. This reanalysis found a similar pattern of changes (data not shown).

Diffusion MRI of the Corticospinal Tract

fMRI

In this study, fMRI was used to delineate hand knob cortical regions for seeding tractography rather than to provide a measure of cortical plasticity. Changes in fMRI patterns with training have been reported in a previous paper (Chapter 5). For this reason, the fMRI activation maps for both baseline and post-training sessions were combined for each participant to delineate the hand knob region. Statistically significant S1M1 activation was unilateral in 5 participants and bilateral in the remaining 17 participants. An fMRI activation pattern from a typical participant is shown in Figure 22. All participants had significant S1M1 activation in the right hemisphere; this was used to seed tractography which delineated the right corticospinal tract. For those participants with bilateral activation, the motor region with significant BOLD response in the left hemisphere was used to delineate the left corticospinal tract. Significant activation was also commonly found in the supplementary motor area (21 participants) and superior parietal lobule (20 participants), but such activation was not used for seeding tractography.

Whole-Tract FA and MD

After training, mean FA of the right corticospinal tract had increased by 3.28% compared with the baseline measurement ($p=0.0029$ uncorrected; $p<0.05$ FWE for two comparisons; SEM 1.1%; median 2.01%), driven predominantly by a mean 2.2% decrease in radial diffusivity (median 1.34% decrease). MD of the right corticospinal tract was unchanged ($p>0.1$). FA and MD of the left corticospinal tract were also unchanged (both $p>0.05$). When the five participants who did not display left-hemispheric fMRI activation were also excluded from the right-hemispheric results, mean change in FA in the right corticospinal tract strengthened to a 3.95% increase ($p<0.004$ uncorrected; SEM 1.31%; median 3.45%). When these analyses were repeated with a voxel inclusion criteria of $FA \geq 0.2$, or with tensor maps calculated with older version of MRTrix (2.9) which uses a different tensor-fitting algorithm, the same pattern of results was obtained (data not shown). Although the seeds were identical for each time point, we sought to alleviate concerns that results were due to some unforeseen complication with fMRI seeding, and reran the analysis defining each corticospinal tract in a much more simplistic manner – tracks connecting the precentral gyrus to the brainstem. A similar pattern of results was seen, albeit with numerically smaller degrees of change in the right hemisphere (data not shown), as one may expect from a substantially less anatomically-specific method.²⁴⁹

Along-Tract Analysis

On the basis of an apparent increase in FA, a reanalysis was conducted to determine whether FA change occurred throughout the corticospinal tract. The right corticospinal tract was split into seven equal-length sections from which FA was resampled (Figure 22). A factorial ANOVA fed mean bin-FA values yielded significant effects of *time-point* ($p < 0.001$), and all controlled-for factors (see methods; all $p < 0.001$) but the *bin * time-point* interaction was not significant ($p = 0.42$), implying

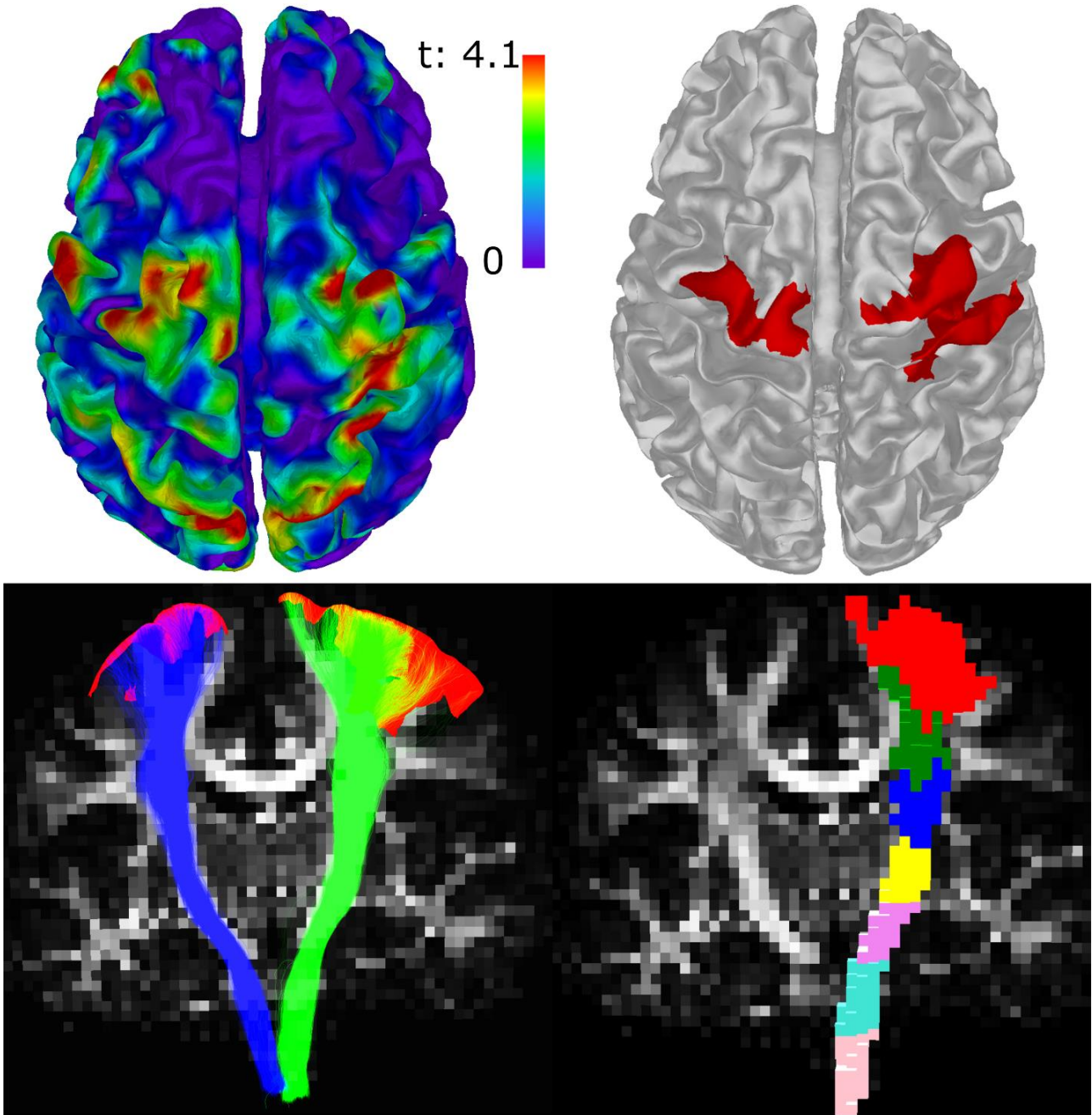


Figure 22. *fMRI-tractography for a representative participant. Top Left: fMRI t-value map for learned-task versus rest. Top Right: Areas of significant fMRI activation (red) after filtering and transforming to the grey-matter white-matter interface (silver; see text). Bottom Left: Left (blue) and right (green) corticomotor tracts, elucidated with tractography seeded from the thresholded fMRI (red), overlaid on the fractional anisotropy image. Bottom Right: 3D rendering of voxels crossed by the right corticomotor tract, broken into seven bins.*

change was relatively consistent (did not significantly differ) throughout the length of the tract. Unadjusted mean FA increased by 2.10 – 4.3% across the seven bins (Figure 23). This same pattern of results was found when the requirement for voxels to have an FA ≥ 0.2 was applied, or MRTrix 2.9 was used for tensor fitting (data not shown).

Diffusion MRI of the Frontal Cortex

Wholebrain tractography and related procedures were successful for all available participants. Given that we were unable to detect MD changes for the corticospinal tracts, we opted to solely measure FA for tracts associated with the middle frontal gyrus. This is because MD arguably has lower interpretability and specificity when applied to major white-matter pathways, and a severe multiple-comparisons penalty would be associated with collecting this measure. FA increased for tracts connecting the right middle frontal gyrus to (A) the right caudate nucleus in 17 of 22 participants ($p < 0.05$ FWE; median 1.78% increase), and (B) the right SMA in 18 of 22 participants ($p < 0.05$ FWE; median 1.71% increase). These changes appeared to be driven mainly by numerical decreases in radial diffusivity (median change: Caudate, -0.86%, SMA, -0.99%), rather than increases in axial diffusivity (Caudate, 0.59%, SMA, 0.35%). No significant changes were found in the left hemisphere.

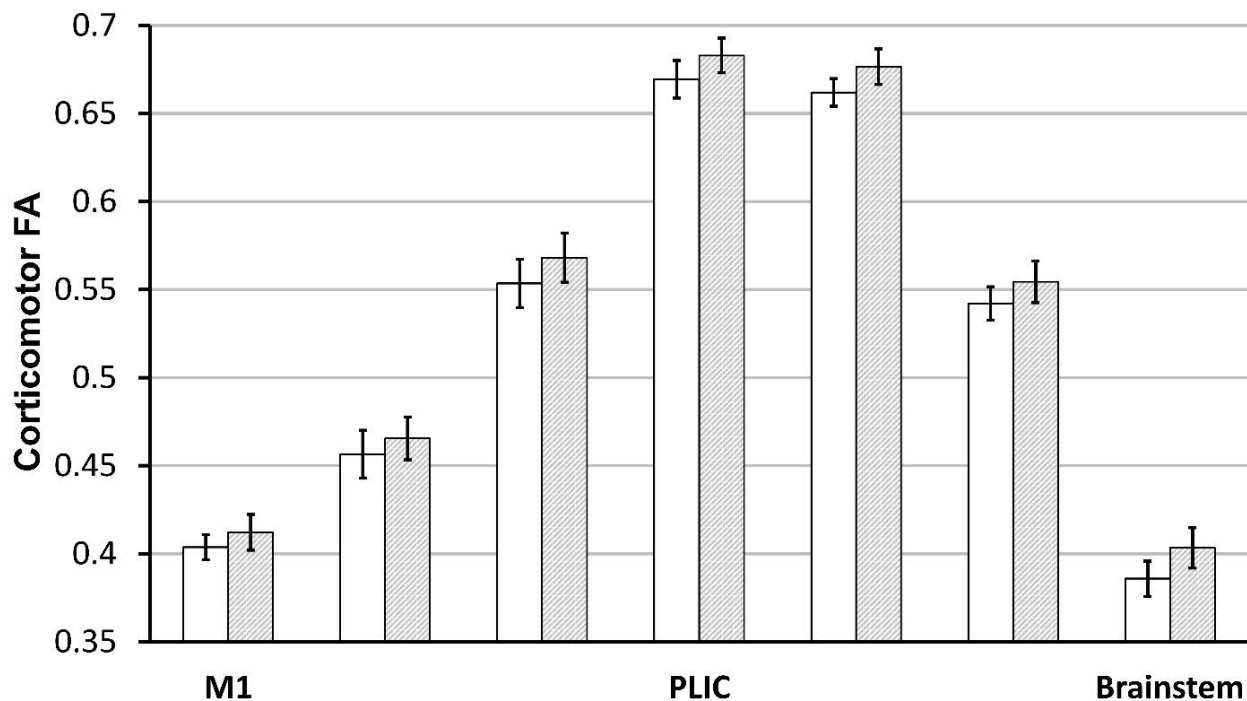


Figure 23. Change in unadjusted FA in the right corticomotor tract, by bin. White and grey bars indicate FA before and after training, respectively. The leftmost bars represent the most superior bin sampled (motor cortex); the rightmost bars represent the most inferior bin sampled (brainstem). Error bars denote SEM. Differences between time points were statistically significant and did not differ by bin. Abbreviations: PLIC, posterior limb of the internal capsule; M1 primary motor cortex.

Discussion

In this study, 23 right-handed participants practiced a finger-thumb opposition task with their left hand over a four-week period. Neuroimaging revealed a variety of brain changes throughout motor-related areas in the right hemisphere. Previously, we reported reduced fMRI activation, increased TMS motor evoked potentials of the corticospinal tract, and suggested cortical thickness increases throughout the motor system, including the dlPFC. Here we found that FA increased significantly throughout the length of the right corticospinal tract (Figure 23). Investigation of the basal ganglia revealed a significant increase in FA (4.9%) and a trend toward decreased MD (-0.83%) of the right caudate nucleus, as well as significantly decreased MD in the left NAcc (-1.3%) and a trend toward decreased FA of the right NAcc (-3.2%). On the basis of these changes we investigated white-matter connections between the middle frontal gyrus (where cortical thickness changes were reported) and the caudate nucleus (Right hemisphere: FA increase in 77% of participants; Left hemisphere, not significant), and also with the SMA (Right hemisphere: FA increase in 82% of participants; Left hemisphere, not significant). Notably, changes found in all measures were unilateral – appearing solely in the right (‘trained’) hemisphere, with the exception of FA in the nucleus accumbens, which trended towards bilateral changes. Whether these unilateral changes are at odds with the bilateral behavioural improvements seen is explored later in this section. Combined with our findings from TMS, cortical thickness and fMRI, the present work provides compelling evidence that neuroplasticity associated with a specific motor learning task occurs throughout the motor system, and can be robustly measured using a multimodal approach.

Sensorimotor Cortex

Motor output from the brain predominantly originates from the sensorimotor cortex,^{258,259} and it was from the corticospinal tract that we saw an increase in FA, driven predominantly by changes in radial diffusivity. From the same dataset we previously reported changes in cortical thickness, fMRI maps, and TMS maps (Chapter 5). The locations of such changes are consistent with brain stimulation work in which areas responsible for motor output of the fingers have been mapped.²³⁴

Although it is difficult to ascertain precisely what our previously reported changes in cortical thickness represent at a cellular level,⁹⁴ they lend credence to the diffusion changes found, for which we can hypothesise a biological origin. The task practiced by our participants involved sustained, rapid, repetitive use of the digits of the non-dominant hand in a manner different from those expected for most daily activities. Given that myelination has previously been demonstrated to occur in response to electrical activity,^{170,240} and we can expect action potentials to traverse the entire length of the corticospinal tract, it is not unreasonable⁹⁴ to surmise that an approximately uniform increase

in myelination could result from extensive practice of this task. Although we present this hypothesis tentatively, it is consistent with our observations of altered radial diffusivity, an approximately-uniform change in FA across the tract length, as well as with the TMS measures we previously reported in these participants. Once the technique has sufficiently matured,²⁶⁰ myelin water imaging may provide a useful tool to confirm or refute plasticity of this kind in motor skill learning paradigms. Because of its role, it is likely that the FA changes we have seen in the corticospinal tract reflect the extensive practice of fine finger movements in general, and have not arisen because of the unique aspects of this particular sequence. In other words, while grey-matter and functional changes previously reported are likely to reflect sequence-specific learning, it is unlikely that the corticospinal tract changes reported here could solely ‘encode’ and improve execution of the specific practiced sequence. This is a testable hypothesis that future studies could address.

This study is the first to report tract-specific WM changes in response to motor skill learning, and the first study of its kind in which dMRI changes are supported by concurrent TMS changes. While we are cognisant of the work by Palmer et al,¹⁷⁶ who performed another longitudinal study involving fMRI guided tractography, this work focussed on simple strength training rather than motor skill learning, and utilised an alternative approach to tractography seeding and categorisation that is possibly susceptible to cross-sulcal smoothing and other issues.²⁴⁹ Unlike the present study, changes in fMRI activation in the strength training study of Palmer et al. were also absent, as were changes in FA, which one might expect to be more sensitive than changes in MD for much of the corticospinal tract, given its large size and unbranching nature.

Dorsolateral Prefrontal Cortex and Anterior Striatum

The pre- and post-central gyri are known for their roles in subconscious motor output. By contrast, top-down control of motor output, for error-correction, is predominantly associated with activation of the dlPFC, in which we previously reported cortical thickness changes, and the caudate nucleus,^{215,216} in which we saw changes in microstructure. Functional MRI studies have also previously implicated the dlPFC and striatum as playing a key role in motor learning: fast learning of sequential motor tasks modulates activity in these areas.²¹⁹ Inhibiting NMDA receptor currents in the striatum has also been shown to severely disrupt motor learning in mice, without disrupting pre-existing motor behaviours or other forms of learning.²⁶¹ There is also a growing body of evidence that the NAcc plays a role in goal-directed behaviours.²⁵²

Anatomically, both the caudate nucleus and nucleus accumbens receive direct input from the dlPFC, suggesting that changes in the basal ganglia may have been driven by extensive utilisation of top-down motor-control networks, as may be expected when learning a task that requires a high

degree of coordination. This hypothesis is supported by our finding of increased FA in connections between the middle frontal gyrus and both the caudate nucleus and SMA, as may be expected from extensive excitation of these pathways. It is also supported by the fact that we did not see changes in the putamen, the other primary input area to the basal ganglia, whose input predominantly originates from more posterior motor areas that play a lower-order role in motor processes.²¹⁶

Generalisation to the Untrained Hand

Improvements in task performance were seen for both sequences in both hands, despite only one sequence with the non-dominant hand being trained. Such cross-hemisphere generalisation is at odds with one smaller (n=6) previous study employing a similar learning task,²²¹ but consistent with findings from several other motor studies utilising other tasks.^{238,239} Our fMRI analyses revealed that, after training, execution of the trained sequence with the left hand elicited reduced activation relative to the control sequence, *bilaterally* (Chapter 5). However, no changes in the left hemisphere were revealed by either structural or diffusion MRI. This discrepancy suggests that altered fMRI and behavioural measures of the ‘untrained’ side may reflect changes to the grey matter, such as LTP or altered neurite density, that were too subtle for changes in either measure. It may also reflect increased intercortical inhibition originating from the right hemisphere, though this seems at odds with the diminished relative activity reported in the right hemisphere. Techniques such as neurite orientation dispersion and density imaging,¹⁷¹ bilateral TMS, EEG, and fMRI tasks targeting the opposite hand may allow future techniques to shine light on this process.

Strengths and Limitations

The changes that we have indexed here are relatively subtle. This should be expected – a healthy person performs hundreds of learned complex tasks on a daily basis; the addition of a novel task may be expected to invoke changes that allow, or are represented by, circuit adaptation, but should not be expected to evoke large changes in brain structure. As practice-induced changes are expected to be subtle, caution must be taken in the analysis and interpretation of data to avoid type I errors.²²⁹

One strength of the current study was overcoming and controlling for potential sources of error. First, tractography-based studies could conceivably be biased by inconsistent seeding distances from white/grey matter interface, or changes in diffusion metrics of voxels containing grey-matter near seeding locations. To eliminate the possibility that mean change in FA was due to a subset of voxels shifting the whole-tract mean, we binned the tract into sections and demonstrated that change did not significantly differ at any one location in the tract. This also ascertained that changes in FA did not simply index change in other fibres which cross the corticospinal tract near the cortical surface. Second, we controlled for variable diffusion tensor fitting by demonstrating a lack of change

in corticospinal tracts in the untrained hemisphere, and replicating results using an alternative tensor-fitting algorithm. Finally, and critically, the changes reported were consistent with changes in TMS measures, and backed by increases in skill performance, cortical thickness changes, and altered fMRI activation in the sensorimotor cortex and superior parietal lobule (Chapter 5).

It is reasonable to assert that the two primary sources of error for ROI-based dMRI analyses are variability in the tensor fitting algorithm and variability in ROI placement. As ROIs were generated on single-participant templates it is unlikely that a bias in their placement took place. Results were also similar when alternative packages were used to generate our ROIs or fit the diffusion tensors.

The pattern of subtle brain changes seen, taken in context of our functional findings, suggests that motor learning involves structural brain changes. It should be noted, however, that our study lacked a second follow-up time point, and so it is ambiguous as to whether our detected changes reflect semi-permanent changes that accompany ability improvement, or whether they are a side effect of microstructural (e.g. vascular, dendritic) change that subsides once performance improvement reaches a plateau. Similarly, further studies are required to determine whether white matter changes such as these take place in response to the first few hours of training, or progressively over the longer training period.

Conclusion

In response to unilateral motor-coordination training, diffusion MRI revealed changes in the anterior striatum and white matter connections between this region and the right ('trained') middle frontal gyrus. FA of white matter connecting the right frontal gyrus and right SMA also appeared to improve. Finally, FA increased throughout the length of the right corticospinal tract. These changes were consistent with concurrently recorded changes in fMRI, TMS, cortical thickness, and performance improvements outlined in detail in a separate paper. These results imply that, while some areas may be critical for driving motor learning, this process evokes widespread functional, structural, and microstructural changes across the motor system, and that effective motor rehabilitation schemes may be able to achieve widespread brain changes without necessarily needing to target specific aspects of motor processing individually.

Supplementary Materials

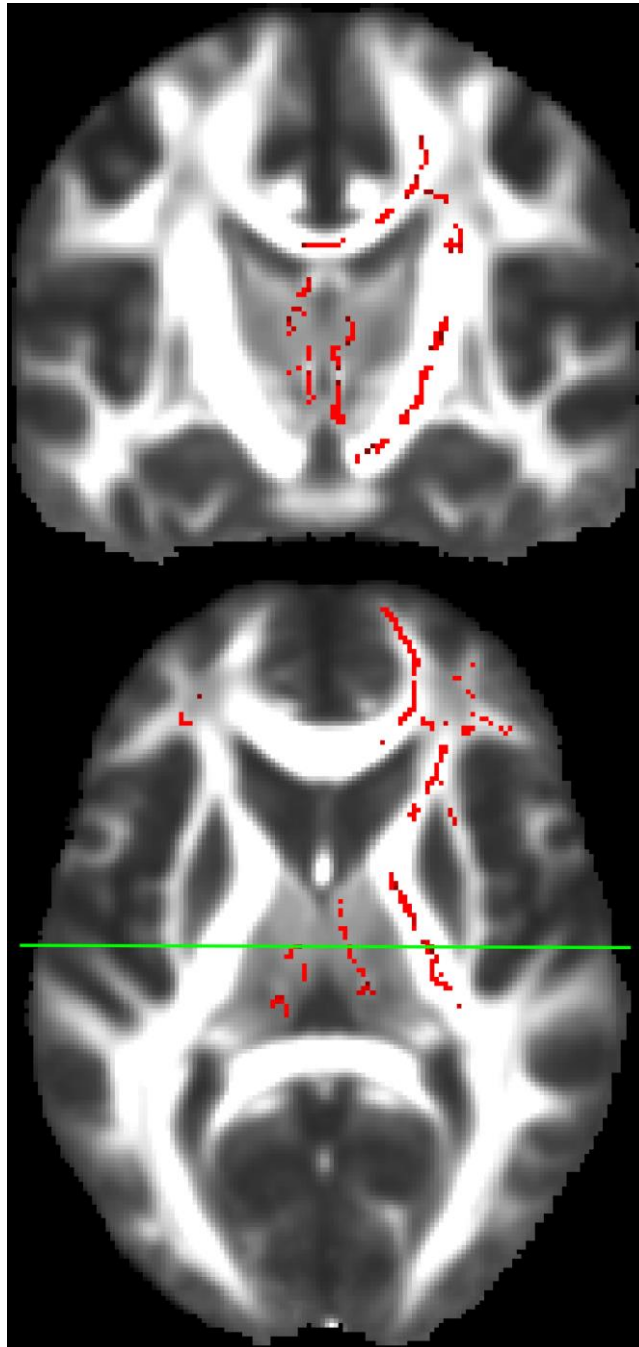
Tract Based Spatial Statistics

Method

Preprocessed diffusion MRI data (see Main Text) were utilised from 22 participants. Fractional anisotropy (FA) and mean diffusivity (MD) maps were calculated using MRTrix 2.9. A whole-brain analysis using the standard tract-based spatial statistics (TBSS) pipeline²⁶² was conducted. A paired analysis was achieved by subtracting the post-training timepoint from the baseline time-point after registration to the template, and conducting a one-sample T-test with threshold-free cluster enhancement using FSL 'randomise'.²⁶³ An exploratory re-analysis using a recently introduced ANTS-Syn based voxel-based analysis method²⁶⁴ was also conducted. This method may be less prone to type-I errors than TBSS by utilising single-participant templates and ANTS registration with a white-matter mask rather than a skeletonisation procedure.²⁶⁴ This was conducted in accordance with the procedures and parameters detailed by Schwarz et al.²⁶⁴

Results

After correction for multiple comparisons, the ANTS-based analysis revealed only a 4-voxel cluster in the external capsule bordering the putamen. For the TBSS analysis, no voxels showed significant change ($p < 0.05$) after controlling for multiple comparisons. In light of our TMS and tractography findings, we reduced the multiple-comparison threshold of the TBSS analysis to $p < 0.15$ FWE to search for any patterns of change. In this exploratory analysis, a large number of voxels reached threshold in the frontal lobes bilaterally, throughout the presumed right corticomotor tracts, the right and left thalamus, and some areas of the corpus callosum (Supplementary Figure 5).



Supplementary Figure 5. Training-related changes in white matter. 'Significant' voxels in the exploratory TBSS analysis (Red) in which the statistical threshold was relaxed to $p < 0.15$ FWE, overlaid with the mean FA image. Voxels consistent with the locations of the right corticomotor tracts, corpus callosum connecting the sensorimotor cortices, bilateral thalamus, and both frontal lobes exceeded this threshold. The top image shows a coronal slice at the level of the line on bottom (axial) image. Right of the image is right of the brain. Voxels did not exceed this threshold in the corticomotor tracts of the 'untrained' hemisphere.

Chapter 7

Measuring Neuroplasticity in the Mitii Cerebral Palsy Rehabilitation Trial

This chapter consists of unpublished work in which the fMRI-guided tractography method introduced in Chapter 3 was applied to neuroimaging data from the ‘Move It To Improve It’ (Mitii™) virtual reality therapy clinical trial.¹³ Although the trial provided limited improvement in outcome measures for the impaired limb, this neuroimaging analysis demonstrates the feasibility of conducting longitudinal analyses of brain structure in children with this condition. The present analysis also suggests that a concern when conducting such studies is data quality (e.g. due to compliance issues during scanning), rather than processing issues associated with the fMRI-guided tractography pipeline. These findings lead to a more rigorous investigation into factors affecting power in Chapter 8 in the hopes that such an investigation could reduce barriers to similar future studies involving people with brain injury.

Data acquisition was conducted by Prof. Boyd’s group, of which I was a part. Analyses for this section have been designed, conducted, interpreted, and written by myself. In addition to Prof Boyd’s team, Professors Rose and Cunnington played roles in planning different aspects of the Mitii trial. All three reviewed and edited this chapter.

Introduction

As discussed in Chapter 2, by understanding how present therapy induces neurological changes in children with brain injuries, rehabilitative therapies may be able to be adjusted or designed to provide better outcomes. Chapter 5 and Chapter 6 described neuroplasticity findings in healthy adults who had undergone motor training. Changes were widespread, and particularly prevalent in white matter pathways, as indexed using diffusion MRI tractography and TMS. Such findings hold particular promise for neurorehabilitation in CP, because approximately 43% of children with this condition present with white matter lesions.⁷ Regarding the measurement of white matter plasticity, although TMS can induce headaches in children with UCP (Chapter 2), diffusion MRI is a painless and safe procedure, for which the method described in Chapter 4 has been demonstrated to work well in the presence of pathology.

This brief chapter reports on the measurement of neuroplasticity in children with UCP undergoing rehabilitative therapy using the surface-based fMRI-seeded tractography method.

Methods

This work described in this chapter aimed to measure the presence of any FA changes in the corticomotor tracts for children with UCP who had undergone rehabilitative therapy. Imaging and clinical data were acquired as part of the Move it to improve it (Mitii™) Clinical Trial.¹³ The details of this trial are published elsewhere.¹³ Briefly, children with UCP were provided with home-based, self-driven, virtual-reality based therapy developed and owned by the Elsass Foundation, Denmark. This therapy consisted of video games that could be played via natural bodily movements that were tracked by a computer camera (Figure 24). Games targeted a variety of cognitive and motor skills, and the difficulty could be adjusted remotely by clinicians to suit the needs of each participant. The target therapy time was at least 30min a day, for 6 days per week, over 20 weeks (60 hours of therapy). Children were assigned to Mitii therapy during the first 20 weeks of the trial, or during the second 20 weeks of the trial. Children received standard care throughout the trial. For the present analysis, imaging data acquired at two time points were used to assess longitudinal brain changes in each child. Children with adequate quality MRI scans before and after Mitii therapy were labelled as the *treatment* group. For this group, *baseline* and *follow-up* scans referred to the pre- and post-treatment scans, respectively. Those remaining children who had two adequate quality pre-treatment scans were

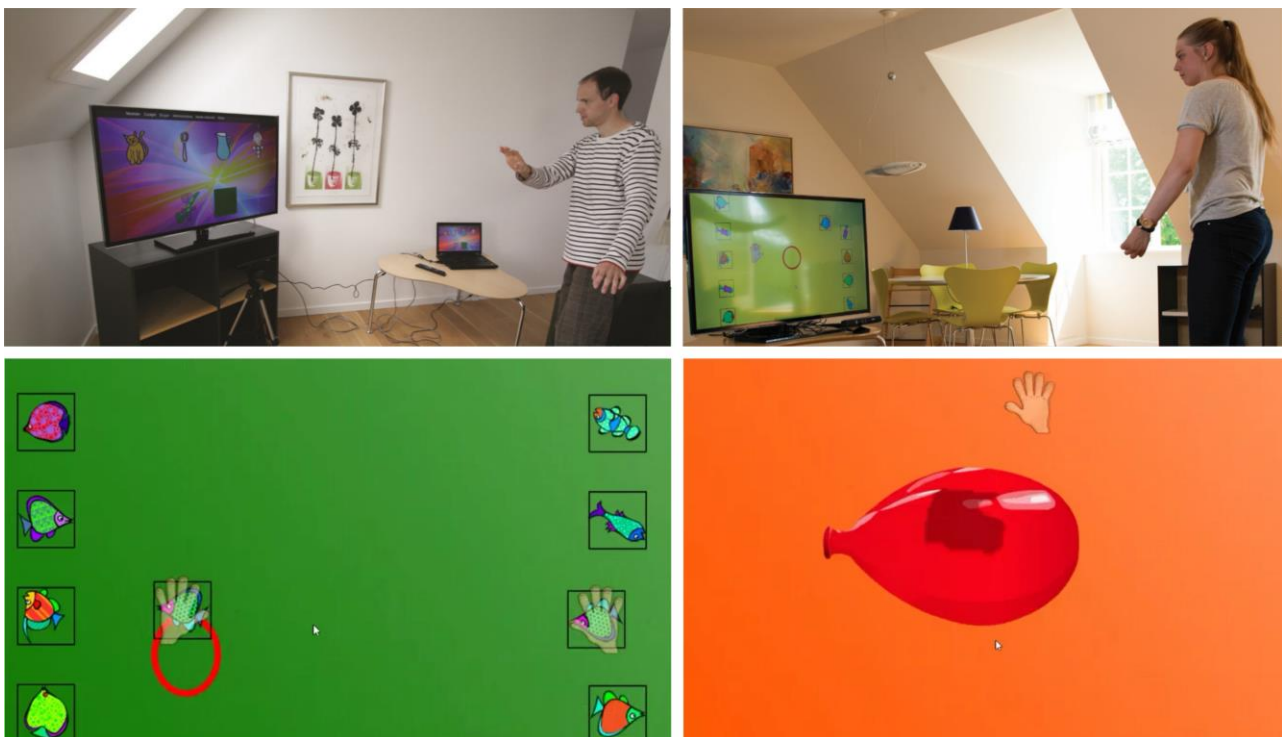


Figure 24. The Mitii system in action. Top: Demonstrators moving their hands to play games. In the version of Mitii used in the present work, a normal web camera was used and green bands were worn on the children's upper limbs to aid tracking. Bottom Left: Screenshots from a game in which both hands must be used to pick up matching images of fish. Bottom Right: Game in which the hand must be repeatedly moved up and down in to inflate a balloon. Images used with permission from Mitii Development and the Elsass Foundation.

labelled as belonging to the *control* group. For this group, *baseline* and *follow-up* scans referred to first and second pre-treatment scans, respectively.

Children were assessed clinically with a variety of tools at both time points. The present analysis focusses on three related measures of upper-limb motor function: the MUUL (Melbourne Unilateral Upper Limb Assessment), AHA (Assisting Hand Assessment), and motor component of the AMPS (Assessment of Motor and Processing Skills). The MUUL assessment provides insight into movement range, accuracy, dexterity and fluency of the more-impaired upper limb with particular focus on reaching, grasping, releasing, and manipulating simple objects. The AHA measures how effectively the more-impaired hand and arm are used in bimanual performance. The AMPS is designed to evaluate a person's quality of performance in personal or instrumental activities of daily living, using tasks prioritised by the individual.

The surface-based fMRI-seeded tractography method described in Chapter 4 was used to elucidate whether any improvements in clinical measures after Mitii therapy were reflected in microstructure changes of the corticospinal tract, as previously seen in healthy adults after motor learning (Chapter 6). Functional, structural, and diffusion MRI parameters, tasks, and related analysis methods, have been previously described in Chapter 4. As in Chapter 6, binarised fMRI maps (hand tapping task; $p < 0.05$ FWE) from each time point were combined for each participant to provide a seeding region for tractography. Tractography at each time point was conducted using the same structural mesh and seeding region, transformed into native diffusion MRI space, as previously described. As MRTrix 3 had not yet been released at the time of analysis, MRTrix 2.9 was used for FA calculation. Although absolute differences *between* these versions are noticeable, results described in Chapter 6 revealed that longitudinal differences are largely unaffected by the version of MRTrix used, so long as the same version is used at each time point.

Results

Sixty-six children underwent MR scanning during the trial. Of these, 25 participants were not scanned at two sequential time points, 12 displayed excessive motion artefacts on diffusion and/or fMRI images, and mesh generation failed for 2, leaving datasets from 27 children. Of these, 13 and 14 children were assigned to control and treatment groups, respectively. Clinical data for each group are shown in Table 10. At baseline, the control and treatment groups displayed similar clinical assessments for the Gross Motor Function Classification System (GMFCS), the Manual Abilities Classification System (MACS), MUUL, and AHA. MUUL assessments were not able to be collected at both time points for three children in each group.

At follow-up, clinical improvements in the treatment group were not significantly greater than improvements seen in the control group for MUUL and AHA assessments (one-tailed Bonferroni corrected t-test $p > 0.05$; Figure 25). The motor component scores of AMPS (Assessment of Motor and Processing Skills) did increase to a greater degree in the treatment group than the control group (0.40 vs -0.10 on a 4-point scale; $p < 0.01$). Although the increase seen in the treatment group meets the criteria for clinical significance (> 0.30 logits),²⁶⁵ baseline scores for this measurement were significantly lower in the treatment group at baseline (treatment 1.16 vs control 1.45; $p < 0.05$), making the direct comparison of these improvements difficult to assess. To achieve a more valid comparison, three participants were removed from each group: those with the highest baseline AMPS from the control group, and those with the lowest baseline AMPS from the treatment group. Resulting mean baseline AMPS scores were 1.33 and 1.32 for the control and treatment groups respectively ($p = 0.92$).

	Control	Treatment	Difference
n	13	14	N/A
Age	12.34 ± 2.86	11.67 ± 2.16	p=0.50
Male	5	5	N/A
GMFCS I, II	8, 5	8, 6	N/A
MACS I, II	3, 10	4, 10	N/A
MUUL	108.5 ± 14.3	110 ± 13.5	p=0.83
AHA	69.2 ± 9.2	71.9 ± 11.7	p=0.50
AMPS	1.45 ± 0.32	1.16 ± 0.39	p<0.05

Table 10. Baseline characteristics of control and treatment groups. The ± symbol indicates mean ± standard deviation; integers represent participant counts. The difference column indicates whether the population means differed between groups, as assessed by uncorrected t-tests. Abbreviations: AHA, Assisting Hand Assessment; AMPS, Assessment of Motor and Processing Skills; GMFCS, Gross Motor Function Classification System; MACS, Manual Abilities Classification System; MUUL, Melbourne Unilateral Upper Limb Assessment; N/A, Not Applicable.

In this subanalysis, positive improvement was still statistically significantly higher in the treatment group ($p < 0.01$), but fell slightly below clinical significance (mean improvement 0.29 logits).

Mean FA and mean MD of the corticospinal tract did not change in either hemisphere for either group (one-tailed paired t-tests; all $p > 0.05$ uncorrected; Figure 25), and did not change more in the treatment group than control group for either hemisphere (one-tailed paired t-tests for FA increase or MD decrease; all $p > 0.05$ uncorrected).

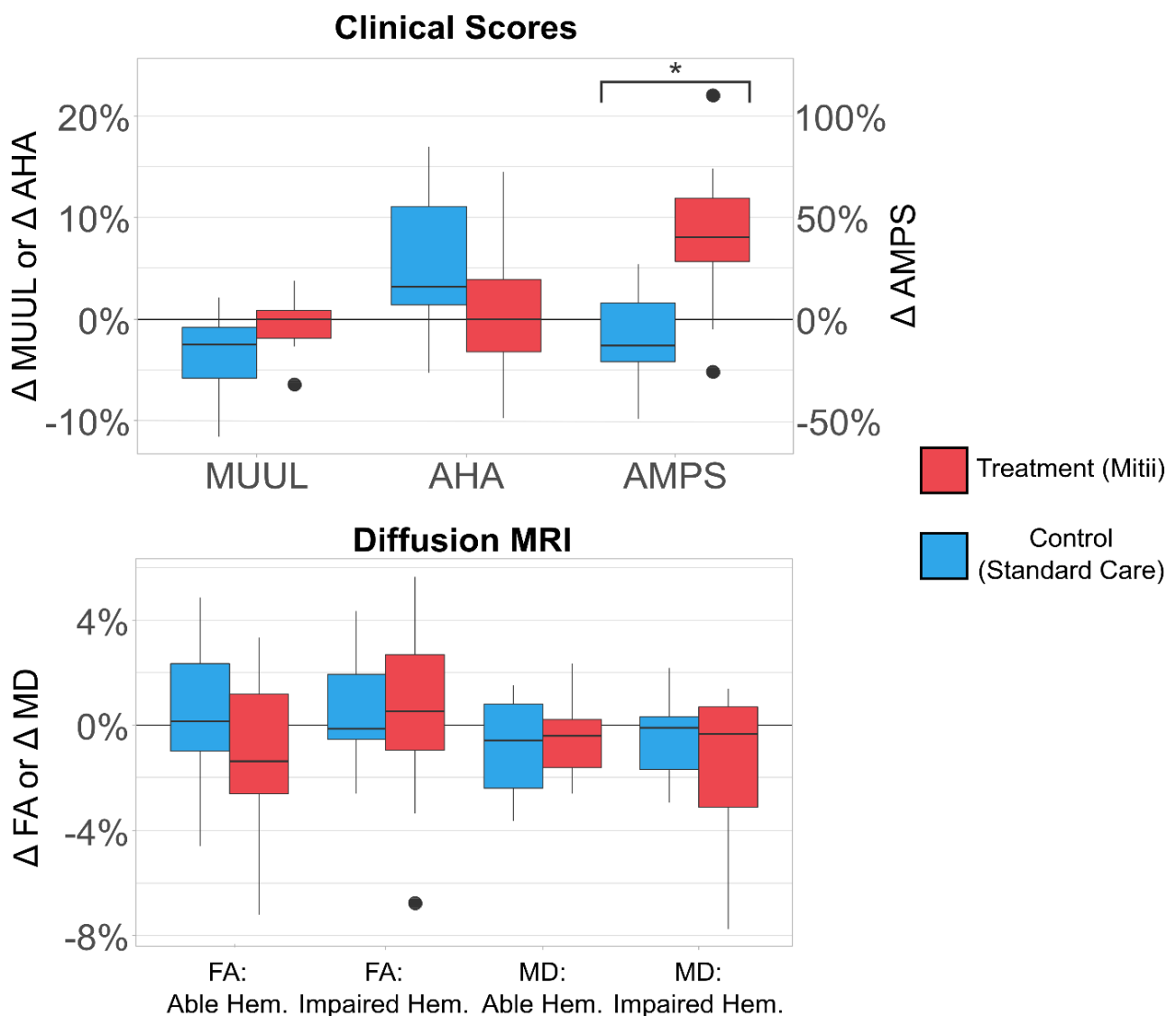


Figure 25. Change in clinical scores and diffusion statistics of the corticospinal tracts in children with CP after 20 weeks. Children who received Mitii rehabilitation therapy are shown in red; children who received standard care are shown in blue. Dots indicate outliers, as defined by Tukey.²⁹⁴ Top: Significant improvements in clinical scores after Mitii therapy were seen only for AMPS. Bottom: Significant changes were not seen in mean FA or mean MD of the corticospinal tracts of either hemisphere. Abbreviations: Able Hem., Able (less affected) hemisphere; AHA, Assisting Hand Assessment; AMPS, Assessment of Motor and Processing Skills; Impaired Hem., (more affected) Hemisphere; FA, fractional anisotropy of the corticospinal tract; MD, mean diffusivity of the corticospinal tract; MUUL, Melbourne Unilateral Upper Limb Assessment.

Discussion

This chapter describes an attempt to measure changes in the microstructure of the corticospinal tracts in children with UCP enrolled in the Mitii clinical trial. The treatment group did not display significantly greater changes in FA nor MD within either corticospinal tract. As discussed in Chapter 3, the most important contextual information for the measurement of brain change is the degree of behavioural improvement. With this in mind, the lack of white matter changes is expected, given a lack of improvement in the more direct measures of motor ability for the upper limb (MUUL and AHA). Although the treatment group showed relatively larger improvement in the AMPS scores, when groups were made equivalent with respect to baseline scores, the mean change in the treatment group (0.29 logits on a 4-point Likert scale) was marginally below threshold for clinically relevant improvement (> 0.3 logits).

It is important to note that the lack of clinical improvement reported here was not due to biased participant selection – for example, clinical improvement correlating with behavioural issues during scanning. Concretely, the trial as a whole ($n=92$ children after attrition) reported no clinically significant differences between groups for any measure of impaired upper limb function.¹⁴ It was suggested that the potential efficacy of Mitii therapy for upper limb function may have been limited by the enrolment of children with relatively high motor function, and also by the treatment's lack of grasping or object manipulation tasks.¹⁴ The mean dose of therapy received (32.4 hours) was also around half the target dose of 60 hours, which may have also played a role.

A compounding issue for the work presented here is statistical power. No published power analysis for neuroimaging measures in such a context was available during data collection nor data analysis. Subsequently conducted analyses, presented in Chapter 8, found that the present analysis was underpowered to detect small brain changes, even if moderate behavioural improvements were demonstrated in response to therapy.

Although it is important to demonstrate that diffusion measures will not demonstrate change when there is little-to-no clinical improvement, this overall result unfortunately provides little insight into the neuroplasticity associated with effective neurorehabilitation. Although the present work was limited to data from the Mitii trial, moderate-to-strong behavioural evidence exists for the effectiveness of more standard therapies, such as mCIMT and BIM (see Chapter 2).¹² This suggests that clinical trials of these methods may be more suitable for investigating brain changes associated with clinical improvement. Neuroimaging can be expensive, and so it is important that researchers have a clear understanding of the power and practical limitations of the method in question. With regards to the fMRI-guided tractography method introduced in this thesis, the previous chapters

demonstrated correlations between clinical scores and diffusion metrics, and the ability to detect brain changes when abilities improve. The present chapter has demonstrated the feasibility of conducting a longitudinal study in children with CP. The final important barrier to investigation of intervention-induced neuroplasticity in individuals with CP is understanding the statistical power of this method, and how to maximise it. The present work suggests that two major sources of power loss may be cancelled scans (attrition) or compliance issues when scanning, rather than issues with data processing. To better quantify the influence of such issues, and to make strong recommendations for future trials, a more rigorous investigation into this methods' power, and factors which influence it, is covered in the following chapter.

Chapter 8

Measuring Neuroplasticity Associated with Cerebral Palsy Rehabilitation: An MRI based Power Analysis

This chapter consists of the paper *Measuring Neuroplasticity Associated with Cerebral Palsy Rehabilitation: An MRI based Power Analysis*. This chapter has been accepted for publication in the *International Journal of Developmental Neuroscience*. This paper aims to further reduce the barriers to measuring neuroplasticity in a rehabilitative context by calculating required enrolment sizes for a two-time-point randomized controlled trial. Specifically, this paper reports the number of children with unilateral cerebral palsy required to detect increases in cortical thickness, FA of the corticospinal tract using standard tractography, and FA of the corticospinal tract using the method described in Chapter 4.

With relevance to this thesis, this chapter formally addresses Aim 4: *to utilise the information above to perform a power analysis that can be used to plan neuro-rehabilitative studies in children with cerebral palsy*. This analysis makes a number of recommendations allowing study designs to minimise resource wastage and ensure adequate enrolment numbers, such that studies can reasonably expect to be able to ascertain the efficacy of their chosen treatment strategy with regards to inducing brain changes. In addition, by calculating the test-retest reliabilities of the novel fMRI-guided tractography method and standard ROI-seeded tractography, this chapter completes requirements of Aim 2: *address the need for algorithms that can reliably detect subtle structural brain changes and that perform well in the presence of pathology*. This chapter demonstrates that the fMRI-driven diffusion method is markedly more reliable in cohorts with pathology than ROI-based tractography.

As joint-first author on this publication, I conducted all diffusion analyses, and generated the single-participant templates relied upon for cortical thickness measures. I wrote the large majority of the manuscript and interpreted the results to generate the practical recommendations that are made in the paper. Alex Pagnozzi, the co-author, was responsible for calculating cortical thickness using the provided templates, converting calculated variances into power-curves and required enrolment counts. Mr Pagnozzi and I both conceived of the factors and levels of analyses which were to be taken into account and reported. Dr Fiori manually defined our brain regions of interest. All authors reviewed the manuscript and contributed academically during the editing process.

Publication Information

Reid, LB; Pagnozzi, AM; Fiori, S; Boyd, RN; Dowson, N; Rose, SE. Measuring Neuroplasticity Associated with Cerebral Palsy Rehabilitation: An MRI based Power Analysis. *International Journal of Developmental Neuroscience (In Press)*

Minor changes have been made in response to examiner feedback.

This work also appeared in abstract form and has been accepted for presentation at an international conference as follows:

Reid LB, Pagnozzi A, Fiori S, Boyd RN, Rose SE. Measuring Neuroplasticity Associated with Cerebral Palsy Rehabilitation: An MRI based Power Analysis In: International Symposium on Biomedical Imaging. Melbourne; 2017

Abstract

Researchers in the field of child neurology are increasingly looking to supplement clinical trials of motor rehabilitation with neuroimaging in order to better understand the relationship between behavioural training, brain changes, and clinical improvements. Randomised controlled trials are typically accompanied by sample size calculations to detect clinical improvements but, despite the large cost of neuroimaging, not equivalent calculations for concurrently acquired neuroimaging measures of changes in response to intervention. To aid in this regard, a power analysis was conducted for two measures of brain changes that may be indexed in a trial of rehabilitative therapy for cerebral palsy: cortical thickness of the impaired primary sensorimotor cortex, and fractional anisotropy of the impaired delineated corticospinal tract. Power for measuring fractional anisotropy was assessed for both region-of-interest-seeded and fMRI-seeded diffusion tractography. Taking into account practical limitations, as well as data loss due to behavioural and image-processing issues, estimated required participant numbers were 101, 128 and 59 for cortical thickness, region-of-interest-based tractography, and fMRI-seeded tractography, respectively. These numbers are not adjusted for study attrition. Although these participant numbers may be out of reach of many trials, several options are available to improve statistical power, including careful preparation of participants for scanning using mock simulators, careful consideration of image processing options, and enrolment of as homogeneous a cohort as possible. This work suggests that smaller and moderate sized studies give genuine consideration to harmonising scanning protocols between groups to allow the pooling of data.

Highlights

- Power analysis for imaging-measures of neuroplasticity in cerebral palsy
- Details enrolment numbers needed to detect changes in structural and diffusion MRI
- A range of assumptions tested, including differences in treatment response
- Recommendations made for studies with under 100 participants for improving power

Introduction

Motor rehabilitation for children with cerebral palsy (CP) is currently hampered by our lack of understanding of how the brain responds to rehabilitative therapy at microscopic and macroscopic scales.¹⁰³ Researchers are increasingly looking to quantify brain reorganisation in clinical trials of motor rehabilitation in order to better understand the relationship between behavioural training, brain changes, and clinical improvements, and/or to index subtle changes which may not be reflected in clinical assessments.¹³ This information may ultimately inform rehabilitation, for example by elucidating factors that interfere with motor learning, such as maladaptive plasticity, or disrupted network deficits that prevent neuroplastic changes¹⁰³.

MRI data can be analysed in a variety of ways to acquire metrics of brain changes, including changes in cortical thickness, and changes in diffusion metrics of white matter.¹⁰³ Cortical thickness is a structural measure related to several neurophysiological changes, including variations in neuronal, glial and synaptic density.⁹⁴ This measure has been used to quantify structural changes related to plasticity in animal studies,¹⁶⁶ and correlated with cognitive performance in several human studies.^{266–268} Diffusion MRI is typically used to investigate white-matter microstructure, and metrics such as fractional anisotropy (FA) applied to the corticospinal tract have been found to correlate with a number of clinical scores in CP.^{103,179} A small number of longitudinal studies have demonstrated that motor training can induce changes in cortical thickness and diffusion metrics in animals¹⁶⁶ and in adults who do not have CP.^{80,237} Speech therapy has also been demonstrated to alter cortical thickness of the left posterior superior temporal gyrus in children with children with CP.²⁶⁹

Power analyses are relied on to plan clinical-trial enrolment numbers, but are usually based on expected behavioural improvements, rather than secondary image-derived measures of neuroplasticity potentially conducted as part of these trials. Clinical trials based on behavioural changes alone may be underpowered for detecting changes with neuroimaging, because neuroimaging and clinical changes may have substantially different effect sizes and variance. Underpowered trials are wasteful in terms of time and resources but, to the best of the authors' knowledge, no literature is readily available for ensuring rehabilitative trials are sufficiently powered with respect to neuroimaging. The present work aims to address this gap by providing participant numbers required to detect secondary-outcome changes in both cortical thickness and tractography-derived diffusion metrics in white matter, which may occur as a result of primary therapeutic intervention. Required n values for a variety of effect sizes are presented. These effect sizes are based on published literature and brain changes measured in a longitudinal motor-learning study of healthy

adults.^{270,271} Population-appropriate variances were calculated by applying methods from this study to images from children with unilateral CP. This work pertains specifically to studies wishing to detect the amplitude of structural and/or microstructural measures in specific motor-related regions. It should be noted that alternative analysis methods which investigate the ‘typicality’ of imaging findings,^{272,273} originally developed for functional MRI analyses, have distinctly different form of hypothesis to most randomised controlled trials of neurorehabilitation, and so are considered out of scope for the present manuscript.

Methods

Participant numbers were calculated for a theoretical longitudinal study in which MR imaging took place immediately prior to, and immediately following, several weeks or months of treatment. It was assumed that such a study would utilise a paired parametric test (e.g. t-test) for differences in cortical thickness, or differences in FA of the delineated corticospinal tract using ROI-seeded or functional MRI (fMRI) seeded diffusion tractography. The general power analysis equation is described below before the description of values and sources of its parameters for each imaging metric.

Statistical Analyses

The power analyses were performed using the ‘pwr’ package in R statistical software.²⁷⁴ This test computes the sample size required to achieve a certain statistical power threshold (which is defined as one minus probability of a false negative finding), of a one-sided, paired t-test for a predefined effect size. Statistical power was varied between three thresholds; 0.8, 0.9 and 0.95, which represent a 20%, 10% and 5% chance of a false negative finding, respectively. A standard alpha value of 0.05 was used for all analyses. The longitudinal effect size for the power analysis was computed using the Cohen’s d formula as follows:

$$effect\ size = \frac{\mu_{post} - \mu_{pre}}{\sqrt{(\sigma_{measurement}^2 + \sigma_{response}^2)}}$$

where μ_{pre} and μ_{post} are the mean MRI measures from pre-treatment and post-treatment time points respectively. The variations of this formula includes two sources of variance; the measurement error ($\sigma_{measurement}$) and the variance in the longitudinal response to therapy ($\sigma_{response}$). Variance in response to treatment was set at 10% of the mean change, based on the variance in behavioural improvements reported in rehabilitative trials for CP.^{275,276} These measurement and response to therapy variances are provided in Supplementary Table 1, while participant numbers for 5% and 15% variances in response are provided in Supplementary Figure 8. Therefore, assuming a null hypothesis

of no longitudinal change ($\mu_0 = 0$), the calculation of the sample size n using the software package can be approximated with the following equation:

$$n = \frac{\left(z_{1-\frac{\alpha}{2}} + z_{1-\beta}\right)^2}{\text{effect size}^2}$$

where $z_{1-\frac{\alpha}{2}}$ represents a standardised z -distribution of the test statistic at the $\alpha = 0.05$ cut-off for significance, and $z_{1-\beta}$ represents the same standardised distribution at the $(1 - \beta)$ power threshold.²⁷⁷ For each imaging modality, mean change in MRI measures and measurement error were based on quantitative data, as described below.

Cortical Thickness

Power was calculated for a hypothetical analysis that measured change in cortical thickness in the primary sensorimotor cortex of the impaired hemisphere. An ROI-based approach was assumed, as altered neural development in CP can invalidate assumptions of structure-function homogeneity across the cohort or hamper the accurate registration of anatomy, which would affect approaches such as voxel-based morphometry. A variety of expected cortical thickness increases were explored; these were based on published studies^{166,278,279} of this cortical thickness in different circumstances (Table

CT change	Notes
6%	Realistic/safe estimate for current therapies. At least one successful study of motor training in healthy adults detected subtle and/or highly localised CT changes which may be difficult to detect with ROI based methods. ²⁷¹ Measurement errors of approximately 4% have also been reported in Freesurfer-based longitudinal studies, implying that CT changes near this number are likely to be difficult to detect with realistic cohort sizes. ²⁸⁴
8%	Balanced estimate for effective therapy over 6-month time frame.
10%	Optimistic data-driven estimate (extremely effective therapy). This change in CT has been observed in rats that underwent 1 month of motor training. ¹⁶⁶
12%	Heavily optimistic estimate (extremely effective therapy). This change in CT has been observed between the injured and uninjured hemispheres in a cross-sectional cohort of children with CP. ²⁷⁹ This difference reflects recovery of these participants' entire 7-16 years of life, which can be considered as an upper limit one can expect from several months of therapy.

Table 11. The four effect sizes used for the power calculation. The authors' opinions are provided on how realistic each effect size is for a randomised controlled trial of present rehabilitative therapy. Abbreviations: CT, cortical thickness; ROI, region of interest

11). Based on this literature, an increase of 8% was considered to be a balanced estimate of change for effective therapies conducted over a 6-month time frame (See Table 11).

An outline of the cortical thickness pipeline is shown in Figure 26, and is described in detail below. An estimate of variance due to measurement error was obtained from five children with unilateral cerebral palsy (4 male; mean age 13.2y; age-range 9 – 15.8y; 4 GMFCS II; 1 GMFCS I; 3 right-sided hemiplegia), enrolled in the control arm of the Mitii clinical trial.¹³ The pathology present in this cohort was fairly homogeneous with respect to injury type and location (Supplementary Figure 6). These children underwent two MRI scans 20 weeks apart. As no intervention took place between these two scans, differences in measures of cortical thickness between the two scans is indicative of measurement error. This data is referred to herein as the ‘UCP-dataset’. Ethics approval for the aforementioned trial was granted by the University of Queensland Human Research Ethics Committee and the Royal Children’s Hospital Brisbane. Written informed consent was obtained from each participant’s legal guardian.

Cortical thickness analyses utilised T1 MPR volumes (TR/TE: 1900/2.32ms; 0.9mm isotropic; Siemens Tim Trio 3T) that underwent N4 bias field correction,²⁸⁰ intensity normalisation and skull stripping. For longitudinal analyses, it is important to utilise a structural template for each participant that is unbiased to either pre- or post-treatment images, as labelling cortical regions on each image directly can result in uneven deformations or inconsistent labelling. Inconsistencies of this nature can produce false positive results and lower statistical power.²²⁹ Here, structural templates were constructed for each participant by first rigidly registering scans from each time point together using Advanced Normalization Tools (ANTs; v2.1.0, source pulled 9th Feb 2016) SyN (symmetric) transformation.²³⁰ An unbiased mid-point of these two time points was then produced by transforming both images by half of the resulting transformations, and then averaging them together (Figure 26). This template was then converted to sharper, final template using the ‘antsMultivariateTemplateConstruction’ script.

The accuracy of the brain mask around the cortical motor regions was carefully inspected, as both the under-segmentation of the grey matter or the erroneous inclusion of dura would affect cortical thickness measures. Tissue segmentation was performed on this structural template using a patch based segmentation approach.²⁵⁰ The obtained tissue segmentations were transformed back to each time point’s image space using the inverse transformations obtained from the single-participant template construction. Cortical thickness was obtained for each time point using a voxel-based Laplacian approach,²⁸¹ which has been previously demonstrated on children with CP. Cortical regions corresponding to motor function, including the pre- and post-central gyri, supplementary motor area

and the superior parietal lobe, were each manually delineated on the single participant template by a paediatric neurologist (S.F.). The inverse transformations were again used to transform these masks to time-point-1 and time-point-2 image spaces, allowing cortical thickness measures in the cortical motor regions to be isolated at each time point.

Diffusion MRI Tractography

Power was also calculated for a hypothetical analysis that measured change in average FA values across the whole delineated corticospinal tract in each hemisphere after intervention. Participant numbers were independently calculated to achieve an 80% power of detecting a significant difference

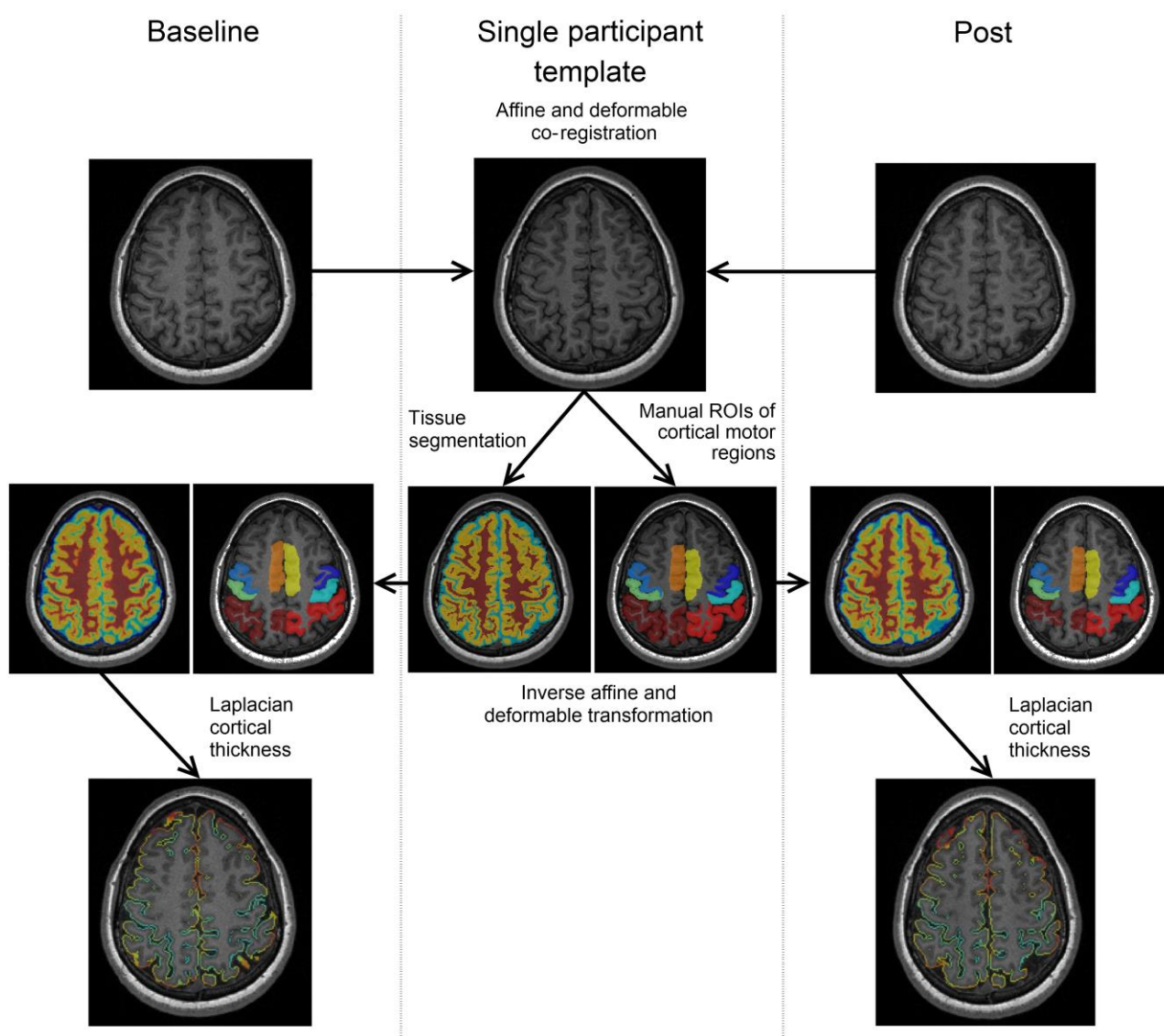


Figure 26. An illustration of the cortical thickness pipeline used to estimate the effect size for the power analysis. Images from both time points are combined into a single-participant image. Tissue segmentation and manual definition of regions of interest (ROIs) are performed on this image, then propagated back to each time point. Cortical thickness is then estimated for each time point. This method reduces the influence of tissue segmentation or ROI definition inconsistencies on final results.

FA change	ROI-seeded tractography	fMRI-seeded tractography
1%	Optimistic data driven estimate for very effective therapy. Such change has been demonstrated in healthy adults who mastered a unilateral motor task. ²⁷⁰ Unlike adults, the presence of pathology makes it less likely that sulcal boundaries are functional boundaries in children with CP.	Realistic/safe estimate for current therapies.
1.5%	Optimistic data-driven estimate (extremely effective therapy).	Balanced estimate for effective therapy over a 6-month time frame.
2%	Heavily optimistic estimate (extremely effective therapy).	Optimistic estimate for very effective therapy.
3%	Unrealistic estimate for present therapies.	Heavily optimistic estimate for very effective therapy. Such change has been demonstrated in healthy adults who mastered a unilateral motor task. ²⁷⁰ Behavioural improvements and anatomical homogeneity in this study were greater is typically reported in trials of CP therapy.

Table 12. Effect sizes for fractional anisotropy change used in this power analysis. The authors' opinions are provided on how realistic each effect size is for a randomised controlled trial of present rehabilitative therapy; see text for details.

with training for two versions of such an analysis: ROI-seeded tractography and surface-fMRI-seeded tractography.

Due to the dearth of literature reporting diffusion changes observed in children with CP undergoing longitudinal therapy, the amounts of expected longitudinal change were based on a healthy adult ('HA') dataset from a recent study, in which 24 healthy adults practiced a novel fine-motor task with their non-dominant hand for ten minutes a day for four weeks.²⁷⁰ This study found substantial improvements in task performance that were accompanied by changes in functional MRI, cortical thickness (voxel-based analysis), TMS maps and the delineated corticospinal tract FA in the 'trained' hemisphere. Importantly, in this study, both ROI seeded tractography and surface-fMRI seeded tractography were conducted. To ascertain the impact choice of methodology on required participant numbers, both methods were tested for FA changes between 1% and 3%: values reported in the aforementioned study (Table 12). Note that although these changes were not based on children with UCP, and so the effect of rehabilitative therapy may differ, this range of FA values represents a wide scope from realistic to heavily optimistic effects of therapy. The use of the HA dataset was

within the bounds of an approval originally granted by the University of Queensland Human Research Ethics Committee, for which participants gave written informed consent.

To ascertain measurement error associated with each of these methods, both approaches were conducted on the UCP-dataset. For both methods, FA was sampled from the generated tracts, and the average across the whole tract taken. Mean measurements from the second time point were then subtracted from those of the first time point and the variance of these differences computed.

ROI-seeded tractography

To calculate FA measurement error, ROI-seeded tractography was performed on the UCP-dataset using manually defined ROIs corresponding to the primary motor cortex. Acquired during each scan-session was a 64-direction high-angular resolution diffusion image sequence with $b=3000\text{s/mm}^2$, one $b = 0$ image, whole brain coverage, and $2.34 \times 2.34 \times 2.5\text{mm}$ spatial resolution. A relatively standard HARDI dMRI pipeline was used that has been published in detail elsewhere.^{58,190} In brief, this pipeline included extensive pre-processing of dMRI data, and utilised MRTrix 3 (<https://github.com/MRtrix3/mrtrix3>)¹⁸⁰ to estimate fibre orientation distributions via constrained spherical deconvolution.

For each dataset, registration between the previously generated single-participant T1 template and diffusion b_0 diffusion image was calculated with FSL FLIRT using boundary-based registration.¹⁸⁶ The inverse of this transform allowed the expert-drawn M1 labels (see above) to be projected into diffusion space. MRTrix3 was used to generate 20,000 corticospinal streamlines passing from each M1 label, through the posterior limb, to the brain stem. Constraining these tracts required 2D axial labels of the brainstem and posterior-limb of the internal capsule. These were delineated manually (L.B.R.) on up-sampled track-density images for each dataset using ITK-SNAP.¹⁹¹

With respect to degree of FA change, in the HA dataset, atlas-based ROI-seeded tractography of the delineated corticospinal tract reported a mean FA change slightly below 1%. Although the authors consider it optimistic to detect the same level of change in a CP rehabilitative study, testing for lower levels of change was not conducted as substantially smaller changes are difficult to interpret.

Surface-fMRI seeded tractography

Functional MRI provides an alternative to using structural ROIs to seed tractography. With fMRI seeded tractography, an fMRI analysis is conducted to identify motor regions, and the resulting

activation used as the seed region of interest. A surface-based fMRI+tractography approach was selected, as this has been demonstrated to delineate the corticospinal tract in children with UCP in a more clinically-informative manner than a naïve fMRI-seeding approach.²⁴⁹ This approach was also found to be more robust to the presence of severe pathology, including cases where ROI methods can be expected to fail.²⁴⁹

To calculate measurement error in a UCP population, surface-based fMRI tractography was conducted on the UCP dataset. During each scan session, two block-design task-based fMRI scans were collected, each consisting of 90 echo planar images (TR/TE 3000/30ms; 3mm isotropic; full brain coverage; online distortion correction using point-spread function mapping). Each scan consisted of nine 30-second blocks, alternating between ‘stop’ and ‘move’ conditions. Participants were instructed to tap their hand, by full extension at the wrist, in time with this cue in the ‘move’ condition, and to remain still during the ‘stop’ condition. A visual cue consisting of the words ‘move’ or ‘stop’ was visible at all times, in addition to an auditory click that was delivered at 1 Hz. Participants utilised their more able hand during the first scan, and their less able hand during the second scan. The long block lengths and simple task used were aimed at reducing the influence of various biological factors associated with cerebral palsy.¹⁸¹ It should be stressed that functional data were used to seed tractography only and were neither designed nor intended to be directly interpreted.

Surfaces were generated from each single-participant template (Figure 27). Each fMRI-session was analysed individually in surface space, using methods and parameters described previously.²⁴⁹ This included 5mm of surface-smoothing, and motion scrubbing where frame-wise displacement¹⁶⁵ exceeded 0.9mm. Contrast was set as move > stop, and statistical significance was set at $p < 0.05$ after family-wise error correction. Manual filtering of significant activation was then carried out, as described previously,²⁴⁹ to retain only the largest ROI near the hand-knob on the right S1M1. For each participant, identical seeding region for each time-points’ tractography was generated by performing a union of regions of significant activation from each time-point. This seeding region was expanded such that total seeding area was at least 200mm² in participants who displayed significant fMRI activation, but whose total seeding area would otherwise be below this size. Tractography from this seeding region was performed using established methods,²⁴⁹ including use of cluster-based filtering to restrict analysis to the delineated corticospinal tracks.

With respect to estimated FA change, the aforementioned neuroplasticity motor-training study reported FA change, elucidated with this surface-based fMRI approach, of 3.28%. Because rehabilitation trials in CP typically report lower degrees of behavioural improvement than the

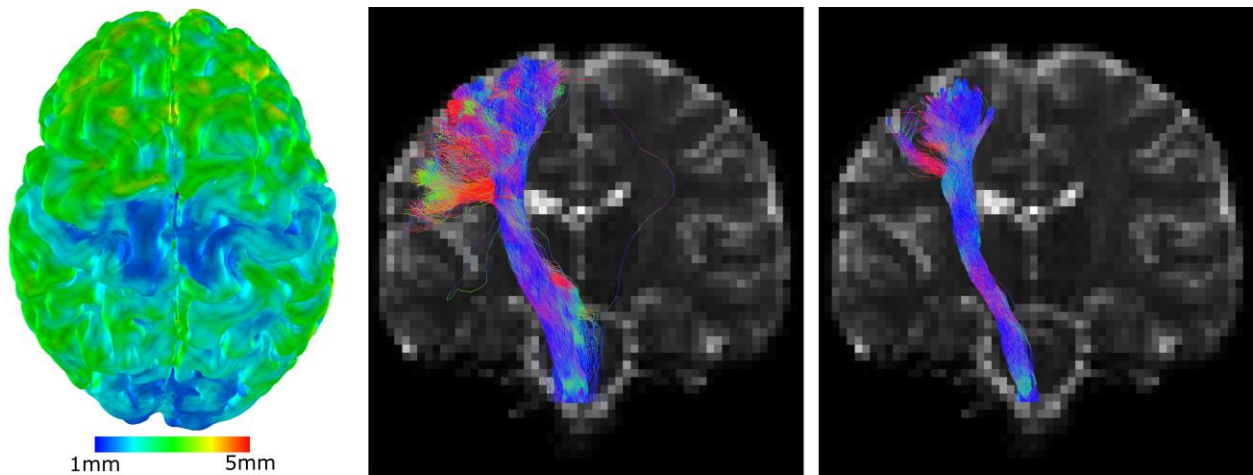


Figure 27. Example of cortical thickness (left), projected onto the pial surface; ROI-seeded diffusion tractography (middle); and surface-fMRI seeded tractography (right) in a single participant with CP. Tracks from all slices are shown, overlaid on a diffusion b_0 image. Note the higher anatomical specificity of the surface-fMRI seeded method, relative to the ROI-seeded method. Left of images is left of the participant.

aforementioned study,²⁸² an FA change of 1.5% was considered to be a balanced estimate for effective therapy over a six month time frame.

Accounting for Data Exclusions

When studying children with brain pathology, acquired data must often be excluded due to motion artefacts or software instability in the presence of brain lesions. Based on the sample size computed from the power analyses, n_{power} , an extra analysis was performed to determine the practical number of children required to undergo scanning, given a probability that a scan is able to be both acquired and processed successfully, $P(successful)$. This probability, which was ranged between 60% and 100% represents the probability of obtaining an image free of motion artefacts. Because each child must successfully undergo scanning twice in a longitudinal study, the final number of participants was computed based on the square of this probability, as shown below.

$$n_{needed} = n_{power} / P(successful)^2$$

This equation was checked against historical imaging data for over 100 children with UCP, aged 5 – 18 years, acquired by the authors. It was confirmed to that the number of excluded participants in a two time-point study could be predicted by squaring the number of individual time-point datasets that were rejected due to motion or processing issues (data not shown). Based on the authors' historical rates of data rejection, the text focusses on a 75% probability of success for structural imaging, and a 65% probability of success for fMRI-seeded and ROI-seeded diffusion MRI. The primary reason for data rejection for the authors' data were motion artefacts. Success was generally lower in diffusion analyses due to the longer scan time and thus higher likelihood of motion during acquisition.

Although fMRI-seeded tractography requires two sets of good images (fMRI and diffusion), historical data acquired by the authors showed similar success rates with ROI-based diffusion analyses because of automated cortical parcellation has a high failure rate when pathology is present.

Results

To detect a change in cortical thickness of the sensorimotor cortex with 80% power, the number of children required to successfully complete imaging was between 25 and 106, depending on the expected effect size of treatment (Figure 28). These numbers rose to between 33 and 138 to achieve power of 90%. For the ‘balanced’ estimate of an 8% expected change, the number of children required to complete imaging was 57, 77 and 95 for powers 80%, 90% and 95%, respectively. Power curves for supplementary motor and superior parietal areas are supplied in Supplementary Figure 8.

To detect a change in FA of the delineated corticospinal tract using *ROI-seeded* tractography with 80% power, the number of children required to successfully complete imaging was between 7 and 56, depending on the expected effect size of treatment (Figure 28). These numbers rose to between 9 and 77 to achieve power of 90%. For the most realistic estimate of a 1% change in FA, number of children required to complete imaging was 56, 79 and 93 for powers 80%, 90% and 95%, respectively.

Required imaging counts to achieve an 80% power for surface-based *fMRI-seeded* tractography were substantially lower, between 3 (for a heavily optimistic expectation of change) and 22, for a safer expected effect size (Figure 28). For the ‘balanced’ estimate of a 1.5% change in delineated corticospinal FA, the number of children successfully completing two scans was 9, 13 and 16 for powers of 80%, 90%, and 95%, respectively.

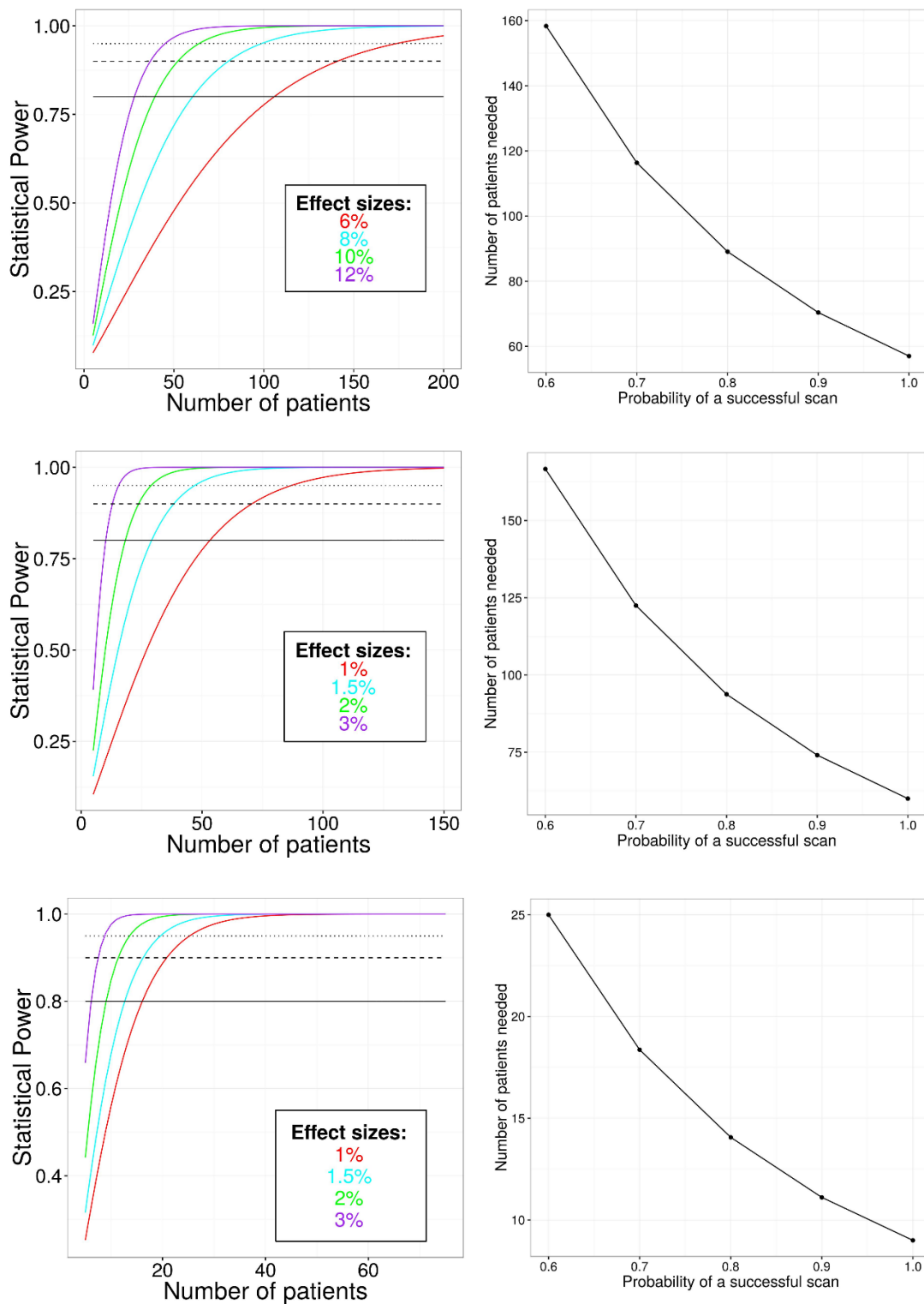


Figure 28. Power analysis curves. Graphs in the left column denote the relationships between power and number of participants for a variety of expected changes in cortical thickness (top row), ROI-seeded tractography (middle row) and surface-fMRI-guided tractography (bottom row), assuming successful scans in all instances. Three power thresholds are illustrated, 80% (full line), 90% (dashed line) and 95% (dotted line). Graphs in the right column display the number of children required to be scanned at both time points taking into account a variety of success rates of scanning and image processing ($P(\text{success})$). These are displayed for changes of 8%, 1%, and 1.5% in cortical thickness (top), ROI-seeded tractography (middle) and surface-fMRI-seeded tractography (bottom), respectively.

Accounting for Data Exclusions

Practical issues related to participant cooperation, imaging artefacts, and processing difficulties will significantly affect the number of participants required. To achieve 80% power, assuming a 75% probability of a successful scan, 101, 106 and 16, participants are required to undergo scanning for cortical thickness (8% change), ROI-based tractography (1% change) and fMRI tractography (1.5% change) respectively (Figure 28). It is notable that achieving successful diffusion and fMRI scans is much more difficult than acquiring T1 images, due to the scan lengths and/or participant interaction required. At a 65% probability of success required participant numbers are to 142 and 21 for ROI-seeded and fMRI-seeded tractography methods, respectively.

Due to the heterogeneity seen in cerebral palsy populations, a study with a low number of participants is unlikely to fairly represent the variety of pathology and other factors observed in the general population (see Discussion). For this reason, the above number-to-scan calculation was repeated for a target of 25 participants. As shown in Figure 29, 45 or 60 participants are needed to be scanned in order to achieve this target, assuming $P(\text{success})$ of 75% or 65%, respectively.

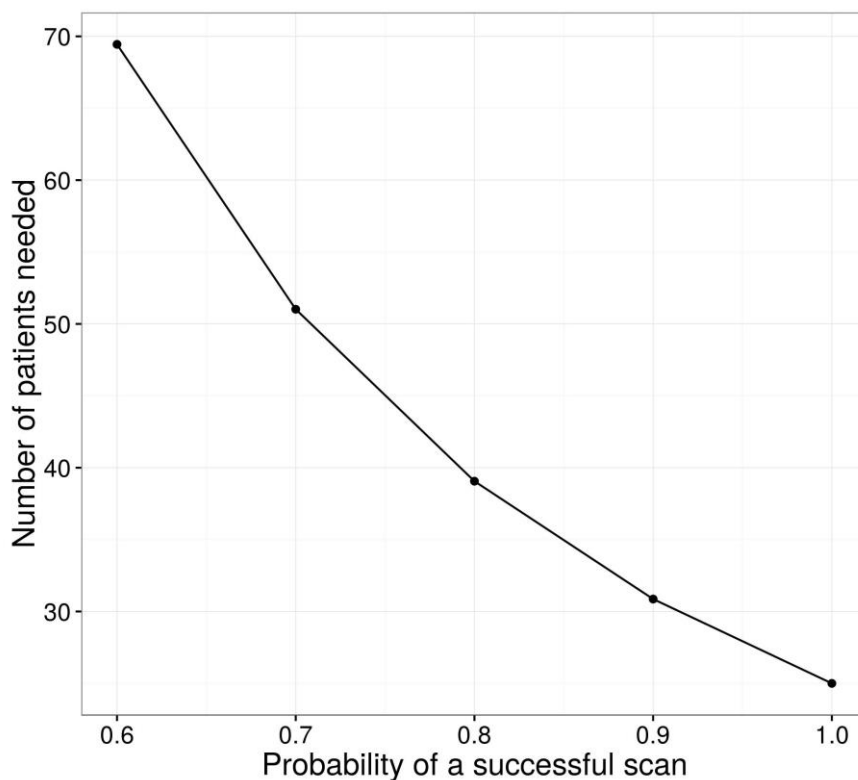


Figure 29. Number of participants needs to scan in order to successfully analyse 25 participants.

Discussion

The present study calculated number of children with unilateral cerebral palsy required to undergo scanning and intervention in order for a neurorehabilitative study to detect changes in cortical thickness of the more-impaired primary sensorimotor cortex, or FA of the more-impaired delineated corticospinal tract using either M1 *ROI-seeded* or *surface-fMRI seeded* tractography. It is important to note that the values here assume that all enrolled participants attend all scans – they do not account for general trial attrition. Attrition was purposefully not accounted for, as each study cohort may display substantially different drop-out rates due to socioeconomic, cultural, and trial-specific factors (such as length). To achieve a number-to-enrol, it is important that the number-to-scan values reported here are also adjusted by the expected attrition rate of the trial in question.

Cortical Thickness

Measuring change in cortical thickness required 101 participants to undergo scanning to achieve an 80% power, assuming a mean cortical thickness change of 8%, and a scan-and-analysis success rate of 75% per scan-session. As the calculations presented here indicate that the primary factor determining statistical power was the reliability of the cortical thickness measure (Supplementary Figure 7), a study may be able to improve its statistical power by achieving more sensitive or reliable measures of cortical thickness change. One means of doing so is to collect multispectral data (T1, T2, and proton density sequences) at high resolutions, as this can improve grey-matter estimations in a number of software standard packages. The other main driver of required participant numbers for cortical thickness analysis was scan-and-process success rates. For example, a study with a scan-and-process success rate of 90% needs approximately half the number of enrolled participants than a study which loses one in three scans. An important means of improving statistical power is, thus, to give adequate consideration to the preparation and conduction of scans. Pre-existing protocols that address these issues have been published, with impressive success rates.²⁸³ A complimentary means of reducing data loss is to give ample consideration to processing software. Some mainstream packages, particularly with their default pipelines, make assumptions about brain structure that do not apply to brain-injured populations and as a result, even in healthy participants, can result in a dataset rejection rates above 35%.^{284,285} Utilisation of simpler methods that make fewer assumptions of brain structure, such as those utilised here,^{281,285} can help to minimise the loss of data and thus improving a study's statistical power. Finally, teams interested in this measure with unavoidably underpowered trials should consider active collaboration with other groups to harmonise imaging protocols, allowing for data to be aggregated across similar interventional studies. Note that multi-centre studies will carry

with them an additional degree of variability due to the use of multiple scanners, though the effect of this on diffusion or cortical thickness measurements is beyond the intended scope of the present work.

Diffusion MRI Tractography

Tractography seeded by ROIs of M1, manually delineated by an expert neuroanatomist, required 106 or 128 participants to detect a 1% change in delineated corticospinal FA at 80% power, assuming the 75% or 65% scan-session success rates, respectively. Although it may be tempting to assume a greater degree of FA change may take place, which would reduce required participant numbers (Figure 28), such an assumption is contrary to existing evidence; higher values were only presented here for direct comparison with *fMRI-seeded* tractography. By contrast, surface-fMRI guided tractography required only 42 participants to detect the same degree of change at a 65% scan-session success rate, due to its substantially lower test-retest error in the UCP cohort. According to a motor learning study in healthy adults,²⁷⁰ this method can also be expected to display greater mean FA changes than an ROI based approach, presumably due to its greater anatomical specificity (Figure 27). When the expected degree of change for surface-fMRI guided tractography was raised to a more realistic 1.5% – slightly under half of the degree of change demonstrated in the aforementioned study – this number fell further, to 21.

It is clear, then, that the primary driver of power in tractography analyses is the processing method. In fact, the numbers presented here suggest that even moderately large randomised controlled trials are unlikely to find genuine white-matter changes of the delineated corticospinal tract without resorting to an fMRI-guided approach, or similar. Although an fMRI-based diffusion analysis pipeline may require substantial investment to set up, the savings associated with fewer scans is likely to provide a substantial, if not complete, financial offset. We note that the fMRI-based method requires a specific motor task, which will require meaningful consideration of participants' abilities and of the specific region that is expected to be targeted by the intervention (e.g. hand knob within M1, or the equivalent region in re-organised brains). When using such an approach, the present analysis suggests that statistical power is not the primary concern. It is important to remember that cerebral palsy is a highly heterogeneous condition. As such, even large demonstrated brain changes in smaller cohorts will not generalise to the general CP populous. For this reason, although not based on hard calculation, it is recommended that studies aim to successfully scan and process data from no fewer than 25 participants, and ensure a test partition of no less than 25% of the available data when constructing predictive models to verify the generalisability of the model. As shown in Figure 29, a $P(\text{success})$ of 65% requires attempting to scan approximately 59 children, ignoring general attrition.

For studies restricted to utilising manually or automatically delineated ROIs for tractography seeding, improving statistical power will rely on reducing variability of response to treatment; using scanning protocols designed to reduce participant anxiety and behavioural issues; and opting for software pipelines that are robust to pathology (which may require manual delineation of ROIs). One practical step toward reducing variable response to treatment is to enrol as homogenous a cohort as possible in terms of CP subtype, severity, and pathology. This is likely to minimise the variance in response to treatment and thus improve the statistical power of longitudinal trials. This also carries the added benefit of improving interpretability, but may reduce the generalisation of results to people with dissimilar pathology. Another action that can be taken is to opt for treatment delivery that is actively monitored, or individually customisable, to better enable participants with more severe pathology or situationally-difficult circumstances to achieve results. Finally, head motion is common in children with intellectual disability. Adequate preparation of participants, ideally with mock scanners, is likely to improve the rates of successfully obtaining artefact-free scans, boosting the power of the study.

Alternative Measures

With high required enrollee counts, particularly for cortical thickness, it is not unreasonable to consider whether it is worth utilising alternative measures of brain change. The authors prefer not to rely on voxel-based analyses such as (standalone) fMRI using available software packages, voxel-based morphometry (VBM), or tract-based spatial statistics (TBSS) for this purpose. In order to conduct groupwise voxel based analyses, especially standalone fMRI, make a number of assumptions that are invalidated by pathology.¹⁸¹ These include the assumptions of uniform anatomy, and uniform structure-function relationships, across participants. The data retention rates amongst such methods may also be reduced in CP cohorts due to the instability of non-linear registration methods when pathology is present.²⁸⁵ By contrast, ROI-based analyses assume only that change will occur *somewhere* within the region of interest for each participant, and do not rely at all upon inter-subject anatomical correspondence or non-linear registration methods. Although fMRI analyses can be performed in an ROI-based manner, there is presently no guarantee that this will be more sensitive than the methods detailed here. Furthermore, the interpretation of fMRI is complex in CP populations and is most robust when supplemented by independent neuroimaging measures.^{103,181}

In a related note, readers may also consider whether it is worth forming a different form of hypothesis in order to make smaller neuroimaging studies (<25 participants) more viable. Certainly, alternative forms of hypotheses are possible, such as calculating the proportion of the population whom can be expected to see a brain change meeting certain criteria (observed brain change

‘typicality’).^{273,286} As indicated earlier, a discussion on these forms of hypotheses is well outside the scope of the present work. It is worth noting, however, that biological insight into neurorehabilitation in CP is presently awaiting characterisation of induced brain changes’ qualities (such as type, location, and amplitude). Such characterisation is more explicitly tested with the hypotheses utilised in the present paper.

Limitations

The experiments reported here tested many different sets of assumptions, using data-driven parameters where possible, but some limitations remain. Perhaps the largest remaining limitation is that it is not presently known whether brains impaired by cerebral palsy are capable of similar levels of plasticity to a brain free of pathology. There is some evidence to suggest that this may be age dependent,^{36,287} a factor not included in the present model due both to a lack of data, and to a desire for the results to be broadly applicable. A second limitation is that both cortical thickness and myelination change during typical development with age.^{288,289} A consequence of this is that long-term studies must account for age at each time point, either directly or with a control cohort, to avoid misconstruing development as intervention-induced brain change. Another limitation is that the variance in longitudinal changes in structural and diffusion measures was only measured from five children with CP, and as such may not be representative of children with CP outside this age range or with different underlying brain pathologies. In these instances, we recommend that researchers compute their own power using the equation from the Statistical Analyses section, substituting in their own more accurate estimates of effect size and variance.

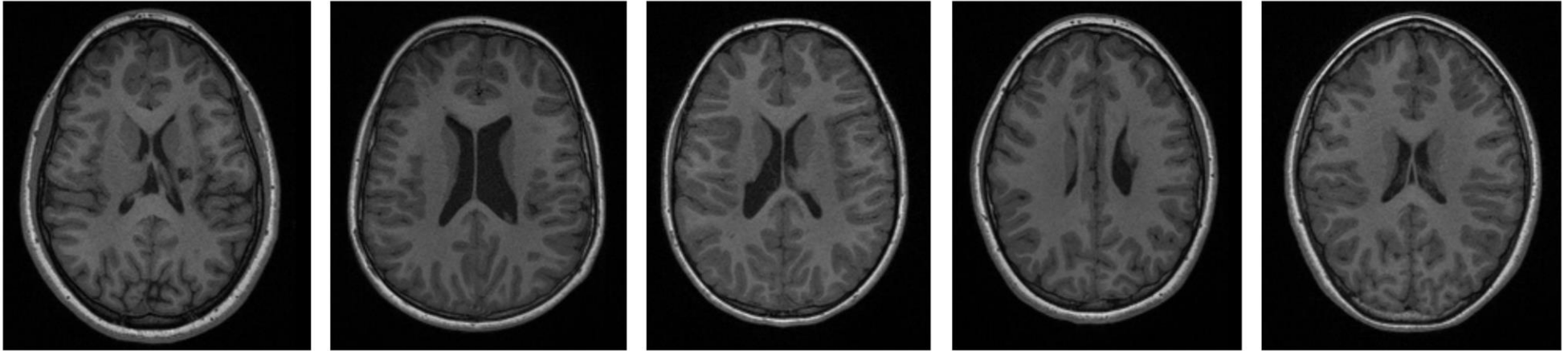
Conclusions

Based on data driven parameters and practical limitations, calculations reported that 101 participants were required for longitudinal measurement of cortical thickness in the impaired sensorimotor cortex. For the measurement of FA in the impaired delineated corticospinal tract, these numbers were 128 for ROI-seeded tractography, and 59 for fMRI seeded tractography, respectively. These numbers must be multiplied by a constant factor to take into account expected study attrition. Although these participant numbers may be excessive for many rehabilitative trials, several options are available to improve statistical power, including ample preparation of participants for scanning, careful consideration of image processing options, and enrolment of as homogeneous a cohort as possible. Smaller and more moderate-sized studies can still realise the full potential of their datasets by harmonising scanning protocols in order to allow the pooling of data.

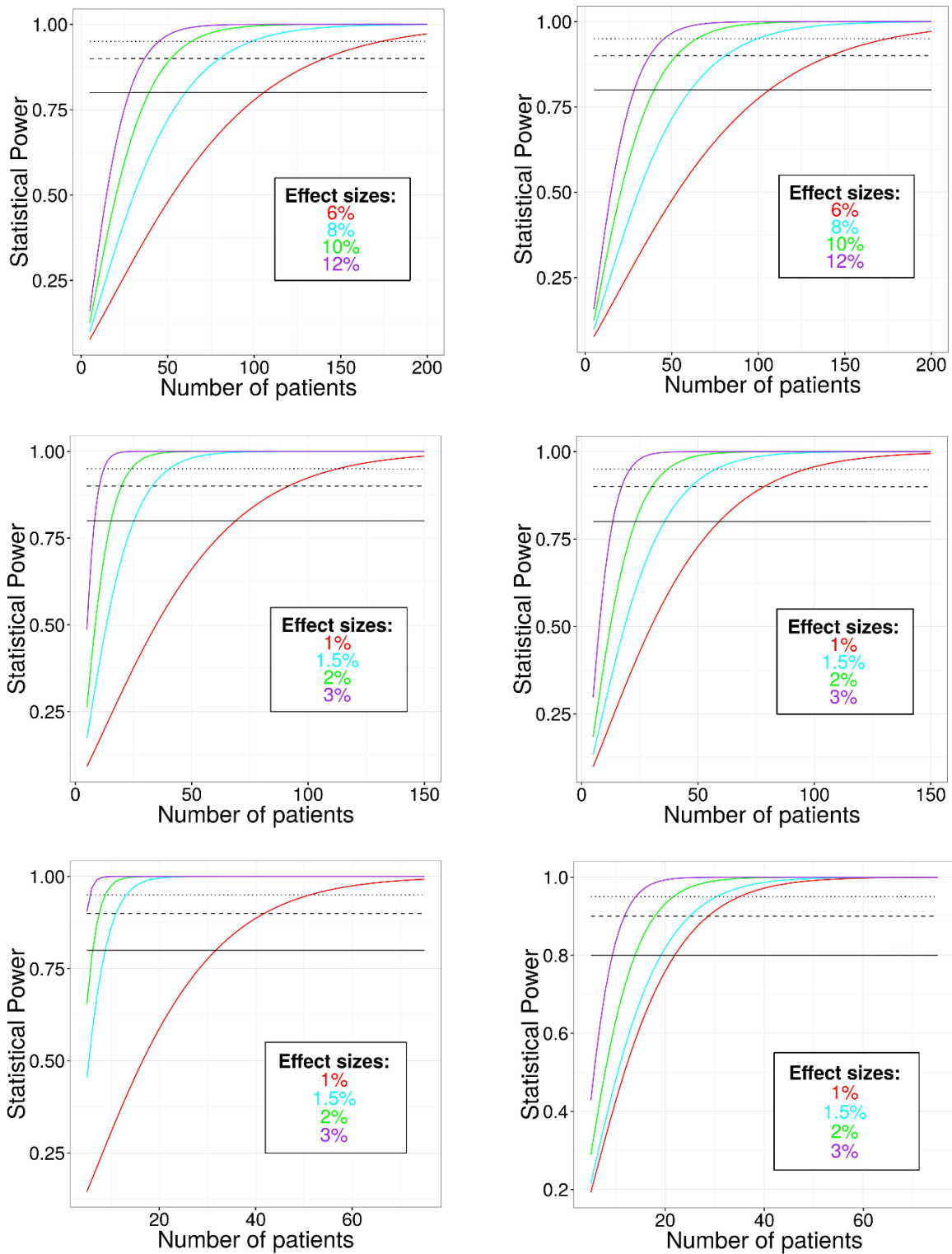
Supplementary Materials

Neuroimaging measures	Estimate of effect size	$\sigma_{measurement}$	$\sigma_{response} = 5\%$	$\sigma_{response} = 10\%$	$\sigma_{response} = 15\%$
Cortical thickness	8%	0.412	0.0005	0.0024	0.0053
ROI-seeded tractography	1%	6.28e-04	2.5e-05	1e-04	2.25e-04
Surface-fMRI seeded tractography	1.5%	1.54e-04	3.75e-05	1.5e-04	3.38e-04

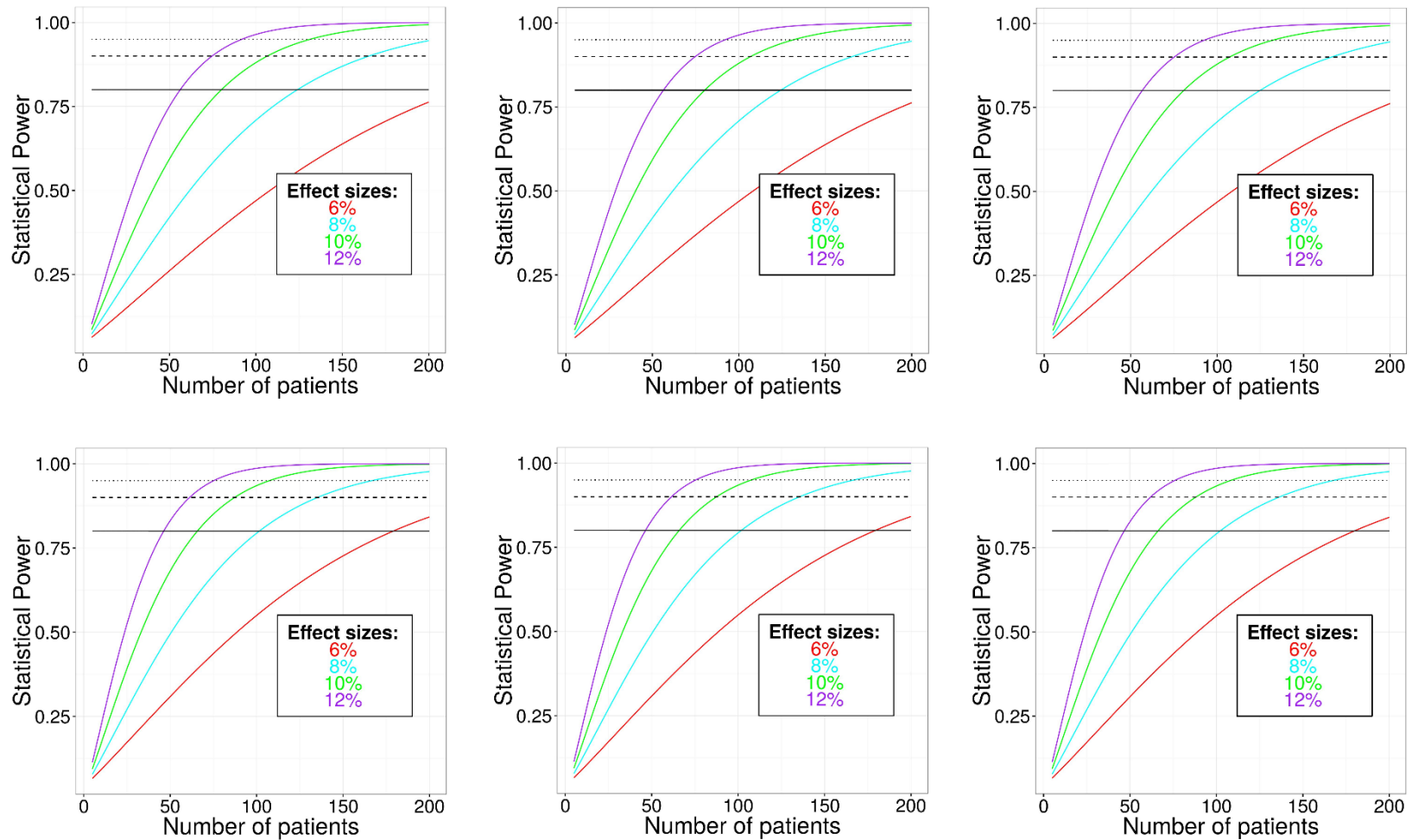
Supplementary Table 1. The values of variance used in the power analysis, including measurement error ($\sigma_{measurement}$) and variance in response to treatment ($\sigma_{response}$), for both structural and diffusion measures.



Supplementary Figure 6. Representative axial slices illustrating the brain pathology of the structural MRI of the five children with UCP, who underwent two scans, without rehabilitation in-between, to obtain estimates of measurement variance



Supplementary Figure 7. Power analysis curves. Curves represent number of participants needed for a variety of expected changes in cortical thickness (top row), ROI-seeded tractography (middle row) and surface-fMRI-guided tractography (bottom row), assuming successful scans in all instances. Curves in the left column represent a 5% standard deviation in response to therapy, curves on the right represent a 15% standard deviation in response to therapy, based on previous rehabilitative trials for CP. Three power thresholds are illustrated as horizontal black lines: 80% (full line), 90% (dashed line) and 95% (dotted line).



Supplementary Figure 8. Power analysis curves. Curves represent number of participants needed for a variety of expected changes in cortical thickness in the posterior parietal lobe (top row) and supplementary motor cortex (bottom row). The different columns represents different standard variations of participant response to treatment: 5% (left column), 10% (middle column), and 15% (right column). Three power thresholds are illustrated as horizontal black lines: 80% (full line), 90% (dashed line) and 95% (dotted line).

Chapter 9

Grand Discussion

Novel Contributions

This thesis presents a series of novel works that together significantly reduce barriers toward the measurement of brain plasticity associated with neurorehabilitation, and also contribute considerably toward understanding the neurological processes associated with normal motor learning. A series of six papers, and one unpublished chapter, were presented that directly addressed the goals of this thesis:

1. Critically review the potential for functional MRI, when used alone, to measure brain changes in a rehabilitative context
2. Address the need for algorithms that can reliably detect subtle structural brain changes and that perform well in the presence of pathology
3. Combine the aforementioned principles and methods in order to measure a variety of brain changes in healthy adults learning a novel motor task, then to interpret such information together in a way that may improve our understanding of neuroplasticity at a biological level
4. Utilise the information above to perform a power analysis that can be used to plan neuro-rehabilitative studies in children with cerebral palsy

The main findings of these papers are summarised below.

Measurement of Neuroplasticity with fMRI

Chapter 2, published in *Nature Reviews Neurology*, explored the potential for measures of brain change to transform neurorehabilitation, with a particular focus on motor issues in unilateral cerebral palsy. This chapter suggested a variety of methods were available, one of the most popular being task-based functional MRI. Chapter 3 critically explored this method's potential for the measurement of neuroplasticity in people with brain injury. A variety of issues were identified, including a high degree of uncertainty surrounding interpretation, confounds related to disease states, reliability issues with small cohorts, and the ability for processing steps intrinsic to the technique to artificially produce 'differences' between time points. Although many of these issues were known prior to publication, the compounding effect of these had not been explored. It was concluded that, although the method applied to a single-participant may be useful to identify certain brain regions, interpretation of subtle changes between time points in people with brain injury was not justifiable. This chapter also explored alternatives and solutions to the problems raised. This exploration determined that the best

course of action for an imaging study wishing to investigate neuroplasticity was to take a multimodal approach.

A Means of Detecting Brain Changes in the Presence of Pathology

Measuring structural brain changes associated with learning presents a very difficult challenge because changes can be expected to be subtle, but most techniques are relatively insensitive, especially when acquisitions must be performed within reasonable scanning times. Furthermore, the presence of brain pathology can result in standard analyses behaving erratically. Brain pathology can also invalidate assumptions one must make in order to interpret these results from these methods, such as standard relationships between anatomical locations and functions.

Chapter 4 described a novel diffusion MRI analysis procedure designed to overcome these difficulties, the utility of which was demonstrated throughout the remainder of this thesis. These difficulties were overcome using a number of novel features. Firstly, fMRI activation was utilised to identify relevant motor areas. This means that registration to atlases, and assumptions about structure-function relationships were no longer necessary. Functional MRI also increases the sensitivity of the technique by focusing on regions specifically involved with a certain task, rather than the entire motor area. Importantly, the fMRI analysis was conducted on a surface, rather than in voxel-space, which reduced activation transfer across sulci during smoothing or due to low image resolution. This method also constrained tractography using a surface, generated from the high-resolution T1, rather than using low resolution voxel-based masks generated from diffusion images (as is typical). Finally, this method utilised machine learning to decipher corticospinal from thalamocortical tracts, rather than rely solely on accurate ROI placement. This allows tracks to be labelled based on their position and shape, rather than only the positions of one or two aspects, and removes the requirement for accurate S1 and M1 cortical labels. The result of these factors was a pipeline that outperformed a standard cutting-edge fMRI-based approach in terms of tractography coherency, data rejection rates and correlation strengths between diffusion metrics and clinical scores

Measurement of Brain Changes in Healthy Adults

Before embarking on an investigation into neuroplasticity in a rehabilitative context, it is important to ensure that similar processes are moderately well understood, and can be measured, in people without neurological issues. Although a small number of neuroplasticity studies of healthy adults existed in the literature, these studies used vastly different training paradigms; different imaging techniques, which were predominantly mono-modal; and typically very small cohort sizes. These factors have stymied researchers' abilities to integrate and interpret this information together; that is,

to form a cohesive picture of neural changes that accompany motor training. In response, Chapter 5 and Chapter 6 of this thesis described a substantial study which reported brain changes in healthy adults learning a single-handed motor coordination task. Measures of brain change were indexed with TMS, fMRI, tractography, ROI-based diffusion MRI, behaviour and measures of cortical thickness. Almost all measures showed degrees of change solely in motor related areas of the ‘trained’ hemisphere, consistent with two non-mutually exclusive hypotheses. The first was that training improved the performance of cortical areas that were already responsible for performing the motor task prior to training, through an LTP-like process. This is an important finding as most fMRI-based studies have been based on the premise that motor learning is associated with regions of tissue taking on new responsibilities. The second finding was that white matter associated with these motor areas presented changes in microstructure in a manner consistent with activity-dependent myelination. This second finding is particularly promising for neurorehabilitation in unilateral CP as a large portion of this population present with white matter injury. As these white matter changes were reliable and detectable using the tractography pathology-robust method introduced in Chapter 4, it is reasonable to consider this type of investigation a priority for imaging trials of motor neurorehabilitation.

Power Analysis for Neuroplasticity with MRI

Chapter 7 described an attempt to follow up on the adult study by searching for corticospinal tract FA changes in children with UCP who were enrolled in a randomised controlled trial of Mitii™ virtual reality rehabilitative therapy. Unfortunately, unlike the adult study, participants in this trial did not show significant improvement in behavioural measures of motor function in the affected upper limb. As could be expected, changes in corticospinal tract diffusion metrics were resultantly unchanged. Although disappointing, this investigation demonstrated the ability of the fMRI-driven tractography method to perform reliably in a longitudinal trial in which participants presented with considerable pathology. It also raised questions about the power of such studies, noting that randomised controlled trials are typically planned around expected behavioural improvements, not neuroimaging, which makes it hard to ascertain whether null results represent lack of change, or lack of statistical power.

To address this gap in the literature, a power analysis was conducted so that future studies could be adequately planned for the measurement of neuroplasticity using diffusion MRI (corticospinal FA) or structural MRI (cortical thickness). This analysis, described in Chapter 8, reported that most studies of this type would need higher than average numbers of enrollees (59 – 108 before general attrition) to be adequately powered for this task. However, a consideration of the influencing factors meant that a number of recommendations could be made for studies to reduce these numbers where possible. These recommendations included investment into pre-scan

preparation for participants to reduce data-loss, investing effort in participants struggling to improve behaviourally to reduce variability in behavioural outcomes, and utilizing the surface-based fMRI seeded tractography method to boost signal-to-noise. Another important recommendation was that small and medium studies consider harmonizing protocols to ensure that data can be pooled across studies for more powerful analysis.

Implications, Limitations and Future Work

The work presented in this thesis has significantly increased knowledge about the brain changes that underlie motor-learning in healthy adults. With an understanding of these processes, similarities or differences in motor rehabilitation can now be investigated in a targeted way, in hope that resulting findings can be harnessed to improve neurorehabilitative efficacy. This work also reduced a number of barriers to such investigation, by making a wide range of data-driven recommendations on effective methodology, interpretation, required sample sizes and the effects of data loss. Importantly, key to this thesis was the description and demonstration of a novel diffusion MRI measurement pipeline that is demonstrably robust to pathology and sensitive to subtle brain changes.

A number of limitations exist in the present thesis, many of which cannot be easily quantified given the present state of scientific knowledge. For example, it is implicitly assumed that the ability of injured and uninjured brains to adapt is not significantly different, or at least that the same general types of neuroplasticity (e.g. myelination) occur with motor-training for rehabilitative or non-rehabilitative skill improvement. These assumptions are not baseless – there is no reason to believe that the basic physiological processes of healthy neurons or glia are altered in CP populations – but have also not yet been demonstrated. In essence, this is a ‘Catch-22’ scenario – prior to this work, there were high barriers to investigating these features. The current thesis helps alleviate these barriers, particularly by quantifying precisely how much brain change can be expected from a training regimen in a healthy population, and providing means to do so in people with cerebral palsy.

One barrier that the present work has failed to lower is the proportion of diffusion data discarded during processing. Although standard atlas-based packages such as Freesurfer are unstable in the presence of pathology and so can result in loss of ~30% of all data, motion during fMRI scanning is nearly at a similar level in children with UCP. As demonstrated, however, the methods used in the present thesis are substantially more sensitive, and so the impact of this data loss is less severe. Furthermore, reducing data-rejection was also not a primary goal of this thesis, and it could be argued that relying on imaging techniques for this purpose is akin to ‘parking an ambulance at the bottom of the cliff’. Adequate preparation and child-friendly scan routines will always be more ideal

than attempting to ‘clean’ motion corrupted data, and at least one study has described specific behavioural techniques effective for this purpose since data for this thesis was acquired.²⁸³ Utilisation of such techniques may see future use of the present methodology improve data rejection rates above those of standard packages.

Although future directions for UCP are hopefully relatively clear from this discussion, it is worthy of note that the tractography pipeline presented in this thesis is suitable for any participant cohort for whom imaging can be acquired. Since publication of this work, our laboratory has been approached, and is now planning, to utilise this technique to measure sensory-related neuroplasticity in children with spastic CP, and for neurosurgical planning of patients with epilepsy or brain tumours. The use of surfaces also lends this method to conducting ‘atlas free’ segmentations of brain structure based purely on tractography – a technique now being developed by our group.

References

1. Rosenbaum P, Paneth N, Leviton A, Goldstein M, Bax M, Damiano D, et al. A report: the definition and classification of cerebral palsy April 2006. *Dev Med Child Neurol Suppl.* 2007 Feb;109(April):8–14.
2. Boyd RN, Jordan R, Pareezer L, Moodie A, Finn C, Luther B, et al. Australian Cerebral Palsy Child Study: protocol of a prospective population based study of motor and brain development of preschool aged children with cerebral palsy. *BMC Neurol.* 2013 Jan;13(1):57.
3. Parkinson KN, Gibson L, Dickinson HO, Colver AF. Pain in children with cerebral palsy: a cross-sectional multicentre European study. *Acta Paediatr.* 2010 Mar;99(3):446–51.
4. Australian Cerebral Palsy Register Group. The Australian Cerebral Palsy Register Report 2013 [Internet]. Sydney; 2013.
5. Towsley K, Shevell MI, Dagenais L. Population-based study of neuroimaging findings in children with cerebral palsy. *Eur J Paediatr Neurol.* 2011 Jan;15(1):29–35.
6. Krägeloh-Mann I, Horber V. The role of magnetic resonance imaging in elucidating the pathogenesis of cerebral palsy: a systematic review. *Dev Med Child Neurol.* 2007 Feb;49(2):144–51.
7. Bax M, Tydeman C, Flodmark O. Clinical and MRI correlates of cerebral palsy: the European Cerebral Palsy Study. *JAMA.* 2006 Oct 4;296(13):1602–8.
8. Eyre J a., Taylor JP, Villagra F, Smith M, Miller S. Evidence of activity-dependent withdrawal of corticospinal projections during human development. *Neurology.* 2001 Nov 13;57(9):1543–54.
9. Holmefur M, Kits A, Bergström J, Krumlinde-Sundholm L, Flodmark O, Forsberg H, et al. Neuroradiology can predict the development of hand function in children with unilateral cerebral palsy. *Neurorehabil Neural Repair.* 2013;27(1):72–8.
10. Novak I, Hines M, Goldsmith S, Barclay R. Clinical prognostic messages from a systematic review on cerebral palsy. *Pediatrics.* 2012 Nov;130(5):e1285-312.
11. Boyd RN, Ziviani J, Sakzewski L, Miller L, Bowden J, Cunnington R, et al. COMBIT: protocol of a randomised comparison trial of COMBined modified constraint induced movement therapy and bimanual intensive training with distributed model of standard upper limb rehabilitation in children with congenital hemiplegia. *BMC Neurol.* 2013 Jan;13(1):68.
12. Sakzewski L, Ziviani J, Boyd RN. Efficacy of upper limb therapies for unilateral cerebral palsy: a meta-analysis. *Pediatrics.* 2014 Jan;133(1):e175-204.
13. Boyd RN, Mitchell LE, James ST, Ziviani J, Sakzewski L, Smith A, et al. Move it to improve it (Mitii): study protocol of a randomised controlled trial of a novel web-based multimodal training program for children and adolescents with cerebral palsy. *BMJ Open.* 2013 Jan;3(4).
14. James S, Ziviani J, Ware RS, Boyd RN. Randomized controlled trial of web-based

- multimodal therapy for unilateral cerebral palsy to improve occupational performance. *Dev Med Child Neurol. In Press*. 2015 Jun;57(6):530–8.
15. Mitchell L, Ziviani J, Oftedal S, Boyd R. The effect of virtual reality interventions on physical activity in children and adolescents with early brain injuries including cerebral palsy. *Dev Med Child Neurol*. 2012 Jul;54(7):667–71.
 16. Fasoli SE, Fragala-Pinkham M, Hughes R, Hogan N, Krebs HI, Stein J. Upper limb robotic therapy for children with hemiplegia. *Am J Phys Med Rehabil*. 2008;87(11):929–36.
 17. Qiu Q, Ramirez D a, Saleh S, Fluet GG, Parikh HD, Kelly D, et al. The New Jersey Institute of Technology Robot-Assisted Virtual Rehabilitation (NJIT-RAVR) system for children with cerebral palsy: a feasibility study. *J Neuroeng Rehabil*. 2009;6:40.
 18. Fluet GG, Qiu Q, Kelly D, Parikh HD, Ramirez D, Saleh S, et al. Interfacing a haptic robotic system with complex virtual environments to treat impaired upper extremity motor function in children with cerebral palsy. *Dev Neurorehabil*. 2010;13(5):335–45.
 19. Ladenheim B, Altenburger P, Cardinal R, Monterroso L, Dierks T, Mast J, et al. The effect of random or sequential presentation of targets during robot-assisted therapy on children. *NeuroRehabilitation*. 2013;33(1):25–31.
 20. Gilliaux M, Renders a., Dispa D, Holvoet D, Sapin J, Dehez B, et al. Upper Limb Robot-Assisted Therapy in Cerebral Palsy: A Single-Blind Randomized Controlled Trial. *Neurorehabil Neural Repair*. 2014;29(2):183–92.
 21. Sakzewski L, Ziviani J, Abbott DF, Macdonell R a L, Jackson GD, Boyd RN. Randomized trial of constraint-induced movement therapy and bimanual training on activity outcomes for children with congenital hemiplegia. *Dev Med Child Neurol*. 2011 Apr;53(4):313–20.
 22. Sakzewski L, Ziviani J, Boyd RN. Delivering evidence-based upper limb rehabilitation for children with cerebral palsy: barriers and enablers identified by three pediatric teams. *Phys Occup Ther Pediatr*. 2014 Nov;34(4):368–83.
 23. Sakzewski L, Miller L, Ziviani J, Abbott DF, Rose S, Macdonell RAL, et al. Randomized comparison trial of density and context of upper limb intensive group versus individualized occupational therapy for children with unilateral cerebral palsy. *Dev Med Child Neurol. In Press*. 2015;
 24. Miller L, Ziviani J, Ware RS, Boyd RN. Mastery motivation as a predictor of occupational performance following upper limb intervention for school-aged children with congenital hemiplegia. *Dev Med Child Neurol*. 2014 Oct;56(10):976–83.
 25. Taub E, Ramey SL, DeLuca S, Echols K. Efficacy of constraint-induced movement therapy for children with cerebral palsy with asymmetric motor impairment. *Pediatrics*. 2004;113(2):305–12.
 26. Charles JR, Wolf SL, Schneider J a, Gordon AM. Efficacy of a child-friendly form of constraint-induced movement therapy in hemiplegic cerebral palsy: a randomized control trial. *Dev Med Child Neurol*. 2006;48(8):635–42.
 27. Sakzewski L, Ziviani J, Abbott DF, Macdonell R a L, Jackson GD, Boyd RN. Equivalent retention of gains at 1 year after training with constraint-induced or bimanual therapy in

- children with unilateral cerebral palsy. *Neurorehabil Neural Repair*. 2011;25(7):664–71.
28. Yang JF, Livingstone D, Brunton K, Kim D, Lopetinsky B, Roy F, et al. Training to enhance walking in children with cerebral palsy: are we missing the window of opportunity? *Semin Pediatr Neurol*. 2013 Jun;20(2):106–15.
 29. Westerga J, Gramsbergen A. Development of locomotion in the rat: the significance of early movements. *Early Hum Dev*. 1993;34(1–2):89–100.
 30. Martin JH, Choy M, Pullman S, Meng Z. Corticospinal system development depends on motor experience. *J Neurosci*. 2004;24(9):2122–32.
 31. Friel K, Chakrabarty S, Kuo H-C, Martin J. Using motor behavior during an early critical period to restore skilled limb movement after damage to the corticospinal system during development. *J Neurosci*. 2012 Jul 4;32(27):9265–76.
 32. Eyre J a. Corticospinal tract development and its plasticity after perinatal injury. *Neurosci Biobehav Rev*. 2007 Jan;31(8):1136–49.
 33. Guzzetta A, Boyd RN, Perez M, Ziviani J, Burzi V, Slaughter V, et al. UP-BEAT (Upper Limb Baby Early Action-observation Training): protocol of two parallel randomised controlled trials of action-observation training for typically developing infants and infants with asymmetric brain lesions. *BMJ Open*. 2013;3(2):1–11.
 34. Eliasson A-C, Sjöstrand L, Ek L, Krumlinde-Sundholm L, Tedroff K. Efficacy of baby-CIMT: study protocol for a randomised controlled trial on infants below age 12 months, with clinical signs of unilateral CP. *BMC Pediatr*. 2014;14:141.
 35. Taub E. Harnessing brain plasticity through behavioral techniques to produce new treatments in neurorehabilitation. *Am Psychol*. 2004 Nov;59(8):692–704.
 36. Andersen SL. Trajectories of brain development: point of vulnerability or window of opportunity? *Neurosci Biobehav Rev*. 2003 Jan;27(1–2):3–18.
 37. Merzenich MM, Van Vleet TM, Nahum M. Brain plasticity-based therapeutics. *Front Hum Neurosci*. 2014 Jun 27;8(June):1–16.
 38. Kleim J a, Jones T a. Principles of experience-dependent neural plasticity: implications for rehabilitation after brain damage. *J Speech Lang Hear Res*. 2008;51(1):S225–39.
 39. Meunier S, Russmann H, Shamim E, Lamy J-C, Hallett M. Plasticity of cortical inhibition in dystonia is impaired after motor learning and paired-associative stimulation. *Eur J Neurosci*. 2012 Mar;35(6):975–86.
 40. Gillick BT, Krach LE, Feyma T, Rich TL, Moberg K, Thomas W, et al. Primed low-frequency repetitive transcranial magnetic stimulation and constraint-induced movement therapy in pediatric hemiparesis: A randomized controlled trial. *Dev Med Child Neurol*. 2014;56(1):44–52.
 41. Murase N, Duque J, Mazzocchio R, Cohen LG. Influence of interhemispheric interactions on motor function in chronic stroke. *Ann Neurol*. 2004 Mar;55(3):400–9.
 42. Marquez J, van Vliet P, Mcelduff P, Lagopoulos J, Parsons M. Transcranial direct current

- stimulation (tDCS): Does it have merit in stroke rehabilitation? A systematic review. *Int J Stroke*. 2013 Oct 22;10(3):1–11.
43. Nair DG, Renga V, Lindenberg R, Zhu L, Schlaug G. Optimizing recovery potential through simultaneous occupational therapy and non-invasive brain-stimulation using tDCS. *Restor Neurol Neurosci*. 2011 Jan;29(6):411–20.
 44. Lindenberg R, Renga V, Zhu LL, Nair D, Schlaug G. Bihemispheric brain stimulation facilitates motor recovery in chronic stroke patients. *Neurology*. 2010 Dec 14;75(24):2176–84.
 45. Fregni F, Boggio PS, Mansur CG, Wagner T, Ferreira MJL, Lima MC, et al. Transcranial direct current stimulation of the unaffected hemisphere in stroke patients. *Neuroreport*. 2005 Sep 28;16(14):1551–5.
 46. Zimerman M, Heise KF, Hoppe J, Cohen LG, Gerloff C, Hummel FC. Modulation of training by single-session transcranial direct current stimulation to the intact motor cortex enhances motor skill acquisition of the paretic hand. *Stroke*. 2012 Aug;43(8):2185–91.
 47. Grecco LAC, de Almeida Carvalho Duarte N, Mendonça ME, Cimolin V, Galli M, Fregni F, et al. Transcranial direct current stimulation during treadmill training in children with cerebral palsy: a randomized controlled double-blind clinical trial. *Res Dev Disabil*. 2014 Nov;35(11):2840–8.
 48. Stefan K, Kunesch E, Cohen LG, Benecke R, Classen J. Induction of plasticity in the human motor cortex by paired associative stimulation. *Brain*. 2000;123 Pt 3:572–84.
 49. Damji O, Kotsovsky O, Kirton A. Evaluating developmental motor plasticity after perinatal stroke with paired associative stimulation. *Stroke*. 2012;43 (11):e144–5.
 50. Liepert J, Miltner WH, Bauder H, Sommer M, Dettmers C, Taub E, et al. Motor cortex plasticity during constraint-induced movement therapy in stroke patients. *Neurosci Lett*. 1998 Jun 26;250(1):5–8.
 51. Rose S, Guzzetta A, Pannek K, Boyd R. MRI structural connectivity, disruption of primary sensorimotor pathways, and hand function in cerebral palsy. *Brain Connect*. 2011 Jan;1(4):309–16.
 52. Draganski B, Gaser C, Busch V, Schuierer G, Bogdahn U, May A. Neuroplasticity: changes in grey matter induced by training. *Nature*. 2004 Jan 22;427(6972):311–2.
 53. Gauthier L V, Taub E, Perkins C, Ortmann M, Mark VW, Uswatte G. Remodeling the brain: plastic structural brain changes produced by different motor therapies after stroke. *Stroke*. 2008 May;39(5):1520–5.
 54. Staudt M, Grodd W, Gerloff C, Erb M, Stitz J, Krägeloh-Mann I. Two types of ipsilateral reorganization in congenital hemiparesis: a TMS and fMRI study. *Brain*. 2002 Oct;125(Pt 10):2222–37.
 55. Staudt M, Gerloff C, Grodd W, Holthausen H, Niemann G, Krägeloh-Mann I. Reorganization in congenital hemiparesis acquired at different gestational ages. *Ann Neurol*. 2004 Dec;56(6):854–63.

56. Farmer SF, Harrison LM, Ingram DA, Stephens JA. Plasticity of central motor pathways in children with hemiplegic cerebral palsy. *Neurology*. 1991 Sep;41(9):1505–10.
57. Guzzetta A, Bonanni P, Biagi L, Tosetti M, Montanaro D, Guerrini R, et al. Reorganisation of the somatosensory system after early brain damage. *Clin Neurophysiol*. 2007 May;118(5):1110–21.
58. Pannek K, Boyd RN, Fiori S, Guzzetta A, Rose SE. Assessment of the structural brain network reveals altered connectivity in children with unilateral cerebral palsy due to periventricular white matter lesions. *NeuroImage Clin*. 2014 Jan;5:84–92.
59. Tsao H, Pannek K, Fiori S, Boyd RN, Rose S. Reduced integrity of sensorimotor projections traversing the posterior limb of the internal capsule in children with congenital hemiparesis. *Res Dev Disabil*. 2014 Feb;35(2):250–60.
60. Hoon AH, Stashinko EE, Nagae LM, Lin DDM, Keller J, Bastian A, et al. Sensory and motor deficits in children with cerebral palsy born preterm correlate with diffusion tensor imaging abnormalities in thalamocortical pathways. *Dev Med Child Neurol*. 2009 Sep;51(9):697–704.
61. Staudt M, Braun C, Gerloff C, Erb M, Grodd W, Krägeloh-Mann I. Developing somatosensory projections bypass periventricular brain lesions. *Neurology*. 2006 Aug 8;67(3):522–5.
62. Kurz MJ, Becker KM, Heinrichs-Graham E, Wilson TW. Neurophysiological abnormalities in the sensorimotor cortices during the motor planning and movement execution stages of children with cerebral palsy. *Dev Med Child Neurol*. 2014 Jun 14;56(11):1072–7.
63. Scheck SM, Pannek K, Fiori S, Boyd RN, Rose SE. Quantitative comparison of cortical and deep grey matter in pathological subtypes of unilateral cerebral palsy. *Dev Med Child Neurol*. 2014;56(10):968–75.
64. Sterling C, Taub E, Davis D, Rickards T, Gauthier L V, Griffin A, et al. Structural neuroplastic change after constraint-induced movement therapy in children with cerebral palsy. *Pediatrics*. 2013 May;131(5):e1664-9.
65. Golomb MR, McDonald BC, Warden SJ, Yonkman J, Saykin AJ, Shirley B, et al. In-Home Virtual Reality Videogame Telerehabilitation in Adolescents With Hemiplegic Cerebral Palsy. *Arch Phys Med Rehabil*. 2010 Jan;91(1):1–8.e1.
66. Sutcliffe TL, Logan WJ, Fehlings DL. Pediatric constraint-induced movement therapy is associated with increased contralateral cortical activity on functional magnetic resonance imaging. *J Child Neurol*. 2009 Oct;24(10):1230–5.
67. Cope SM, Liu X-C, Verber MD, Cayo C, Rao S, Tassone JC. Upper limb function and brain reorganization after constraint-induced movement therapy in children with hemiplegia. *Dev Neurorehabil*. 2010 Feb;13(1):19–30.
68. Juenger H, Linder-Lucht M, Walther M, Berweck S, Mall V, Staudt M. Cortical neuromodulation by constraint-induced movement therapy in congenital hemiparesis: an fMRI study. *Neuropediatrics*. 2007 Jun;38(3):130–6.
69. Juenger H, Kuhnke N, Braun C, Ummenhofer F, Wilke M, Walther M, et al. Two types of exercise-induced neuroplasticity in congenital hemiparesis: A transcranial magnetic

stimulation, functional MRI, and magnetoencephalography study. *Dev Med Child Neurol*. 2013 Oct;55(10):941–51.

70. Rossini PM, Barker AT, Berardelli A, Caramia MD, Caruso G, Cracco RQ, et al. Non-invasive electrical and magnetic stimulation of the brain, spinal cord and roots: basic principles and procedures for routine clinical application. Report of an IFCN committee. *Electroencephalogr Clin Neurophysiol*. 1994 Aug;91(2):79–92.
71. Ferrari A, Cioni G. The Spastic Forms of Cerebral Palsy [Internet]. 1st ed. Ferrari A, Cioni G, editors. *The Spastic Forms of Cerebral Palsy*. Milano: Springer Milan; 2010 [cited 2014 Oct 23]. 331–356 p.
72. Kobayashi M, Pascual-Leone A. Transcranial magnetic stimulation in neurology. *Lancet Neurol*. 2003;2(3):145–56.
73. Rossini PM, Rossi S. Transcranial magnetic stimulation: diagnostic, therapeutic, and research potential. *Neurology*. 2007 Feb 13;68(7):484–8.
74. Frye RE, Rotenberg A, Ousley M, Pascual-Leone A. Transcranial magnetic stimulation in child neurology: current and future directions. *J Child Neurol*. 2008 Jan;23(1):79–96.
75. Sohn YH, Kaelin-Lang a, Jung HY, Hallett M. Effect of levetiracetam on human corticospinal excitability. *Neurology*. 2001;57(5):858–63.
76. Hadjipanayis A, Hadjichristodoulou C, Youroukos S. Epilepsy in patients with cerebral palsy. *Dev Med Child Neurol*. 1997 Oct 29;39(10):659–63.
77. Gilbert DL, Garvey M a., Bansal AS, Lipps T, Zhang J, Wassermann EM. Should transcranial magnetic stimulation research in children be considered minimal risk? *Clin Neurophysiol*. 2004;115(8):1730–9.
78. Jones DK. Studying connections in the living human brain with diffusion MRI. *Cortex*. 2008 Sep;44(8):936–52.
79. Raffelt D, Tournier J-D, Rose S, Ridgway GR, Henderson R, Crozier S, et al. Apparent Fibre Density: a novel measure for the analysis of diffusion-weighted magnetic resonance images. *Neuroimage*. 2012 Feb 15;59(4):3976–94.
80. Scholz J, Klein MC, Behrens TEJ, Johansen-Berg H. Training induces changes in white-matter architecture. *Nat Neurosci*. 2009 Nov 11;12(11):1370–1.
81. Nagee LM, Hoon a H, Stashinko E, Lin D, Zhang W, Levey E, et al. Diffusion tensor imaging in children with periventricular leukomalacia: variability of injuries to white matter tracts. *AJNR Am J Neuroradiol*. 2007 Aug;28(7):1213–22.
82. Sakkalis V. Review of advanced techniques for the estimation of brain connectivity measured with EEG/MEG. *Comput Biol Med*. 2011;41(12):1110–7.
83. Hämäläinen M, Hari R, Ilmoniemi RJ, Knuutila J, Lounasmaa O V. Magnetoencephalography—theory, instrumentation, and applications to noninvasive studies of the working human brain. *Rev Mod Phys*. 1993;65(2):413–97.
84. Sharon D, Hämäläinen MS, Tootell RBH, Halgren E, Belliveau JW. The advantage of

combining MEG and EEG: Comparison to fMRI in focally stimulated visual cortex. *Neuroimage*. 2007;36(4):1225–35.

85. Papadelis C, Ahtam B, Nazarova M, Nimec D, Snyder B, Grant PE, et al. Cortical Somatosensory Reorganization in Children with Spastic Cerebral Palsy: A Multimodal Neuroimaging Study. *Front Hum Neurosci*. 2014 Sep 12;8(September):1–15.
86. Nyström P. The infant mirror neuron system studied with high density EEG. *Soc Neurosci*. 2008;3(3–4):334–47.
87. Southgate V, Johnson MH, Osborne T, Csibra G. Predictive motor activation during action observation in human infants. *Biol Lett*. 2009 Dec 23;5(6):769–72.
88. Southgate V, Johnson MH, El Karoui I, Csibra G. Motor system activation reveals infants' on-line prediction of others' goals. *Psychol Sci a J Am Psychol Soc / APS*. 2010;21(3):355–9.
89. Nyström P, Ljunghammar T, Rosander K, Von Hofsten C. Using mu rhythm desynchronization to measure mirror neuron activity in infants. *Dev Sci*. 2011;14(2):327–35.
90. Ertelt D, Small S, Solodkin A, Dettmers C, McNamara A, Binkofski F, et al. Action observation has a positive impact on rehabilitation of motor deficits after stroke. *Neuroimage*. 2007;36(SUPPL. 2):T164–73.
91. Burzi V, Marchi V, Boyd RN, Mazziotti R, Moscarelli M, Sgherri G, et al. Brain representation of action observation in human infants. *Dev Med Child Neurol*. 2015;57(Supplement s2):26–30.
92. Wilde E a, Merkle TL, Bigler ED, Max JE, Schmidt AT, Ayoub KW, et al. Longitudinal changes in cortical thickness in children after traumatic brain injury and their relation to behavioral regulation and emotional control. *Int J Dev Neurosci*. 2012 May;30(3):267–76.
93. Scheck S, Rose S, Boyd R. Cortical thickness of medial temporal gyrus and pre-central gyrus correlates with upper limb function in unilateral cerebral palsy. In: *Abstracts of the 6th Biennial Conference of the Australasian Academy of Cerebral Palsy & Developmental Medicine*. Brisbane: Wiley-Blackwell Publishing; 2012 [cited 2014 Dec 5]. p. 75–93.
94. Zatorre RJ, Fields RD, Johansen-Berg H. Plasticity in gray and white: neuroimaging changes in brain structure during learning. *Nat Neurosci*. 2012 Apr;15(4):528–36.
95. Lerch JP, Yiu AP, Martinez-Canabal A, Pekar T, Bohbot VD, Frankland PW, et al. Maze training in mice induces MRI-detectable brain shape changes specific to the type of learning. *Neuroimage*. 2011 Feb 1;54(3):2086–95.
96. Carp J. The secret lives of experiments: methods reporting in the fMRI literature. *Neuroimage*. 2012 Oct 15;63(1):289–300.
97. Thirion B, Pinel P, Mériaux S, Roche A, Dehaene S, Poline J-B. Analysis of a large fMRI cohort: Statistical and methodological issues for group analyses. *Neuroimage*. 2007 Mar;35(1):105–20.
98. Boyd R, Sakzewski L, Ziviani J, Abbott DF, Badawy R, Gilmore R, et al. INCITE: A randomised trial comparing constraint induced movement therapy and bimanual training in

children with congenital hemiplegia. *BMC Neurol.* 2010 Jan 12;10(3):4.

99. Heller R, Stanley D, Yekutieli D, Rubin N, Benjamini Y. Cluster-based analysis of fMRI data. *Neuroimage.* 2006 Nov 1;33(2):599–608.
100. Woo C-W, Krishnan A, Wager TD. Cluster-extent based thresholding in fMRI analyses: pitfalls and recommendations. *Neuroimage.* 2014 May 1;91:412–9.
101. Walther M, Juenger H, Kuhnke N, Wilke M, Brodbeck V, Berweck S, et al. Motor cortex plasticity in ischemic perinatal stroke: a transcranial magnetic stimulation and functional MRI study. *Pediatr Neurol.* 2009 Sep;41(3):171–8.
102. Logothetis NK. What we can do and what we cannot do with fMRI. *Nature.* 2008 Jun 12;453(7197):869–78.
103. Reid LB, Rose SE, Boyd RN. Rehabilitation and neuroplasticity in children with unilateral cerebral palsy. *Nat Rev Neurol.* 2015;11(7):390–400.
104. Caeyenberghs K, Wenderoth N, Smits-Engelsman BCM, Sunaert S, Swinnen SP. Neural correlates of motor dysfunction in children with traumatic brain injury: exploration of compensatory recruitment patterns. *Brain.* 2009 Mar;132(Pt 3):684–94.
105. Van de Winckel A, Klingels K, Bruyninckx F, Wenderoth N, Peeters R, Sunaert S, et al. How does brain activation differ in children with unilateral cerebral palsy compared to typically developing children, during active and passive movements, and tactile stimulation? An fMRI study. *Res Dev Disabil.* 2013 Jan;34(1):183–97.
106. Inguaggiato E, Sgandurra G, Perazza S, Guzzetta a, Cioni G. Brain reorganization following intervention in children with congenital hemiplegia: a systematic review. *Neural Plast.* 2013 Jan;2013:356275.
107. Lima FPS, Lima MO, Leon D, Lucareli PRG, Falcon C, Cogo JC, et al. fMRI of the sensorimotor cortex in patients with traumatic brain injury after intensive rehabilitation. *Neurol Sci.* 2011 Aug;32(4):633–9.
108. Kim Y-H, Park J-W, Ko M-H, Jang S-H, Lee PKW. Plastic changes of motor network after constraint-induced movement therapy. *Yonsei Med J.* 2004 Apr 30;45(2):241–6.
109. Sacco K, Cauda F, D’Agata F, Duca S, Zettin M, Virgilio R, et al. A combined robotic and cognitive training for locomotor rehabilitation: evidences of cerebral functional reorganization in two chronic traumatic brain injured patients. *Front Hum Neurosci.* 2011 Jan;5(November):146.
110. Nair DG, Hutchinson S, Fregni F, Alexander M, Pascual-Leone A, Schlaug G. Imaging correlates of motor recovery from cerebral infarction and their physiological significance in well-recovered patients. *Neuroimage.* 2007 Jan 1;34(1):253–63.
111. Tombari D, Loubinoux I, Pariente J, Gerdelat A, Albucher J-F, Tardy J, et al. A longitudinal fMRI study: in recovering and then in clinically stable sub-cortical stroke patients. *Neuroimage.* 2004 Nov;23(3):827–39.
112. Guzzetta A, Staudt M, Petacchi E, Ehlers J, Erb M, Wilke M, et al. Brain representation of active and passive hand movements in children. *Pediatr Res.* 2007 Apr;61(4):485–90.

113. Mackey A, Stinear C, Stott S, Byblow WD. Upper limb function and cortical organization in youth with unilateral cerebral palsy. *Front Neurol*. 2014 Jan;5(July):117.
114. Favre I, Zeffiro T a, Detante O, Krainik A, Hommel M, Jaillard A. Upper limb recovery after stroke is associated with ipsilesional primary motor cortical activity: a meta-analysis. *Stroke*. 2014 Apr;45(4):1077–83.
115. Marshall RS, Perera GM, Lazar RM, Krakauer JW, Constantine RC, DeLaPaz RL. Evolution of cortical activation during recovery from corticospinal tract infarction. *Stroke*. 2000 Mar 1;31(3):656–61.
116. Schaechter JD, Perdue KL. Enhanced cortical activation in the contralesional hemisphere of chronic stroke patients in response to motor skill challenge. *Cereb Cortex*. 2008 Mar;18(3):638–47.
117. Jang SH, You SH, Hallett M, Cho YW, Park C-M, Cho S-H, et al. Cortical reorganization and associated functional motor recovery after virtual reality in patients with chronic stroke: an experimenter-blind preliminary study. *Arch Phys Med Rehabil*. 2005 Nov;86(11):2218–23.
118. Michielsen ME, Selles RW, van der Geest JN, Eckhardt M, Yavuzer G, Stam HJ, et al. Motor recovery and cortical reorganization after mirror therapy in chronic stroke patients: a phase II randomized controlled trial. *Neurorehabil Neural Repair*. 2011;25(3):223–33.
119. Könönen M, Tarkka IM, Niskanen E, Pihlajamäki M, Mervaala E, Pitkänen K, et al. Functional MRI and motor behavioral changes obtained with constraint-induced movement therapy in chronic stroke. *Eur J Neurol*. 2012 Apr;19(4):578–86.
120. Sutcliffe TL, Gaetz WC, Logan WJ, Cheyne DO, Fehlings DL. Cortical reorganization after modified constraint-induced movement therapy in pediatric hemiplegic cerebral palsy. *J Child Neurol*. 2007 Nov;22(11):1281–7.
121. Salinet ASM, Haunton VJ, Panerai RB, Robinson TG. A systematic review of cerebral hemodynamic responses to neural activation following stroke. *J Neurol*. 2013 Nov;260(11):2715–21.
122. Jaillard A, Martin CD, Garambois K, Lebas JF, Hommel M. Vicarious function within the human primary motor cortex? A longitudinal fMRI stroke study. *Brain*. 2005 May;128(Pt 5):1122–38.
123. Cramer SC, Crafton KR. Somatotopy and movement representation sites following cortical stroke. *Exp brain Res*. 2006 Jan;168(1–2):25–32.
124. Bestmann S, Swayne O, Blankenburg F, Ruff CC, Teo J, Weiskopf N, et al. The role of contralesional dorsal premotor cortex after stroke as studied with concurrent TMS-fMRI. *J Neurosci*. 2010 Sep 8;30(36):11926–37.
125. de Bode S, Mathern GW, Bookheimer S, Dobkin B. Locomotor training remodels fMRI sensorimotor cortical activations in children after cerebral hemispherectomy. *Neurorehabil Neural Repair*. 2007;21(6):497–508.
126. Wilke M, Staudt M, Juenger H, Grodd W, Braun C, Krägeloh-Mann I. Somatosensory system in two types of motor reorganization in congenital hemiparesis: topography and

function. *Hum Brain Mapp.* 2009 Mar;30(3):776–88.

127. Holmström L, Vollmer B, Tedroff K, Islam M, Persson JKE, Kits A, et al. Hand function in relation to brain lesions and corticomotor-projection pattern in children with unilateral cerebral palsy. *Dev Med Child Neurol.* 2010 Feb;52(2):145–52.
128. Jindahra P, Petrie A, Plant GT. The time course of retrograde trans-synaptic degeneration following occipital lobe damage in humans. *Brain.* 2012 Feb;135(Pt 2):534–41.
129. Bendlin BB, Ries ML, Lazar M, Alexander AL, Dempsey RJ, Rowley H a, et al. Longitudinal changes in patients with traumatic brain injury assessed with diffusion-tensor and volumetric imaging. *Neuroimage.* 2008 Aug 15;42(2):503–14.
130. Riley JD, Le V, Der-Yeghiaian L, See J, Newton JM, Ward NS, et al. Anatomy of stroke injury predicts gains from therapy. *Stroke.* 2011 Feb;42(2):421–6.
131. Zandbelt BB, Gladwin TE, Raemaekers M, van Buuren M, Neggers SF, Kahn RS, et al. Within-subject variation in BOLD-fMRI signal changes across repeated measurements: quantification and implications for sample size. *Neuroimage.* 2008 Aug 1;42(1):196–206.
132. Pascual-Leone A, Amedi A, Fregni F, Merabet LB. The plastic human brain cortex. *Annu Rev Neurosci.* 2005;28:377–401.
133. Duffau H, Sichez JP, Lehericy S. Intraoperative unmasking of brain redundant motor sites during resection of a precentral angioma: evidence using direct cortical stimulation. *Ann Neurol.* 2000 Jan;47(1):132–5.
134. Sasaki K, Gemba H. Compensatory motor function of the somatosensory cortex for the motor cortex temporarily impaired by cooling in the monkey. *Exp brain Res.* 1984 Jan;55(1):60–8.
135. Raghavan P, Santello M, Gordon AM, Krakauer JW. Compensatory motor control after stroke: an alternative joint strategy for object-dependent shaping of hand posture. *J Neurophysiol.* 2010 Jun;103(6):3034–43.
136. Kitago T, Liang J, Huang VS, Hayes S, Simon P, Tenteromano L, et al. Improvement after constraint-induced movement therapy: recovery of normal motor control or task-specific compensation? *Neurorehabil Neural Repair.* 2013 Feb;27(2):99–109.
137. Roby-Brami A, Feydy A, Combeaud M, Biryukova E V, Bussel B, Levin MF. Motor compensation and recovery for reaching in stroke patients. *Acta Neurol Scand.* 2003 May;107(5):369–81.
138. Johansen-Berg H, Matthews PM. Attention to movement modulates activity in sensori-motor areas, including primary motor cortex. *Exp brain Res.* 2002 Jan;142(1):13–24.
139. Pascual-Leone a, Grafman J, Hallett M. Modulation of cortical motor output maps during development of implicit and explicit knowledge. *Science.* 1994 Mar 4;263(5151):1287–9.
140. Rehme AK, Fink GR, Von Cramon DY, Grefkes C. The role of the contralesional motor cortex for motor recovery in the early days after stroke assessed with longitudinal fMRI. *Cereb Cortex.* 2011;21(April):756–68.

141. McDowd JM, Filion DL, Pohl PS, Richards LG, Stiers W. Attentional abilities and functional outcomes following stroke. *J Gerontol B Psychol Sci Soc Sci*. 2003 Jan;58(1):P45-53.
142. Bottcher L, Flachs EM, Uldall P. Attentional and executive impairments in children with spastic cerebral palsy. *Dev Med Child Neurol*. 2010 Feb;52(2):e42-7.
143. Mathias JL, Wheaton P. Changes in attention and information-processing speed following severe traumatic brain injury: a meta-analytic review. *Neuropsychology*. 2007 Mar;21(2):212-23.
144. Wylie GR, Genova H, DeLuca J, Chiaravalloti N, Sumowski JF. Functional magnetic resonance imaging movers and shakers: does subject-movement cause sampling bias? *Hum Brain Mapp*. 2014 Jan;35(1):1-13.
145. Rehme AK, Eickhoff SB, Rottschy C, Fink GR, Grefkes C. Activation likelihood estimation meta-analysis of motor-related neural activity after stroke. *Neuroimage*. 2012 Feb 1;59(3):2771-82.
146. Meyer BU, Rörich S, Gräfin von Einsiedel H, Kruggel F, Weindl A. Inhibitory and excitatory interhemispheric transfers between motor cortical areas in normal humans and patients with abnormalities of the corpus callosum. *Brain*. 1995 Apr;118 (Pt 2(2):429-40.
147. Heinen F, Kirschner J, Fietzek U, Glocker FX, Mall V, Korinthenberg R. Absence of transcallosal inhibition in adolescents with diplegic cerebral palsy. *Muscle Nerve*. 1999 Feb;22(2):255-7.
148. Takeuchi N, Ikoma K, Chuma T, Matsuo Y. Measurement of transcallosal inhibition in traumatic brain injury by transcranial magnetic stimulation. *Brain Inj*. 2006 Aug;20(9):991-6.
149. Jo HJ, Lee J-M, Kim J-H, Shin Y-W, Kim I-Y, Kwon JS, et al. Spatial accuracy of fMRI activation influenced by volume- and surface-based spatial smoothing techniques. *Neuroimage*. 2007 Jan 15;34(2):550-64.
150. Geissler A, Lanzenberger R, Barth M, Tahamtan AR, Milakara D, Gartus A, et al. Influence of fMRI smoothing procedures on replicability of fine scale motor localization. *Neuroimage*. 2005 Jan 15;24(2):323-31.
151. Price CJ, Crinion J, Friston KJ. Design and analysis of fMRI studies with neurologically impaired patients. *J Magn Reson Imaging*. 2006 Jun;23(6):816-26.
152. Andersen SM, Rapcsak SZ, Beeson PM. Cost function masking during normalization of brains with focal lesions: still a necessity? *Neuroimage*. 2010 Oct 15;53(1):78-84.
153. Nichols TE. Multiple testing corrections, nonparametric methods, and random field theory. *Neuroimage*. 2012;62(2):811-5.
154. Friston KJ, Worsley KJ, Frackowiak RS, Mazziotta JC, Evans a C. Assessing the significance of focal activations using their spatial extent. *Hum Brain Mapp*. 1994;1(3):210-20.
155. Hillary FG, Biswal B. The influence of neuropathology on the FMRI signal: a measurement

of brain or vein? *Clin Neuropsychol.* 2007 Jan;21(1):58–72.

156. Werring DJ, Clark C a, Barker GJ, Miller DH, Parker GJ, Brammer MJ, et al. The structural and functional mechanisms of motor recovery: complementary use of diffusion tensor and functional magnetic resonance imaging in a traumatic injury of the internal capsule. *J Neurol Neurosurg Psychiatry.* 1998 Dec;65(6):863–9.
157. Altamura C, Reinhard M, Vry M-S, Kaller CP, Hamzei F, Vernieri F, et al. The longitudinal changes of BOLD response and cerebral hemodynamics from acute to subacute stroke. A fMRI and TCD study. *BMC Neurosci.* 2009 Jan;10:151.
158. Murata Y, Sakatani K, Hoshino T, Fujiwara N, Kano T, Nakamura S, et al. Effects of cerebral ischemia on evoked cerebral blood oxygenation responses and BOLD contrast functional MRI in stroke patients. *Stroke.* 2006 Oct;37(10):2514–20.
159. Bonakdarpour B, Parrish TB, Thompson CK. Hemodynamic response function in patients with stroke-induced aphasia: implications for fMRI data analysis. *Neuroimage.* 2007 Jun;36(2):322–31.
160. Mayer AR, Toulouse T, Klimaj S, Ling JM, Pena A, Bellgowan PSF. Investigating the properties of the hemodynamic response function after mild traumatic brain injury. *J Neurotrauma.* 2014 Jan 15;31(2):189–97.
161. Roc AC, Wang J, Ances BM, Liebeskind DS, Kasner SE, Detre J a. Altered hemodynamics and regional cerebral blood flow in patients with hemodynamically significant stenoses. *Stroke.* 2006 Feb;37(2):382–7.
162. Krainik A, Hund-Georgiadis M, Zysset S, von Cramon DY. Regional impairment of cerebrovascular reactivity and BOLD signal in adults after stroke. *Stroke.* 2005 Jun;36(6):1146–52.
163. Grefkes C, Fink GR. Connectivity-based approaches in stroke and recovery of function. *Lancet Neurol.* 2014;13(February):206–16.
164. Rehme AK, Eickhoff SB, Wang LE, Fink GR, Grefkes C. Dynamic causal modeling of cortical activity from the acute to the chronic stage after stroke. *Neuroimage.* 2011;55(3):1147–58.
165. Siegel JS, Power JD, Dubis JW, Vogel AC, Church J a, Schlaggar BL, et al. Statistical improvements in functional magnetic resonance imaging analyses produced by censoring high-motion data points. *Hum Brain Mapp.* 2014 May 17;35(5):1981–96.
166. Anderson BJ, Eckburg PB, Relucio KI. Alterations in the Thickness of Motor Cortical Subregions After Motor-Skill Learning and Exercise. *Learn Mem.* 2002;9:1–9.
167. Rijntjes M, Hamzei F, Glauche V, Saur D, Weiller C. Activation changes in sensorimotor cortex during improvement due to CIMT in chronic stroke. *Restor Neurol Neurosci.* 2011 Jan 1;29(5):299–310.
168. Jansen M, White TP, Mullinger KJ, Liddle EB, Gowland P a., Francis ST, et al. Motion-related artefacts in EEG predict neuronally plausible patterns of activation in fMRI data. *Neuroimage.* 2012;59(1):261–70.

169. Xiong J, Ma L, Wang B, Narayana S, Duff EP, Egan GF, et al. Long-term motor training induced changes in regional cerebral blood flow in both task and resting states. *Neuroimage*. 2009 Mar 1;45(1):75–82.
170. Ishibashi T, Dakin K a, Stevens B, Lee PR, Kozlov S V, Stewart CL, et al. Astrocytes promote myelination in response to electrical impulses. *Neuron*. 2006 Mar 16;49(6):823–32.
171. Zhang H, Schneider T, Wheeler-Kingshott C a., Alexander DC. NODDI: Practical in vivo neurite orientation dispersion and density imaging of the human brain. *Neuroimage*. 2012;61(4):1000–16.
172. Jones EG. Cortical and subcortical contributions to activity-dependent plasticity in primate somatosensory cortex. *Annu Rev Neurosci*. 2000;23(1):1–37.
173. Elhabian S, Gur Y, Vachet C, Piven J, Styner M, Leppert IR, et al. Subject-Motion Correction in HARDI Acquisitions: Choices and Consequences. *Front Neurol*. 2014;5(December):86–7.
174. Cherubini A, Luccichenti G, Péran P, Hagberg GE, Barba C, Formisano R, et al. Multimodal fMRI tractography in normal subjects and in clinically recovered traumatic brain injury patients. *Neuroimage*. 2007 Feb 15;34(4):1331–41.
175. Zhu D, Zhang T, Jiang X, Hu X, Chen H, Yang N, et al. Fusing DTI and fMRI data: a survey of methods and applications. *Neuroimage*. 2014 Nov 15;102 Pt 1:184–91.
176. Palmer HS, Håberg a K, Fimland MS, Solstad GM, Moe Iversen V, Hoff J, et al. Structural brain changes after 4 wk of unilateral strength training of the lower limb. *J Appl Physiol*. 2013 Jul 15;115(2):167–75.
177. Beckung E, Hagberg G. Neuroimpairments, activity limitations, and participation restrictions in children with cerebral palsy. *Dev Med Child Neurol*. 2002;44(5):309–16.
178. Arnfield E, Guzzetta A, Boyd R. Relationship between brain structure on magnetic resonance imaging and motor outcomes in children with cerebral palsy: A systematic review. *Res Dev Disabil*. 2013 Jul;34(7):2234–50.
179. Scheck SM, Boyd RN, Rose SE. New insights into the pathology of white matter tracts in cerebral palsy from diffusion magnetic resonance imaging : a systematic review. *Dev Med Child Neurol*. 2012;54(8):684–96.
180. Tournier J-D, Calamante F, Connelly A. MRtrix: Diffusion tractography in crossing fiber regions. *Int J Imaging Syst Technol*. 2012 Mar;22(1):53–66.
181. Reid LB, Boyd RN, Cunningham R, Rose SE. Interpreting Intervention Induced Neuroplasticity with fMRI: The Case for Multimodal Imaging Strategies. *Neural Plast*. 2016;2016:1–13.
182. Jo HJ, Lee J-M, Kim J-H, Choi C-H, Gu B-M, Kang D-H, et al. Artificial shifting of fMRI activation localized by volume- and surface-based analyses. *Neuroimage*. 2008 Apr 15;40(3):1077–89.
183. Van Leemput K, Maes F, Vandermeulen D, Suetens P. Automated model-based tissue classification of MR images of the brain. *IEEE Trans Med Imaging*. 1999;18(10):897–908.

184. Bourgeat P, Chételat G, Villemagne VL, Fripp J, Raniga P, Pike K, et al. β -Amyloid burden in the temporal neocortex is related to hippocampal atrophy in elderly subjects without dementia. *Neurology*. 2010;74(2):121–7.
185. Jenkinson M, Bannister P, Brady M, Smith S. Improved optimization for the robust and accurate linear registration and motion correction of brain images. *Neuroimage*. 2002;17(2):825–41.
186. Greve DN, Fischl B. Accurate and robust brain image alignment using boundary-based registration. *Neuroimage*. 2009;48(1):63–72.
187. Sochen N, Deriche R, Perez LL. The Beltrami flow over implicit manifolds. *Proc Ninth IEEE Int Conf Comput Vis*. 2003;
188. Yousry T a., Schmid UD, Alkadhi H, Schmidt D, Peraud A, Buettner A, et al. Localization of the motor hand area to a knob on the precentral gyrus. A new landmark. *Brain*. 1997;120(1):141–57.
189. Tournier J-D, Calamante F, Connelly A. Determination of the appropriate b value and number of gradient directions for high-angular-resolution diffusion-weighted imaging. *NMR Biomed*. 2013 Dec;26(12):1775–86.
190. Pannek K, Guzzetta A, Colditz PB, Rose SE. Diffusion MRI of the neonate brain: acquisition, processing and analysis techniques. *Pediatr Radiol*. 2012 Oct;42(10):1169–82.
191. Yushkevich P a., Piven J, Hazlett HC, Smith RG, Ho S, Gee JC, et al. User-guided 3D active contour segmentation of anatomical structures: significantly improved efficiency and reliability. *Neuroimage*. 2006 Jul 1;31(3):1116–28.
192. Calamante F, Tournier J-D, Jackson GD, Connelly A. Track-density imaging (TDI): super-resolution white matter imaging using whole-brain track-density mapping. *Neuroimage*. 2010 Dec;53(4):1233–43.
193. Fisher AG, Jones KB. Assessment of motor and process skills. Three Star Press Fort Collins, CO; 1999.
194. Johnson LM, Randall MJ, Reddihough DS, Oke LE, Byrt TA, Bach TM. Development of a clinical assessment of quality of movement for unilateral upper-limb functon. *Dev Med Child Neurol*. 1994;36(11):965–73.
195. Andrade a, Kherif F, Mangin JF, Worsley KJ, Paradis a L, Simon O, et al. Detection of fMRI activation using cortical surface mapping. *Hum Brain Mapp*. 2001 Feb;12(2):79–93.
196. Oosterhof NN, Wiestler T, Downing PE, Diedrichsen J. A comparison of volume-based and surface-based multi-voxel pattern analysis. *Neuroimage*. 2011 May 15;56(2):593–600.
197. Anticevic A, Dierker DL, Gillespie SK, Repovs G, Csernansky JG, Van Essen DC, et al. Comparing surface-based and volume-based analyses of functional neuroimaging data in patients with schizophrenia. *Neuroimage*. 2008 Jul 1;41(3):835–48.
198. Smith RE, Tournier J-D, Calamante F, Connelly A. SIFT: Spherical-deconvolution informed filtering of tractograms. *Neuroimage*. 2013 Feb 15;67:298–312.

199. Barnea-Goraly N, Weinzimer S a., Ruedy KJ, Mauras N, Beck RW, Marzelli MJ, et al. High success rates of sedation-free brain MRI scanning in young children using simple subject preparation protocols with and without a commercial mock scanner--the Diabetes Research in Children Network (DirecNet) experience. *Pediatr Radiol.* 2014 Feb;44(2):181–6.
200. Yendiki A, Koldewyn K, Kakunoori S, Kanwisher N, Fischl B. Spurious group differences due to head motion in a diffusion MRI study. *Neuroimage.* 2013 Nov 21;88C:79–90.
201. Sanes JN, Donoghue JP. Plasticity and primary motor cortex. *Annu Rev Neurosci.* 2000;23:393–415.
202. Xu T, Yu X, Perlik AJ, Tobin WF, Zweig J a, Tennant K, et al. Rapid formation and selective stabilization of synapses for enduring motor memories. *Nature.* 2009 Dec 17;462(7275):915–9.
203. Nudo RJ, Wise BM, SiFuentes F, Milliken GW. Neural substrates for the effects of rehabilitative training on motor recovery after ischemic infarct. *Science.* 1996 Jun 21;272(5269):1791–4.
204. Hoy RR, Nolen TG, Casaday GC. Dendritic sprouting and compensatory synaptogenesis in an identified interneuron follow auditory deprivation in a cricket. *Proc Natl Acad Sci U S A.* 1985 Nov;82(22):7772–6.
205. Barron HC, Vogels TP, Emir UE, Makin TR, O’Shea J, Clare S, et al. Unmasking Latent Inhibitory Connections in Human Cortex to Reveal Dormant Cortical Memories. *Neuron.* 2016 Apr 6;90(1):191–203.
206. Kong NW, Gibb WR, Tate MC. Neuroplasticity: Insights from Patients Harboring Gliomas. *Neural Plast.* 2016;2016:2365063.
207. Bliss T V, Collingridge GL. A synaptic model of memory: long-term potentiation in the hippocampus. *Nature.* 1993 Jan 7;361(6407):31–9.
208. Matsuzaki M, Honkura N, Ellis-Davies GCR, Kasai H. Structural basis of long-term potentiation in single dendritic spines. *Nature.* 2004 Jun 17;429(6993):761–6.
209. Chang Y. Reorganization and plastic changes of the human brain associated with skill learning and expertise. *Front Hum Neurosci.* 2014;8(February):35.
210. Rioult-Pedotti M-SS, Friedman D, Donoghue JP. Learning-induced LTP in neocortex. *Science (80-).* 2000 Oct 20;290(5491):533–6.
211. Costa RM, Cohen D, Nicoletis MAL. Differential corticostriatal plasticity during fast and slow motor skill learning in mice. *Curr Biol.* 2004 Jul 13;14(13):1124–34.
212. Amunts K, Schlaug G, Jäncke L, Steinmetz H, Schleicher A, Dabringhaus A, et al. Motor cortex and hand motor skills: structural compliance in the human brain. *Hum Brain Mapp.* 1997;5(3):206–15.
213. Milton J, Solodkin A, Hlustík P, Small SL. The mind of expert motor performance is cool and focused. *Neuroimage.* 2007 Apr 1;35(2):804–13.
214. Pearce a J, Thickbroom GW, Byrnes ML, Mastaglia FL. Functional reorganisation of the

- corticomotor projection to the hand in skilled racquet players. *Exp brain Res.* 2000 Jan;130(2):238–43.
215. Kübler A, Dixon V, Garavan H. Automaticity and reestablishment of executive control-an fMRI study. *J Cogn Neurosci.* 2006 Aug;18(8):1331–42.
 216. Chevrier AD, Noseworthy MD, Schachar R. Dissociation of response inhibition and performance monitoring in the stop signal task using event-related fMRI. *Hum Brain Mapp.* 2007;28(12):1347–58.
 217. Orban P, Peigneux P, Lungu O, Albouy G, Breton E, Laberenne F, et al. The multifaceted nature of the relationship between performance and brain activity in motor sequence learning. *Neuroimage.* 2010 Jan 1;49(1):694–702.
 218. Floyer-Lea a, Matthews PM. Distinguishable brain activation networks for short- and long-term motor skill learning. *J Neurophysiol.* 2005 Jul;94(1):512–8.
 219. Dayan E, Cohen LG. Neuroplasticity subserving motor skill learning. *Neuron.* 2011 Nov 3;72(3):443–54.
 220. Doyon J, Bellec P, Amsel R, Penhune V, Monchi O, Carrier J, et al. Contributions of the basal ganglia and functionally related brain structures to motor learning. 2009;199:61–75.
 221. Karni A, Meyer G, Jezzard P, Adams MM, Turner R, Ungerleider LG. Functional MRI evidence for adult motor cortex plasticity during motor skill learning. *Nature.* 1995 Sep 14;377(6545):155–8.
 222. Ma L, Wang B, Narayana S, Hazeltine E, Chen X, Robin DA, et al. Changes in regional activity are accompanied with changes in inter-regional connectivity during 4 weeks motor learning. *Brain Res.* 2010;1318:64–76.
 223. Bezzola L, Mérillat S, Gaser C, Jäncke L. Training-induced neural plasticity in golf novices. *J Neurosci.* 2011 Aug 31;31(35):12444–8.
 224. Reid LB, Sale M V, Cunnington R, Mattingley JB, Rose SE. Structural brain changes following four weeks of unimanual motor training: evidence from fMRI-guided diffusion MRI tractography. *Hum Brain Mapp.* VOLUME(ISSUE):PAGES.
 225. Hallett M. Transcranial magnetic stimulation and the human brain. *Nature.* 2000 Jul 13;406(6792):147–50.
 226. Roth Y, Amir A, Levkovitz Y, Zangen A. Three-Dimensional Distribution of the Electric Field Induced in the Brain by Transcranial Magnetic Stimulation Using Figure-8 and Deep H-Coils. *J Clin Neurophysiol.* 2007 Feb;24(1):31–8.
 227. Sale M V., Ridding MC, Nordstrom MA. Cortisol inhibits neuroplasticity induction in human motor cortex. *J Neurosci.* 2008 Aug 13;28(33):8285–93.
 228. Schabrun SM, Stinear CM, Byblow WD, Ridding MC. Normalizing Motor Cortex Representations in Focal Hand Dystonia. *Cereb Cortex.* 2009 Sep 1;19(9):1968–77.
 229. Thomas AG, Marrett S, Saad ZS, Ruff DA, Martin A, Bandettini PA. Functional but not structural changes associated with learning: An exploration of longitudinal Voxel-Based

- Morphometry (VBM). *Neuroimage*. 2009;48(1):117–25.
230. Avants BB, Epstein CL, Grossman M, Gee JC. Symmetric diffeomorphic image registration with cross-correlation: evaluating automated labeling of elderly and neurodegenerative brain. *Med Image Anal*. 2008 Feb;12(1):26–41.
231. Luders E, Narr KL, Thompson PM, Rex DE, Woods RP, DeLuca H, et al. Gender effects on cortical thickness and the influence of scaling. *Hum Brain Mapp*. 2006;27(4):314–24.
232. Lancaster JL, Tordesillas-Gutiérrez D, Martinez M, Salinas F, Evans A, Zilles K, et al. Bias between MNI and Talairach coordinates analyzed using the ICBM-152 brain template. *Hum Brain Mapp*. 2007 Nov;28(11):1194–205.
233. Wahnoun R, Benson M, Helms-Tillery S, Adelson PD. Delineation of somatosensory finger areas using vibrotactile stimulation, an ECoG study. *Brain Behav*. 2015 Oct;5(10):e00369.
234. Penfield W, Boldrey E. Somatic Motor and Sensory Representation in the Cerebral Cortex of Man as Studied by Electrical Stimulation. *Brain*. 1937;60(4):389–443.
235. Ziemann U, Ilić T V, Pauli C, Meintzschel F, Ruge D. Learning modifies subsequent induction of long-term potentiation-like and long-term depression-like plasticity in human motor cortex. *J Neurosci*. 2004 Feb 18;24(7):1666–72.
236. Di Lazzaro V, Ziemann U. The contribution of transcranial magnetic stimulation in the functional evaluation of microcircuits in human motor cortex. *Front Neural Circuits*. 2013;7(February):18.
237. Taubert M, Draganski B, Anwander A, Müller K, Horstmann A, Villringer A, et al. Dynamic properties of human brain structure: learning-related changes in cortical areas and associated fiber connections. *J Neurosci*. 2010 Sep 1;30(35):11670–7.
238. Hicks RE, Gualtieri CT, Schroeder SR. Cognitive and Motor Components of Bilateral Transfer. *Am J Psychol*. 1983 Jan;96(2):223.
239. Teixeira L a. Timing and force components in bilateral transfer of learning. *Brain Cogn*. 2000 Dec;44(3):455–69.
240. Demerens C, Stankoff B, Logak M, Anglade P, Allinquant B, Couraud F, et al. Induction of myelination in the central nervous system by electrical activity. *Proc Natl Acad Sci U S A*. 1996 Sep 3;93(18):9887–92.
241. Savas JN, Toyama BH, Xu T, Yates JR, Hetzer MW. Extremely long-lived nuclear pore proteins in the rat brain. *Science*. 2012 Feb 24;335(6071):942.
242. Yeung MSY, Zdunek S, Bergmann O, Bernard S, Salehpour M, Alkass K, et al. Dynamics of oligodendrocyte generation and myelination in the human brain. *Cell*. 2014 Nov 6;159(4):766–74.
243. Song JH, Skoe E, Banai K, Kraus N. Training to improve hearing speech in noise: biological mechanisms. *Cereb Cortex*. 2012 May;22(5):1180–90.
244. Madhyastha T, Mérillat S, Hirsiger S, Bezzola L, Liem F, Grabowski T, et al. Longitudinal reliability of tract-based spatial statistics in diffusion tensor imaging. *Hum Brain Mapp*. 2014

Sep;35(9):4544–55.

245. Jones DK, Symms MR, Cercignani M, Howard RJ. The effect of filter size on VBM analyses of DT-MRI data. *Neuroimage*. 2005 Jun;26(2):546–54.
246. Bach M, Laun FB, Leemans A, Tax CMW, Biessels GJ, Stieltjes B, et al. Methodological considerations on tract-based spatial statistics (TBSS). *Neuroimage*. 2014 Oct 15;100:358–69.
247. Baek SO, Jang SH, Lee E, Kim S, Hah JO, Park YH, et al. CST recovery in pediatric hemiplegic patients: Diffusion tensor tractography study. *Neurosci Lett*. 2013 Dec 17;557 Pt B:79–83.
248. Sale M V., Reid LB, Cocchi L, Pagnozzi AM, Rose SE, Mattingley JB. Structural and functional brain changes following four weeks of unimanual motor training: evidence from behaviour, neural stimulation, cortical thickness and functional MRI. *Hum Brain Mapp*. VOLUME(ISSUE):PAGES.
249. Reid LB, Cunnington R, Boyd RN, Rose SE. Surface-Based fMRI-Driven Diffusion Tractography in the Presence of Significant Brain Pathology: A Study Linking Structure and Function in Cerebral Palsy. Yap P-T, editor. *PLoS One*. 2016 Aug 3;11(8):e0159540.
250. Manjon J V, Coupe P. volBrain: an online MRI brain volumetry system. *Front Neuroinform*. 2016;10(30).
251. Næss-Schmidt E, Tietze A, Blicher JU, Petersen M, Mikkelsen IK, Coupé P, et al. Automatic thalamus and hippocampus segmentation from MP2RAGE: comparison of publicly available methods and implications for DTI quantification. *Int J Comput Assist Radiol Surg*. 2016 Jun 20;(In Press).
252. Mannella F, Gurney K, Baldassarre G. The nucleus accumbens as a nexus between values and goals in goal-directed behavior: a review and a new hypothesis. *Front Behav Neurosci*. 2013;7(October):135.
253. Lu MT, Preston JB, Strick PL. Interconnections between the prefrontal cortex and the premotor areas in the frontal lobe. *J Comp Neurol*. 1994 Mar 15;341(3):375–92.
254. Smith RE, Tournier J-D, Calamante F, Connelly A. SIFT2: Enabling dense quantitative assessment of brain white matter connectivity using streamlines tractography. *Neuroimage*. 2015 Oct 1;119:338–51.
255. Modat M, Ridgway GR, Taylor ZA, Lehmann M, Barnes J, Hawkes DJ, et al. Fast free-form deformation using graphics processing units. *Comput Methods Programs Biomed*. 2010 Jun;98(3):278–84.
256. Sahama I, Sinclair K, Fiori S, Doecke J, Pannek K, Reid L, et al. Motor pathway degeneration in young ataxia telangiectasia patients: A diffusion tractography study. *NeuroImage Clin*. 2015;9:206–15.
257. R Core Team. R: A Language and Environment for Statistical Computing [Internet]. Vienna, Austria: R Foundation for Statistical Computing; 2015.
258. Matyas F, Sreenivasan V, Marbach F, Wacongne C, Barsy B, Mateo C, et al. Motor Control

by Sensory Cortex. *Science* (80-). 2010 Nov 26;330(6008):1240–3.

259. Borich MR, Brodie SM, Gray WA, Ionta S, Boyd LA. Understanding the role of the primary somatosensory cortex: Opportunities for rehabilitation. *Neuropsychologia*. 2015 Dec;79(Pt B):246–55.
260. Alonso-Ortiz E, Levesque IR, Pike GB. MRI-based myelin water imaging: A technical review. *Magn Reson Med*. 2015 Jan;73(1):70–81.
261. Dang MT, Yokoi F, Yin HH, Lovinger DM, Wang Y, Li Y. Disrupted motor learning and long-term synaptic plasticity in mice lacking NMDAR1 in the striatum. *Proc Natl Acad Sci U S A*. 2006 Oct 10;103(41):15254–9.
262. Smith SM, Jenkinson M, Johansen-Berg H, Rueckert D, Nichols TE, Mackay CE, et al. Tract-based spatial statistics: voxelwise analysis of multi-subject diffusion data. *Neuroimage*. 2006 Jul 15;31(4):1487–505.
263. Smith SM, Nichols TE. Threshold-free cluster enhancement: addressing problems of smoothing, threshold dependence and localisation in cluster inference. *Neuroimage*. 2009 Jan 1;44(1):83–98.
264. Schwarz CG, Reid RI, Gunter JL, Senjem ML, Przybelski SA, Zuk SM, et al. Improved DTI registration allows voxel-based analysis that outperforms tract-based spatial statistics. *Neuroimage*. 2014 Jul 1;94(3):65–78.
265. Fisher A, Jones K. Assessment of Motor and Process Skills, Vol. 1: Development, standardization, and administration manual. revised.. 7th ed. *Vol. 1*. Three Star Press Fort Collins, CO; 2010.
266. Narr KL, Woods RP, Thompson PM, Szeszko P, Robinson D, Dimtcheva T, et al. Relationships between IQ and Regional Cortical Gray Matter Thickness in Healthy Adults. *Cereb Cortex*. 2007 Sep 1;17(9):2163–71.
267. Dickerson BC, Feczko E, Augustinack JC, Pacheco J, Morris JC, Fischl B, et al. Differential effects of aging and Alzheimer’s disease on medial temporal lobe cortical thickness and surface area. *Neurobiol Aging*. 2009 Mar;30(3):432–40.
268. Shaw P, Greenstein D, Lerch J, Clasen L, Lenroot R, Gogtay N, et al. Intellectual ability and cortical development in children and adolescents. *Nature*. 2006 Mar;440(7084):676–9.
269. Kadis DS, Goshulak D, Namasivayam A, Pukonen M, Kroll R, De Nil LF, et al. Cortical thickness in children receiving intensive therapy for idiopathic apraxia of speech. *Brain Topogr*. 2014 Mar;27(2):240–7.
270. Reid LB, Sale M V., Cunnington R, Mattingley JB, Rose SE. Structural and functional brain changes following four weeks of unimanual motor training: evidence from fMRI-guided diffusion MRI tractography. *bioRxiv*. 2016;
271. Sale M V, Reid LB, Cocchi L, Pagnozzi AM, Rose SE, Mattingley JB. Structural and functional brain changes following four weeks of unimanual motor training: evidence from behaviour, neural stimulation, cortical thickness and functional MRI. *bioRxiv*. 2016 Nov 17;
272. Friston KJ, Holmes a P, Worsley KJ. How many subjects constitute a study? *Neuroimage*.

1999 Jul;10(1):1–5.

273. Friston KJ, Holmes a P, Price CJ, Büchel C, Worsley KJ. Multisubject fMRI studies and conjunction analyses. *Neuroimage*. 1999;10(4):385–96.
274. The R Development Core Team. R: A language and environment for statistical computing. R Foundation for Statistical Computing. Vienna, Austria; 2008.
275. Eliasson A-C, Krumlinde-sundholm L, Shaw K, Wang C. Effects of constraint-induced movement therapy in young children with hemiplegic cerebral palsy: an adapted model. *Dev Med Child Neurol*. 2005 Apr;47(4):266–75.
276. Gordon AM, Hung Y-C, Brandao M, Ferre CL, Kuo H-C, Friel K, et al. Bimanual training and constraint-induced movement therapy in children with hemiplegic cerebral palsy: a randomized trial. *Neurorehabil Neural Repair*. 2011 Oct;25(8):692–702.
277. Chow S-C. Sample size calculations for clinical trials. *Wiley Interdiscip Rev Comput Stat*. 2011 Sep;3(5):414–27.
278. Iscan Z, Jin TB, Kendrick A, Szeglin B, Lu H, Trivedi M, et al. Test-retest reliability of freesurfer measurements within and between sites: Effects of visual approval process. *Hum Brain Mapp*. 2015 Sep;36(9):3472–85.
279. Pagnozzi AM, Dowson N, Fiori S, Doecke J, Bradley AP, Boyd RN, et al. Alterations in regional shape on ipsilateral and contralateral cortex contrast in children with unilateral cerebral palsy and are predictive of multiple outcomes. *Hum Brain Mapp*. 2016;3603(October 2015):3588–603.
280. Tustison NJ, Avants BB, Cook PA, Zheng Y, Egan A, Yushkevich PA, et al. N4ITK: improved N3 bias correction. *IEEE Trans Med Imaging*. 2010 Jun;29(6):1310–20.
281. Pagnozzi AM, Dowson N, Doecke J, Fiori S, Bradley AP, Boyd RN, et al. Automated, quantitative measures of grey and white matter lesion burden correlates with motor and cognitive function in children with unilateral cerebral palsy. *NeuroImage Clin*. 2016;11:751–9.
282. Hoare B, Imms C, Carey L, Wasiak J. Constraint-induced movement therapy in the treatment of the upper limb in children with hemiplegic cerebral palsy: a Cochrane systematic review. *Clin Rehabil*. 2007;21:675–85.
283. Theys C, Wouters J, Ghesquière P. Diffusion tensor imaging and resting-state functional MRI-scanning in 5- and 6-year-old children: Training protocol and motion assessment. *PLoS One*. 2014;9(4):1–7.
284. Iscan Z, Jin TB, Kendrick A, Szeglin B, Lu H, Trivedi M, et al. Test-retest reliability of freesurfer measurements within and between sites: Effects of visual approval process. *Hum Brain Mapp*. 2015 Sep;36(9):3472–85.
285. Pagnozzi AM, Gal Y, Boyd RN, Fiori S, Fripp J, Rose S, et al. The need for improved brain lesion segmentation techniques for children with cerebral palsy: a review. *Int J Dev Neurosci*. 2015;
286. Friston KJ, Holmes a P, Worsley KJ. How many subjects constitute a study? *Neuroimage*.

1999 Jul;10(1):1–5.

287. Johnston M V. Plasticity in the developing brain: implications for rehabilitation. *Dev Disabil Res Rev*. 2009 Jan;15(2):94–101.
288. Zielinski BA, Prigge MBD, Nielsen JA, Froehlich AL, Abildskov TJ, Anderson JS, et al. Longitudinal changes in cortical thickness in autism and typical development. *Brain*. 2014 Jun;137(Pt 6):1799–812.
289. Bennett IJ, Madden DJ, Vaidya CJ, Howard D V, Howard JH. Age-related differences in multiple measures of white matter integrity: A diffusion tensor imaging study of healthy aging. *Hum Brain Mapp*. 2010 Mar;31(3):378–90.
290. Gordon AM. To constrain or not to constrain, and other stories of intensive upper extremity training for children with unilateral cerebral palsy. *Dev Med Child Neurol*. 2011;53(SUPPL.4):56–61.
291. Gordon AM, Schneider J a., Chinnan A, Charles JR. Efficacy of a hand-arm bimanual intensive therapy (HABIT) in children with hemiplegic cerebral palsy: A randomized control trial. *Dev Med Child Neurol*. 2007;49(11):830–8.
292. Volpe BT, Krebs HI, Hogan N, Edelstein OTR L, Diels C, Aisen M. A novel approach to stroke rehabilitation: robot-aided sensorimotor stimulation. *Neurology*. 2000;54(10):1938–44.
293. Schaechter JD, Moore CI, Connell BD, Rosen BR, Dijkhuizen RM. Structural and functional plasticity in the somatosensory cortex of chronic stroke patients. *Brain*. 2006 Oct;129(Pt 10):2722–33.
294. Tukey JW. *Exploratory Data Analysis*. 1st ed. Pearson; 1977.